Decentralized Dynamic Power Control for Wireless Backbone Mesh Networks

by

Thomas Otieno OLWAL

Submitted in partial fulfilment of the requirement for the degree

DOCTOR TECHNOLOGIAE: ENGINEERING: ELECTRICAL

DOCTOR OF PHILOSOPHY: COMPUTER SCIENCE

in the

Department of Electrical Engineering & French South African Institute of Technology (F'SATI)

Tshwane University of Technology

and

University of Paris-Est

Supervisors: Professor Barend Jacobus VAN WYK

Professor Patrick SIARRY

Co-Supervisors: Professor Karim DJOUANI

Professor Yskandar HAMAM

May 2010

Declaration and Copyright

"I hereby declare that the thesis submitted for the degree of Doctorate Technology: Engineering: Electrical, at the Tshwane University of Technology, is my own original work and has not previously been submitted to any other institution of higher education. I further declare that all sources cited or quoted are indicated and acknowledged by means of a comprehensive list of references".

TO OLWAL

DATE

May 14, 2010

Dedication

To my family

Acknowledgments

I would like to express thanks to my advisors, Prof. Barend Jacobus VAN WYK, Prof. Karim DJOUANI, Prof. Patrick SIARRY, Prof. Yskandar HAMAM and Dr. Ntsibane NTLATLAPA for their encouragement, suggestions, guidance, invaluable advice and friendship. I would like to thank them and acknowledge their support and patience with regards to my questions throughout the duration of this study. It is indeed, a great honour to work with them.

Special thanks to Prof. Fred OTIENO for motivating my initial coming to the Republic of South Africa to further my education. Indeed, Prof. Fred and Prof. Ben deserve special appreciation for offering me the opportunity to pursue a doctorate. I am grateful to Joe ODHIAMBO for wonderful accommodation throughout the duration of this study.

I would like to thank all staff members of the Meraka Institute at the Council for Scientific and Industrial Research (CSIR) for a conducive and interactive atmosphere during my research. Special thanks to Kagiso CHIKANE, former CSIR Meraka Institute Centre Manager, for pieces of advice and encouragement. I would like to express appreciation to Mama Sonja HALL and the HR team for their administrative support. Many thanks to the Wireless Africa Research Team for useful discussions and suggestions while presenting my progress at weekly seminars.

I am grateful to my parents for their patience, love and prayers. Special thanks and congratulations go to my wife for her patience, love and daily words of encouragement. Million dollar thanks to all my friends and colleagues for their continued friendship and enormous support.

I would like to acknowledge the Meraka Institute for offering me a studentship programme and taking full responsibility to defray all my study fees. The Tshwane University of Technology, the University of Paris-Est and the University of Nairobi are greatly appreciated for giving me the opportunity to pursue a PhD degree.

Finally, I am indebted to my creator, God for granting me abundant grace without measure and being faithful to me over many years of my life.

Thomas OLWAL

May 2010

Pretoria, South Africa.

Abstract

The remarkable evolution of wireless networks into the next generation to provide ubiquitous and seamless broadband applications has recently triggered the emergence of Wireless Mesh Networks (WMNs). The WMNs comprise stationary Wireless Mesh Routers (WMRs) forming Wireless Backbone Mesh Networks (WBMNs) and mobile Wireless Mesh Clients (WMCs) forming the WMN access. While WMCs are limited in function and radio resources, the WMRs are expected to support heavy duty applications: that is, WMRs have gateway and bridge functions to integrate WMNs with other networks such as the Internet, cellular, IEEE 802.11, IEEE 802.15, IEEE 802.16, sensor networks, et cetera. Consequently, WMRs are constructed from fast switching radios or multiple radio devices operating on multiple frequency channels. WMRs are expected to be self-organized, self-configured and constitute a reliable and robust WBMN which needs to sustain high traffic volumes and long "online" time. However, meeting such stringent service expectations requires the development of decentralized dynamic transmission power control (DTPC) approaches.

This thesis addresses the DTPC problem for both single and multiple channel WBMNs. For single channel networks, the problem is formulated as the minimization of both the link-centric and network-centric convex cost function. In order to solve this issue, multiple access transmission aware (MATA) models and algorithms are proposed. For multi-radio multi-channel (MRMC) WBMNs, the network is modelled as sets of unified channel graphs (UCGs), each consisting of interconnected active network users communicating on the same frequency channel. For each UCG set, the minimization of stochastic quadratic cost functions are developed subject to the dynamic Link State Information (LSI) equations from all UCGs. An energy-efficient multi-radio unification protocol (PMMUP) is then suggested at the Link-Layer (LL). Predictive estimation algorithms based on this protocol are proposed to solve such objective functions. To address transmission energy and packet instabilities, and interference across multiple channels, singularly-perturbed weakly-coupled (SPWC) control problems are formulated. In order to solve the SPWC transmission power control problem, a generalized higher-order recursive algorithm (HORA) that obtains the Riccati Stabilizing Solutions to the control problem is developed. The performance behaviours of the proposed models and algorithms are evaluated both analytically and through computer simulations. Several simulations are performed on a large number of randomly generated topologies. Simulation and analytical results confirm the efficacy of the proposed algorithms compared to the most recently studied techniques.

Table of Contents

List of Tables

List of Figures

Glossary

BLVN	Bi-directional Logical Visible Neighbour Set
CDMA	Code Division Multiple Access
CSMA/CA	Carrier Sense Multiple Access/Collision Avoidance
DTPC	Dynamic Transmission Power Control
EBIA	Effective Band Interference Estimation Based DTPC Algorithm
GCOM	Generalized Cross-Layer Occupation Measure
HORA	Higher Order Recursive Algorithm
LL	Link-Layer
LSI	Link State Information
MAC	Medium Access Control
MAC-TSP	MAC Dependent Transmission Scheduling Probability
MAI	Multiple Access Interference
MANET	Mobile Ad Hoc Network
MATA	Multiple Access Transmission Awareness
MRMC	Multi-Radio Multi-Channel
MRSIP	Multi-Radio Multi-Channel Interaction States Prediction
MRSUP	Multi-Radio Multi-Channel Unification States Prediction
MUP	Multi-Radio Unification Protocol
NIC	Network Interface Card or Radio Device
PMMUP	Energy-Efficient MRMC Unification Protocol at the Link-Layer
SIR/SINR	Signal to Interference plus Noise Ratio
SPWC	Singularly Perturbed Weakly Coupled
UCG	Unified Channel Graph
User	Wireless Radio Link
VoIP	Voice over Internet Protocol
WBMN	Wireless Backbone Mesh Network
WMC	Wireless Mesh Client
WMN	Wireless Mesh Network
WMR	Wireless Mesh Router

Chapter 1

Introduction

With the massive growth of wireless networks into the next generation to provide better services, an important technology, wireless mesh networks (WMNs), has recently emerged. WMNs have attracted immense interest, from those who research wireless networks, during the past decade. This sudden interest emanates from developments which indicate that the WMNs can offer ubiquitous communication and seamless broadband applications. Architecturally, WMNs are hybrid networks composed of a mixture of static and mobile nodes interconnected via wireless links to form a multi-hop wireless ad hoc network (WANET). The static nodes are usually called wireless mesh routers (WMRs) while mobile nodes are generally termed wireless mesh clients (WMCs), as shown in Figure 1.1. In WMNs, each node operates not only as a host but also as a router, forwarding packets of data on behalf of other nodes that may not be within direct wireless transmission range of their destinations. While static WMRs form wireless backbone mesh networks (WBMNs), the WMCs access the Internet through WBMNs as well as directly meshing with each other [1]. The WMCs form traditional mobile wireless ad hoc networks (MANETs) which provide end-user applications [2]. However, the WMRs which access WMCs voluntarily relay huge backbone traffic to the Internet via a few fixed gateways, and perform internetworking integration. These roles render WMNs quite distinct from the traditional wireless networks, such as the wireless sensor networks (WSNs) [3], MANETs [2], Wireless Fidelity (Wi-Fi) and cellular networks [4, 5].

Wireless mesh networks (WMNs) are classified into three standard activities, namely IEEE 802.11, IEEE 802.15, and IEEE 802.16 mesh networks [6]. The working group within the IEEE 802.11, called IEEE 802.11s has been formed to standardize the extended service set (ESS) [7]. The main objective is to define the MAC and PHY layers for mesh networks that extend coverage with no single point of failure. Consequently, the IEEE 802.11 ESS mesh defines an architecture and protocol that create an IEEE 802.11 wireless distribution system (WDS). The WDS supports both broadcasts/multicasts and unicast delivery of packets at the MAC layer using radio-aware metrics over self-configuring multi-hop topologies [7]. In terms of power management, the IEEE 802.11s standard demonstrates two power

management modes implemented at all mesh stations. The first mode is the active mode and the second mode is the power save mode. In active mode the stations stay awake all the time while in power save mode, the stations alternate between awake and doze states, as determined by the frame transmission and reception rules. However, during transmission of a packet, stations use maximum power level implying that proposing a transmission power control scheme would improve the power management significantly. On the other hand, IEEE 802.15.5 working group has been established to investigate the necessary mechanisms in the PHY and MAC layers that can enable mesh networking in the wireless PANs [8]. Thus, power control mechanism would ensure this standard maintains mesh networking topology. The IEEE 802.16 mesh networks working group aims at determining the possible mechanisms in the PHY and MAC layers which can serve the broadband wireless access in metropolitan area (i.e., last mile) and support point to multi-point connection oriented Quality of Service (QoS) communications that extend fibre optic backbones. However, the IEEE 802.16 mesh standard demonstrates several limitations such as lack of scalability, a connectionless MAC (i.e., so QoS of real-time services cannot be guaranteed). It also assumes no interference between two hops away (i.e., a situation of hidden terminal problem) [9].

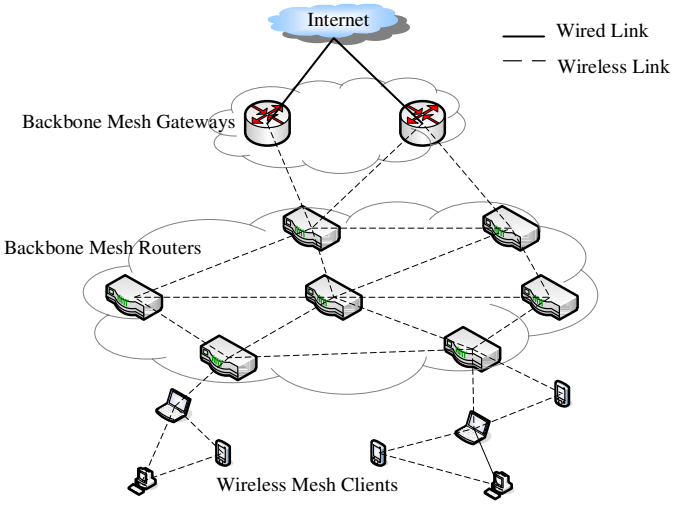

Figure 1.1: Hybrid Wireless Mesh Network architecture

Numerous significant attributes of the wireless backbone mesh network (WBMN) can be identified as follows. Firstly, the WBMN is dynamically self-organized and self-configured. That is, the WMRs in the mesh network automatically establish and maintain stable network connectivity. This feature provides the end-users with many advantages, such as low up-front

cost, easy network maintenance, robustness, and reliable service coverage. Secondly, the WMRs establish redundant paths between the sender and the receiver of the wireless connection. This feature provides path reliability against single points of failure. It also creates network robustness against node or path failures due to Radio Frequency (RF) interference, obstacles or power outages by providing multiple alternative routes. Thirdly, the WMRs are constructed using advanced radio technologies, for example, multiple radio interfaces, software defined radios and smart antennas. These radio technologies may be designed to support either the same or different wireless access network technologies. The motivation behind advanced radio technologies is the performance of simultaneous WMC network access and backbone traffic routing. As a result, the backbone network capacity of diverse service applications (e.g., VoIP, video and data) may be increased substantially without compromising the specific QoS constraints. The network capacity is the sum of the throughput provided to all end-users in the network. That is, the magnitude of the spatial re-use and the fairness of medium access. Finally, WMRs perform gateways and bridge functionalities. This is to enable the integration of WMNs with various existing wireless network technologies, such as WSNs, Wi-Fi, WiMAX, Wireless Region Area Network (WRAN) and cellular networks [10]. As a benefit to network operators and subscribers, WBMNs can extend the service coverage of these technologies, even up to the furthest of far flung remote and rural areas [11].

Based on these significant attributes, WMN technology promises several emerging and commercially interesting applications. Examples include broadband home networking, community and neighbourhood networks, enterprise networking, coordinated and collaborative network management and intelligent transportation systems. Indeed, WMN has now made it possible for cash strapped Internet Service Providers (ISPs) and others to roll out robust and reliable wireless broadband services at a reasonable cost [6]. Such ambitious applications have triggered several challenges that researchers must address before WMN can realize its full application potential. In order to automatically access and forward huge volumes of traffic over a long period of time and to automatically internetwork with other existing technologies, network capacity, and connectivity and energy-efficiency issues must be addressed for WBMNs. These are the problems which decentralized Dynamic Transmission Power Control (DTPC) must tackle.

The DTPC is the method of selecting transmission power levels from a set of transmission power settings of a wireless radio interface, for every packet, and is subject to both the network and application dynamics [12]. The network dynamics include wireless channel

conditions [13], modulation and coding variations, network RF interference fluctuations, received signal-to-interference ratio (SIR) variations, queue conditions, topology changes and power source outages [5]. The application variations involve the diverse QoS for voice, video or data applications [14]. Because the wireless medium is naturally distributed, decentralized DTPC approaches are investigated in this work. In such an approach, only the local state information is utilized in real-time by each wireless transmitter to select proper transmission power levels. Moreover, decentralized algorithms indicate low message overhead costs across the network compared to the centralized algorithms [15].

1.1 Problem Statement

The main objective of this investigation is to develop decentralized DTPC solutions maintained at the Link-Layer of the protocol stack for the purpose of maximizing network capacity of WBMNs while minimizing energy consumption and maintaining fault-tolerant network connectivity.

In general, WBMNs are expected to extend the coverage range of existing wireless technologies through multi-hop communication without sacrificing the channel or network capacity. This can be ensured by providing shorter link distances (or hops), less multiple access interference (MAI) among adjacent nodes and more efficient frequency re-use within an interference range of a transmitter [16-18]. The design criterion is that the power level should be high enough to suppress the co-channel interference but no higher than that which will create unnecessary contention and collisions among nodes. Channel contention and collisions may in turn compromise the overall network throughput. However, capacity maximization techniques for the WBMN with multiple radio systems still face a number of challenges [19-21]. For instance, switching and process coordination delays stemming from multiple channels, MAI effects across multiple adjacent channels, energy outage problems, non fault-tolerant and non-scalable network connectivity [22], [23].

In order to conserve transmission power while maintaining fault-tolerant connectivity, the transmission power level should be low enough to conserve the supply energy, experience less MAI, report a minimal average node degree and maintain short hop-lengths. This power level, however, should not result in a partitioned network. To reduce control delays, the power level adjustment should be fast enough to limit queue delays due to packet arrivals from upper layers but no faster than that which will cause queue perturbations between residual energy and packet sizes at the buffer. However, in terms of energy outage problems,

in the recent past it has been argued by a number of researchers that WMRs usually do not possess strict constraints on power consumption [1]. Nonetheless, with remote applications, such WMRs may run on battery power (e.g., solar-power or mechanical vibrations) with limited maintenance or replacement [11]. Moreover, mesh routers may also be equipped with low cost multiple radios or high speed wireless radio interfaces. The motivation is to perform backbone routing, client network access and internetworking integration functionalities. However, the challenges involved include multiple queue instabilities owing to speed variations between residual energy and packets, and the expected long "online" time: consequently, accelerated transmission energy depletion and shorter battery lifetime [6].

Thus, owing to such design constraints, the transmission power level needs to be adaptive to changes in the Link State Information (LSI) so that retransmissions in high error-prone wireless channels can be avoided. Such LSI may include the wireless link transmission packet rate, RF interference, user-centric and network-centric quality measures, transmission ranges and residual energy. Exploiting such information renders the flexibility and adaptability benefits of the cross-layer interaction useful. In order to manage the interaction between non-adjacent layers in a systematic organized manner while preserving the modularity of each layer [24], an energy-efficient Link-Layer (LL) protocol will be suggested in this study. In addition to controlling packet synchronization, flow control and adaptive channel coding, this LL protocol should coordinate the transmission power adjustment by multiple radio interfaces operating over multiple error-prone wireless channels [25]. The advantage is that the LL periodically monitors the quality of LSI on each radio interface with each of its neighbours and performs power optimization. Subsequently, when the time comes to send a packet to a neighbour, it selects the correct radio(s) with optimal transmission power(s) with which to forward the packet. In addition, the LL protocol allows for the use of localized information across the layers in order to derive an optimal transmission power level that improves capacity, energy conservation and network connectivity. Thus, such a consideration is expected to contribute to a number of desirable features of the WMNs: network collaborations, internetwork integration, multi-hop and multi-point to multi-point (M2M) communication and scalability.

1.2 Research Aims

The purpose of studying optimal DTPC is to achieve:

1. **High Throughput Performance**. One, most crucial, aim of DTPC solutions for WMRs is to ensure maximum network capacity: the maximum number of conversations that a receiver station can handle within some Signal-to-Interference (SIR) constraint. This network capacity can be measured by throughput performance which describes the amount of transmitted packets that are successfully received in a reasonable amount of time.
2. **Significant Transmission Power-Saving Performance.** The transmission power control by itself saves power resources. However, the use of high speed radios and/or multiple radio interfaces built on the WMRs may not guarantee a proper throughput and energy balance. Thus, this study aims to conserve energy further by employing energy-awareness strategies while developing optimal transmission power control algorithms.
3. **Reliable Network Connectivity Performance.** Network connectivity is characterized by average node degree, fault-tolerance and spanner structure metrics. Keeping a minimum average node degree while maintaining redundant multiple short hop-lengths provides robustness and reliability against node or path failures. In WBMNs, nodes or links fail due to RF interference, obstacles and power source outages. These metrics are achieved through topology control algorithms using the transmit power adjustment.

1.3 Delimitations

This investigation will not involve the following:

1. Wireless Mobile Ad Hoc Networks (MANETs): This is because mobile nodes are portable nodes with a highly constrained power supply and are usually constructed on single radio technologies. Thus, they cannot support automatic and simultaneous accessing and forwarding of high volumes of traffic over long periods of operation. Extensive studies addressing power control problems in MANETs over the past years do exist [26].
2. Centralized power control algorithms: Such algorithms require an infrastructure base station which possesses information concerning the entire network. However, gathering such information in real-time across the whole network incurs communication overheads. In contrast, WBMNs need to be self-organized and self-configured: that is, each node or

radio automatically joins the network when it is added or heals the network when it is down so that the network establishes routes without any central control.

3. Topology Control Algorithms: The explicit topology control sub-problem in a wireless mesh network (WMN) has been dealt with recently [26-30]. However, this thesis is limited to the transmission range information affecting network connectivity, that is, the transmission power level determines how far a node connects with its neighbours; hence, the need to estimate the connectivity range prior to adjustment of the transmission power.
4. Joint cross-layer resource management: Joint cross-layer resource allocation and power control involves excessive message signalling across different layers. Such signalling assumes maximum transmission power and, thus, is not scalable in general. Furthermore it has been pointed out that most message interactions across different layers do not preserve the modularity of the layers [24]. Performing optimal power control and cross-layer resource allocation indeed adds to the design's complexity and as a result it is not realistic, considering the extensive problem dimensions of multi-radio multi-channel (MRMC) wireless systems.
5. Hardware Implementations and field-testing: Due to time constraints, the study will be limited to simulation investigations. The objectives of the research can be adequately assessed by both analytical and computer simulations only.

1.4 Underlying Assumptions

This study will assume that:

1. Wireless mesh routers (WMRs) can operate in energy-constrained environments; for instance, rural and remote areas where nodes are battery-powered and frequent battery replacements may not be feasible.
2. WMRs can operate with heterogeneous transmission ranges: In other words, any node can connect to another node in the network using a transmission range that may be completely different from one node to the other. Therefore, the established network topology need not be uniformly distributed.
3. Channels are statically assigned: For the duration of a time-slot comprising neighbour discovery, power optimization and packet transmission time scales, channel assignment does not alter. We note that dynamic channel assignments during a time-slot (or at run time) may not only incur run time overhead costs but are also NP-hard problems in wireless systems [19, 20, 31]. Moreover, wireless fading naturally violates the ideal

orthogonality of multiple channels. This assumption is reasonable, considering the power control problems, even for delay sensitive applications [14]. Nonetheless, channels may be re-assigned randomly at the end of every transmission time-slot.

4. The network is connected when each node uses the maximum transmission ranges and thus the maximum transmission power levels. Thus, no single node can be disconnected while operating at maximum transmission power.
5. There is a finite number of nodes, channels in a network, and radio interfaces at a node. This assumption justifies realistic network instances while it also simplifies the design accordingly.

1.5 Motivation

This investigation is motivated by the need to develop DTPC techniques so that a high network capacity, low energy consumption and reliable network connectivity can be achieved for the distributed WBMNs. The rationale behind this research is described below.

1.5.1 Decentralized versus Centralized Approach

As mentioned previously, a decentralized approach models and controls the transmission power of one single transmitter, while the algorithm only relies on local information. A centralized approach requires a common arbiter which possesses all the information regarding the established connections and channel gains at hand, and controls all the transmission power levels in the network. The former case is the only practical one causing less overhead costs. The decentralized approaches maintain the autonomy of each wireless mesh router (WMR) in order to meet the objectives of self-organization and self-configuration. On the other hand, the centralized approach requires extensive control signalling in the network; however, it will suffer from additional time delays and is not robust to single points of failures. Therefore, decentralized dynamic power controllers (DTPC) are proposed in this study.

1.5.2 Dynamic Control Theory versus Game Theory

Theory of dynamic control implements robust filters which are based on the temporal correlation of the interference and channel states in order to compensate for time-varying disturbances [32]. In addition, each WMR may be equipped with multiple radios and

channels, and possesses multi-dimension Link State Information (LSI). State space control theory may effectively be used to model such large dimensions so that predictive algorithms are conveniently used to derive optimal power output signals. Thus, state space modelling offers generic solutions together with reduced control delays, that is, measuring and control signalling time delays [33]. On the other hand, game theory is an analytical tool often used to model individual, independent decision makers (IDMs) whose actions potentially affect all other IDMs in the system [34]. Two categories exist, cooperative and non-cooperative games [35]. According to Branzei, *et al.* [36], cooperative game theory is concerned primarily with coalitions, i.e., groups of IDMs, who coordinate their actions and pool their winnings. Consequently, one of the key problems addressed by cooperative game theory is how to divide or allocate resources or benefits among the members of the formed coalition. In this manner, cooperative game theory strives to understand the interplay between an efficient and a fair allocation of resources [37]. In [36], cooperative game theory is broadly categorized in three models, i.e., crisp games, fuzzy games and multi-choice games. Cooperative games with crisp coalitions are cooperative games with transferable utility (TU-games), while cooperative games with fuzzy coalitions model situations where IDMs have the possibility to cooperate with different participation levels, varying from non-cooperation to full cooperation, and where the obtained reward depends on the level of participation. However, in a multi-choice game each IDM has a finite number of action levels to participate with when cooperating with other IDMs in the same coalition. On the other hand, a non-cooperative game comprises an optimization among *individual* IDMs with selfish objective functions [35]. Several DTPC techniques in Ad Hoc networks have been formulated using game theory. Game theory allows one to completely decouple independent power control decisions from the large-scale interconnected wireless system, to a reduced-scale level. However, the main difficulty is how to find the Nash Equilibrium of a non-cooperative game possessing a large number of IDMs participating in adverse wireless channel conditions [38]. Even the Nash Bargaining Solution in cooperative games that achieves a good compromise between fairness and power efficiency in a scarce resource allocation, demonstrates a complex implementation challenge with an expanded system dimension [34]. Although theory of differential Nash games will be exploited in this thesis [39], dynamic control techniques remain key solutions in meeting our design objectives.

1.5.3 Predictive versus Non-predictive Algorithms

The advantage of predicting channel gains and interference levels is that of being able to update the power levels at a reduced control delay and hence a low computational energy consumption. Predictive power control algorithms rely on temporal correlations between future, previous, and present measurements [40]. In practice, the transmission power iteration time-instants are expected to be faster than the network state evolution time-scales. Therefore, predictive power control algorithms allow "online" measurements of states and facilitate fast convergence of the optimal power signals relative to a given run time. On the other hand, non-predictive power control algorithms are based on only the current and previous measurements. They are slow in yielding optimal solutions. They use outdated measurements to update the power levels. Therefore, this study considers adaptive predictive approaches in order to reduce transmission power adjustment delays.

1.5.4 Asynchronous versus Synchronous Algorithms

Asynchronous power execution algorithms require that each radio interface performs its power adjustment steps independently of other radio interfaces on the same node or other neighbouring nodes. In other words, such a radio interface can proceed with its next cycle without waiting for other radio interfaces to finish their current iteration interval. In contrast, synchronous algorithms require that before proceeding to the next cycle, a radio interface that has finished its execution interval must wait for others to finish their current iteration (i.e., the execution interval is synchronized). The latter approach naturally supports packet stripping mechanisms over multiple channels with minimum re-sequencing problems at the receiver. The former approach is strongly applicable to large scale WMNs with no central controllers. In addition, WMRs may be constructed on high speed radios and/or multiple radios to perform asynchronous access and forward functions. Furthermore, each node may be completely heterogeneous in design that is, with different processing speeds, memory diversity, varying energy supply technologies, and different transmission ranges. Thus, running asynchronous algorithms naturally improves performance efficiency. Moreover, the controllers are allowed to run independently of each other in a completely asynchronous manner, such that controllers with lower state dimensions will release more updated information about their trajectories compared with the synchronous cases. Only the controllers with the largest dimensions will perform as much iteration as is performed in the synchronous case. Therefore, it is expected that asynchronous algorithms will display faster

convergence. The proposed asynchronous algorithms in this dissertation still maintain the simple structure of the synchronous algorithms.

1.5.5 Link-Layer versus Physical Layer

As mentioned previously, the Link-Layer (LL) handles packet synchronization, flow control and adaptive channel coding. In addition to these roles, the LL protocol effectively preserves the modularity of cross-layers and provides desirable WMN scalability [25]. Scalable solutions managed by the LL ensure that the network capacity do not degrade with increase in the number of hops or nodes between the traffic source and destination. This is because the LL is strategically located just right on top of the medium access control (MAC) and just below the network layer. Message interactions across layers do not incur excessive overheads. As a result, dynamic transmission power executions per packet basis are expected to yield optimal power signals. Furthermore, if each node is configured with multiple MACs and radios, then the LL may function as a *virtual* MAC that hides the complexity of multiple lower layers from unified upper layers [41]. It may also coordinate the operations of separate radios in a more efficient and reliable manner. On the other hand, the physical layer executes transmission power control based on only signal-to-interference plus-noise ratio (SIR), interference and channel gains [5]. However, physical layer power control does not take into account MAC problems prevalent in multi-hop networks [42, 43]. Indeed, such power control techniques may not necessarily provide a good trade-off between energy consumption, fairness and network throughput [44].

1.6 Contributions and Publication Synopsis

In this study, mathematical programming models for power control problems are developed. Optimal adaptive predictive algorithms to solve such problems are proposed at the Link-Layer. The main contributions of this thesis are described and our publications are cited in the following.

1.6.1 Mathematical Programming Models

This thesis provides three mathematical programming models for formulating the decentralized DTPC problem in WBMNs [21, 23, 45-48] . In each model, the DTPC problem is represented as an optimization problem at the link level (i.e., also referred to as *user*)

composed of objective functions subject to a set of Link-Layer (LL) constraints, imposed by the link or network and/or the application. The models are decentralized in order to meet the self-organization and self-configuration, and scalability requirements of WBMN. These models may be summarized as follows:

- *Minimizing the convex cost function of joint SIR-deviation and aggregate interference for a single radio wireless network:* This model strikes a balance between user-centric quality of service (QoS) and the network-centric QoS. The user-centric QoS includes maximum user throughput, minimal queue delay, and maximum battery life. The network-centric QoS includes maximum network capacity, multi-hop network fairness, robust network connectivity and elongated network lifetime. The objective function is developed from multiple access transmission awareness (MATA) models; specifically, medium access control dependent transmission scheduling probability (MAC-TSP) and the generalized cross-layer occupation measure (GCOM) models are developed. While the MAC-TSP models the multiple access interference (MAI) and SIR states, the GCOM describes the states from all the protocol layers that affect transmission power optimization managed by the LL.

- *Minimizing the stochastic quadratic cost function within each channel subject to Intra-channel and Cross-channel dynamic equations for a multi-radio multi-channel (MRMC) wireless network:* This model is developed to maximize network capacity while minimizing transmission energy consumption and maintaining reliable network connectivity. Because of the multiple radio and channel configurations, the entire WMN is first divided into Unified Channel Graphs (UCGs) sets. A UCG set comprises radio interface pairs interconnected via a wireless medium while operating on a common frequency channel. The Link State Information (LSI) is derived for each UCG set and then generalized as state space models. The stochastic quadratic cost function is adopted in order to incorporate model uncertainties as well as to indicate the trade-off between the size of uncertain states (or LSI) and the power control action. Specifically, the objective ensures selecting a transmission power sequence at each user in such a manner that the following LSI transitions at the receiver will be met:

- *actual SIR level will track the target SIR level*
- *actual Network Interference will track the target interference level*
- *actual Rate will track the achievable link rate*
- *actual Connectivity range will track the target transmission range.*

- *Minimizing the stochastic quadratic cost function of a singularly-perturbed and weakly-coupled dynamic MRMC wireless network:* This model is provided in order to maximize network throughput while minimizing the energy consumption at the backbone nodes. Due to energy outages arising from the battery charging and/or discharging, and the variations of the packet levels at the queue, singular perturbations may be modelled at the queue system. Markov chain models may be employed to approximate such phenomena. In addition, because of the multiple adjacent channel interference, a weak-coupling model has been developed. These models are formulated as singularly-perturbed weakly-coupled (SPWC) differential Nash games control problems. The objective is to minimize the singular-perturbations and weak-couplings causing packet retransmissions at the WBMN.

1.6.2 Adaptive Predictive Algorithms

This thesis provides several adaptive predictive algorithms for the DTPC problems in WBMNs. These are based on three protocols suggested at the LL. Synopses of the algorithms are outlined and the publications are cited as follows:

- *Multiple Access Transmission Aware (MATA) protocol for single channel wireless mesh network (WMN):*

  First, an energy-efficient bi-directional logical visible neighbour (BLVN) algorithm is derived. This algorithm allows each transmitting radio interface to identify its active neighbours before performing power optimization. To reduce medium access contentions, neighbour identifications are performed using a fraction of maximum transmission power at a node. Employing this framework, a localized topology-based power control algorithm has been developed which calculates the optimal transmission power so that (1) network connectivity is maintained, (2) node transmission power is reduced to cover only the nearest neighbours, and (3) network lifetime is extended [27-30].

  Second, under MATA protocol, a scalable MAC-TSP based DTPC algorithm has been developed. The MAC-TSP defines the probability that a packet will successfully be

transmitted by each link using a selected transmission power level, given the physical, MAC and the BLVN topology information. This algorithm reduces multiple access interference (MAI) including those from hidden terminals. It also provides optimal power level solutions so that network capacity is improved and energy consumption is minimal [45]. An extension of this study to multi-radio problems can be found in [49]. In a general situation, a power adjustment policy that depends on average cross-layer information fluctuations rather than instantaneous variations has been published in [23]. The advantage is that such a power control policy maintained at the LL, relying on imperfect and often delayed information provides much power saving on average compared to that of some recent proposed techniques such as [12, 50].

Third, a generalization of the MAC-TSP referred to as a generalized cross-layer occupation measure (GCOM) based DTPC algorithm is developed. This algorithm describes the probability that an individual link chooses a certain transmission power level knowing the LSI across layers of the protocol stack. Depending on the traffic application and multiple transmission activity (MTA), each user adjusts its power dynamically so as to minimize the average convex cost function [47]. The benefits are that network capacity is increased while utilizing carrier-sensed multiple access together with collision avoidance (CSMA/CA) schemes.

Fourth, MATA-based models and algorithms are rigorously analysed for convergence.

- *An energy-efficient power selection multi-radio multi-channel unification protocol (PMMUP) supported at the Link-Layer:*

  First*,* this study proposes a multi-radio multi-channel link state information (LSI) interaction prediction (MRSIP) algorithm. MRSIP predicts the LSI from lower level multiple MACs [46] and UCGs in order to optimize the transmission power levels for each link (user). Based on this algorithm, the DTPC problems related to a heterogeneous connectivity range in the WBMN have been studied in [51]. Co-channel and cross-channel interference minimization issues have been investigated in [48]. The work in [46] generalizes an MRSIP algorithm in terms of throughput maximization and energy-efficiency.

  Second, a variation of MRSIP called MRSUP (i.e., unification) is also proposed. MRSUP predicts the LSI from the upper layers of the protocol stack. Aware of such information alongside the residual energy, each link optimizes its objective function and

produces optimal power levels. Autonomous transmission power adaptation based on this algorithm has been published in [21, 46]. The benefits of PMMUP algorithms are that they increase network capacity without compromising energy outages by allowing each mesh router to perform network access and traffic forwarding in the backbone network.

Third, convergence and stability analysis of the asynchronous MRSIP and MRSUP is reported in [52].

- *Singularly-perturbed weakly-coupled PMMUP for wireless mesh routers (WMRs):* Based on the knowledge of the queue perturbations and cross-channel interference effects, a differential Nash equilibrium strategy is developed. Corresponding to this equilibrium, a generalized higher-order recursive algorithm (HORA) is proposed. The HORA provides a stabilizing solution for the decoupled algebraic regulator Riccati equation (ARRE). This algorithm has been analysed for system convergence. Some of the results of this work have been submitted for publication [53].

1.7 Thesis Organization

The remainder of this thesis consists of 5 chapters structured as shown in Figure 1.2.

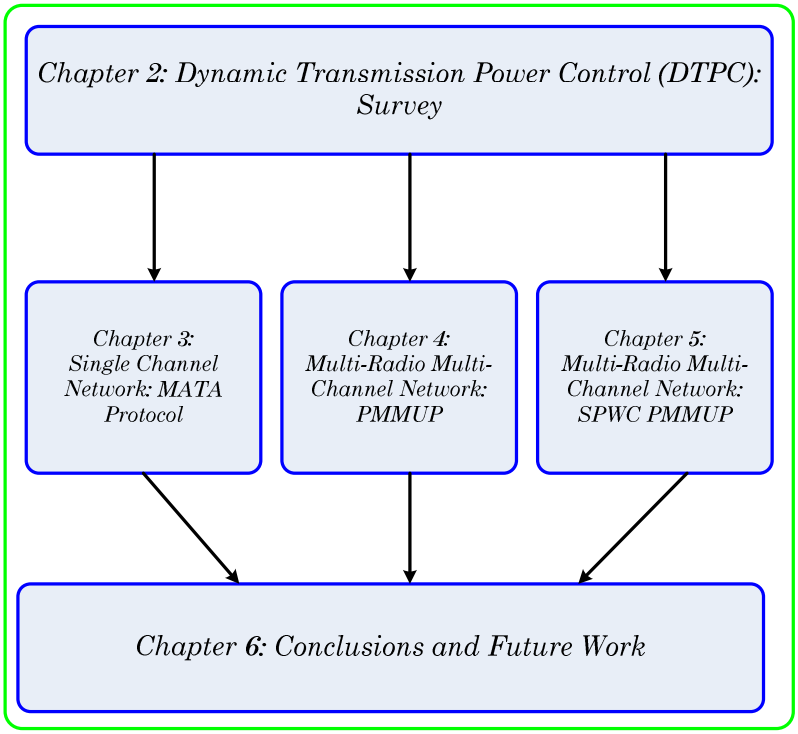

Figure 1.2: Thesis structure

Chapter 2 presents an overview of the dynamic transmission power control (DTPC): decentralized approaches. The taxonomy of the solution techniques is constructed. In short, they are classified in terms of mathematical programming, game theory, dynamic control, network protocol heuristics and the proposed LL based dynamic control solutions.

Chapter 3 furnishes a multiple access transmission aware (MATA) protocol for developing optimal transmission power signals within a Bi-directional Logical Visible Neighbour (BLVN) set on the same frequency channel. MATA based models and algorithms are derived. Analytical and simulation tests are performed in order to validate the efficacy of MATA based algorithms.

Chapter 4 is concerned with wireless mesh routers (WMRs) containing multiple radios and multiple channels (MRMCs). In this chapter, WBMN is divided *virtually* into a set of unified channel graphs (UCGs). Based on each UCG set, a decentralized DTPC problem is formulated. To solve this problem, an energy efficient power selection MRMC unification protocol (PMMUP) is developed. Adaptive transmission power control algorithms are derived. The performances of these algorithms are tested by means of analysis and extensive simulations.

Chapter 5 first models the WBMNs with MRMC configuration as singularly-perturbed weakly-coupled wireless systems. This chapter then develops a generalized higher-order recursive algorithm (HORA) that stabilizes the algebraic regulator Riccati equation (ARRE). Analytical and simulation results that demonstrate the efficacy of the proposed DTPC solution are furnished.

Chapter 6 concludes the research work, summarizes the researcher's contributions, his perspectives, and provides direction for future work.

Chapter 2

Dynamic Power Control: A Survey

2.1 Background Information

In the recent past, the wireless backbone mesh networks (WBMNs) have been assumed to be power-unconstrained since they are expected to handle high traffic loads over longer periods of time [6, 54]. The reason is that WMRs forming the WBMNs operate on stable electric power outlets [55]. Moreover, such backbone nodes are equipped with fast-switching radios [56, 57] and/or multiple radios operating on single and/or orthogonal multiple wireless channels [58]. Nonetheless, these configurations exacerbate such transmission power control problems as energy consumption, connectivity and interference irrespective of the types of power sources [31, 59, 60]. It is noted that over many years, several transmission power control algorithms have been suggested in order to address these problems (e.g., [5, 61, 62]). Indeed, depending on different wireless network architectures, researchers have provided specific solutions to specific problem definitions. In wireless cellular networks (e.g., [5]), the decentralized control of the mobile battery power is achieved through the uplink (mobile-to-base station) power control methods [62]. In wireless sensor networks (e.g., [63]), the transmission power control difficulty arises between sensor nodes and the sink base stations (e.g., [61, 64]). However, for self-organized and self-configured WBMN the transmission power control problems need to be localized at each WMR [6]. In such architecture, the source clients (WMCs) transmit their data to the nearest WMR using uplink channels. This WMR then sends the data over multi-hop paths to reach a WMR that is currently in range of the destination client. The destination WMC receives its data via a downlink channel [65]. In this regard, the uplink (client-to-router) communication exploits well known uplink power control schemes (e.g.,[66, 67]). The downlink (router-to-client) transmissions utilize the conventional downlink power control schemes (e.g.,[68]). This investigation, however, focuses on the decentralized router-to-router power control schemes of the WBMNs. The aim is to increase the network capacity at the backbone networks while maintaining the needed scalability.

2.2 Taxonomy of Dynamic Power Control Approaches

In the light of extensive related works in the literature, the ambition is not to furnish a complete coverage of the area in this thesis, but rather to outline some important and central contributions to the WBMNs. Some examples of the DTPC problems in distributed wireless cellular networks (WCNs) have been provided by [5, 33, 62]. Power control that deals with WCDMA wireless systems have been furnished by (e.g.,[69, 70]), while those approaches associated with WiMAX based WMNs have been proposed in (e.g.,[67, 68, 71]). For instance, the WCDMA air interface of the universal mobile telecommunication system (UMTS) is organized in frames of 10 ms duration of 15 timeslots and each slot includes one power control command [72]. The power control comprises the outer loop which sets the target SIR and the inner loop which adjusts the transmit power in order to keep the SIR equal to the target. On the other hand, the IEEE 802.16e based mesh networks operate both in FDD and TDD modes. Power control algorithms are implemented by the base station which send the command to the mobile stations in order to regulate their transmit power levels according to the SIR constraints at the base station [73]. As specified in IEEE 802.11 standard, the maximum transmit power is limited to 200mW (23 dBm) for the middle band of the 5 GHz, which is suitable for indoor environments. A DTPC-enabled 802.11a device is allowed to choose any of the 15 transmit power levels from -19dBm [2]. Power control solutions in wireless sensor networks (WSNs) have been discussed by [3, 61, 63, 64, 74] and in wireless ad hoc networks (MANETs) by [15, 26, 43, 75-77]. Joint DTPC and network cross-layer resource management have been addressed for WMNs [78-81]. Based on such reviews, the DTPC problem can be assumed to be an optimization formulation irrespective of the solution techniques considered [5]. Thus, the power control optimization is purely described by four tuples: optimization variables, objective function, constraint set, and constant parameters.

This section presents a taxonomy of the proposed approaches or algorithms regarding the DTPC issues. Although these algorithms are general to wireless networks, such theories can easily be applied in ad hoc WMNs with single radio configurations [82]. The broad classification includes: mathematical programming theory, game-theory, dynamic control theory and network protocol heuristics. Some past contributions in these categories include: mathematical programming (e.g., [12, 83-87]), Branch and Bound theory [57, 88], power controlled network protocols (e.g., [18, 26, 77, 89-95]), simulated annealing [87], game theory (e.g., [35, 96-99]), predictive methods (e.g., [12, 100, 101]), Kalman filter methods

(e.g., [32, 102]) and cross-layer approaches (e.g.,[103-106], [84, 107]). These techniques may be classified hierarchically as shown in Figure 2.1.

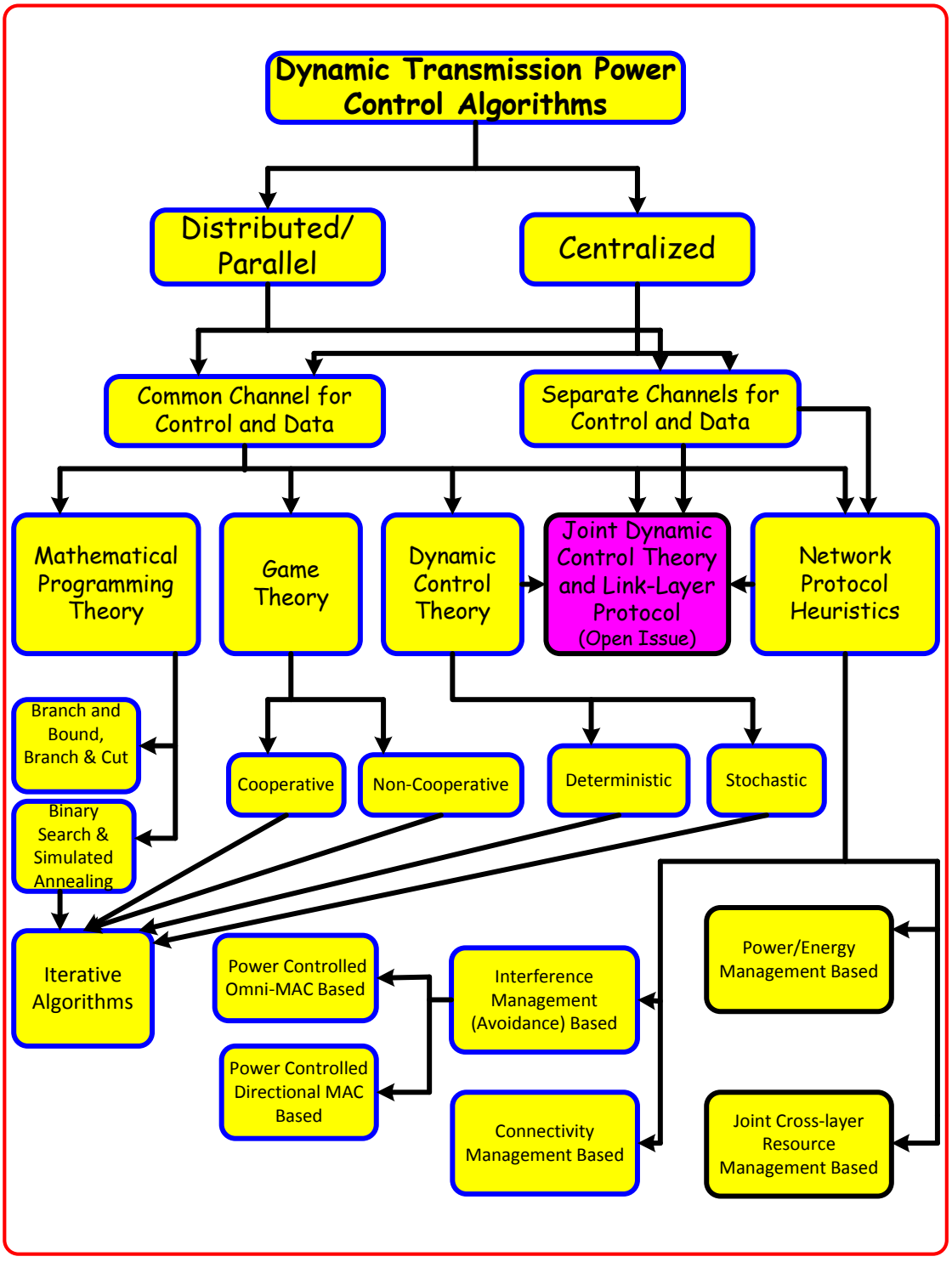

Figure 2.1: Taxonomy of DTPC algorithms

2.3 Publications Based on Mathematical Programming

In wireless cellular or Ad Hoc networks, the quality of service (QoS) is interference-limited [85]. Therefore, most of the DTPC problems can be formulated as optimization problems composed of a cost function subject to a set of constraints imposed both by the service or application and the network or system [108]. For example, the DTPC problem can be formulated as a nonlinear optimization with a system-wide objective, for example, maximizing the total system throughput or the worst user throughput, subject to QoS constraints from individual users, for example, on data rate, delay, and outage probability [85]. However, in a multi-hop wireless system, the optimal DTPC problem is known to be an NP-hard [109] while the time complexity of the optimal algorithm increases rapidly with the size of the problem, that is, the number of power levels and nodes in the system. Due to the complexity of the DTPC problem, most of the studies in the literature have developed heuristics while optimal algorithms are developed only for restricted cases or for small problems [110]. Many of these efforts have been dedicated to solving Signal-to-Interference plus noise ratio (SIR or SINR) based power optimization problems. The well known distributed constrained DTPC algorithm that maximizes the attained user SIR subject to maximum power constraints is found in [111]. Algorithms that minimize total power consumption in the presence of large-scale fading were found in [112, 113]. Certain algorithms minimize total transmission power consumption over a set of discrete available power levels (e.g., [35]). Still other algorithms seek to minimize the outage probability of the SIR (e.g., [88, 114]).

In [115], Tang, *et al.* examined joint link scheduling and power control with the objective of throughput maximization. The maximum of throughput link scheduling with power control has been formulated as a mixed integer linear programming (MILP) problem so as to furnish optimal solutions. To obtain a good trade-off between throughput and fairness, a new parameter called the demand satisfaction factor (DSF) has been defined and an effective polynomial-time heuristic algorithm developed. Numerical results have demonstrated that the bandwidth can be fairly allocated among all links or flows by solving the MILP formulation or by using the heuristic algorithm. The drawback of this model is that centralised arbiters that allocate bandwidth are assumed; thus the power expended needs to be accounted for. The MILP formulations have also been used by Ramamurthy, *et al.* [116] to study link scheduling

and power control in WMNs with directional antennas. Although the use of directional antennas allows network fairness in bandwidth usage, the heuristic algorithms derived perform optimally only at light traffic loads. This implies that, there can be no performance guarantee at heavy traffic loads.

Based on broadcasting in wireless networks so as to reach several nodes with a single transmission, Montemanni, *et al.* [86, 87, 117-119] investigated a minimum power symmetric connectivity problem in wireless networks. The minimum power broadcast (MPB) problem requires the assignment of transmission powers to the nodes in such a manner that the network is connected and the total power consumption is minimized. To achieve this goal, authors have formulated the problem in terms of a mixed integer programming (MIP) and applied different solution heuristics. In [117, 118], the branch and cut algorithms have been used. In [87], Montemanni, *et al.* have adopted a simulated annealing in order to obtain sub-optimal solutions. In [119], the authors presented a comprehensive review on different solution techniques to the MPB problem in wireless networks. Montemanni performed several comparative simulation tests against the broadcast incremental power (BIP) algorithms [120]. The BIP was based on constructing minimum power broadcast trees by adding new nodes to the tree on a minimum incremental cost basis until all intended destination nodes were included. The simulation results demonstrated that MPB outperformed the BIP algorithms in terms of energy-efficiency. It should be noted that broadcasts result in message duplications and thus network flooding problems.

Numerous studies on Integer Linear Programming (ILP) for power optimization formulations have been conducted by, for example, [5, 79, 88, 95, 114, 116, 121]. Power and rate control outage based on multiple access interference (MAI) and heterogeneous traffic sources have been proposed by [88, 114]. The authors solved the total rate maximization problem by suggesting a base receiver station for all the nodes. They set the SINR outage probability, total transmission power and achievable rate as the model constraints. In order to solve this problem, authors have adopted two power control algorithms: the outer and inner loop power control algorithms. The outer loop power control is responsible for setting the target SINR at the receiver input. The inner loop control compensates for channel variations induced by fast fading phenomena. The inner loop attempts to adjust the powers of each node in order to meet a target level for the SINR. The optimal solution has been obtained using the branch and bound (BB) criteria [110].

From a different perspective, Tadonki and Jose Rolim [95, 122] have solved the dual power management problem in wireless sensor networks (WSN). These authors have

considered a given network scenario with two possible transmission powers (e.g., low and high). They have investigated the problem of finding a minimum size subset of nodes such that if they are assigned high transmission power while the others are assigned low transmission power, then the network will be strongly connected. Simulation results of the exact solutions yielded efficient execution time and solution quality. The approach has assumed, however, that each node possesses only two powers, which is thus a restrictive assumption. In order to formulate scheduling problems using the ILP techniques, Capone and Carello [79] have addressed both power control and rate adaptation. The authors laid down an objective function of minimizing the number of used time slots subject to transmission power constraints as an ILP. They used a column generation approach to solve the minimal power variables. Column generation that computes a lower bound for the problem and the heuristics that compute feasible integer solutions were suggested [121]. Numerical results have shown that such an approach can solve small size instances whereas, for larger difficulties, solving the pricing problem to optimality becomes difficult; therefore the whole approach becomes slow. This method has assumed a centralised arbiter to maintain and distribute time slots across the system and thus minimize overhead costs that exacerbate retransmission problems [123].

In order to achieve power optimization in low SINR channels, Vasudevan, *et al.* [124] have formulated an optimization problem to optimally assign power to nodes in the data-gathering tree for the purpose of maximizing the lifetime of the tree, which is equivalent to the time until network partition, due to battery outage, is reached. In order to solve this problem, they have proposed a *binary search* algorithm for optimal power assignment among nodes, which maximizes the tree lifetime. Using turbo codes as an example of a channel coding technique that compensates for low SINR channels, these authors have demonstrated significant improvements in network lifetimes. However, turbo codes are computationally complex techniques and the aspect of time costs in running a binary search has not been investigated yet.

For a generalized SIR regime, Chiang [84] has presented a distributed power control algorithm that is coupled with existing transmission control protocols (TCPs) in order to increase the end-to-end throughput and energy efficiency of the network. Authors have first formulated a nonlinear constrained utility maximization with “elastic” link capacities [108]. They have subsequently proved the convergence of the coupled algorithm with the global optimum of the joint power control and congestion control, for both synchronised and asynchronous implementations. They have discovered that the rate of convergence is

geometric and that a desirable modularity between the transport and physical layers can be maintained. Both analytic and simulation results have illustrated the robustness of the algorithm to channel-outage and path-loss estimation errors. However, the algorithm swops simplicity of implementation for performance optimality. The authors in [85] have shown that in the high SIR regime, these nonlinear, and apparently difficult, non-convex optimization problems can be transformed into convex optimization problems in the form of geometric programming (GP). In the medium to low SIR regime, some of these constrained nonlinear optimizations of power control cannot be turned into tractable convex formulations, but a heuristic can be used to compute the optimal solution, in most cases, by solving a series of GPs through the approach of successive convex approximations. These techniques for power control, together with their implications to admission control and pricing in wireless networks, are illustrated by several numerical examples. Although the GP method with regards to certain applications, it requires high SIR channels [81]. The use of a convex GP for which an Interior Point Method algorithm can be applied is investigated by [125]. The authors have generalized the problem of joint optimization of transmit power-time and bit energy efficiency by employing convex optimization. The nonlinearity of the problem renders the said problem difficult to solve at reasonably low energy levels.

2.3.1 Summary

In summary, mathematical programming theory (MPT) provides a generalized tool for formulating the DTPC problem. However, feasible optimal solutions may not exist, depending on the dimensions of the problem. Such situations require sub-optimal heuristics. Furthermore, the MPT may not yield reliable solutions in stochastic wireless channels unless robust filters are implemented. Based on its generalization attribute, the MPT will be invoked in this thesis to formulate the DTPC problems, and optimal dynamic control theory will be employed to solve the problems.

2.4 Publications Based on Game Theory

In wireless communication systems, the transmission power of each user (or link) contributes to the interference experienced by the other users [126]. Given that there is a limited battery power available at each node but that each user demands unlimited utility satisfaction, effective and efficient power control strategies ought to be in place [34, 127]. These may be

designed to achieve user oriented quality of service (QoS) or system capacity (network oriented) objectives or both [128]. In order to address the strategic DTPC problems, Srivastava, *et al*. [129] assessed game-theoretic analysis of Ad Hoc networks in terms of power control and waveform adaptation, medium access control (MAC), routing decisions, and node participation. Game theory is the ability to model individual, independent decision makers (IDMs) whose actions potentially affect all other IDMs in the system [34]. Game-theoretic models analyze existing protocols and resource management schemes, and design equilibrium-inducing mechanisms that provide incentives for individual IDMs to behave in socially-constructive ways [130]. Game theory is broadly categorized in terms of cooperative approach to optimization (or team theory) and non-cooperative games [35]. Numerous DTPC publications based on the team theory can be found in, for example, [34, 38, 96, 97, 131, 132] while those examining the non-cooperative game theory are found in, for example, [98, 133]. According to the assessment by Koskie [127], most of the previous contributions have contextualized game theory for mobile nodes. We outline the DTPC based on game theory applicable to the wireless backbone mesh networks (WBMNs).

2.4.1 Team Theory

Goodman and Mandayan [131] proposed a utility-based network assisted power control (NAPC). The power control algorithm was implemented by means of SIR balancing, with the assistance of the network that broadcasts the common SIR target for all users. This means that NAPC requires coordination by the network, which has to inform terminals of the best target SIR for current conditions. The utility levels achieved with NAPC are comparable to those achieved by a non-cooperative power control game with pricing [134]. However, network broadcasts cause network flooding problems [92, 94, 135]. The main drawback is that NAPC requires coordination by the network through broadcasts and thus NAPC lacks fault-resilience.

Jean and Jabbari [132] proposed a game-theoretic delay-sensitive multi-rate power control for CDMA wireless networks with variable path-loss. In order to arrive at this goal, these researchers have applied stochastic game-theory which models the dynamism of the cellular uplink power-control problem. A vector of buffer states is assigned to the nodes and captures the statistics of packet arrivals from higher layers and packet departures via successful transmissions, neither of which is deterministic. Jean and Jabbari then evaluate the stationary Nash equilibrium that is a function of buffer level variation in time (i.e., congestion) and

allows for multi-rate transmission in evolving channel conditions. In both static path-loss and dynamic shadowing path-loss environments, the stochastic game equilibrium calculated compares very favourably to the traditional single-agent and often approaches the performance of centralised optimization. The assignment of buffer states and CDMA codes across the system requires centralized base stations and results in signalling overhead costs [5].

In [96], the authors studied the performance of a distributed and asynchronous power control scheme for a spread spectrum wireless ad hoc network. In this scenario, network users exchange prices that reflect their loss in utility due to perceived interference. The prices are then used to determine optimal (i.e., utility maximizing) power levels for each user. Simulation results have shown that with logarithmic utilities, the pricing algorithm exhibits rapid convergence with the unique optimal power allocation. In another contribution, Huang, *et al.* [97] have considered a distributed power control scheme in a spread spectrum (SS) wireless ad hoc network, in which each user announces a price that reflects the current interference level. These authors have assumed that node users voluntarily cooperate with each other by exchanging interference information. Given these prices, Huang, *et al.* presented an asynchronous distributed algorithm for updating power levels, and provided conditions under which this algorithm converges to an optimal power allocation. This algorithm was then linked to myopic best response updates of a fictitious game. Its convergence was characterized using super-modular game theory [130]. Super-modular games are those characterized by "strategic complementarities": in other words, when one IDM carries out a higher action, the others want to do the same. However, motivations behind voluntary cooperation among nodes have not been properly substantiated.

Altman, *et al.* [38] have considered the situation where N nodes share a common access point. With each node there is an associated buffer and channel state which alters in time. Each node dynamically selects both the power and the admission control to be adapted so as to maximize the expected throughput, which depends on the actions and states of all the nodes, given their power and delay constraints. Using Markov Decision Processes, these authors analysed the single node optimal policies under different model parameters. In [35], an uplink power control problem where each node wishes to maximize its throughput (which depends on the transmission powers of all nodes) but exerts a constraint on the average power consumption, has been investigated. These authors assumed that a finite number of power levels are available to each wireless node; also, that the decision of a node to select a particular power level depends on its channel state. Two cases are considered: that of full

state information and that of local state information. In each case, the authors have proposed both cooperative and non-cooperative power control. However, a cellular radio system has been assumed even in the case of local state information and thus the method does not consider scalable attributes of multi-hop WBMNs [4]. In [136], the transmission power control problem with SINR as the objective function is investigated. This investigation involves two scenarios: selfish and cooperative games. However, the analysis is provided for only two users. Such an approach is too restrictive.

2.4.2 Non Cooperative Game Theory

Koskie and Zapf [128] have demonstrated how the power control problem in wireless networks is formulated as a non-cooperative game in which users choose to trade off between SIR error and transmission power usage, that is, minimizing the SIR error at the cost of high transmission power usage. They have proposed distributed power control strategies based on the use of Newton iterations possessing third-order rather than quadratic convergence. A realistic CDMA cell model has been used to simulate the proposed algorithms. Simulation results indicated that the use of Newton iterations to accelerate the convergence of the static Nash power control algorithm significantly decreased the number of iterations required for convergence. The advantage of the third-order algorithms over the second order ones appeared to eliminate the slight overshoot observed in early iterations. It should be noted that a CDMA cell model requires a centralised arbiter; hence, the procedure with regards to how independent users were assigned codes and with what power level was not discussed by the authors.

In [98], a game-theoretic approach to energy-efficient power control in multicarrier CDMA systems has been proposed. In multi-carrier direct-sequence CDMA (DS-CDMA), the data stream for each user is divided into multiple parallel streams. Each stream is first spread using a spreading sequence and then transmitted on a carrier [137]. Therefore, a multi-carrier CDMA combines the benefits of orthogonal frequency-division multiplexing (OFDM) with those of CDMA for the next-generation high data-rate wireless systems. In order to achieve their goal, Meshkati, *et al.* [98] have formulated the power control problem as a non-cooperative game in which each user decides how much power to transmit over each carrier in order to maximize its own utility. The utility function considered measures the number of reliable bits transmitted over all the carriers per joule of energy consumed. The utility function also reflects the user's preference regarding the SIR and the transmitter power [99].

Meshkati, *et al.* [98] have demonstrated that, for all linear receivers including the matched filter, the de-correlator, and the minimum-mean-square-error detector, a user's utility is maximized when the user transmits only on its "best" carrier. This is the carrier that requires the least amount of power to achieve a particular target signal-to-interference-plus-noise ratio (SINR) at the output of the receiver. Conditions have been described that must be satisfied by the channel gains for a Nash equilibrium to exist. The distribution of users among the carriers at equilibrium was also characterised. An iterative and distributed algorithm for reaching the equilibrium (when it exists) was presented. It has been shown that the proposed approach results in significant improvements in the total utility achieved at equilibrium compared with a single-carrier system as well as a multicarrier system in which each user maximizes its utility over each carrier independently. However, the proposed technique trades-off complexity for optimality; consequently, efficient power consumption is difficult to guarantee.

In [133], a game-theoretic power management in multi-input multi-output (MIMO) Ad Hoc networks has been proposed. The power allocation at each user is built into a non-cooperative game where a utility function is identified and maximized. Owing to poor channel conditions, some users experience very low data transmission rates even though their transmission power is high. Therefore, a mechanism for shutting down link users is proposed in order to reduce co-channel interference and improve energy-efficiency. Compared to multiuser water-filling and gradient projection methods, for example, [98], the proposed game-theoretic approach utilizing the link user shut-down mechanism allows the MIMO ad hoc network to achieve the highest energy and the highest system capacity.

Xing and Chandramouli [99] have proposed a stochastic learning solution for a distributed discrete power control game in wireless data networks. The said researchers first noted that a simple discretization of the continuous transmitter power level does not guarantee convergence and uniqueness. Consequently, they have proposed two probabilistic power adaptation algorithms and analysed their theoretical properties along with the numerical behaviour. The distributed, discrete power control problem has been formulated as an N-node, non-zero sum game by [129]. In this game each user evaluates a power strategy by computing a utility value. This evaluation is performed using a stochastic iterative procedure. These authors [99] have approximated the discrete power control iterations by an equivalent ordinary differential equation and proved that the proposed stochastic learning power control algorithm converges on a stable Nash equilibrium [129]. The drawback is that the convergence times may be too long relative to the packet duration.

Thomas, *et al.* [138] have presented a cognitive network approach to achieve the objectives of power and spectrum management. The authors classified the problem as a two phased non-cooperative game and made use of the properties of potential game theory to ensure the existence of, and convergence to, a desirable Nash Equilibrium. Although this is a multi-objective optimization and the spectrum problem is NP-hard, this selfish cognitive network constructs a topology that minimizes the maximum transmission power while simultaneously using, on average, less than 12% extra spectrum, as compared to the ideal solution. With a related formulation, Closas *et al.* [139] use a non-cooperative game theory to design a fully distributed network topology control algorithm using optimal transmit adjustment. Simulation results have shown that for a relatively low node density, the probability that the proposed algorithm leads to a connected network is close to one.

Huang, *et al.* [140] have proposed two auction mechanisms, the SINR auction and the power auction, that determine relay selection and relay power allocation in a distributed fashion. For a single relay network case, the authors show that the power auction achieves the most efficient allocation by maximizing the total rate increase and that the SINR auction is flexible in trading off fairness and efficiency. For both auctions, the distributed best response bid updates globally converged with the unique Nash Equilibrium in a completely asynchronous manner. The same results were obtained when considering generalised networks with multiple relays. Using a similar approach, Jindal *et al.* [141] considered non-iterative power control algorithms with mutually interfering users and a common target SINR. Each transmitter knows the channel quality of its intended receiver, but has no knowledge of (potential) interference from other transmitters. The said authors have considered fractional power control policies that fall between channel inversion (i.e., full channel compensation, 1/H) and constant transmission power (i.e., no channel compensation, H = 1). They have considered a spatially distributed (decentralised) network, representing either a wireless Ad Hoc network or unlicensed spectrum usage by many nodes (e.g., Wi-Fi or spectrum sharing systems [34]). The disadvantages of iterative power controls are, for example, a feedback channel with the required latency that may not be available or where the convergence times may be too long relative to the packet duration. However, it can be argued that selecting only the fractional or constant transmission power levels is also restrictive.

2.4.3 Summary

In summary, non-cooperative games are quite useful in formulating decentralised DTPC problems but finding the Nash Equilibrium in an error-prone wireless system is NP-hard [38]. Although cooperative approach to optimization (team theory) has been proposed, voluntary actions taken by an IDM in order to favour others, are difficult to motivate in real time [35, 130]. Even the Nash Bargaining Solution (NBS) that achieves a good compromise between fairness and efficiency with a small system dimension guarantees no better performance with an expanded system dimension [34]. Based on the expanded dimension of the link state information (LSI), affecting the optimality of the DTPC, the required feedback latency may not be available at each IDM [33]. Furthermore, the WMRs require collaborative protocols [6]. This thesis will address the topic of a coalition and individual scope objective function formulation offering the benefits of the two types of games. It will exploit dynamic control techniques to solve the problem formulation.

2.5 Publications Based on Dynamic Control Theory

The DTPC is an important means to reduce mutual interference between the users (i.e., by lowering power), while compensating for time-varying propagation conditions (i.e., by raising power) [142]. The transmission powers are controlled using feedback while the feedback results in dynamic behaviour that critically affects the network performance (i.e., throughput and delay) [112]. Methods from control theory have been employed to analyse the dynamic effects and to design appropriate control strategies (e.g., [33]). The basic block diagram for the DTPC problem formulation with interpreted signals is illustrated by Figure 2.2. The DTPC algorithm updates transmission power levels by using quality related measurements from the environment. The output from a wireless radio system (plant) is exacerbated by time-varying external disturbances such as channel states and interference. The DTPC algorithms based on such time-varying random channels for wireless cellular systems have been researched extensively (e.g., [5, 33, 112, 142-144]). The objectives are to achieve the desired quality measures [145, 146].

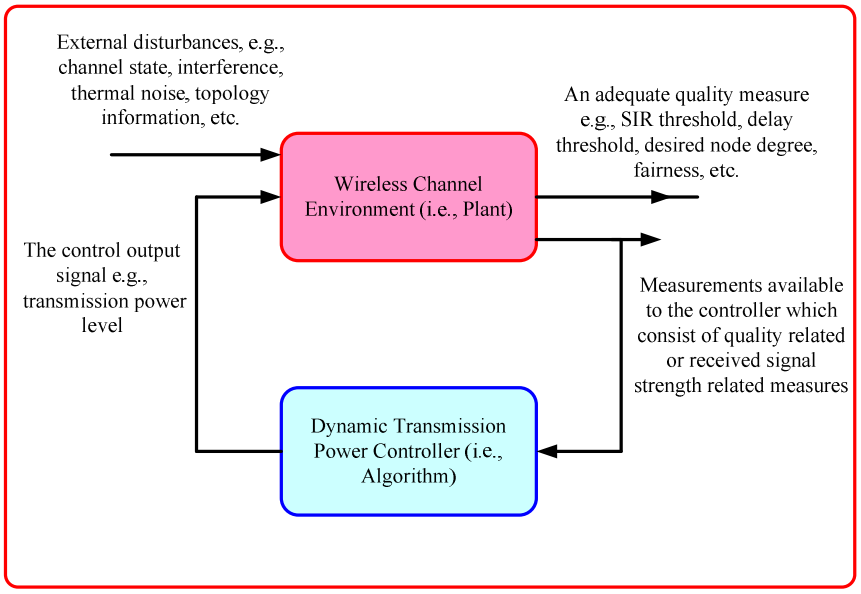

Figure 2.2: The basic block diagram (Adapted from [33])

In [33], Gunnarsson has motivated the need to compute powers locally for each wireless connection. Methods from control theory have been used to analyse existing algorithms locally and to design local controllers with improved performance. On a global level, Gunnarsson has provided results with regards to the stability and convergence of the designed controllers. The results were illustrated by simulations using both small and large-scale simulation environments. However, the algorithms are mainly based on only the SIR measurements by the base station from the connected node. The approach limits its application to single-hop wireless networks whereby hidden terminal problems (HTPs) are not dominant. In [12], both user-centric and network-centric power control objectives were considered. Each user adjusts the transmission power level dynamically based on the network interference and SINR measurements. Both the interference and SINR are predicted before adjusting the transmission power to an optimal level. The robustness of the algorithms was investigated against time-varying and noisy channel conditions. The advantage of adapting the transmission power in this way is that a user can choose to be either greedy or energy efficient. Greedy users tend to increase their transmission power levels so as to maximize their SINR. On the other hand, energy-efficient users tend to lower or possibly power down so as to save their transmission power. The method, however, relies on the base station to assign individual user-CDMA codes. The aggregate interference is estimated due to forward transmissions. In contrast, WBMNs would require bidirectional control signalling whereby aggregate interference takes care of the backward transmission as well [147].

In [148], the researchers provided for a distributed on-line power control of Ad-Hoc networks with user-specific SIR requirements. Their algorithm yields the minimum transmitter powers that satisfy the SIR requirements. The only drawback is that their algorithm requires that the channel gains between nodes in the Ad Hoc networks be constant during the transmission power adaptation. This is reasonable only in the case where the time scale for transmission power adaptation is much faster than the time scale of the channel variability (i.e., stationary users, slowly-varying channels). Yates [149] extended the work by Foschini and Miljanic [148], whereby each user is iteratively assigned to a fixed base station at which its SIR is highest. The aforementioned researchers have developed a general proof of the synchronous and totally asynchronous convergence of predicted power iteration. However, it can be inferred that a centralised receiver base station assigns orthogonal codes to nodes. The centralised controller possesses knowledge of the channel states for all the users in the system [144]. Nonetheless, such a method is too restrictive to apply to decentralised general WBMNs [15].

Holliday, *et al.* [144] discussed the power control problem and its relation to the call admission problem for Ad Hoc networks. They have pointed out that the power control design in wireless networks depends on channel condition dynamics [143]. As a result they have developed an appropriate stochastic approximation power optimality algorithm. This algorithm is modified to track non-stationary equilibrium (i.e., users entering and leaving the system) that performs an admission control. They have also suggested that the iterations of the stochastic approximation algorithms can be decoupled to form fully distributed online power and admission control algorithms for ad hoc wireless networks with time-varying channels. However, the algorithm has been based on the physical layer channel conditions. Algorithms that resolve both rate and power control problems are suggested by Subramanian and Sayed [107]. Formulations are based on a state space model with and without channel condition uncertainties [150, 151]. The algorithms have been found to be robust against SIR measurement uncertainties for single hop channels [112].

In [112, 113], the stochastic dynamic optimization technique has been used to minimize the total combined mobile receiver operating in log-normal fading channels. A similar approach was followed by [152] to adaptively optimize the quantization of the feedback SIR. In the same context, Neely, *et al.* [142] exploited the convex optimization theory in order to study the dynamic power allocation for and routing of time-varying wireless networks. Their main contributions were the formulation of a general power control for such wireless networks, the characterization of the network layer capacity region and the development of

capacity achieving routing and power allocation algorithms. These algorithms hold for systems with general arrival and channel processes and offer delay guarantees at the queuing systems. However, these algorithms required a centralized arbiter and thus not feasible for Ad Hoc networks [153].

Based on the convex formulations, Olama, *et al.* [112] have suggested using a stochastic power control model for time-varying long term fading (TV LTF) wireless networks. The TV LTF captures both space and time variations. The proposed TV LTF is represented by a stochastic differential equation driven by Brownian motion. The Brownian motion allows viewing the wireless channel as a dynamic system solvable by adaptive and non-adaptive estimation techniques. Using similar formulations, Hande *et al.* [154] have solved the joint power control and SIR assignment problem. They resolve the coupled constraint set problem by using a re-parameterization approach and the left Perron Frobenius eigen-vectors. They have developed a distributed algorithm that can achieve any Pareto-optimal SIR assignment, and consequently, a distributed algorithm that picks out a particular Pareto-optimal SIR assignment and the associated powers through utility maximization [5].

Adaptive predictive power control for the uplink channel in DS-CDMA systems has been proposed by [40]. The authors first analysed the conventional closed-loop power control system. The analysis was performed using a prediction technique for estimating the channel-power fading profile. This prediction technique is based on oversampling the power measurements. The proposed scheme performs significantly in terms of minimizing the power-error variance. Characterization of the predictive closed-loop power control algorithms of a reverse link DS-CDMA system can be found in [155]. The main drawback of the Adajani and Sayed [40] predictive algorithm is that base stations are required in order to provide the nodes with future channel states based on the previous and present measurements. This power control algorithm does not scale properly as the network density in a geographical cell increases [153]. Shoarinejad, *et al.* [156] have proposed integrated distributed predictive power control and dynamic channel assignment (DCA). This has been achieved by first deriving a minimum interference DCA algorithm. They then designed Kalman filters in order provide the predicted measurements of both the channel gains and the interference levels. The predicted information is in turn used to update the power levels. The local and global stability of the network have been analysed and extensive computer simulations carried out to demonstrate the improvement in performance, under the dynamics of user arrivals and departures, and base station handoffs. It has been observed that call droppings and call blockings are decreased while, on average, fewer channel reassignments per call are required.

The main drawback is that the approach has been investigated under the centralized FDMA and TDMA schemes. Transmission power levels for distributing such control signalling in real-time has not been outlined [101, 157].

In [32, 102, 158, 159], Leung proposed transmission power control algorithms based on the tracking of the interference power at the receiver by Kalman filter. In [159], link adaptation and power control for streaming services was investigated by Leung, *et al.* In [158], Leung remarked that power control algorithms, proposed earlier for packet-switched time division multiple access (TDMA) wireless networks, do not yield performance gain for short message length and/or moderate control delay [32, 158]. As a consequence, they have introduced an error margin in determining the transmission power obtained from tracking the interference prediction error [158]. This algorithm has been later applied to packet voice service applications [83]. It has been discovered that by introducing such an error margin, SINR performance can be significantly improved even for short messages (i.e., the performance yields little temporal correlation for the interference prediction) and control delay (i.e., that incurred in measuring the interference power and passing the power control information from the receiver to the transmitter). The medium access control allows, at most, one terminal in each sector or cell to send data at any one time. Furthermore, the base station knows which terminal is scheduled to transmit at different times. In general wireless ad hoc networks, random medium contentions are dominant while there is a need to devise power control, taking into account such phenomena.

Koskie and Gajic [62] have generalized the main results on SIR based power control algorithms in wireless radio systems. Their aim was to increase network capacity, extend battery life, and improve quality of service (QoS). Recent approaches solving power distribution problems have exploited Kalman filters, dynamic estimators, and non-cooperative Nash game theory. In this context, Koskie and Gajic [100] have presented optimal SIR-Based power control strategies for wireless CDMA networks. They have designed control algorithms that explicitly consider the trade-off between the cost of transmit power and SIR error. In this case the cost of each node consists of a weighted sum of power, power update, and SIR error. The authors assume that the interference levels do not change significantly from one measurement to the next and are slower than the time-scales of the power updates. Simulation results have demonstrated the superiority of the proposed controller to the power balancing algorithm in minimizing power usage and SIR error.

2.5.1 Summary

In summary, most of the DTPC algorithms studied in literature are predictive in order to reduce the control system delay. Based on the temporal correlation of interference and the SINR, previous works have exploited robust filters to estimate the channel state conditions. However, it has been inferred that base stations assign orthogonal CDMA codes or TDMA slots to mobile nodes in their cell or sector and a possible high transmission power level may be used. In spite of many decentralized control algorithms, most algorithms rely on the physical layer SIR measures for the optimal DTPC. However, according to Kumar and Kawadia [76], the DTPC algorithms are affected by a number of link state information (LSI) across the network protocol stack. We can argue that these LSIs, too, do have temporal correlations and thus can be modelled using state space techniques solvable by predictive approaches. If the overall WBMN is considered to comprise a large number of interconnected distributed control loops, then methods from control theory may be used to assess the stability and dynamic behaviour of the network. The rationale lies in the need to improve throughput, energy-efficiency, fault-tolerant connectivity, and node coexistence.

2.6 Power Controlled Network Protocol Heuristics

Figure 2.3 illustrates a single transmission from node A to node B in a co-channel environment with other nodes of the network. Table 2.1 provides the motivation behind such illustrations. If node A chooses a minimum power level (i) then significant power saving and better spatial re-use may be achieved, but hidden terminal problems (HTPs) around node B may aggravate the network throughput. If node A uses a power level (ii) then not much power saving and network fairness can be achieved. On the other hand, if node A chooses a maximum power level (iii), then all HTPs are resolved but spectrum re-use and energy consumption are inefficient and thus may aggravate network throughput (capacity) even further. Therefore, if node A uses a "proper" power level (iv) then a fair trade-off between power and network capacity may be attained. Allocating the transmission power level dynamically on a per-packet basis requires the cross-layering information [76]. This area has been widely studied for the general wireless Mobile Ad Hoc and Sensor Networks but research has missed the specialized attributes of the WBMNs. This section outlines studies relevant to the WBMN context and highlights the open issues addressed in the present study.

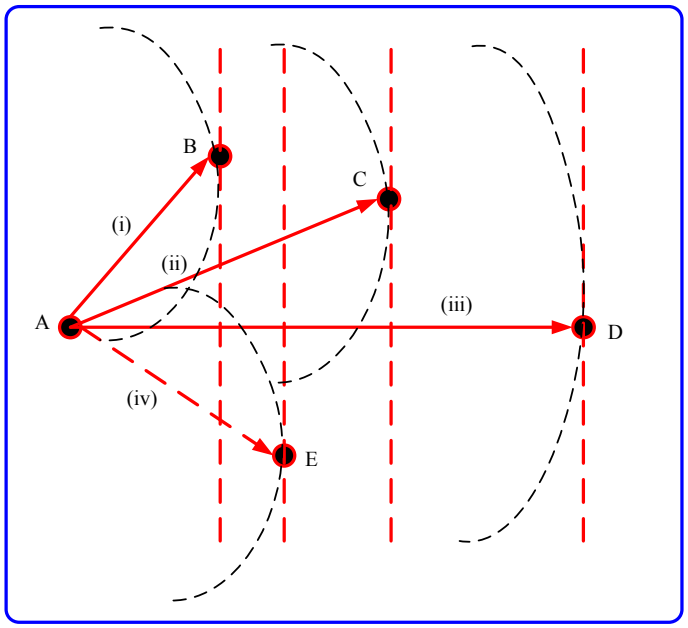

Figure 2.3: Motivating DTPC (node A to node B) for single channel networks

Table 2.1: Summary of TPC Motivation

Action	Advantages	Disadvantages
(i) A-B at minimum power	Save power and better spatial re-use	Maximum HTPs e.g., contention and collisions and aggravated network throughput
(ii) A-C at some power > min power	Some power saving, some fairness, some spatial reuse	
(iii) A-D at maximum power	Interference avoidance i.e., suppressed HTPs	Poor spatial reuse, inefficient power use and bandwidth unfairness
(iv) A-E at properly controlled power	Optimal saving, optimal network capacity and optimal fairness	

2.6.1 Publications Based on Omni Directional-MAC Protocol

The role of the medium access control (MAC) protocol is to modify the transceiver parameters (e.g., transmission power levels and antenna beams) or radio resources (e.g., channels) or the topology of a network. At MAC level the aim is to reduce energy consumption, improve throughput or both. Our focus in this review falls on how the MAC protocol adjusts the transmission power level dynamically for every packet transmitted. This section covers only central contributions in this area relevant to the static WBMNs.

2.6.1.1 Common Channel Based

In [42], Cheng, *et al.* have reviewed the distributed MAC protocols in terms of the objectives and methodology as applied to the resource allocation problems in the WMNs. Research

carried out on varying the transmission power level on a per-packet basis in Ad Hoc networks has been thoroughly conducted by [4, 17]. In the conventional way, maximum transmission power level is used for request-to-send (RTS) and clear-to-send (CTS) packets while the minimum required transmission power is used for data and acknowledgement (DATA-ACK) packets in order to save energy [4, 92]. However, RTS-CTS packet exchanges reserve a large floor space for DATA-ACK conversations, thereby degrading the spatial reuse by other network users. In order to eliminate hidden terminal problems (HTPs), [17, 160] have introduced a power controlled MAC (PCM) protocol. In PCM, RTS-CTS packets are transmitted at maximum power and data is periodically also transmitted at maximum power; the data is otherwise sent at optimal power to conserve energy. The periodic maximum power for data transmissions enable nodes in the sender's carrier sense zone to stay suppressed throughout the sender's transmission. This asymmetric transmission power results in unfairness of medium access among users [161]. In fact, transmission power control increases the number of hidden terminals in the network and exacerbates the unfairness of the medium access for less powerful links in the network. The SHUSH technique proposed by Sheth and Han [162] tackles the unfairness problem among the low and high transmission power nodes. The SHUSH technique suggests a reactive transmission power control for wireless MAC protocols. SHUSH is grafted into the reactive strategy of SHUSHing the interferer [163]. Only after interference occurs do the nodes react by identifying the source of interference via the header fields in the interfering packets. Nodes initiate the control packets at optimal power needed to reach and SHUSH the interferer. The DATA-ACK packets are exchanged, also at optimal transmission powers. Autonomous power adjustment for RTS-CTS packets in addition to that of the DATA-ACK packets has been well studied by Chen, *et al.* [160].

Muqattash and Krunz [18] have proposed POWMAC: a single-channel power-control protocol for throughput enhancement in wireless Ad Hoc networks [164-166]. Instead of alternating between the transmission of control (i.e., RTS-CTS) and data packets, as done in the 802.11 scheme [4, 164], POWMAC uses an access window (AW) to allow for a series of RTS-CTS exchanges to take place before several concurrent data packet transmissions can commence. The length of the AW is dynamically adjusted, based on localized information, to allow for multiple interference-limited concurrent transmissions to take place in the same vicinity of a receiving terminal. Simulation results have demonstrated that significant throughput and energy gains are obtainable with POWMAC protocol. However, it is difficult to implement synchronization between nodes during the access window (AW). POWMAC does not solve the interference problem either. Siam and Krunz [166] have enhanced the

throughput and energy performance of the POWMAC and the IEEE 802.11 standard protocols. They have integrated multi-input multi-output (MIMO) capabilities into these protocols and noted that the MIMO systems double the bit rate per link over the single-input single-output (SISO) systems (i.e., use of single antenna). Throughput gains in the MIMO systems are observed at a non-negligible energy cost. However, MIMO systems are not energy efficient techniques.

Ding, *et al.* [167] have proposed a per-frame-based transmission power control protocol, DEMAC in IEEE 802.11 at a low PHY rate. The aim is to avoid network interference, improve throughput and save energy. In DEMAC, the transmit power of RTS is used to find the interference in the network. The receiver calculates the optimal transmit power for the data frame based on the data payload and the current interference. CTS, DATA and ACK would then be transmitted with this optimal transmit power. Although DEMAC avoids network interference at both the sender and receiver side, yields a good throughput and is energy saving, it does not take into account a high PHY rate. The DEMAC employs maximum power with RTS packets and thus evidences poor spatial re-use. Jia, *et al.* [44] have improved on the work by Ding, *et al.* [167] by proposing a scheme that carefully combines collision avoidance and spatial re-use for IEEE 802.11 MAC protocols. Simulation results indicated that up to 40% throughput increase and 3 times more data delivery could be achieved with the same amount of energy under single-channel, single-transceiver design conditions. Although the authors have provided a theoretical analysis in order to justify the scheme and simulation results, interference avoidance and fairness was assumed only at the receiver side. Li, *et al.* [168] proposed an adaptive transmission power control protocol (ATPMAC) which can enable several concurrent transmissions without interfering with each other while incurring minimal signalling overhead costs. Considering the single channel and single transceiver nodes Ad Hoc networks, ATPMAC has shown up to 136% throughput improvement compared to the IEEE 802.11 in a random topology. The method, however, does not take into account interference effects at the sender's side [169].

In order to allow fairness, Ho and Liew [170, 171] have proposed and investigated two distributed adaptive power control algorithms that minimize mutual interference among links while avoiding the hidden nodes [172, 173]. Hidden nodes cause unfair bandwidth distributions and bandwidth oscillations [173]. The two algorithms adapt the transmission power of each transmitter link to the positions of its surrounding links in addition to the connectivity requirements with its receiver link. The algorithms demand that links that do not mutually interfere with one another remain non-interfering while existing interfering links

can be made non-interfering after the adjustment of transmission power. Also, no new hidden nodes will be created [173]. By means of extensive experiments, the authors observed that the proposed algorithms achieve a good balance between the scalability of the network capacity (which is related to the exposed node) and fairness (which is related to the hidden node) in wireless networks [174].

In [63], Correia, *et al.* performed experiments on two dynamic transmission power adjustments in MAC protocols for wireless sensor networks (WSNs). The first approach employs dynamic power adjustments by exchanging information among nodes, and the second one calculates the ideal transmission power according to signal attenuation in the link. Both methods used a clear channel assessment (CCA) mechanism (i.e., one that does not exploit channel reservation, e.g., RTS-CTS messages). Nodes periodically sample the signal strength if there are ongoing transmissions in order to determine the maximum noise level (base noise). If the sampled signal strength is higher than the base noise, then the protocol detects ongoing transmission and the transmission power is dynamically and accordingly adjusted by the node [175]. The CCA mechanism has the advantage of mitigating collisions over the reservation based schemes. In another paper, Correia, *et al.* [176] extensively discussed the benefits of the transmission power control MAC protocols, examined the issues in the implementation of such protocols and summarized the results of their first evaluation using existing hardware [89].

In [145], the authors established an effective transmission power control mechanism by understanding the dynamics between link qualities and the received signal strength indicator and link quality indicator (RSSI/LQI) values. They presented empirical results that demonstrate the relationship between the link layer quality and RSSI/LQI. It was observed that the irregularity of radio channel results in radio signal strength variation in different directions, while the signal strength at any point within the radio transmission range displays a detectable correlation with transmission power in a short time period. A similar empirical experiment was studied by Jeong, *et al.* [177]. They based their work on previous studies and evaluated power control algorithms using realistic multi-hop WSN workloads as well as a large Mica2dot based test-bed. The experimental results indicated that the dynamic power control MAC protocol with low duty cycles yields up to 16% more power saving than the fixed power controlled counterparts. The said authors also furnished an empirical and mathematical analysis of micro-solar power systems for WSNs [178]. The WSNs typically possess some fixed central servers in order to aggregate the sensed traffic which is thus not fully distributed.

2.6.1.2 Separate Channels Based

From a different perspective, Dongsheng, *et al.* [91] have emphasized the need to combine both power control (i.e., to reduce energy consumption and increase spatial re-use) and least interference channel assignment (i.e., to reduce collisions and improve fairness) and to combine both the MAC layer and the network layer (i.e., to guarantee network connectivity and eliminate frequent topology changes). This research has been triggered by the fact that the control of transmission power by the use of minimum power not only reduces energy consumption but also brings about more collisions and frequent changes in topology [179]. In order to solve such problems, the authors have proposed a protocol with the following features: independent channels are used to transfer data packets to reduce collisions in data transmissions, control packets are transferred at maximum power and data packets are transferred at proper power in order to reduce energy consumption, guarantee network connectivity and eliminate frequent topology changes. However, the use of maximum power to eliminate HTPs in turn aggravates the spatial re-use and thus poor network capacity.

In order to reduce collisions further, [5, 33, 180] combined the carrier sense multiple access (CSMA) with a spread spectrum-code division multiple access (SS-CDMA) which does not require the central controller [5]. The various authors observed that through the use of local coordination only, packet collisions were completely avoidable by employing the hybrid MAC protocol and power control. A better trade-off between bandwidth usage and latency could also be noted compared to IEEE 802.11 MAC [4]. The authors have assumed a decentralized SS-CDMA but have not further investigated how codes are spread across the network as well as the transmission power cost.

It has been well argued that minimizing the transmit power (i.e., to eliminate exposed node problems (ENPs)) not only improves spectral re-use and reduces energy consumption but also introduces HTPs [42]. In order to eliminate HTPs, Lai, *et al.* [181] presented a power control interference avoidance (IA) scheme. They demonstrated a proper way to adjust the transmission power of the control packets and data packets in such a manner that large interference range problems are resolved and low energy is consumed compared to IEEE 802.11. This is achieved by first dividing the channel into separate control and data channels. The RTS, CTS and ACK packets are sent in control channels while DATA packets are sent in data channels. The RTS and DATA packets are subsequently sent by means of a smaller transmission power (i.e., a tenth of the maximum power) and CTS and ACK packets are sent

by means of a larger power (i.e., the maximum power) in order to suppress the interferers within the vicinity of the receiver [182]. However, they did not estimate the interference within the vicinity of the transmitter during control signalling exchanges [147].

In order to utilize the radio spectrum efficiently and resolve potential contention among nodes using the medium, a dynamic channel assignment with power controlled (DCA-PC) MAC protocol is proposed [183]. The overall bandwidth is divided into one control channel and several data/application channels. The purpose of the control channel is to assign data channels to hosts and to resolve the potential contention while using data channels. Data channels each for one host are used to transmit data packets and acknowledgements. Each host is equipped with two half-duplex transceivers. The control transceiver operates on the control channel to exchange control packets with other hosts and to obtain rights to access data channels. The data transceiver dynamically switches to one of the data channels to transmit data packets and acknowledgements. The data channels are used with proper power control while control channel are used with maximum power level. The added benefits are that while a multi-channel provides an improved network performance as the number of the nodes causing contention and collision increases, the transmission power control provides spatial re-use and minimizes energy consumption. If a node is empowered to access multiple channels such as in CDMA technology, then a node can utilize multiple codes simultaneously or dynamically switch from one code to another as needed. In this way, the authors achieved the channel assignment, multiple access and power control solutions in an integrated framework [184-187]. It should however, be noted that assigning channels, estimating cross-layer states and performing the DTPC may cause system delay problems. Multi-radio configurations have been designed to resolve delay problems of this kind [41]. However, not many studies exist in the literature with regards to the multi-radio DTPC problems in statically assigned channels [21].

2.6.1.3 Summary

In summary, the above power-controlled MAC protocols assume that nodes have equal reception sensitivity and radiate equal power in all directions. The argument behind this assumption is that if any node can cause interference at a receiver then it will most likely hear the CTS from that receiver and defer from transmitting. However, when directional antennas are used, the radiated power and reception sensitivity between any two nodes become a function of the angular orientation of these nodes. Thus, using omni-directional power for

RTS-CTS and data packets, even at different levels, can no longer prevent all potential interferers from transmitting [188]. However, when directional antennas are employed without invoking proper power control, typical MAC protocols for the IEEE 802.11 Ad Hoc mode may face several medium access problems. For example, interference from minor lobes and HTPs may cause medium access unfairness [189]. Hence, this thesis addresses the issue of accessing and forwarding traffic simultaneously while maintaining bandwidth fairness by means of power controlled multiple channel MAC protocols.

2.6.2 Publications Based on Directional MAC Protocol

The use of directional antennas offers the numerous benefits of a wireless Ad Hoc network, that is, extended communication range, better spatial reuse, capacity improvement, and suppressed interference [188]. While numerous studies exist in this regard, the focus falls on the WBMNs.

Capone and Martignon [78, 190] have argued that while adaptive antennas may improve the utilization of the wireless medium (i.e., increased network capacity) by reducing radio interference and the impact of the exposed node problem, they can exacerbate the HTP [90]. Consequently, information about the reservation of the wireless medium needs to be distributed to the maximum possible extent without interfering with the connections already established in the network. In order to achieve an improved total traffic which is accepted by the network (i.e., capacity) and fairness between competing connections, Capone and Martignon [78] proposed a scheme in which RTS-CTS frames are sent in all antenna sectors at the maximum allowed power that does not cause interference with the ongoing transmissions. The DATA-ACK packets' exchange then takes place directionally with the minimum necessary power. Instead of using maximum power for control traffic, one should employ power efficient antenna radiation gain.

Arora, *et al.* [188] suggested a power-controlled MAC protocol for directional antennas that ameliorates HTPs and improves energy-saving [90]. The protocol used separates control and data channels to reduce collisions. This allows for the dynamic adjustment of data-packet transmission power to such a degree that this power is just enough to overcome interference at the receiver. In [90], Arora and Krunz proposed a load control access protocol (LCAP) that allows transmissions to take place along already reserved directions, provided that the SINR at the receiving nodes remains above the predefined SINR. The proposed LCAP manages throughput and energy trade-off in a power-controlled (interference-limited) wireless

communications with directional antennas. The LCAPs are categorized into two types; interference-based LCAP and the overall throughput based LCAP. In the former, when a new user is to be admitted, the service provider estimates the expected total interference due to the addition of this new user. The increase in the interference depends on the user's quality of service (QoS) requirements (bit rate, required bit-error-rate, etc.). The new user is admitted only if the total expected interference is below a predefined threshold. In the latter case, the prospective user is not admitted if the total normalized throughput following the admission is expected to exceed a predefined threshold. The simulation results have demonstrated that the combined gain from concurrent transmissions using directional antennas and power control provides a good trade-off between network throughput and energy consumption.

In [191], Alawieh, *et al.* analysed the benefits of transmission power control on throughput and energy consumption in Ad Hoc networks with directional antennas. The researchers first constructed an interference model for such antennas based on the honey grid model in order to calculate the maximum interference [192]. Subsequently, they developed a collision avoidance model [181]. The authors also presented the maximum end-to-end throughput under the maximum interference constraints. It was noted that selecting a smaller carrier sense threshold (i.e., interference range) will severely impact on the spatial re-use whereas a larger carrier sense threshold will yield excessive interference among concurrent transmissions [16]. Hence, a need exists for an appropriate selection of the carrier sense threshold so that power control can reduce collisions significantly.

2.6.2.1 Summary

In summary, the use of directional antennas and performing power control allows improved throughput and energy-saving since they possess a higher gain than their equivalent omni-directional counterparts. However, frequent beam switching to specific target receivers may turn out to be energy-inefficient [192]. To access and route traffic simultaneously, sectored antennas driven by power controlled dual-band radios or soft-ware defined radios might be desirable [52, 57, 192].

2.6.3 Publications Based on Power Management

In order to sustain a longer lifetime for wireless networks on limited energy resources, two major approaches have been proposed: transmission power control and sleep schedules. While transmission power control reduces the radio power consumption in the transmission

state, the sleep scheduling reduces the radio power consumption in the idle state by turning off radios when not in use. Hence, the integration of the two is often referred to as power management [193]. A detailed taxonomy of power management protocols for wireless networks have been provided by Zheng, *et al.* [194]. Numerous DTPC contributions exist in this context for mobile Ad Hoc and WSNs. We outline works that are relevant to the attributes of WBMNs.

Jamieson, *et al.* [195] have proposed a power-saving technique for multi-hop Ad Hoc wireless networks called Span. Span has been based on the observation that when a region of a wireless Ad Hoc network contains a sufficient density of nodes, only a small number of them need to be switched on at any time in order to forward and coordinate traffic for active connections. Experimental design has proved that the system lifetime of a Span 802.11 network is a factor of two better than a Standard 802.11 network. Span yields an improved latency and competitive bandwidth. Xu, *et al.* [196] presented two topology control protocols that extend the lifetime of dense Ad Hoc networks while preserving connectivity, the ability for nodes to reach each other. The methods conserve energy by identifying redundant nodes and turning their radios off. The first method is that of Geographical Adaptive Fidelity (GAF), which identifies redundant nodes by their physical location and a conservative estimate of their radio range. The other method is cluster-based energy conservation, which directly observes radio connectivity in order to determine redundancy and therefore can be more aggressive regarding radio fading. Analysis, simulation and experimental tests have demonstrated that both protocols are robust with regards to node failures, radio propagation and node deployment density. However, since these proposals have focussed on the network operations and neighbour discovery, Hsu and Hurson [197] applied probabilistic wake-up based power management to neighbour monitoring which aims to reduce energy consumption while preserving the effectiveness of misbehaving node detection.

An asynchronous power save protocol has been discussed in depth by [198]. In this protocol, neighbours that wish to communicate, estimate their relative phase difference between their sleep and wake cycles. A station then uses this phase information to transmit its pending packets over the available periods most efficiently. The advantage is that stations can adjust their phase relationships to avoid contention and reduce latency for delay sensitive flows. In a recent study Feeney, *et al.* [199] investigated the impact of wakeup schedule distribution in asynchronous power saving protocols regarding the performance of multi-hop wireless networks. The asynchronous wakeup schedules create an uncoordinated pattern of times at which nodes will attempt to transmit. Simulation data indicated that the capacity

associated with the best wake-up patterns is significantly larger than that of the worst ones. The result gives an insight into the behaviour of such protocols and serves as a feasibility study indicating the potential benefit of mechanisms by which nodes adapt their wake-up schedules in order to obtain improved performance.

Instead of placing inactive components into low power states using a single dynamic power management (DPM) policy, Dhiman and Rosing [200] suggested making a selection among a set of DPM policies using a machine learning algorithm. This algorithm adapts to changes in workloads and guarantees quick convergence with the best performing policy for each work load. In a similar spirit, unified power management architecture (UPMA) for supporting radio power management in WSNs is furnished [201, 202]. The UPMA provides a set of standard interfaces that allow different sleep scheduling policies to be easily implemented on top of various MAC protocols at the data link layer and an architectural framework for composing multiple power management policies into a coherent strategy based on application needs. A minimum power configuration that minimizes the aggregate radio power consumption of all radio states has been suggested by Xing, *et al.* [203]. However, in both Klues, *et al.* [202] and Xing, *et al.* [203], the transmission power choices and the sleep scheduling decisions of nodes are coordinated according to the current network workload. The UPMA enables cross-layer coordination and the joint optimization of different power management strategies that exist at multiple network layers while allowing them to carry out independent implementations [204].

Zheng and Kravets [205] have proposed an on-demand power management framework for multi-hop wireless networks. In this framework, power management decisions are driven by data transmission in the network. Nodes maintain soft-state timers that determine power management transitions. By monitoring routing control messages and data transmissions, these timers are set and refreshed on demand. Only nodes on the communication path along which a connection is routed are kept active while all the other nodes can switch to the power-save mode. The benefit achieved is that soft states are aggregated across multiple flows and the system's maintenance requires no additional out-of-band messages. However, no incentive has been given to keep some nodes active while others sleep. Motivated by the observation that explicit and periodic re-computation of the backbone topology [196] is costly with respect to its additional bandwidth overhead, a probabilistic power management framework been constructed by Li and Li [206]. They believe that any schemes involving periodic and local broadcasts of messages do not scale well as the number of node densities increases. Since each node needs to broadcast a message during each broadcasting interval, as

the number of nodes increases, such broadcasts will eventually saturate the residual capacity of the network, thereby causing collisions and disruptions to the ongoing data traffic. The contributions of the probabilistic (odds) approach guarantee network scalability, uninterrupted ongoing traffic, network parameter flexibility and compatibility with IEEE 802.11 MAC layer standard. However, Odds suffers from heavyweight computations, a prime consumer of the network energy. Odds has not proved whether or not an optimal transmission power is used for selected active nodes.

Zhang, *et al.* [207] have proposed a time-division multiple-access (TDMA) based multi-channel MAC protocol called TMMAC in order to save power for Ad Hoc networks. TMMAC requires only a single half-duplex radio transceiver on each node. In addition to explicit frequency negotiation, TMMAC introduces a lightweight explicit time negotiation in order to exploit the advantage of both multiple channels and TDMA so as to set inactive nodes to doze mode. The simulation evaluation has shown 113% higher communication throughput and 74% less per packet energy over the state-of-the-art multi-channel MAC protocols for single transceiver wireless devices. The drawback of TMMAC is that time negotiations are difficult to distribute across the network without incurring bandwidth overheads. While single half-duplex radio transceiver operations are energy-efficient, such configurations coupled with multiple channels require sophisticated switching and thus exacerbate delay [208].

Wang, *et al.* [208] considered the joint design of opportunistic spectrum access (i.e., channel assignment) and adaptive power management for multi-radio multi-channel wireless local area networks (WLANs). Their motivation has been the need to improve throughput, delay performance and energy efficiency [209]. In order to meet their objective, they have suggested a power-saving multi-channel MAC (PSM-MMAC) protocol which is capable of reducing the collision probability and the wake state of a node. The design of the PSM-MMAC relied on the estimation of the number of active links, queue lengths and channel conditions during the ad hoc traffic indication message (ATIM) window [4, 210]. From numerous simulation results, a good trade-off was observed for throughput, delay performance and energy-efficiency compared to the previous approaches [210, 211].

2.6.3.1 Summary

In summary, power control by alternating the dormant state and transmission state of a transceiver is an effective means to reduce the power consumption significantly. However,

most previous studies have emphasized that wake-up and sleep schedule information are distributed across the network. The overhead costs associated with this have not yet been thoroughly investigated. Furthermore, transmission powers for active connections have not been optimally guaranteed. This thesis will consequently investigate the problem of energy-inefficient DTPC whereby nodes whose queue loads and battery power levels are below predefined thresholds are allowed to doze or otherwise participate voluntarily in the network.

2.6.4 Publications Based on Connectivity Management

In order to attain desirable network connectivity attributes, minimal average node degree (e.g., [212, 213]), fault tolerant connectivity (e.g., [214, 215]) and spanner network structure (e.g., [216-218]), topology control algorithms (TCAs) using optimal transmission power adjustment (TCATPA) have been studied (e.g., [22, 27-30, 213]). The topology of a multi-hop wireless network refers to the set of communication links between node pairs used explicitly or implicitly by a routing mechanism. The WBMN topology is affected by many factors: weather conditions, medium obstacles, interference, channel noise, battery power outage, the power levels and antenna radiation directions [179]. Our interest is to adjust the transmission power level of each node dynamically based on the desired connectivity attributes. In Figure 2.4, a connection from node A to node B with transmission power levels (i), (ii), (iii), and (iv) may result in a dis-connected, a fully connected, a critically connected and a 'properly' connected network, respectively. Table 2.2 furnishes a summary of the advantages and disadvantages of choosing various transmission power levels (i.e., homogenous ranges). The heterogeneous network is a generic model of this homogenous scenario.

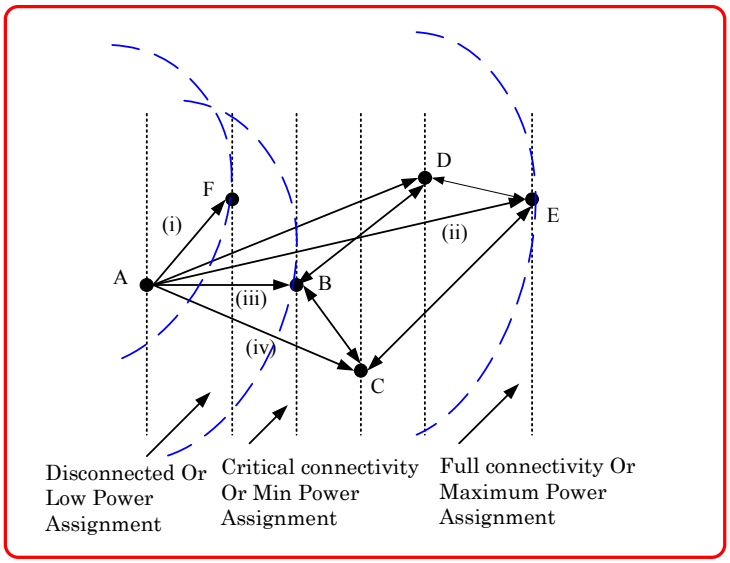

Figure 2.4: Connectivity range adjustment for node A to node B: homogenous case

Table 2.2: Summary of Topology Control Based DTPC Motivation

Action	Advantages	Disadvantages
(i) A-F, Low connectivity range	Significant power saving and enhanced multi-hop routing (fault-tolerance).	Node A and B are disconnected directly by one hop and routing delays may occur.
(ii) A-E, Maximum connectivity range	Fully connected network and user-specific quality of service (QoS) improvement e.g., reduced user latency.	Very high energy consumption and thus short network life, very high node A degree e.g., F, B, C, D and F, and increased congestion to other nodes.
(iii) A-B, Critical connectivity	Power saving and some network capacity improvement.	Critical resilience to topology changes, dominant unfairness from hidden nodes.
(iv) A-C, properly adjusted connectivity range	Minimum average node A degree e.g., F, B and C, enhanced multi-hop, high spatial re-use and improved network capacity.	Fair energy loss and suppression to immediate neighbours, thus introducing bandwidth unfairness

Numerous studies on the DTPC based on the TCA for distributed wireless networks have been conducted (e.g., [22, 27-30, 213, 219]. In [213], the authors studied the problem of adjusting transmit powers of nodes to create a desired network topology. They formulated the transmit power adjustment problem as a constrained optimization problem. In this case, the connectivity and bi-connectivity were taken as constraints and the maximum power used as an optimization objective. They suggested the so called Connected MinMax Power (CMP) and Biconnectivity Augmentation with MinMax Power (BAMP) problems. These problems assumed a given multi-hop wireless network, $M = (N, L)$, where N is a set of nodes in the entire network and $L: N \to (Z_0^+, Z_0^+)$ is a set of coordinates on the plane denoting the location of the nodes. Specifically, the CMP problem finds a per-node minimal transmit power assignment $p: N \to Z^+$, such that the induced graph of (M, λ, p) is connected, and

$Max_{u\in N}(p_u)$ is minimum. The induced graph is represented as: $G=(V,E)$, where V is a set of vertices corresponding to nodes in N, and E is a set of undirected edges such that $(u,v)\in E$ if and only if $p_u \geq \lambda(d(u,v))$, and $p_v \geq \lambda(d(u,v))$. The BAMP problem attempts to find a per-node minimal set of power increases $\delta(u)$ in such a manner that the induced graph of $(M,\lambda,p_u+\delta(u))$ is bi-connected, and $Max_{u\in N}(p_u+\delta(u))$ is minimum. In order to solve these problems, the authors proposed two centralized algorithms for static networks and two distributed heuristics for mobile networks. The aforementioned work [193] minimized the *maximum* transmission power rather than the *total* power to maintain system scalability.

Authors in [215, 220] have suggested a transmission power adjustment scheme related to the approach by Ramanathan and Rosales [213]. They have shown that each node makes local decisions concerning its transmission power which collectively guarantee global connectivity. Specifically, a node receiving directional information increases its transmission power gradually until it finds a neighbour node in every direction. Simulation results have indicated that with low transmission power adjustment and low node degree attainment, the network lifetime is increased and traffic interference is reduced [221]. Tan and Seah [221] have proposed the critical neighbour (CN) scheme, which adaptively adjusts the transmission power of individual nodes according to route and traffic demands in order to reduce the level of interference amongst nodes in the network. Simulation results have indicated that the CN scheme records higher throughput and lower end-to-end delays than the unmodified version.

Li, *et al.* [219] studied the strong minimum power restricted topology control problem in wireless sensor nodes in order to adjust the limited transmission power for each wireless node and to find a power assignment that reserves the strong connectivity and achieves minimum energy cost in the wireless nodes. Simulation results have demonstrated their efficiency.

Calinescu, *et al.* [222] have reported analytical power assignment problems. Calinescu, *et al.* [223] calculated approximation algorithms for the Min-Power Symmetric Connectivity, Min-Power Strong Connectivity and Min-Power Broadcast. They also considered a special treatment for the important case of Power Symmetric Connectivity in the Euclidean norm with node-dependent transmission efficiency. In [222], they analysed the assignment and concluded that adjusting transmission power can present strong network connectivity.

The authors in [218, 224] generalized the work in [213, 215]. They addressed the problem of finding the minimum power assignment of each individual node in such a way that the

undirected *induced* communication graph represents a *spanner* of the communication graph when all nodes transmit at their *maximum* power. The term, induced undirected communication graph, is defined by an edge uv if and only if $p_{uv} \le p_u$ and $p_{uv} \le p_v$ with p_u and p_v as power settings for node u and v, respectively. However, if all wireless nodes transmit with their *maximum* power $p_{\max}$ then the *induced* communication graph is called the *original* communication graph, or simply a unit disk graph (UDG). It should be noted that at maximum power, each node may possess information about all possible network topologies. The term, a *spanner,* means that the length of the shortest path in the induced communication graph at most represents some constant multiplied by the length of the shortest path in the original communication graph. However, the minimum power assignment does not always guarantee the minimum average node degree in spite of a strongly connected network [218].

The authors in [218] developed a polynomial time algorithm that minimizes the maximum assigned power. They also presented a polynomial time approximation method to minimize the total transmission radius of all nodes. The algorithm and approximation are based on two heuristics. Simulation studies were conducted to verify their efficacies. However, the minimization of the *total* transmission radii implies that each node possesses global knowledge of the network at the expense of communication overheads. The approach holds little practical value since battery power-life is localized. An energy-efficient extension to the work by [218] has been found in [217]. Khan, *et al*. [217] and Choi, *et al.* [225] presented a distributed construction of the minimum spanning tree (MST) problem. This problem was formulated as a geometric weighted MST problem:, that is, given an arbitrary set N of nodes in a plane, find a tree T spanning N such that $\sum_{(u,v)\in T} d^{\alpha}(u,v)$ is minimized, where $d(u,v)$ is the distance of an edge, $(u,v)\in T$ according to the Euclidean norm and $\alpha=[2,4)$ depicts environments with multiple-path interference or local noise. Khan, *et al*. identified that in Kruskal's algorithmic construction [216], the MST which minimizes $\sum_{(u,v)\in T} d(u,v)$ also minimizes $\sum_{(u,v)\in T} d^{\alpha}(u,v)$ for any $\alpha>0$. In order to solve the distributed MST problem, they developed the so called *Nearest Neighbour Tree* (NNT) algorithms with low energy complexity. The NNT operates on the idea that each node independently chooses a unique *rank,* a quantity from a totally ordered set, and this node connects to the *nearest* node of higher rank. This precludes overhead cycles with the edges

already chosen. The only information that needs to be exchanged is the rank. However, the procedure on how to evaluate the set of ranks has not been furnished.

Gerharz, *et al.* [214, 226] introduced a simple distributed algorithm that assigns individual transmission powers to wireless devices. The authors proposed a cooperative nearest neighbour topology (CNNT) control strategy. Each device is assigned the lowest transmission power that connects it to the *k*-nearest "neighbours". Node *A* is the neighbour of a node *B* if and only if there is a bidirectional link between *A* and *B*. Through simulations, the topologies created by the CNNT algorithm without any global knowledge are as effective as the topologies resulting from the best choice of a common transmission power (which would require global knowledge) in terms of the achievable throughput. The CNNT was thus an improvement of NNT. However, common transmission power adjustment does not only cause excessive message overheads across the network but also assumes prior to this the network nodes are uniformly distributed.

Li and Hou [206] proposed two localized topology control algorithms for general wireless networks with each node possessing different maximal transmission power. The two algorithms are: the Directed Relative Neighbourhood Graph (DRNG) and the Directed Local Spanning Sub-graph (DLSS). In both algorithms, each node independently creates its neighbour set by adjusting the transmission power and defines the network topology by using only local information. These authors have proved that both the DRNG and the DLSS can preserve network connectivity, the out-degree of any node in the resulting topology generated by the DRNG or DLSS is bounded by a constant and the DRNG and the DLSS can preserve network bi-directionality.

Aron, *et al.* [29] considered the problem of topology control for hybrid wireless mesh networks (WMNs) with heterogeneous transmission ranges. A localized distributed topology control algorithm was developed which calculates the optimal transmission power so that network connectivity is maintained, node transmission power is reduced to cover only the nearest neighbours and network lifetime is extended. These goals have been confirmed by means of numerous simulation tests. However, mobile mesh clients have not been considered in spite of investigations of the hybrid mesh architecture. In other works, Aron, *et al.* [27, 28, 30] proposed the local minimum shortest-path tree (LM-SPT) and/or the local neighbourhood shortest-path tree (LN-SPT) algorithms suited for WBMNs. The algorithms are distributed with each node using only the information gathered locally in order to determine its own transmission power. The implementation takes place in two phases. The first phase is to construct a minimum local or neighbourhood shortest-path tree. The other phase is to

gradually remove all unidirectional links. The researchers performed several simulation tests and noted that the resultant network topology preserved the network connectivity, reduced the average node degree, ensured evenly distributed power consumption among the nodes and significantly reduced the total power consumption leading to a longer network lifetime [196].

In a similar framework to that of the work in [225], Bhatia, *et al.* [212] investigated a power balancing problem in energy constrained multi-hop wireless networks. The objective is to minimize the maximum average power used by the nodes in such a way that no node uses more power than the others. The authors have formulated the problem of two power assignments under the constraint that the network connectivity is maintained. However, such a problem has been shown to be an NP-hard and also hard to approximate [215]. Because establishing the maximum average power is not feasible with a fully decentralized algorithm, the distributed localized heuristics proposed to solve this problem have demonstrated that the algorithm can reduce the average power significantly when compared with algorithms that assign a common power [214]. However, excessive message overhead costs across the network remained un-resolved by [212].

Li, *et al.* [227] proposed a distributed mechanism to build a sparse power efficient network topology for non-uniform Ad Hoc wireless networks. In order to achieve their goal, they first extended the Yao structure [228] in order to build a spanner with a constant length and power stretch factor for the mutual inclusion graph. They then suggested two efficient localized algorithms to construct connected sparse network topologies. They discovered that both algorithms incur communication costs $O(n)$, where each message contains $O(\log n)$ bits. The proposed structure requires the use of maximum power in a sparse topology; hence it is an energy-inefficient technique.

2.6.4.1 Summary

It is worthwhile to conclude that a decentralized power adjustment is useful in topology control problems, which are graph-theoretic problems [179]. Optimal graph-theoretic methods, however, assume a global optimisation space, otherwise, they are often NP-hard problems [215]. An optimal assignment of power by each node requires information across the network and thus incurs overhead costs [213]. Furthermore, the unit disk graphs (UDGs) employed in the solution assume a 2-D plane or flat earth surface problem [179]. However,

the earth's surface is composed of topographical obstructions [146]. Many applications to structuring monitoring and underwater networks present a 3-D plane power control problem [229]. The topology control based power control algorithms over-rely on the position of neighbour nodes in order to preserve the connectivity, maximum node degree, conserve energy and minimize interference. However, locations are complicated by several spatial factors [146]. In order to meet most of the stringent requirements for control of topology, our thesis considers localized range predictions in order to adjust transmission power level dynamically.

2.6.5 Publications Based on Joint Cross-layer Resource Management

In their seminal paper, Kawadia and Kumar [76] remarked that power control in wireless networks is a cross-layer design problem. This occurs because the transmission power level affects signal quality and thus influences the physical layer, determines the neighbouring nodes that can hear the packet and consequently impacts on the network layer, affects interference which causes medium access issues and congestion, thus affects the medium access control (MAC) and transport layers. Furthermore, power control aims at desirable throughput, delay and energy consumption performance [80, 89]. Some of the power control jointly performed with cross-layer protocols will be reviewed in this section.

Wang, *et al.* [50] proposed a joint scheduling and power control algorithm, supporting multicasting traffic in multi-hop wireless Ad Hoc networks. Multicasting enables data delivery to multiple recipients in a more efficient manner than traditional unicasting and broadcasting. A packet is duplicated only when the delivery path toward the traffic destinations diverges at the node, thus helping to reduce unnecessary transmissions (overheads). The algorithm performed an optimal power control based on the Yates Algorithm [149] and subsequently connections are scheduled when no optimal transmission power solution exists. In other words, scheduling determines which connections should not be allowed so that the connections admitted can enjoy a sufficiently high SINR.

Muqattash, *et al.* [164, 165] proposed a power controlled dual channel (PCDC) protocol that emphasizes the interplay between the MAC and network layers. They explained that the MAC layer indirectly influences the selection of the next-hop by properly adjusting the power of *route request* packets while maintaining network connectivity. Channel gain information obtained mainly from overhead RTS and CTS packets is used to dynamically construct the network topology. They argued that unlike the IEEE 802.11 approach whereby

RTS-CTS packets are used to silence the neighbouring nodes, collision avoidance information (CAI) can be inserted into the CTS packets and sent over an out of band control channel. The CAI is used dynamically to bound the transmission power of potentially interfering nodes in the vicinity of a receiver [18]. Compared to the IEEE 802.11 approach, the proposed protocol achieved a significant increase in the channel utilization and end-to-end network throughput, and a significant decrease in the total energy consumption. On a similar course, the authors contributed towards developing a joint rate and power control with modulation adaptation [125, 230].

Li and Wu [14, 231] studied the power control and dynamic channel allocation for delay sensitive applications in wireless networks. In [14], they investigated QoS-driven power allocation for the downlink of multi-channel, multi-user wireless networks. They subsequently proposed schemes based on multi-user and frequency diversities. Performance evaluations have indicated that such schemes guarantee the QoS requirements compared to those which do not use multi-user diversity and power control. However, this model approach confines it to base-station based wireless cellular networks; hence the applications are limited [153]. A two phase distributed scheduling algorithm to identify a subset of wireless users whose QoS is guaranteed is found in [232]. In the first phase, each link transmits with a probing power and each user determines whether it can be a member of the basic feasible set or not in a distributed manner. In the second phase, a generalized call admission algorithm that attempts to merge as many of the remaining links as possible into the basic feasible set is developed. By means of simulations, the said researchers evaluated the performance of the proposed scheme in terms of average execution time, average packet delay and the maximum of the cycle time.

Narayanaswamy, *et al.* [77] studied the theory, architecture, algorithm and implementation of the COMPOW protocol in wireless Ad Hoc networks. The COMPOW power control protocol for each node selects a common power level, sets this power level to the lowest value which keeps the network connected and maintains the energy consumption close to the minimum. It possesses the property of ensuring the bi-directionality of links due to the reciprocity of electromagnetic waves in space. They noted that the COMPOW protocol simultaneously satisfies the three objectives of maximizing the traffic carrying capacity of the entire network, extending the battery life by providing low power routes, and reducing the contention at the MAC layer. The COMPOW protocol reveals the drawback that all links need to be symmetrical and all nodes must be homogenously distributed. This implies that even a single outlying node can cause every node to use a high power level. An improvement

to the COMPOW protocol was investigated by Bergamo, *et al*. [233]. In Bergamo, *et al.* [233], each node estimates the power necessary to reach its own neighbours so as to yield the energy efficiency required while performing routing algorithms. However, disseminating routing information across the network incurs overhead costs. This fact was not even considered by the said authors.

In order to solve the power control problem for nodes with heterogeneous distribution, Kawadia and Kumar [93] proposed a protocol called CLUSTERPOW. In clustered networks, the CLUSTERPOW protocol allows nodes to use a power level which depends on the destination of the packet so as to maximize spatial re-use and hence network capacity. In particular, every node forwards a packet to a destination d using the smallest power level p such that the destination d is reachable, possibly in multiple hops, using only p. In Kawadia and Kumar [76], the authors have generalized the solution proposed by [93]. They discussed the COMPOW, CLUSTERPOW, MINPOW and LOADPOW power control protocols. In this case, the MINPOW attempts to optimize the total energy consumption globally [222, 223]. In order to achieve this goal, they have presented an architecturally clean implementation of the MINPOW in Linux without assuming any physical layer support. Instead, estimates of link costs are performed using control packets at the network layer. In order to maximize network capacity by increasing spatial re-use, a power control adaptive to the traffic load, called LOADPOW, is introduced. The LOADPOW protocol opportunistically uses a higher transmit power level whenever the network load is low, and lowers the transmit power as the load increases. These authors furnished details of the implementation of these protocols in wireless IEEE 802.11 cards, and the test-bed experimentation using several topology scenarios, and also discussed their performance. Although running routing daemons at each power level has demonstrated no loop cycles, such iterative computations coupled with table maintenance could eventually increase route computation delay.

Park and Sivakumar [234, 235] argued that the use of minimum transmission range and hence the MINPOW protocol might not always result in an optimal throughput. Using throughput and throughput per unit energy optimization criteria, they demonstrated that the optimal transmission power is generally a function of the number of stations, the network size, and the traffic load. As a result, they defined analytical throughput in terms of spatial reuse, hop count and contention time. They substantiated their arguments by means of a comprehensive set of simulation results in both typical and atypical network configurations in terms of number of stations and network density.

Power-aware routing in wireless networks that addresses the inherent conflict between energy efficient communication and the need to achieve desired QoS such as end-to-end communication delay has been thoroughly investigated [94, 236, 237]. For instance, Chipara, *et al.* suggested a real-time power-aware routing (RPAR) protocol that dynamically adapts transmission power and route packets based on packet deadlines. The RPAR possesses salient features, including improving the number of packets meeting their deadlines at low energy cost and using an efficient neighbour manager that quickly discovers forward choices (pairs of a neighbour and a transmission power level) that meet packet deadlines while introducing low communication and energy overheads. However, it is difficult to acquire an eligible neighbour manager that meets the stringent velocity requirements. Simulations based on MICA2 motes have shown that RPAR reduces miss ratio and energy consumption [194].

Gomez and Campbell [238] studied the impact of individual variable-range transmission power control on the physical and network connectivity, network capacity and power savings of wireless multi-hop networks. They demonstrated that the average traffic carrying capacity of nodes suggested by Gupta and Kumar [239] remains constant even when nodes are added to the network. They have also shown that the ratio between the minimum transmission range levels obtained using a common-range and a variable-range based routing protocol is approximately one to two. They also derived a model that approximates the signalling overhead of a routing protocol as a function of the transmission range and topology dynamics for both route discovery and route maintenance. They concluded that routing protocols based on common-range transmission power limit the capacity available to nodes [240]. In spite of the desirable features, the use of variable range may result in medium access unfairness whereby the lower range nodes are suppressed by the higher range ones.

In Li, *et al.* [241], a multi-rate power controlled MAC protocol, called MRPC-MAC, to enable fairness and a multi-rate power controlled routing called MRPC-Routing, to determine the next hop immediately before transmitting packets at the MAC layer, was proposed. The MRPC-MAC and Routing use the effective transport capacity as the routing metric so that short links with high bandwidth are preferred and more concurrent transmissions can be enabled. Although spatial re-use and network throughput could significantly be improved, these authors have not shown how the protocol performs in the case of all short links with low bandwidth.

The problem of joint power control, scheduling and routing in multi-hop wireless networks has received much attention (e.g., [57, 231, 242-246]). The chief motivation has been the need to reduce energy consumption of individual nodes and the overall network

without severely degrading network throughput (i.e., capacity). In connection with this, Hengster [244] exploited two multi-hop routing protocols. One such protocol determines packet routes according to a shortest-path criterion and aims to minimize the total transmission power. The other selects routes that minimize the cumulative energy consumption within the network (i.e., both links and nodes). The algorithm developed jointly performs link scheduling and power control in order to minimize packet delays and transmission powers. However, wireless sensor nodes (WSNs) are assumed that transmit application information to, or receive control information from, a central node. This is not feasible for Ad Hoc type WBMNs.

In cases where the exact end-to-end traffic matrix is unknown, Kashyap, *et al.* [245] proposed algorithms that compute a two-phase routing, schedule and power assignment. Their goal was to minimize the total transmission power in the network over all traffic matrices in a given polytope. They proved the algorithms to be 3-approximations with respect to an optimal algorithm. The drawback is that although the scheme does not require the network to detect changes in the traffic distribution, the limits imposed by the ingress-egress nodes on capacity bounds need to be known across each node in the network. However, an overhead-efficient means to do this has not yet been investigated.

Cruz and Santhanam [242] studied the problem of joint routing, link scheduling and power control to support high data rates for broadband wireless multi-hop networks. They applied the convex optimization problem whereby link scheduling and power control policies are optimized, subject to given constraints (i.e., the minimum average data rate per link and peak transmission power constraints per node). They discovered the sensitivity of the minimal total average power with respect to the average data rate for each link. They noted that shortest path algorithms with link weights set to the link sensitivities can be used to guide the search for optimum routing globally. In this case, it can be determined that optimal allocations do not necessarily route traffic over minimum energy paths. With single channel wireless mesh networks in mind, Gupta [243] designed a joint mechanism that conducts routing in parallel with the scheduling by calculating routes over links that fit completely into the current schedule. The power control algorithm for both these schemes utilizes the minimum power level needed for communication. Nonetheless, the algorithm does not necessarily produce optimal power values.

In Yuan, *et al.* [81], a joint optimization of multicast routing and power control for WMNs have been suggested. The aim is to maximize multicast throughput by proposing a cross-layer optimization model and solving the optimal throughput problem in an efficient and

distributed manner. They discussed the geometric programming method and game-theoretic approach in order to solve the transmission power control problem. Their contribution was to strike a balance between the demand of link bandwidth at the network layer and the supply of link capacity at the physical layer. Although multicast routing ensures reaching multiple receivers in a single transmission, the algorithms proposed demanded information exchange by broadcasting messages. Broadcasting introduces network flooding even if it is localized, and consequently exacerbates the cross-layer optimization problems.

Xi and Yeh [246] proposed optimal distributed power control, routing and congestion control in wireless networks. They assumed a multi-commodity flow model in which power and routing variables are chosen to minimize convex link costs reflecting an average queuing delay. Distributed network algorithms performing joint power control and routing on a node-by-node basis have been established. The benefit of their work is that congestion control can seamlessly be incorporated to optimize the user input rates [84].

Xi and Yeh [123] devised a spectrum allocation scheme that divides the whole spectrum into multiple sub-channels and activates conflict-free links on each sub-band. They then proposed a simple distributed and asynchronous algorithm to feasibly activate links on the sub-bands. For the active links on each sub-band, they developed an optimal power control, traffic routes' and user input rates' algorithms based on the channel states and traffic demands. They proved that under specific conditions the algorithms asymptotically converge to optimal operating points. However, this convergence performance has been subjected to specified conditions and thus may not hold for general conditions [149].

2.6.5.1 Summary

In summary, joint cross-layer resource optimization involves allocations of transmit power level, MAC layer schedules, links, input rates, routes and delay constraints [123, 246]. The benefits are energy-management, throughput improvement and connectivity preservation. However, many cross-layer optimizations from the physical layer to application layer lack proper modularity and scalability [15]. Complex models are presented and sub-optimal solutions are obtained [80]. In order to ensure modularity and scalability, this thesis considers new DTPC protocols at the Link-Layer. The protocol utilizes the information on SINR, MAI, and connectivity range and transmission rate to adjust transmission power level optimally.

2.7 Chapter conclusions and Remarks

The DTPC problems for the wireless networks have been extensively addressed in the literature. The motivations can be outlined as follows: firstly, in order to compensate for the effects of time-varying random wireless channels and thus high SINR; secondly, in order to minimize energy consumption and thus elongate network lifetime; thirdly, in order to reduce MAC problems such as exposed terminal nodes (ETNs), hidden terminal nodes (HTNs), collisions and contentions and spectrum sharing fairness and thus maximize spatial re-use (network capacity); fourthly, in order to improve connectivity attributes such as minimal average node degree and stable or fault-tolerant network connectivity and thus energy-efficient routing; fifthly, in order to minimize congestion and thus optimal end-to-end network throughput and latency. These objectives have been formulated as an optimization problem which tries to strike a balance between minimal use of power at a node and maximal network throughput gain. The attributes of the DTPC optimality are emphasized as follows. The power level should be high enough to avoid interference from the HTPs but no higher, so that it will not create unnecessary contention or collision among nodes in a shared channel. Furthermore, the power level should be low enough to save energy but no lower than this, or it will create a disconnected network. Finally, the transmission power adjustment should be fast enough to eliminate queue delays but no faster so that it will not create queue singular perturbations among multiple radios. Optimal solutions have been conducted based on a number of conceptual frames: mathematical programming, game theory, dynamic control theory and cross-layering protocol heuristics. Nonetheless there are still a number of open issues worth considering for network capacity enhancement in the WBMNs.

- In order to address both forward and backward power controlled message exchanges, the LSI measurements should include both the sides: the transmitter and the receiver.
- In order to effectively address multiple LSI based optimal DTPC algorithms, the LSI should comprise: the SIR deviation, aggregate interference, connectivity range deviation, and link rate deviation. The LSI can then be viewed as state space models.
- In order to address protocol modularity, scalability and delay across multiple layers, the DTPC algorithm should be implemented at the Link-Layer (LL) of the stack.
- In order for the WBMN to perform as mesh client access and backbone traffic routers simultaneously, each WMR should be built from low cost dual or multiple radios. To

coordinate these multi-radio operations, an energy-efficient unification protocol should be developed at the LL.

- In order to ameliorate singular perturbations between power and packet dynamics at the queues, the DTPC protocol should be developed to manage such system instability.

The above open issues have been investigated in Chapters 3, 4 and 5. The DTPC problem has been formulated using mathematical programming, solved using dynamic control theory and managed by the LL protocol. To the best of our knowledge these issues have never been investigated in the past.

Chapter 3

Single Channel Network: MATA Scheme

3.1 Introduction

This chapter presents a multiple access transmission aware (MATA) dynamic transmission power control (DTPC) scheme for single channel wireless backbone mesh networks (WBMNs). This scheme is based on recently proposed DTPC schemes, developed at the physical layer with regards to the wireless cellular context [12, 35]. Instead, this study addresses power controlled MAC scalability issues affecting the capacity performance for the WBMN. WBMNs are composed of static wireless mesh routers (WMRs) that access and route the huge traffic generated by wireless mesh clients (WMCs). WBMNs particularly those operating in energy-constrained environments do face DTPC problems. These problems include accelerated energy depletion due to the long operation time required, multiple access co-channel interference (MACI) due to co-located nodes, poor quality of the received signal owing to adverse channel environment and energy-inefficient cross-layer information exchanges. These problems affect the level of the power and will be modelled in terms of the MATA states in this study.

In order to solve such problems, two decentralized DTPC schemes have been developed. These schemes are based on the awareness of multiple access transmissions occurring in the same frequency channel simultaneously. To realize this, first, a medium access control (MAC) dependent transmission scheduling probability (TSP) model is furnished. This model is simply referred to as the MAC-TSP based DTPC model. It entails a scalable interaction between the physical and MAC layer information exchanges for transmission power control. Second, a generalized cross-layer occupation measure (GCOM) model, which is an extension of the MAC-TSP model, is introduced. The GCOM model involves the general cross-layer information exchanges for transmission power control and energy-efficiency. For each model, a convex cost function is proposed. This function has been formulated as a minimization problem of a user centric (i.e., measured in terms of the quality of the received

signal) and a network centric (i.e., measured in terms of MACI) objectives. The cost function is constrained by the locally available LL information.

Extensive analytical and simulation results that confirm the efficacy of MATA-DTPC models to WBMNs are furnished. Key contributions are two-fold: firstly, a generalized DTPC model independent of specific medium access scheme and of specific WMN technology; secondly, a scalable convex cost function formulation with both user and network centric objectives.

The basic block diagram of the proposed MATA-DTPC model for WBMN is depicted in Figure 3.1. The fundamental concept is that each wireless link (user) gathers neighbourhood bidirectional information, that is, at the sender and receiver sides. Such information is processed as MATA estimates, which are driven to stable conditions by iterating transmission power signals. If the power control system output metric mismatches the desired metric performance, then a feedback loop is initiated. Otherwise, the control system becomes stable and optimal power signals are attained.

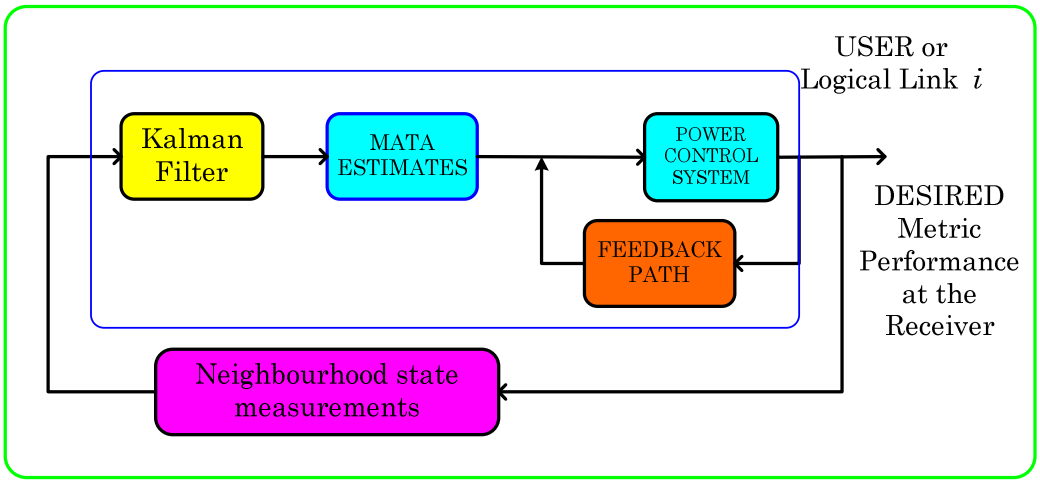

Figure 3.1: Basic block diagram of MATA-DTPC in WBMNs

Tables 3.1 and 3.2 summarize the definitions of common abbreviations and notations used in the rest of this chapter.

Table 3.1: Abbreviation

Abbreviation	*Description*
BLVN	A set of nodes forming Bi-directional Logical Visible Neighbourhood
CCA	Clear Channel Assessment
GCOM	Generalized Cross-Layer Occupation Measure
MAC	Medium Access Control

MACI	Multiple Access Co-Channel Interference
MATA	Multiple Access Transmission Awareness
OCG	Optimal Transmission Power Controller Gain
TSP	Transmission Scheduling Probability

Table 3.2: Notation

Notation	*Description*
$\mathbf{p}$	Transmission Power Vector
$q_{-i}(k)$	Instantaneous MACI against node i's transmission at time k
$\beta_i^r(k)$	Instantaneous Signal-to-Noise Ratio (SINR) between transmitter i and receiver r
$\mathbf{x}_k$	MATA State Vector at Instant time k
$\mathbf{y}_k$	MATA measurement vector at time k
$J_{e\in E}(k)$	User and Network-centric cost function
$\alpha_{e\in E}$	Transmission Power Controller Gain
ω_i	Weight for the cost function
ρ_i	Transmission Scheduling Probability (TSP)
$\rho_i^{u_i}$	Generalized Cross-Layer Occupation Measure (GCOM probability).

3.2 MATA Model Description

3.2.1 Fundamentals

Let N stationary wireless mesh nodes (WMN) be randomly distributed in a space S of a single frequency channel. Suppose each node is assumed to be equipped with an omni-directional transmitter of a carrier sensing range (CSR) at least twice as large as the transmission range (TR) [17]. Nodes are generally assumed to be heterogeneous with different CSRs and TRs [238]. This assumption is reasonable when taking into account that different wireless mesh network (WMN) technologies can co-exist in the same area. Consider a multi-hop network whereby nodes *voluntarily* cooperate to relay each others' messages [22]. Multi-hop communication provides short multiple ranges between source nodes and destination nodes located beyond the sender's transmission range [213].

Let the wireless network be defined by a graph $G=(V,E)$, where V is the set of static nodes and $E\subseteq V^2$ is the set of pairs of devices between which communication is possible via a direct link. It should be noted that the heterogeneity with TRs and the multiple paths

channel fading conditions guarantee that the sets E and V^2 are not necessarily equal [247]. However, we will assume that node failures due to energy depletion are more common than link failures due to environmental dynamics as no mobility is taken into account [247]. Therefore, the distance between devices i and r is denoted as $d(i,r)$ and the power setting which i and r must use to communicate to each other is denoted as $p(i,r)$. Each node is faced with the problem of an undirected minimum power *k*-vertex connected sub-graph [22]. This is necessary in order to ensure bi-directional communication among decentralized nodes with the least possible transmission power consumption [248]. According to [22], a *k*-vertex connected graph has *k* vertex-disjoint paths between every pair of vertices such that even when *k-1* vertices are removed, the network still remains connected. In order to have a *k*-fault tolerant topology, the localized topology control based transmit power adjustment has been given [22, 27-30]. Based on these algorithms, MATA-DTPC assumes the following topology definitions:

Definition 3.1: *accessible neighbourhood set: the accessible neighbourhood set A_i^N is defined as the set of all nodes that forms a direct link with node i when node i transmits at maximum power. The set is*

$$A_i^N = \{ r \in V \mid d(i,r) \le R(i) \}.$$

Here, $R(i)$ is the TR when node i transmits with maximum power.

Definition 3.2: *relay region: the relay region of the transmit-relay node pair $(i,r) \in A_i^N$ is the physical region $RL_{i \to r} \subseteq A_i^N$ such that relaying through the physical location, $Loc(r)$ to any other point $j \in A_i^N$ would consume less power than direct transmission to that point. That is,*

$$p(i,r) + p(r,j) \le p(i,j).$$

Definition 3.3: *logical neighbourhood set: the set is denoted as NS_i^L and a node $r \in NS_i^L$ if and only if there exists an edge (i,r) in a given generated topology. The set is*

$NS_i^L = \{ r \in V \mid i \to r \}$.

Definition 3.4: *bi-directionality: an undirected graph $G' = (V', E')$ generated by a topology control algorithm is bidirectional if $V' = V$, $E' = \{ (i,r) \mid (i,r) \in E(G') \text{ and } (r,i) \in E(G') \}$.*

Definition 3.5: *power cost of an undirected graph $G' = (V', E')$: the power cost with edge costs $p(i,r)$, is defined as*

$$P(G') = \sum_{i \in V'} \max_{\{ r | (i,r) \in E' \}} p(i,r).$$

Definition 3.6: *normal cost of a graph* $G' = (V', E')$ *with edge costs* $p(i,r)$ *is defined as*

$$C(G') = \sum_{(i,r) \in E'} p(i,r).$$

Definition 3.7: *an undirected minimum power k-vertex connected sub-graph (k-UPVCS) of a graph* $G' = (V', E')$ *is a k-vertex connected sub-graph* $H = (V', L)$, $L \subseteq E$ *such that* $P(H) \leq P(H')$ *for any k-vertex connected sub-graph* $H' = (V', L')$, $L' \subseteq E$ *[22].*

Definition 3.7: *an undirected minimum cost k-vertex connected sub-graph (k-UCVCS) of a graph* $G' = (V', E')$ *is a k-vertex connected sub-graph* $H = (V', L)$, $L \subseteq E$, *such that* $C(H) \leq C(H')$ *for any k-vertex connected sub-graph* $H' = (V', L')$, $L' \subseteq E$ *[22].*

3.2.2 The Neighbour Discovery Algorithm

It is to be noted that MATA-DTPC requires each transmitting node to initially identify (or discover) its *active* neighbours before performing power optimization. This is to eliminate interference levels and increase the data rate. The energy-efficient neighbourhood topology discovery procedure is outlined by Algorithm 3.1 as follows:

Algorithm 3.1: bidirectional logical visible neighbour (BLVN) set

Input: $G=(V,E)$

Output: BLVN

Step 1: **initialize:** $A_i^N \subseteq G(V,E)=\varnothing$, $NotNbr=\varnothing$, $LVN(i)=\varnothing$, $BLVN(i)=\varnothing$;

Step 2: Node i broadcasts its identity (ID) "Hello" message with transmission power, $p_i=p_i^{\max}$;

Step 3: Node i receives ACK messages and record location IDs of its neighbours in the set A_i^N.

Step 4: **for** each $r,j\in A_i^N$ and $r\neq j$ **do**

Step 5: **compute:** $d(i,r)$, $p(i,r)$ and $p(i,j)$.

Step 6: **if** $Loc(r)\in RL_{i\to j}$ && $p(i,j)+p(j,r)\le p(i,r)$ **then**

Step 7: **add:** $NotNbr=NotNbr\cup\{r\}$, **else if**

Step 8: $Loc(j)\in RL_{i\to r}$ && $p(i,r)+p(r,j)\le p(i,j)$ **then**

Step 9: **add:** $NotNbr=NotNbr\cup\{j\}$;

Step 10: **remove** non neighbours: $LVN(i)=A_i^N\setminus NotNbr$; *//logical visible neighbour of node* i *//*

Step 11: **if** directed edge $i\to r$ and $i\notin LVN(r)$ **then**

Step 12: **add:** $LVN(r)=LVN(r)\cup\{r\to i\}$, **for** each $r\to i\in LVN(i)$ **do**;

Step 13: **add:** $LVN(r)=LVN(r)\cup\{i\}$, **for** each $i\in LVN(r)$ **do**;

Step 14: **set:** $BLVN(i)=LVN(r)$, $\forall i,r\in V$; *//bidirectional logical visible neighbourhood//*

The resulting BLVN topology set is constructed geometrically as demonstrated by Figure 3.2.

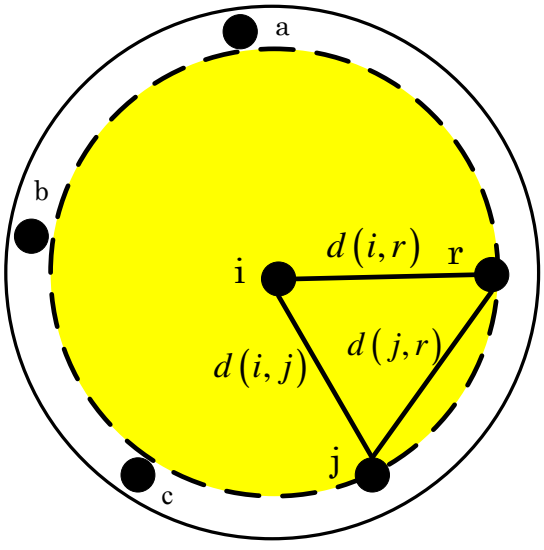

Figure 3.2: Bi-directional Logical Visible Neighbour, $BLVN(i)=\{r,j\}$:

In Figure 3.2, the set of accessible neighbours of node i on full transmission power is denoted as: $A_i^N = \{a,b,c,j,r\}$. A set which is not a logical visible neighbour of i (NotNbr) is denoted as: $NotNbr(i) = \{a,b,c\}$. If $Loc(r)$ satisfies $p(i,j) + p(j,r) \le p(i,r)$, then $LVN(i) = A_i^N \setminus \{r\}$. If $Loc(j)$ satisfies $p(i,r) + p(r,j) \le p(i,j)$, then $LVN(i) = A_i^N \setminus \{j\}$. The $BLVN(i) = LVN(r) = LVN(i)$ of the triangle vertices i, r and j.

3.2.3 Motivation

In the context of MATA models, one seeks to estimate the bidirectional (i.e.., undirected) channel gains, multiple access co-channel interference (MACI) and the localized topology information in a given BLVN set. The transmission power is then dynamically allocated given such MATA information or estimates. This is the so called MATA based DTPC scheme in this thesis. Any sender intending to transmit data first periodically probes the channel conditions, MACI and network topology; this is referred to as a clear channel assessment (CCA) [249]. The CCA is needed during the transmission power adjustment [45]. Several benefits of CCA can be noted: firstly, the CCA for the conditions of the physical (PHY) and medium access control (MAC) layers can improve the quality of service (QoS) at the receivers [17]. Secondly, the utilization of CCA information for power optimization before exchanging actual data/application packets reduces the probability of traffic drops in bad channels. At the LL, dropped packets are adaptively retransmitted. This incurs significant power consumption and excessive network delays [185]. Thirdly, the knowledge of the local topology conditions for transmission power optimization results in fault-tolerant route decisions for multiple hop communications [147]. Therefore, CCA information is first modelled as a MAC transmission scheduling probability (MAC-TSP) and then generalized as a cross-layer occupation measure (GCOM). The MAC-TSP and GCOM both form MATA models. The MATA-DTPC approach carries the advantage of being independent of specific medium access scheme (e.g., TDMA, CSMA, FDMA, CDMA, etc.) and specific WMN technology (e.g., IEEE 802.11, IEEE 802.15, IEEE 802.16, etc.). Finally, Figure 3.3 illustrates the need for a MATA based DPC scheme in single channel wireless networks.

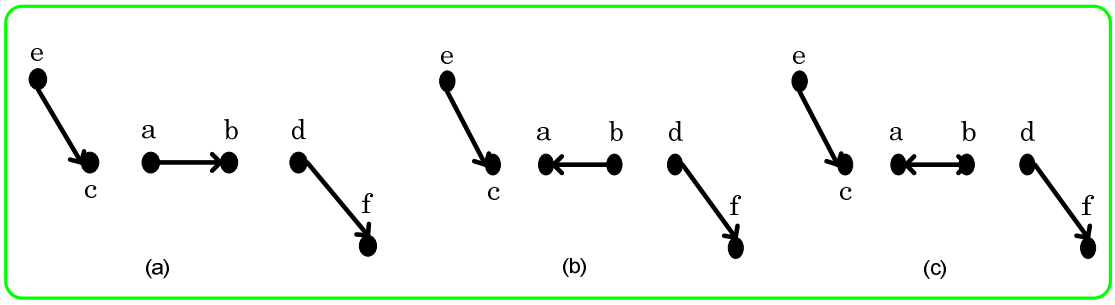

Figure 3.3: Motivating MATA Scheme:

In Figure 3.3a, node n_a transmits to node n_b with probe power $p(a,b)$. At the same *k*th time instant node n_e transmits to node n_c and node n_d transmits to node n_f all transmissions are on the same channel. Powers, $p(e,c)$ and $p(d,f)$ are any values within the maximum power limits. Node n_c is exposed by an omni-directional radiation if distance, $d(a,b) \geq d(a,c)$. Collisions occur at n_c due to exposed terminal problem (ETP). Node n_f receiving from n_d is hidden from link (a,b) transmissions if $p(a,b) \leq p(a,f)$. Transmissions from n_d to n_f cause collisions at n_b due to n_d hidden from n_a (i.e., Hidden terminal problem (HTP)). Figure 3.3b: shows the backward transmissions of the link (a,b) irrespective of the links (e,c) and (d,f) directions. The backward transmissions relay exchanged information to the power controller at the sender end. Figure 3.3c: depicts the bidirectional communication necessary for scalable information gathering.

3.3 MATA State Estimation

3.3.1 Stochastic State Space Model

Using the probe power level, each transmitter-receiver pair i (or user) gathers variable state information such as channel gain, $G_{ii}(k)$, perceived multiple access interference power plus additive white Gaussian noise, $I_i(k)$, received signal to interference plus noise ratio (SINR or SIR), $\beta_i(k)$, normalized queue length to buffer size, $Q_i(k)$, channel normalised bandwidth to the link capacity limit, $\Gamma_i(k)$ and the network connectivity range, $C_i(k)$. Such stochastic state information gathered within a BLVN set can be modelled as [107, 156, 250]:

$$G_{ii}(k+1) = G_{ii}(k)\, g_i(k),$$

$$I_i(k+1) = I_i(k)\, i_i(k),$$

$$\beta_i(k+1) = \beta_i(k)\, s_i(k),$$

$$Q_i(k+1) = Q_i(k)q_i(k),$$
$$\Gamma_i(k+1) = \Gamma_i(k)b_i(k),$$
$$C_i(k+1) = C_i(k)c_i(k), \tag{3-1}$$

where $g_i(k)$, $i_i(k)$, $s_i(k)$, $q_i(k)$, $b_i(k)$ and $c_i(k)$ are Gaussian distributed unit mean random variable noise terms. The noise term $g_i(k)$ refers to the fluctuations in channel gains characterized by the spatial-temporal fading on top of the distance signal propagation path loss. The term $i_i(k)$ represents fluctuations in the interference levels when nodes power up above, or power down below their interference levels, respectively and $s_i(k)$ represents the SIR variations. The queue variations when packets either enter or exit the queue system is denoted by $q_i(k)$ and the increase or decrease in the link bandwidth due to network congestion is denoted by $b_i(k)$. Variations in connectivity range that model the topology changes due to node failures or entry into the network are yielded by $c_i(k)$.

In order to linearize the above models, we introduce a logarithmic scale so that:

$$\bar{G}_{ii}(k+1) = \bar{G}_{ii}(k) + \bar{g}_i(k),$$
$$\bar{I}_i(k+1) = \bar{I}_i(k) + \bar{i}_i(k),$$
$$\bar{\beta}_i(k+1) = \bar{\beta}_i(k) + \bar{s}_i(k),$$
$$\bar{Q}_i(k+1) = \bar{Q}_i(k) + \bar{q}_i(k),$$
$$\bar{\Gamma}_i(k+1) = \bar{\Gamma}_i(k) + \bar{b}_i(k),$$
$$\bar{C}_i(k+1) = \bar{C}_i(k) + \bar{c}_i(k), \tag{3-2}$$

For convenience of notations we drop the subscript i as it should be noted that the dynamics are the same for each user. Let $X_k \triangleq \left[\bar{G}_{ii}(k) \ldots \bar{C}_i(k)\right]^T$ and $\mathbf{w}_k \triangleq \left[\bar{g}_{ii}(k) \ldots \bar{c}_i(k)\right]^T$, where X_k is random variable with realization vector $\mathbf{x}_k$, depicting state information and $\mathbf{w}_k$ is a realization vector of system driving noise terms with zero-mean and some variance $\sigma_{\mathbf{w}}^2$ and is assumed independent of the transmission power selected by a link user. The linear dynamic model stemming from the above equations is given by

$$\mathbf{x}_{k+1} = \mathbf{A}\mathbf{x}_k + \mathbf{w}_k,$$
$$\mathbf{y}_k = \mathbf{C}\mathbf{x}_k + \mathbf{v}_k, \quad (3\text{-}3)$$

where $\mathbf{A} \in \Re^{n \times n}$ is the state identity matrix, $\mathbf{C} \in \Re^{p \times n}$ is the measurement vector $\mathbf{y}_k$ matrix and $\mathbf{v}_k$ is the measurement noise term of zero mean and some variance $\sigma_{\mathbf{v}}^2$. In order to filter out noise terms in the above equations and reliable track states and measurements, the well known Kalman filter method is exploited [251].

3.3.2 The Kalman Filter

The Kalman filter is a set of mathematical equations which provides an efficient computational (recursive) means to estimate the state of a process, in a way that minimizes the mean of the squared error [251]. Let $\mathbf{x} \sim \mathrm{N}(\boldsymbol{\mu}, \Sigma)$ denote the value of a random variable X with a normal probability distribution with mean $\boldsymbol{\mu} = \mathrm{E}[\mathbf{x}_k]$ and covariance $\Sigma = \mathrm{E}\left[(\mathbf{x} - \boldsymbol{\mu})(\mathbf{x} - \boldsymbol{\mu})^T\right]$. The random variable X is a complex vector of wireless MACI, link bandwidth, queue states, received signal quality and neighbour connectivity range. If $\mathbf{y}$ is the value of random variable Y and represents measurement values, then the Kalman filter process model at time step k is given by the following equations:

Dynamic Model:

$\mathbf{x}_k \sim \mathrm{N}(\mathbf{A}_k \mathbf{x}_{k-1}, \Sigma_{\mathbf{x}k})$, where $\Sigma_{\mathbf{x}k} = \mathrm{cov}(\mathbf{w}_k) = \mathrm{E}\left[\mathbf{w}_k^T \mathbf{w}_k\right]$ and $\mathbf{w}_k$ is the dynamic system process noise.

$\mathbf{y}_k \sim \mathrm{N}(\mathbf{C}_k \mathbf{x}_k, \Sigma_{\mathbf{y}k})$, where $\Sigma_{\mathbf{y}k} = \mathrm{cov}(\mathbf{v}_k) = \mathrm{E}\left[\mathbf{v}_k^T \mathbf{v}_k\right]$ and $\mathbf{v}_k$ is the measurement process noise.

Initialization:

$\hat{\mathbf{x}}_0^- = E[\mathbf{x}_0]$ and $\sigma_0^- = E\left[(\mathbf{x}_0 - \hat{\mathbf{x}}_0^-)(\mathbf{x}_0 - \hat{\mathbf{x}}_0^-)^T\right]$.

Update Equations: *Prediction*

$\hat{\mathbf{x}}_k^- = \mathbf{A}_k \hat{\mathbf{x}}_{k-1}^+$: System state transition and the a priori mean value of $P(X_k | Y_{k-1} = \mathbf{y}_{k-1})$ = $P(X_k, \mathbf{y}_{k-1}) / P(\mathbf{y}_{k-1})$.

$\Sigma_k^- = \mathbf{A}_k \sigma_{k-1}^+ \mathbf{A}_k + \Sigma_{\mathbf{x}k}$: a priori Riccati model and the a priori estimate error covariance of $P(X_k | Y_{k-1} = \mathbf{y}_{k-1})$.

Update Equations: *Correction*

$\kappa_k = \Sigma_k^- \mathbf{C}_k^T \left[\mathbf{C}_k \Sigma_k^- \mathbf{C}_k^T + \Sigma_{\mathbf{y}k} \right]^{-1}$: Kalman Filter Gain

$\hat{\mathbf{x}}_k^+ = \hat{\mathbf{x}}_k^- + \kappa_k \left[\mathbf{y}_k - \mathbf{C}_k \hat{\mathbf{x}}_k^- \right]$: Correction process/posterior mean of various distributions encountered while tracking a state variable of a certain fixed dimension using the given dynamic model.

$\Sigma_k^+ = \left[\mathbf{I} - \kappa_k \mathbf{C}_k \right] \Sigma_k^-$: Update Riccati Matrix, a posterior estimate error covariance of various distributions based on the given dynamic model.

3.4 MAC-Scheduling Probability Model

In general, consider distributed spread-spectrum channel signalling methods [185]. Such methods provide anti-jamming capabilities, robustness to multi-path effects and potential for multi-user access [147]. In spread-spectrum systems, distributed transmission power control methods are affected by multiple access co-channel interference (MACI) powers [12]. The MACI powers due to concurrent transmissions by other network users suppress a user's reception quality (i.e., as measured in terms of the received SINR) [143]. The instantaneous MACI level at the receiver node r can be defined by

$$q_{-i}(k, \mathbf{p}_{-i}) = \sum_{j \in V_r \; j \neq i} x_j(k) . g_j^r(k) \; p_j(k) + \eta_r \; . \tag{3-4}$$

Here, $p_j(k)$ and $g_j^r(k)$ denote the interfering power of node j towards receiver, $r \in V_r$ and the corresponding channel gain, respectively. All interfering transmitters other than transmitter i have powers represented as $\mathbf{p}_{-i}(k)$. Notation, η_r refers to the thermal noise power at the receiver node $r \in V_r$. Denote $x_j(k)$ as a binomially-distributed random variable

describing whether a user is active or not. It dictates the number of nodes in the set V_r and V_i that are transmitting concurrently. Let $x_j(k)$ occur with probability ρ_j for all $j \in V_r \cup V_i$. Thus, $x_j(k)$ may be defined as

$$x_j(k) = \begin{cases} 1 \text{ if j transmits at time k} \\ 0 \text{ otherwise} \end{cases}. \tag{3-5}$$

The number of multiple transmission activities (MTA) should be made available to the power control system in order to estimate the MACI level. If the number of MTA at node r is $|V_r| = N_r$, then there are exactly 2^{N_r-1} possible combinations of MTA in the set V_r excluding the transmitting node itself at any given time. Sets of such combinations of MTA can be denoted as $\{\phi_{in}^r\}_{n=1,\ldots,2^{N_r-1}}$ [147]. Table 3.3 depicts possible state combinations of two independently interfering nodes during time period k. Interestingly, Table 3.3 generalizes medium access schemes ranging from the TDMA scheme showing no interference to the CDMA scheme indicating simultaneous activity. Based on this generalization, the transmission power control can be developed at any given instant of time k [47].

Table 3.3: Possible Concurrent MACI States

	Interferer 1	Interferer 2
ϕ_{i1}^r	$x_1 = 0$	$x_2 = 0$
ϕ_{i2}^r	$x_1 = 0$	$x_2 = 1$
ϕ_{i3}^r	$x_1 = 1$	$x_2 = 0$
ϕ_{i4}^r	$x_1 = 1$	$x_2 = 1$

Correspondingly, we can define a random variable $\Phi_i^r(k)$ which indicates the occurrence of a specific combination $\phi_{in}^r(k)$ of independent interferers, interfering with node i's transmission at a certain time k. Thus, the probability that $\Phi_i^r(k)$ assumes the value of $\phi_{in}^r(k)$ for the nth combination of independent interferers can be defined as

$$\Pr\left\{\Phi_i^r(k)=\phi_{in}^r\right\}=\prod_{m\in\bar{\phi}_{in}^r}(1-\rho_m)\prod_{l\in\phi_{in}^r}\rho_l \tag{3-6}$$

Here, $\bar{\phi}_{in}^r$ of the first product term denotes the complement of ϕ_{in}^r in the second product term. That is, the first term of the product function is the probability describing nodes which are *not* transmitting simultaneously with the sender node i at time k. On the other hand, the second term refers to the probability of those *actively* transmitting simultaneously with node i. The medium access probability ρ_l or ρ_m is to be evaluated as follows. Considering the definition in (3-6), assuming unicast traffic and dropping the time index k for reasons of simplicity, the probability υ_i^r that a CCA packet transmitted with power $p_i(k)$ by the node i is successfully received at the node r conditional on certain MACI levels is calculated as:

$$\begin{aligned}\upsilon_i^r &= \Pr\{\textit{successful packet reception at } r\},\\ &= \sum_{n=1}^{2^{N_r}-1}\Pr\left\{\textit{succ. pac. recept.}|\Phi_i^r=\phi_{in}^r\right\}\Pr\left\{\Phi_i^r=\phi_{in}^r\right\},\\ &= \sum_n f\left(\phi_{in}^r\right)\Pr\left\{\Phi_i^r=\phi_{in}^r\right\}.\end{aligned} \tag{3-7}$$

Here, $f\left(\phi_{in}^r\right)$ denotes the probability of successful CCA packet reception by node r due to the transmission of node i using power $p_i^r(k)$, conditioned on a certain MACI level. The functional form of $f\left(\phi_{in}^r\right)$ depends on the specific choice of the PHY-layer aspects such as wireless channel model, modulation and demodulation schemes, channel coding and the receiver designs [252]. If we assume that the forward and backward transmissions are independent, then the joint probability of successful reception of packets at the nodes i and r is given by

$$\begin{aligned}\upsilon_i &= \Pr\{\textit{forward success}, \textit{backward success}\},\\ &= \sum_n^{2^{Nr}-1}\sum_l^{2^{N_i}-1} f\left(\phi_{in}^r\right) f\left(\phi_{rl}^i\right)\Pr\left\{\Phi_i^r=\phi_{in}^r\right\}\Pr\left\{\Phi_r^i=\phi_{rl}^i\right\}.\end{aligned} \tag{3-8}$$

The MAC protocol in place exploits the PHY-layer signalling information in (3-8) and the interaction among other nodes in the topology to determine adaptive scheduling rules for actual application packet transmissions. This can be achieved in a manner which minimizes the number of unsuccessful transmissions. Such a MAC-dependent functional may take the

form $\rho_i = \xi_i(\upsilon_i)$. In general, this functional is a non-linear function of Kalman filter outputs. Its related analysis is complex. In linear representation, $\xi_i(\upsilon_i)$ can be assumed to have an nth derivative throughout the interval $[0,1]$ such that the Maclaurin series expansion is given as

$$\rho_i = \xi_i(\upsilon_i) = \xi_i(0) + \upsilon_i \xi_i'(0) + \ldots + \frac{\upsilon_i^{n-1}}{(n-1)!}\xi_i^{(n-1)}(0) + \frac{\upsilon_i^n}{n!}\xi_i^{(n)}(\varepsilon), \qquad (3\text{-}9)$$

where $0 \le \varepsilon \le \upsilon_i$. The first order approximation of (3-9) is given by

$$\rho_i \approx m\upsilon_i, \text{ where } m = \xi'(0), \quad \text{at } \upsilon_i = 0. \qquad (3\text{-}10)$$

Here, m is a time-varying proportionality design factor for the linear model in (3-10). This proportionality factor relates the PHY-layer successful packet reception probability (PRP) υ_i to the MAC-dependent TSP, ρ_i at any given time k. The determination of the value m involves the network topology in a BLVN region. It is easy to verify that m is inversely proportional to the number of nodes in the neighbourhood of the transmitter and the receiver [147]. Therefore, one can choose $m << 1$ since in a Maclaurin expansion series, the conditional successful packet reception probability, $\upsilon_i = 0$ as the number of MTA gets much larger (i.e., N >>1).

Theorem 3.1: *Given a BLVN(i) set described by* $V_i \cup V_{ri}$ *with* $N > 1$. *If* $m < (N-1)^{-1}$ *then matrix* $\mathbf{M} \in \Re^{N \times N}$ *is non singular regardless of the network topology described by* m.

Proof:

Suppose $\boldsymbol{\rho} = \mathbf{M}\boldsymbol{\upsilon}$ with $m_{ij} = \begin{cases} 1 \text{ if } i = j, \ j \in V_i \cup V_{ri} \\ m \text{ if } i \neq j, \ j \in V_i \cup V_{ri} \\ 0 \text{ if } i \neq j, \ j \notin V_i \cup V_{ri} \end{cases}$ and by design, the diagonal elements of matrix $\mathbf{M}$ are all unity entries and by definition $\mathbf{M}$ and $\mathbf{M}^T$ are said to be diagonally dominant if $\sum_j |m_{ij}| < m_{ii}$, $j \neq i$, $\sum_j m_{ij} < 1$ for all i and $\sum_i m_{ij} < 1$ for all j. Hence, we can let S denote the set of non-zero off-diagonal elements in a specific row or column of $\mathbf{M}$ such

that $\sum_{s\in S} m_{ij}(s) \le (N-1)m$. Thus, from the definition, matrix $\mathbf{M}$ is a positive definite matrix with $m<(N-1)^{-1}$. The positive definiteness property implies that $\mathbf{M}^{-1}$ exists, proving theorem 3.1.

■

3.4.1 Average Multiple Access Co-Channel Interference (MACI)

In reality, channel gains, received signal power, MACI and SINR are random processes fluctuating in time. Power adjustments need to respond to the average trends reflecting true QoS changes rather than instantaneous values [47]. That is, if the number of MTA which is heard by the device r is $|V_r|=N_r$, then there are exactly 2^{N_r-1} possible combinations of MTA in the set V_r excluding the transmitting node itself, during a long time slot. The average MACI is then dependent on the probability that a time-variant random variable $\Phi_{ir}(k)$ has a realization ϕ_{ir} in each combination. Therefore, such an average MACI over all possible combinations of medium access schemes is modelled as [23]

$$\left\langle q_{-ir}(k,\mathbf{p}_{-ir})\right\rangle = \sum_{m=0}^{2^{N_r-1}-1} \Pr\{\Phi_{ir}(k)=\phi_{irm}\} q_{-ir,m}(k,\mathbf{p}_{-ir}),$$

$$= \sum_{m} \prod_{a\in\phi_{irm}}^{Active\ Set} \rho_a \prod_{d\in\bar{\phi}_{irm}}^{Inactive\ Set} (1-\rho_d)\, q_{-ir,m}(k,\mathbf{p}_{-ir}), \qquad (3\text{-}11)$$

where ρ_{ir} for all $(i,r)\in E$ denotes any MAC transmission scheduling probability (MAC-TSP) for any actively transmitting wireless user [23, 45]. The product terms in (3-11) denote the number of users in the *active* and *inactive* sets.

3.5 MATA-Power Optimization

3.5.1 Problem Formulation: MAC-TSP

The main aim of each user is to minimize its convex cost function subject to MAC-TSP constraints. The convex cost function consists of the next step average SINR deviation (i.e., user centric) and the next step average aggregate network MACI (i.e., network centric) falling in the BLVN set [12]

$$\min \; J_{e\in E}(k) = \omega_{e1}\,\Delta^2_{e\in E}(k+1) + \omega_{e2}\left\langle q_{e\in E}(k+1)\right\rangle^2 \tag{3-12}$$

$$\text{Subject to:} \quad x_{e\in E}(k)\in\{0,1\} \;\; \forall e\in E,\; k=1,\ldots,K, \tag{3-13}$$

$$\sum_{(i\to r)\in E} x_i^r(k) + \sum_{(r\to i)\in E} x_r^i(k) \le 1 \quad \forall i,\, r\in V,\, k=1,\ldots,K, \tag{3-14}$$

$$0 \le \rho_{e\in E}(k) \le 1 \quad \forall e\in E,\; k=1,\ldots,K, \tag{3-15}$$

$$\left\{\frac{d_{e\in E}}{R_T^{max}}\right\}^{\nu} p_{e\in E}^{max} x_e(k+1) \le p_{e\in E}(k+1) \le p_{e\in E}^{max} x_e(k+1), \tag{3-16}$$

$$p_{zh}(k+1) \le p_{zh}^{max} - \left[1 - \left\{\frac{d_{zr}}{R_I^{max}}\right\}^{\nu}\right] p_{zh}^{max} x_{zh}(k+1). \tag{3-17}$$

Here, the next step average SINR deviation and interference are given respectively, by

$$\Delta_{e\in E}(k+1) = \gamma_{e\in E} - \left\langle \beta_{e\in E}(k+1)\right\rangle, \tag{3-18}$$

$$\left\langle q_{e\in E}(k+1)\right\rangle = \left\langle q_{-e\in E}(k+1)\right\rangle + \left\langle p_{e\in E}(k+1) G_{e\in E}(k+1)\right\rangle. \tag{3-19}$$

These cost function components are weighted by the network and/or application generated scalars ω_{e1} and ω_{e2}. The weights determine whether a user is self-centred, network-centred or

a trade-off between the two. The instantaneous SINR at the receiver r when a signal is transmitted by sender device i at the beginning of time k is given by

$$\beta_i^r(k) = \frac{S_i\, p_i^r(k) G_i^r(k) x_i^r(k)}{\sum_{(l\to m)\neq(i\to r)} p_l^m(k) G_l^r(k) x_l^m(k) + \eta_r(k)}, \tag{3-20}$$

where S_i is the spreading gain (or the bandwidth expansion factor) of the spread-spectrum system, $p_i^r(k)$ is the transmission power emitted by i on link (i,r), $G_i^r(k)$ is the gain of the radio channel between i and r, η_r is the thermal noise at receiver r.

Constraint (3-13) is a binary constraint that indicates concurrent transmission of link $e\in E$ with other links in the co-channel BLVN set. Equation (3-14) implies that each device is active in, at most, one link in each iteration slot, while constraint (3-15) depicts a pessimistic successful transmission with probability zero and an optimistic successful transmission with probability one. Equations (3-16) and (3-17), respectively, are the necessary and sufficient conditions for a successful transmission under the protocol interference model (PrIM) [57]. Parameters, ν, d_e, R_T^{max} and R_I^{max} are the path-loss exponent, transmission distance, the maximum transmission and interference ranges, respectively for link $e\in E$.

Proofs for equations (3-16) and (3-17) can easily be derived by extending analytical results in [239]. In particular, a link $e\in E$ considers its transmission to be successful if and only if the receiver device r falls within its *transmission range* but outside the interference range of a concurrent transmitting link $(z,h)\in E$. Equation (3-16) offers a practical minimum power level that can be chosen for a channel probing mechanism [253]. It should be noted that PrIM constraints result in poor space re-use (i.e., a low network density). Reducing this transmission range through power control significantly improves the network capacity [57].

3.5.2 Optimal Controller Gain Analysis

Let the decentralized power adjustment law that minimizes the cost function in (3-12) and satisfies MAC-TSP constraints be given by

$$p_{e\in E}(k+1) = p_{e\in E}(k) + \alpha_{e\in E}(k)\left\langle q_{-e\in E}\left(k, \mathbf{p}_{-e\in E}\right)\right\rangle , \tag{3-21}$$

where $\alpha_{e\in E}(k)$ represents the distributed power controller gain, analysed in theorem 3.2.

Theorem 3.2 [108]: *From the distributed cost function (3-12), if $J(\alpha_e)$ is convex on a convex set C, then $J(\alpha_e)$ has at most one local minimum. If such a minimum exists, it is also a global minimum for users in the BLVN set and is attained on a convex set.*

Proof: Suppose there is a local minimum at a point $\alpha_e^* = \arg\min_\alpha \left\{\omega_{e1}\Delta_e^2(\alpha_e) + \omega_{e2}\left\langle q_e(\alpha_e)\right\rangle^2\right\}$ with $\omega_e \triangleq \omega_{e2}/\omega_{e1}$. For any $\alpha_e = \bar{\alpha}_e$ in C, by definition of a local minimum and convexity of $J(\alpha_e)$ [254], we have

$$J(\alpha_e^*) \le J\left((1-\lambda)\alpha_e^* + \lambda\bar{\alpha}_e\right) \le (1-\lambda)J(\alpha_e^*) + \lambda J(\bar{\alpha}_e), \tag{3-22}$$

for λ a sufficiently small positive number. From the extremes of (3-22) we have

$$J(\alpha_e^*) \le (1-\lambda)J(\alpha_e^*) + \lambda J(\bar{\alpha}_e) \ , \tag{3-23}$$

$$\lambda J(\alpha_e^*) \le \lambda J(\bar{\alpha}_e) \ , \tag{3-24}$$

and since $\lambda > 0$, then $\lambda J(\alpha_e^*) \le \lambda J(\bar{\alpha}_e)$, which implies $J(\alpha_e^*)$ is a global minimum by definition, as $\bar{\alpha}_e$ is any point in C [108].

If α_e^* and α_e° are two points at which $J(\alpha_e)$ attains its minimum value z_0, then for $0 \le \lambda \le 1$

$$z_0 \le J\left((1-\lambda)\alpha_e^* + \lambda\alpha_e^\circ\right) \le (1-\lambda)J(\alpha_e^*) + \lambda J(\alpha_e^\circ) = z_0 \tag{3-25}$$

Hence, $J(\alpha_e)$ also attains its minimum at $\alpha_e = (1-\lambda)\alpha_e^* + \lambda\alpha_e^\circ$ and thus the set of solutions is convex.

▪

It should be noted that a unique fixed point p^* can be achieved if the adaptive control gain $\alpha_e(k)$ can be optimum for all $e \in E$ in the BLVN network. This optimum point may be derived from: $\alpha_e^*(k) = \arg_{l \in E} \min J_l(k)$ [45].

Corollary 3.1: *For a link executing the power iteration in (3-21), the optimum controller gain (OCG)* $\alpha_{e \in E}^*(k)$ *in the* k*th iteration can be written as*

$$\alpha_e^*(k) = \frac{A_k - \omega_e \left\langle q_{-e \in E}(k+1) \right\rangle^2 \left\{ \left\langle q_{-e \in E}(k+1) \right\rangle + \left\langle p_{e \in E} G_e(k) \right\rangle \right\}}{B_k \left\{ 1 + \omega_e \left\langle q_{-e \in E}(k+1) \right\rangle^2 \right\}}, \tag{3-26}$$

where

$$A_k = \left\langle q_{-e \in E}(k+1) \right\rangle^2 \gamma_{e \in E} - \left\langle p_{e \in E} G_{e \in E}(k) \right\rangle, \tag{3-27}$$

$$B_k = \left\langle G_{e \in E}\, q_{-e \in E}(k) \right\rangle, \tag{3-28}$$

$$\omega_{e \in E} = \omega_{e2} / \omega_{e1} \ . \tag{3-29}$$

From equations (3-18), (3-12) and (3-29) the notations $\gamma_{e \in E}$ and $\omega_{e \in E}$ are respectively, the target SIR value and the application priority based non-negative weighting factor for the minimization of the objective function in (3-12).

It should be noted that the weighting factor $\omega_e(k) \geq 0$ and the MAC-dependent TSP $0 \leq \rho_e(k) \leq 1$ are locally assigned to each node depending on the MATA states and traffic applications [12].

Proof: The outline of the proof is as follows: If we substitute the value of $p_e(k+1)$ in (3-18) and (3-19) with the expression in (3-21) and evaluate the first partial derivative of (3-12) with respect to $\alpha_{e \in E}(k)$, and set the result to zero, we obtain the result in (3-26).

▪

Corollary 3.2*: Given the BLVN set, each user's power update given by (3-21) is globally optimal with respect to the minimization of the decentralized constrained nonlinear function (3-12) consisting of the average SINR deviation and average MACI.*

Proof: Using the Karush-Kuhn-Tucker conditions [108], it is possible to solve the constrained nonlinear programming problem in (3-12). Suppose the protocol constraints (3-13)-(3-15) hold, then α_e^* is a solution to the convex-programming problem $J(\alpha_e)$ with the predicted power value $p_e(k+1)$ bounded by the minimum and maximum if and only if Lagrange scalars π_1 and π_2 exist such that (α_e^*, π_j^*) is a solution to the saddle point problem [254].

▪

Consequent Proof (Saddle Point) : It is well known from [108] that the saddle point conditions are sufficient to ensure that α_e^* is a solution to the convex-programming problem. The saddle point problem is given by

$F(\alpha_e^*, \pi) \le F(\alpha_e^*, \pi^*) \le F(\alpha_e, \pi^*)$ with $-\infty < \alpha_e < \infty$ and $\pi = [\pi_1, \pi_2] \ge 0$ and (α_e^*, π^*) is the saddle point.

First, substitute the power iteration in (3-21) into constraints in the (3-16) then obtain new constraints defined as

$$\hbar_1(\alpha_e) \triangleq (p_e - p_e^{\max}) / \langle q_{-e}(\mathbf{p}_{-e}) \rangle + \alpha_e \le 0 \ , \tag{3-30}$$

$$\hbar_2(\alpha_e) \triangleq (p_e^{\min} - p_e) / \langle q_{-e}(\mathbf{p}_{-e}) \rangle - \alpha_e \le 0 \ , \tag{3-31}$$

Given that

$$F(\alpha_e, \pi) = J(\alpha_e) + \sum_{j=1}^{2} \pi_j \hbar_j(\alpha_e) \ . \tag{3-32}$$

We have from the saddle point definition that

$$J(\alpha_e^*) + \sum_{j=1}^{2} \pi_j \hbar_j(\alpha_e^*) \le J(\alpha_e^*) + \sum_{j=1}^{2} \pi_j^* \hbar_j(\alpha_e^*) \le J(\alpha_e) + \sum_{j=1}^{2} \pi_j^* \hbar_j(\alpha_e) . \tag{3-33}$$

For the left hand inequality of (3-33) to hold for all $\pi \ge 0$, we must have both $\hbar_j(\alpha_e^*) \le 0$ for all j and $\sum_{j=1}^{2} \pi_j^* \hbar_j(\alpha_e^*) = 0$. We demonstrate this as follows. The left hand inequality is

$$\sum_{j=1}^{2}\pi_j\hbar_j\left(\alpha_e^*\right)\le\sum_{j=1}^{2}\pi_j^*\hbar_j\left(\alpha_e^*\right)\quad . \tag{3-34}$$

If some $\hbar_j\left(\alpha_e^*\right)>0$, then a corresponding $\pi_j>0$ can be chosen large enough so that the inequality (3-34) does not hold. Therefore, $\hbar_j\left(\alpha_e^*\right)\le 0$ for all j. Since $\alpha_e^*\ge 0$ for all transmission power sequence $\left\{p_e(k)\right\}\ge 0$, one concludes that α_e^* satisfies the constraints of the (3-31) of the convex-programming problem.

Also as (3-34) must hold for $\pi=0$, we have $0\le\sum_{j=1}^{2}\pi_j^*\hbar_j\left(\alpha_e^*\right)$. But as $\pi^*\ge 0$, all $\hbar_j\left(\alpha_e^*\right)\le 0$; then $\sum_{j=1}^{2}\pi_j^*\hbar_j\left(\alpha_e^*\right)\le 0$, which implies $\sum_{j=1}^{2}\pi_j^*\hbar_j\left(\alpha_e^*\right)=0$. Thus either $\pi_j^*=0$ or $\hbar_j\left(\alpha_e^*\right)=0$, or both equal zero.

Similarly, from the right hand inequality of (3-33) we obtain

$$J\left(\alpha_e^*\right)\le J\left(\alpha_e\right)+\sum_{j=1}^{2}\pi_j^*\hbar_j\left(\alpha_e\right)\ \text{for all}\ \alpha_e\ge 0.$$

Since $\pi^*\ge 0$, $J\left(\alpha_e^*\right)\le J\left(\alpha_e\right)$ for all $-\infty<\alpha_e<\infty$ from which one concludes that $\hbar_j\left(\alpha_e\right)\le 0$. Consequently, with $\hbar_j\left(\alpha_e^*\right)\le 0$, α_e^* is a solution to the convex programming problem.

■

3.5.3 Optimal Controller Power Analysis

It should be noted that the global optimal MATA power adjustment law in the BLVN set is defined as [45]

$$\mathbf{p}(k+1)=(\mathbf{I}+\mathbf{A})\mathbf{p}(k)+\mathbf{b}, \tag{3-35}$$

$$\text{Subject to: } \mathbf{p}^{lower}\le\mathbf{p}(k+1)\cong\Gamma(\mathbf{p})\le\mathbf{p}^{upper}. \tag{3-36}$$

Here,

$$\mathbf{A}=\begin{bmatrix} \alpha_1^* g_{1\leftrightarrow 1}(k) & \alpha_1^* g_{1\leftrightarrow 2}(k) & \alpha_1^* g_{1\leftrightarrow 3}(k) & \dots & \alpha_1^* g_{1\leftrightarrow N}(k) \\ \alpha_2^* g_{2\leftrightarrow 1}(k) & \alpha_2^* g_{2\leftrightarrow 2}(k) & \alpha_2^* g_{2\leftrightarrow 3}(k) & \dots & \alpha_1^* g_{2\leftrightarrow N}(k) \\ \dots & \dots & \dots & \dots & \dots \\ \dots & \dots & \dots & \dots & \dots \\ \alpha_N^* g_{N\leftrightarrow 1}(k) & \alpha_N^* g_{N\leftrightarrow 2}(k) & \alpha_N^* g_{N\leftrightarrow 3}(k) & \dots & \alpha_N^* g_{N\leftrightarrow N}(k) \end{bmatrix}$$

$$g_{i\leftrightarrow r}(k)=g_i^r(k)=g_r^i(k) \quad \forall i,r\in V,$$

and $\mathbf{b}=\begin{bmatrix}\alpha_1^*\eta & \dots & \dots & \alpha_N^*\eta\end{bmatrix}^T$.

Theorem 3.3: *If the optimal gain vector* $\boldsymbol{\alpha}^*$ *is unique then it implies that power update function* $\Gamma(\mathbf{p})$ *has a unique fixed point at the optimal power vector* $\mathbf{p}^*$.

Proof by contradiction: Suppose $\boldsymbol{\alpha}^a$ and $\boldsymbol{\alpha}^b$ are two distinct fixed points at a and b for all $\boldsymbol{\alpha}=[\alpha_1,\alpha_2,\dots,\alpha_N]^T$ at the same time. Thus, from (3-35) and (3-36), the following properties can be defined:

$$\|\mathbf{I}+\mathbf{A}\|\le\|\mathbf{I}\|+\|\mathbf{A}\|, \qquad \textit{(Triangle Inequality)}$$

$$\left(\|\mathbf{I}\|+\|\boldsymbol{\alpha}\|^T\|\mathbf{G}\|\right)>\|\mathbf{0}\| \quad 0<g_{i\leftrightarrow j}(k)\le 1,$$

$$\|\mathbf{b}\|>\|\mathbf{0}\| \quad \textit{where} \quad \eta>0, \qquad \textit{(non zero)}$$

$$\Rightarrow \alpha_i\neq 0 \quad \forall i=1,2,\dots N. \qquad \textit{(non zero)}$$

$$f(\boldsymbol{\alpha}^a)\ge f(\boldsymbol{\alpha}^b) \text{ if } \boldsymbol{\alpha}^a\ge\boldsymbol{\alpha}^b, \qquad \textit{(monotonicity)}$$

$$\delta f(\boldsymbol{\alpha})>f(\delta\boldsymbol{\alpha}) \quad \forall\delta>1, \qquad \textit{(scalability)}$$

Let us assume that there exists j such that $\alpha_j^a<\alpha_j^b$ for all j. Correspondingly there exists $\delta>1$ such that $\delta\boldsymbol{\alpha}^a\ge\boldsymbol{\alpha}^b$. Thus, there exists for some j, $\delta\boldsymbol{\alpha}^a=\boldsymbol{\alpha}^b$. The monotonicity and scalability implies:

$$f_j(\boldsymbol{\alpha}^b)=\alpha_j^b\le f_j(\delta\boldsymbol{\alpha}^a). \tag{3-37}$$

$$f_j\left(\delta \boldsymbol{\alpha}^a\right) = \delta \alpha_j^a < \delta f_j\left(\boldsymbol{\alpha}^a\right). \tag{3-38}$$

The result in equations (3-37) and (3-38) implies that a and b are two distinct points. Thus, there can be no more than one solution of $\boldsymbol{\alpha}^*$ at the same time. Furthermore if wireless channels hold their states in the duration of the power control, then $\boldsymbol{\alpha}^*$ can be unique with exact solution as shown in (3-26). From *theorem 3.3*, having shown that $\boldsymbol{\alpha}^*$ is unique, then the *proof* that $\Gamma(\mathbf{p})$ has a unique fixed point at $\mathbf{p}^*$ can be found in [149]. However, the uniqueness of $\mathbf{p}^*$ does not necessarily imply the feasibility of the power vector $\Gamma(\mathbf{p})$ in a contention and collision environment [50]. In such situations, the MATA based DPC algorithm becomes necessary. That is, each sender aware of the TSP constraints may decide whether to transmit at a certain time using a controlled degree of power in such a manner that the aggregate MACI component of the objective function in (3-12) is minimized. The remaining sender nodes can then attain feasible power solutions via the execution of transmission power iterations, i.e., $\mathbf{p}(0) \geq \mathbf{p}(1)\ldots$ if $\mathbf{p}(0) > 0$. Hence, the feasibility implies monotonicity [254].

▪

Lemma 3.1: *If* $\mathbf{p}$ *is a feasible power vector for all nodes, then* $\Gamma(\mathbf{p})$ *is a monotonically decreasing sequence of feasible power vectors that is lower bounded by the minimum power and* $\Gamma(\mathbf{p})$ *converges to a unique fixed point* $\mathbf{p}^*$. *Conversely starting from* $\mathbf{p}(0)=0$, *then* $\Gamma(\mathbf{p})$ *is a monotonically increasing sequence of power vectors that is upper bounded by a unique fixed point* $\mathbf{p}^*$.

The *proof* is developed in [149] and extended in [50].

▪

3.5.4 Problem Formulation: GCOM

It should be noted that MAC-TSP models consist of interactions between the physical and MAC layers. However, the transmission power level impacts on connectivity range and hence multi-hop routing decisions. This is a generalized view of a cross-layer design problem.

Suppose $u_i\left(p_i(k+1)\mid \mathbf{y}(k)\right)$, denotes the probability that user i dynamically chooses transmission power value $p_i(k+1)\in \mathbf{p}(k+1)$ in the next time period given cross-layer information $\mathbf{y}(k)\in \mathbf{Y}(k)$ describing the MATA state and application constraints. Then, the generalized cross-layer occupation measure (GCOM) of user i knowing the dynamic power control policy is given by

$$\rho_i^{u_i}\left(\mathbf{y}, p_i(k+1)\right) = \rho_i(k)\, u_i\left(p_i(k+1)\mid \mathbf{y}\right), \tag{3-39}$$

for all $\rho_i^{u_i}\in \boldsymbol{\rho}$. Such a measure gives the steady state probability information that the system is in state $\mathbf{y}^{ss}\in \mathbf{Y}^{ss}$ and the transmission power $p_i^{ss}\in \mathbf{p}^{ss}$ is chosen [255]. The compliment of the GCOM is defined as, $\bar{\rho}_i^{u_i}=1-\rho_i^{u_i}$. The corresponding power policy $u_i\in U$ can be obtained by

$$u_i\left(p_i(k)\mid \mathbf{y}\right) = \frac{\rho_i^{u_i}\left(\mathbf{y}, p_i(k)\right)}{\sum_{\mathbf{p}_{-i}\in \mathbf{p}} \rho_i^{u_i}\left(\mathbf{y}, \mathbf{p}_{-i}\right)}. \tag{3-40}$$

For a given policy and the corresponding GCOM presented in equations (3-40) and (3-39), an average power minimization problem in terms of a convex cost function, subject to a set of cross-layer constraints, is given by [12]:

$$\underset{u\in U}{\text{Min}}\, J_i\left(u_i(k)\right) := \omega_{i1}\left\langle \varepsilon_i(k+1)\right\rangle^2 + \omega_{i2}\left\langle q_i(k+1)\right\rangle^2, \tag{3-41}$$

Subject to:

$$p_i^{\min} \le \left\langle p_i(k+1)\right\rangle \le p_i^{\max}, \tag{3-42}$$

$$\omega_i(k) = \omega_{i2}/\omega_{i1} \ge 0, \tag{3-43}$$

$$0 \le \rho_i^{u_i}\left(\mathbf{y}, p_i\right) \le 1. \tag{3-44}$$

Here,

$$\left\langle \varepsilon_i(k+1) \right\rangle = \left(\overline{\gamma}_i - \gamma_i(k+1) \right) \overline{\rho}_i^{u_i}(\mathbf{y}, p_i), \tag{3-45}$$

where (3-45) denotes the user centric objective function. It measures the quality of the received signal for a user as in (3-18). The space average aggregate interference powers are given by

$$\left\langle q_i(k+1) \right\rangle = \left(q_{-i}(k+1) + \left(p_i(k+1) g_i^r(k+1) \right) \right) \overline{\rho}_i^{u_i}(\mathbf{y}, p_i). \tag{3-46}$$

Expression in (3-46) models the network centric objective function. It measures the impact of the power chosen by a user on the transmissions of other network users. Since (3-41) presents a cost function problem to each user's decisions, the expectations in (3-45) and (3-46) are taken with respect to $\overline{\rho}_i^{u_i} \in \boldsymbol{\rho}$. The decentralised network state space average DTPC algorithm can now be given by

$$\left\langle p_i(k+1) \right\rangle = \left(p_i(k) + \alpha_i^*(k) q_{-i}(\mathbf{p}_{-i}, k) \right) \rho_i^{u_i}(\mathbf{y}, p_i). \tag{3-47}$$

The objective weight function, $\omega_i(k)$ can be defined as $\omega_i(k) = \left(p_i^{\max} / \mathit{Rate\ of\ } i \right)^{-1}$. The weight function depicts the delay sensitivity measure of the application. That is, depending on the priority level of application traffic, each user can either adapt its power in a greedy manner (so that the first term of (3-41) is minimized) or in an overly energy-efficient manner (so that the second term of (3-41) is minimized). In practice, delay sensitive traffic applications enjoy higher priority than bursty traffic applications. Thus, each node must generally evaluate the weight as

$$\text{If } \omega_i(k) = \begin{cases} 0, \text{ delay sensitive applications} \\ \infty, \text{ non delay sensitive applications} \\ 0 < \omega_i < \infty, \text{ otherwise, a trade-off} \end{cases}. \tag{3-48}$$

3.5.5 Summary of MATA Based Algorithm

Based on a given GCOM, and on both the user and application constraints, each node executes a dynamic power control algorithm:

$$\text{If } \rho_i^{\mu_i}(k) = \begin{cases} 0 \quad \textit{then} \ \text{select} \quad \langle p_i(k+1)\rangle = p_i^{\min} \\ 1 \quad \textit{then} \ \text{select} \quad \langle p_i(k+1)\rangle = p_i^{\max} \\ \text{otherwise} \quad \textit{then} \ \text{select} \quad p_i^{\min} < \langle p_i(k+1)\rangle < p_i^{\max} \end{cases} . \tag{3-49}$$

The details of this contribution can be found in our publications [23, 45, 47, 49].

It is worth noting that the MATA based algorithm provides a correction mechanism for the problem of overly greedy algorithms[1]. That is, any user i experiencing $\rho_i^{\mu_i}(k)=0$ will autonomously go onto power-save mode while causing no interference to an actively transmitting user $j \in V_r \cup V_i$ in state $x_j(k+1)$. Conversely, with $\rho_i^{\mu_i}(k)=1$, the sender user i can transmit with up to maximum power, taking advantage of the favourable link condition. However, due to the inherent interference caused to the rest of the network users, the voluntarily relaying nodes may choose to isolate such a persistent interferer. This decision may prompt the transmitting user to lower its transmission power. Consequently, the network may eventually become socially stable in the long run as depicted by simulation results in Section 3.6.

3.6 Performance Evaluations

3.6.1 Simulation Tests, Results and Discussions (MAC-TSP)

For performance tests, MATLAB™ version 7.1 [256] was used, to simulate realistic physical layer wireless radio and MAC layer conditions, which are often simplified in idealized network simulators. Up to fifty mesh nodes were placed randomly within a 1000 x 1000 m^2 area, i.e., a size big enough to deploy a multi-hop network. Each node was assumed with a transmission range of 250 m and the maximum interference range of 500 m. Performance metrics were evaluated by Monte Carlo simulations for 60 independent runs for each random

[1] An overly greedy algorithm refers to users simultaneously adapting their transmission powers to maximum values, causing excessive MACIs in the network.

network configuration or instance. For all network configurations, it was assumed that all nodes have at least one neighbour, and that there were considerable channel contention and collision problems. Such problems could be resolved by employing distributed time-slotted signalling and the bi-directional signalling (or the TSP) exchanges. Packets arrive at the radio link queues according to independent Poisson processes. Packet sizes are 1000 bytes, data rate of 2 Mbps, code spectrum gain of 128 (i.e., for simulation purposes only). A channel bandwidth of 10 MHz was assumed, as was a typical carrier frequency of 2.4 GHz for calculating the signal wavelength for channel gain. Modulation and channel coding techniques were employed as in [257]. It was further assumed that every node has a maximum transmission power (P*max*) of 1000 *m*Watts and a minimum transmission power of 0 *m*Watt. The propagation path loss model exponent and a white Gaussian noise (AWGN) were also assumed to be 4 and 0.001 *m*Watts respectively.

In Fig. 3.4, performance tests of the optimally designed per link or user power control gain as a function of estimated channel states demonstrates that when priority based weighting factor is zero (i.e., greedy strategy) and the channel condition is poor for the purpose of transmission then the gain is a large positive value that decreases exponentially when the channel condition improves. This can be explained as follows. In a bad channel condition and with a zero weighting factor, a mesh radio link or user computes a greedy based optimal transmission power level. This is in order to overcome channel barriers, consequently achieving a user-centric target QoS. However, such greedy power level adjustments result in a high energy source depletion and also cause additional interference to other co-located network users. As the wireless channel conditions become more favourable for packet transmission, such a user lowers the optimal controller gain (OCG), suggesting a low optimal transmission power level. In favourable channel conditions, OCG ensures that the transmission power remains stable during steady state time. Also evident from Fig. 3.4 is that the OCG approaches a zero from negative when the weighting factor is a positive large value (i.e., energy-efficient strategy). This means that each user, in a bad channel chooses to become energy-efficient and lowers its transmission power significantly. In fact, in a persistent bad channel condition, such a user may eventually switch off its transmission power and opt-out of transmissions. As the channel condition becomes more favourable for packet transmission, an energy-efficient user will set a near positive value to the parametric OCG and consequently attain a stable value for the transmission power level.

In Fig. 3.5, the impact of changes in the MAC probability (MAC-TSP) on the autonomous link optimal power control gain at different objective function weight factors is depicted. At

different transmission scheduling probabilities, each interface autonomously chooses the value of the weight factor from a non-negative real range and determines a stable level for the OCG factor. In each time slot the dynamic transmission power is executed until it reaches a steady state. At the beginning, an interface uses a probing power level to gather various aspects of local network information including interference, channel conditions and PHY-layer information. The interface utilizes such information to evaluate the MAC-TSP. The reliability of the MAC-TSP depends on the conditions of the wireless channel at any given time. If the MAC-TSP value is low then the wireless channel condition is unreliable for successful transmission and vice versa. At a zero weighting factor, Fig. 3.5 illustrates that the OCG factor falls rapidly from a high positive value to a near zero level, that is, defined as a stable region as the MAC-TSP value increases. This implies that the OCG factor tracks the channel uncertainties exponentially faster in order to reach the stable region. However, at a unity weighting factor, *a marginal* gain response was noted, that is, the OCG factor falls from a sufficiently large positive value to a negative region and rises monotonically to a stable level. If the weighting factor was taken to be a large positive value then the MAC-TSP versus OCG curve rises monotonically from a large negative to a stable equilibrium region. The observations are due to the fact that an interface decision to select a zero weighting factor allows such an interface to autonomously attain its desired QoS in a time-competitive environment. It is thus, a desirable decision for delay-sensitive QoS applications such as voice traffic. However, the decision incurs a high energy depletion cost. On the other hand, deciding on a non-zero weighting factor implies that the primary goal is to conserve individual energy and to reduce overall network interferences. Such decisions are tolerable by data traffic applications. However, energy-saving decisions may face starvation conflicts, particularly when a device fails to resolve its starvation problem in a number of transmission trials. The impact of this is evidenced in increased queue congestions.

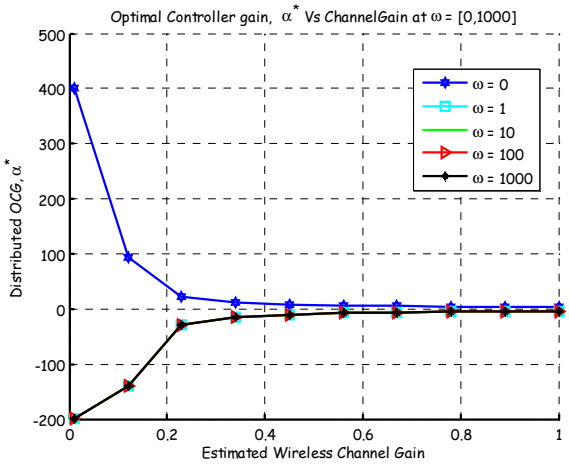

Figure 3.4: The optimal power controller gain versus estimated channel conditions.

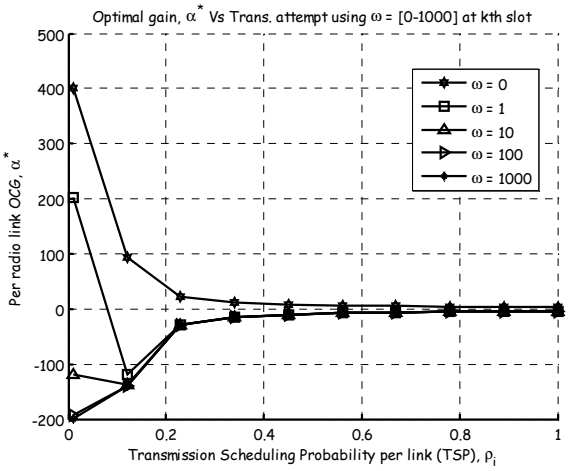

Figure 3.5: Optimal power controller gain versus transmission scheduling probability.

In Fig. 3.6, the parametric OCG graph smoothly tends to a zero value from a large negative, with an increase in MACI levels when the link is energy efficient or delay-insensitive. This implies that, irrespective of the choice of the initial transmission power in each radio link, an energy-efficient radio link attempts to maintain constant and low transmission power levels even as others introduce excessive interferences in the network. At 20 *m*Watts of MACI powers, the parametric OCG is noted to be about -15 when the initial probing power is 60 *m*Watts and about -60 when the initial probing power is 100 *m*Watts. This implies that the initial choice of the transmission power at a node exerts significant effects on the value of the parametric OCG. For a given interference level against an energy-efficient user, the higher the initial power, the larger the magnitude of response of the control system to stability region. That is, the high valued gain suppresses possible energy dissipations. Negative signs of the OCG suggest a reduction in the initial transmission power from high to low levels if a user decides on an energy-efficient strategy.

However, the greedy user's OCG versus MACI at different initial transmission powers is depicted in Fig. 3.7. The values of OCG fall as MACI increases. The fall from the user point of view is explained as follows. Low MACI ensures a high degree of freedom in selecting the power level it will use. Conversely, high MACI suppresses this freedom; hence a fall in the OCG factor. At 10 *m*Watts of the MAI powers, the parametric OCG was noted to be about 100 when the initial transmission power was 60 *m*Watts and about 200 when the initial transmission power was 100 *m*Watts. This implies that for a given MACI level and high initial powers, a greedy radio link increases its power selection rapidly in order to attain the

desired system stability. High transmission power decisions suppress MACI effects at the receiver, yielding reliable receiver decoding estimates. However, suppressing MACI effects at the receiver is a greedy behaviour that results in extra interference for other network users.

For different SINR thresholds or target values, five senders' transmission power iterations and the corresponding received SINR responses are illustrated in Figure 3.8 which depicts that for a random choice of the weighting factor of the designed cost function, that is, between zero and any positive large value, the transmission power iterations converge fast to a nearly fixed point, that is, after three sample epochs in sixty sample epochs of the total simulation time. Furthermore, all radio links can be noted to have met their target QoS, that is, each link has its received SINR as being above the SINR threshold. This implies that in this simulation run, the channel condition is favourable for successful transmission.

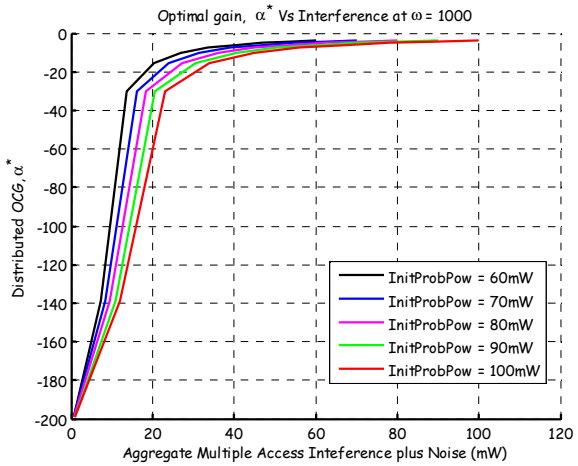

Figure 3.6: The optimal controller gain versus MACI for energy-efficient users

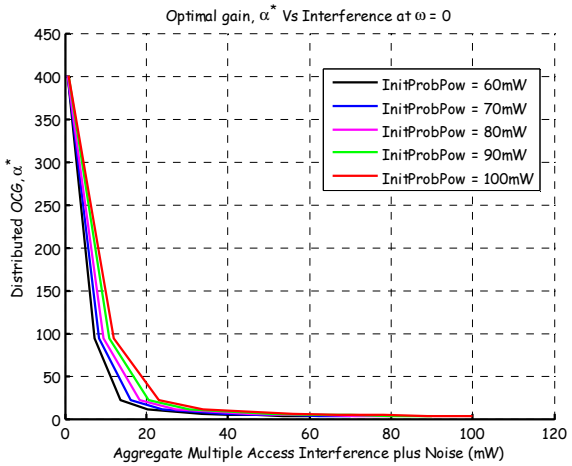

Figure 3.7: The optimal controller gain versus MACI for greedy users

Figure 3.9 depicts an autonomous DTPC policy in which a scalable MAC-TSP is incorporated in the model. It was noted that links 2, 4 and 8 demonstrate transmit power savings aperiodically between time 17-24 seconds and time 40-60 seconds. That is, if such links can compute their scheduling rates independently, they are able to determine whether or not to transmit at the optimal power level. Link 6 performs independent CCA and finds favourable network conditions. Link 6 then joins the network at these periods. In this manner, network capacity can significantly improve via the admission of other network users. The rest of the links execute iterative power selection throughout the steady state time. From the

network perspective, autonomous sleep, wake-ups and power selection procedures improve capacity and power savings.

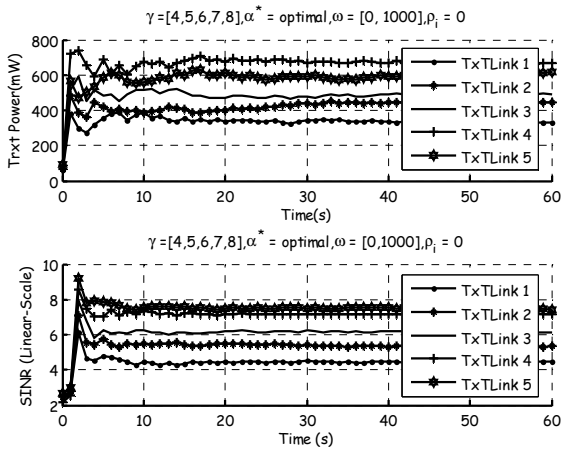

Figure 3.8: Autonomous adaptive transmission power execution

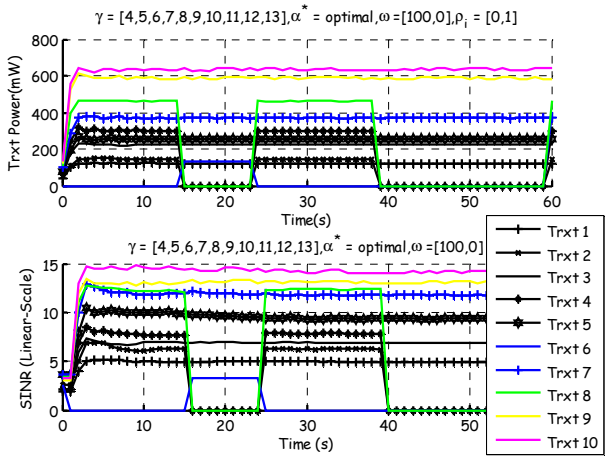

Figure 3.9: Autonomous dynamic power allocation incorporating power saving

In order to investigate the impact of the MAC-TSP based DTPC on throughput performance, additional simulation parameters were specified as: time slot duration = 100 msec, data packet duration = 80 msec, packet arrival rates were 12.8, 51.2, 89.6 and 128 packets per second, and the simulation time = 60 seconds.

Fig. 3.10 shows the impact of autonomous adjustment of the transmission power on the bit reception probability at different network traffic loads. Assuming independent MACI at each sender- receiver pair, the bit delivery ratio-power curve is a monotonically increasing curve. Such observation depicts a greedy algorithm in which case, each link strives to increase its transmission power in order to attain a reliable connection with its receiver. If the MACI and the traffic arrival rates are low then increasing the sender power yields a successful bit delivery ratio. However, the bit delivery ratio degrades for a high network traffic load. This implies that at high packet arrival rates, there are high multiple transmissions and collisions that degrade the bit reception probability. A similar observation can be reported for results in Fig. 3.11. That is, Fig. 3.11 illustrates that at different packet level arrival rates, the packet delivery ratio-transmission power curve monotonically increases. However, the power demand to send packets reliably to the receiver is high, that is, with a highly successful probability of delivery. In particular, over 20 *m*Watts, 40 *m*Watts and 60 *m*Watts of transmission power were needed, respectively to transmit 51.2, 89.6, 128 packets/s of the traffic load.

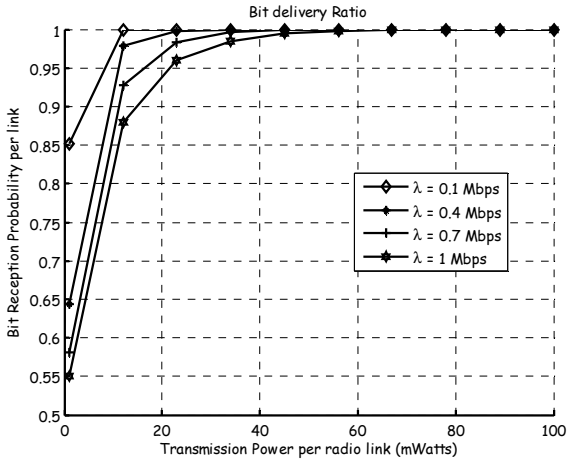

Figure 3.10: Bit delivery rate versus the transmission power

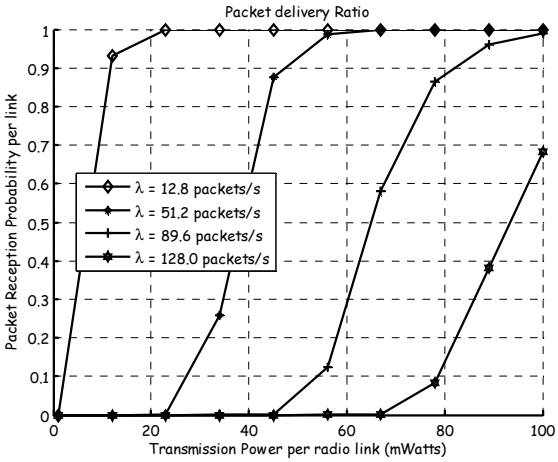

Figure 3.11: Packet rate versus the transmission power

In Fig. 3.12, a comparative performance analysis of average transmission powers after convergence is depicted. In general, the average transmission power drops exponentially as the number of sender users increases. However, the proposed cross-layer based dynamic power control (i.e., MATA-DTPC) indicates more power savings than the recently proposed iterative methods [12, 50]. In Fig. 3.12, 50% more power saving is evident at 15 users compared to the common base station-based method. This implies that the proposed method allows for network density scalability without sacrificing throughput performance.

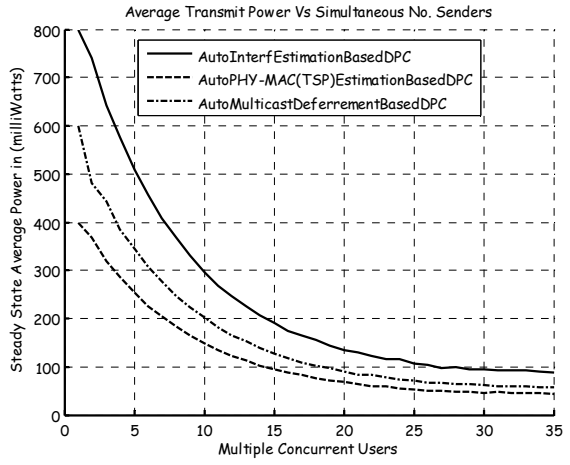

Figure 3.12: Power consumption versus network density

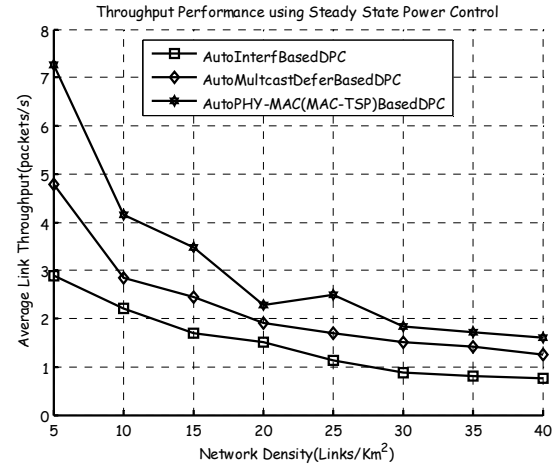

Figure 3.13: Average throughput performance at steady state power versus network density

Figure 3.13 reveals the average link throughput performance with respect to the network density in a square kilometre area. In the simulation, fixed locations of source devices and destination devices were assumed. The average steady state transmission power was used to send DATA packets between any two sender-receiver pairs or users in a local neighbourhood. Sources which could not reach their destinations when using steady state transmission powers did so through multiple hop packet forwarding by intermediate hops. The rate of packets that successfully reached the intended destination was measured and considered as the average link throughput. The same simulation environment was run for multiple interference estimation-type algorithms for unicast and multicast traffic connections [50].

The simulation results show that the average throughput performance degrades as the network becomes denser. This implies that collisions and interference are more likely when the network density grows larger. However, if each link possesses sufficient medium access information, then throughput can be improved significantly. In other words, the choice of optimal transmission power to use for a reliable successful reception depends on the PHY-layer parameters and concurrent activity of the network in the neighbourhood. Simulation results show that the MATA-DTPC method improves throughput performance compared to certain conventional algorithms.

3.6.2 Simulation Tests, Results and Discussions (GCOM)

For simulations, similar settings as in the case of MAC-TSP method are assumed. The power specifications of P*max* = 50 *m*Watts and P*min* = 0 *m*Watt, were assumed. In all simulation runs, we observed a monotonically increasing sequence of power response that converges to a fixed point. The GCOM based DTPC results in a stable SINR condition in the time limit at steady state.

In particular, for different target SINR thresholds, the transmission powers update, regarding five senders and the corresponding received SINR response, are depicted in Fig. 3.14. Figure 3.14 shows how five greedy sender nodes, that is, $\boldsymbol{\omega}=\mathbf{0}$, adjust their transmission powers via the optimum control gain $\boldsymbol{\alpha}^{*}$ in order to attain respective SINR, $\overline{\boldsymbol{\gamma}}=[4,5,6,7,8]$. If the GCOM is $\boldsymbol{\rho}=[\mathbf{0},\mathbf{1})$ for all senders, then each greedy sender attempts to increase its own transmission power selfishly and cause interference to the rest of the network users. Greedy optimal network users aim at achieving the target QoS. Thus, this method is rendered appropriate for delay sensitive traffic while still maintaining appropriate network scalability.

Figure 3.15 illustrates an energy-efficient transmission power adjustment performance and the corresponding received SINR performance. Each sender keeps its transmission power low enough relative to the perceived MACI powers by allocating itself $\omega_i(k) = 100$ and target SINR threshold values, assuming these are the same as shown in Fig. 3.14. The energy-efficient method result indicates that at a steady state more power saving occurs than that of the greedy method as depicted in Fig. 3.14. However, target SINR thresholds are not attained owing to low power modes. Lower power modes lead to network disconnectedness and poor network capacity performance [258]. However, the power saving method may be appropriate to bursty traffic applications which are tolerant of delays.

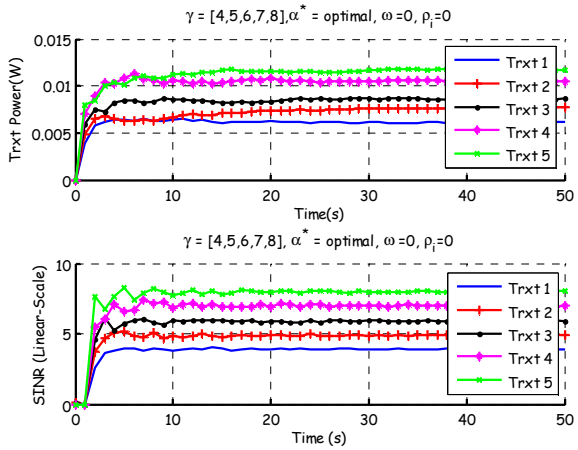

Figure 3.14: Transmission power execution for greedy users

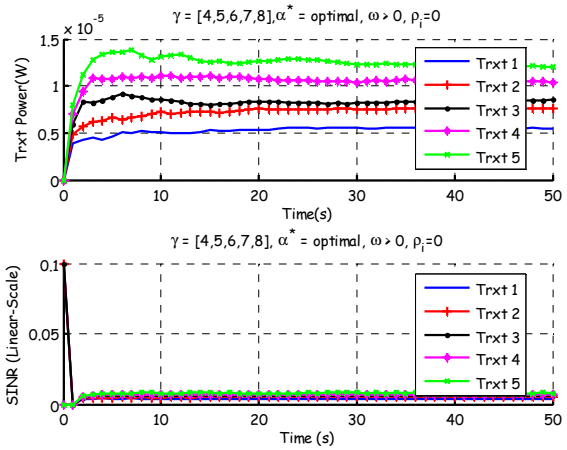

Figure 3.15: Transmission power execution for energy-efficient users

In Fig. 3.16 a random joint greedy and energy-efficient power control performance is depicted. This is useful in balancing power savings and throughput performance. The results depict the scenarios of active and inactive transmission states during a certain common period. The benefits are controlled excessive network interferences and enhanced co-existence feasibility within a given deployment location.

Figure 3.17 illustrates simulation results for a non-zero GCOM ($0 < \rho_i^{u_i} \leq 1$) incorporated in a greedy and energy-efficient DTPC method. In Fig. 3.17, sender 4, at the beginning of simulation, adjusts its transmission power to a value sufficiently minimal to achieve the target SINR threshold in the steady state. At a later time, say after 38 seconds, sender 4 chooses to opt-out of the network participation when an unfavourable channel condition arises. Sender 1 chooses to stay active in the network throughout the power control convergence and

continues to achieve the target QoS. The rest of the users remain inactive throughout the duration of the power control convergence and the transmission of a packet.

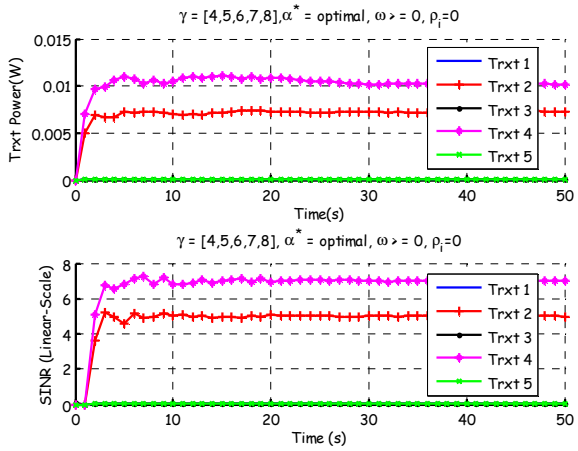

Figure 3.16: Senders 2 and 4 are greedy while senders 1, 3 and 5 are energy-efficient.

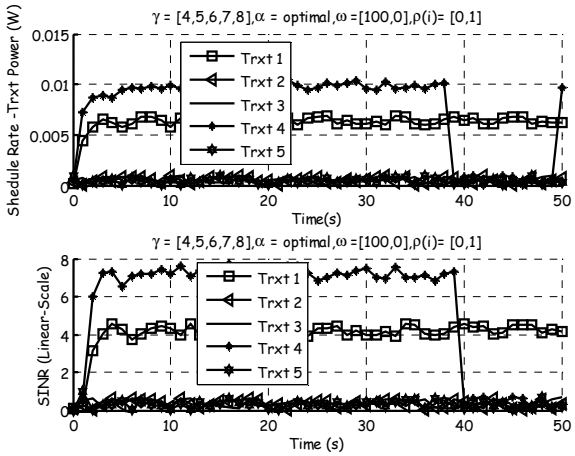

Figure 3.17: TSP based greedy and energy-efficient

Figure 3.18 depicts an average feasibility rate per network scenario versus the number of admitted sender users. The average feasibility rate (feasibility probability) indicates how many senders can be active simultaneously in a specific area without causing MACI significantly, that is, a case when the power vector $\mathbf{p}(k+1)$ converges to a unique fixed solution $\mathbf{p}^*$. Infeasibility implies that no successful transmission can be obtained and that the transmission power vector $\mathbf{p}(k+1)$ does not attain convergence to $\mathbf{p}^*$ in the long run. As shown in Fig. 3.18, the feasibility probability drops sharply as the number of simultaneous active senders increases. However, the proposed algorithm (i.e., based on the GCOM model) can accommodate slightly more active users than certain recently proposed algorithms [12, 50]. This is significant in improving the WMN capacity.

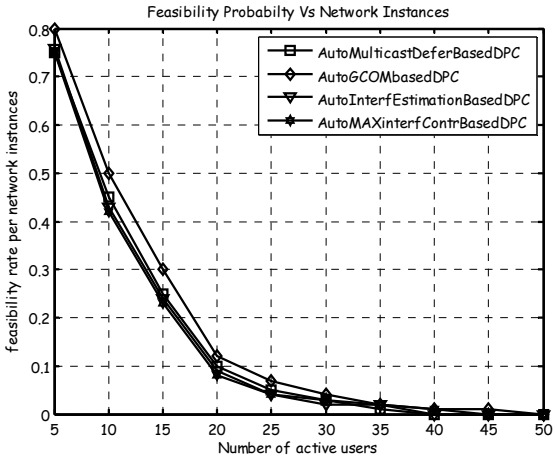

Figure 3.18: Feasibility probability versus number of senders

3.7 Chapter Conclusions and Remarks

In this chapter, a new decentralized dynamic power control (DTPC) scheme based on multiple co-channel access transmission awareness (MATA) has been proposed. The MATA-DTPC scheme is suitable for Wireless Backbone Mesh Networks (WBMNs) equipped with single radios operating on single channels. Two MATA-DTPC models have been formulated. Both are based on joint user-centric and network centric objectives. The first one was referred to as the medium access control dependent transmission scheduling probability (MAC-TSP) model that contains a convex cost function subject to MAC protocol constraints. The second one was referred to as the generalized cross-layer occupation measure (GCOM) model with a convex cost function subject to general cross-layer information interactions. Both models are managed at the Link-Layer.

Analytical results revealed that the DTPC scheme possessed optimal controller gain and transmission power value for each decentralized user. Both the gain and transmission power values were proved to converge to a steady state exponentially. Several simulation results demonstrated that the proposed MATA-DTPC scheme was both optimally greedy and energy-efficient depending on the MATA states. There was significant improvement in network feasibility, scalability and average throughput when the MATA-DTPC was compared with recent leading contributions.

The key contributions of this chapter are two-fold: Firstly, a generalized DTPC model has been derived, independent of medium access schemes (i.e., TDMA, FDMA, CSMA/CA,

CDMA, etc.) and WMN technologies (i.e., IEEE 802.11, IEEE 80.15, IEEE 802.16, etc.). Secondly, a scalable joint user and network centric DTPC strategy has been developed.

However, the MATA-DTPC scheme applies to single radio networks. Typically WBMNs are configured with multiple radios with access and route functionalities. Chapter 4 therefore discusses the DTPC scheme suitable for such networks.

Chapter 4

Multi-Radio Multi-Channel Wireless Networks: PMMUP Scheme

4.1 Introduction

This chapter addresses the problems of transmission power control in multi-radio multi-channel (MRMC) wireless networks. Such networks demand high energy resources during operation. The co-located radios and wireless channels experience cross-channel interference that degrades network capacity. Even if the signals are orthogonal when transmitted, the radio channel may affect this orthogonality. Time delays and lack of synchronization in the entire network as well as fading and other effects violate the orthogonality. Under these conditions, the receiver risks interference effects from adjacent channels. The MRMC configuration also introduces topology control problems arising from the increased dimension of non-overlapping channels and connectivity scenarios. In order to address interference problems and improve spectrum efficiency, several approaches have implemented channel assignments [20, 259, 260]. Also, topology control related problems have been addressed [59, 261]. However, such conventional approaches have assumed that high performing nodes are not subjected to power constraints. That is, all nodes are plugged into electrical power outlets during operation. Despite numerous recent works on joint power control and channel assignments [60, 183], the key emphasis has been placed on the minimization of maximum power output constraints. The motivation is to reduce interference and control network topology. Moreover, such methods require that the global network power constraints from all nodes be available to the central controller [262]. However, major challenges revolve around the need for scalability and the utilization of at least one power controlled channel for application traffic. This in turn results in the need for high throughput performance without compromising power conservation and topology stability [1].

Therefore, this chapter considers WBMNs utilizing MRMC capabilities. In order to achieve the desired energy-efficient network, the MRMC network is first divided into sets of unified channel graphs (UCGs). A UCG is defined as a set of radio interface pairs interconnected via a wireless medium sharing the same frequency channel. Under the decentralized paradigm, each wireless link or a *user* predicts Link State Information (LSI) consisting of signal-to-interference noise ratio (SINR), aggregate interference, packet transmission rate and the link connectivity range. The LSI may model network capacity and may allow for the evaluation of optimal transmission power signals, that is, each user minimizes a quadratic cost function of the LSI subject to the transmission power constraints. In order to coordinate the functions of different users, an energy-efficient power selection MRMC unification protocol (PMMUP) at the LL is proposed [21, 46, 48, 51, 52]. The PMMUP performs a *virtual* MAC at the LL and connects multiple MACs and radio interfaces with the unified higher layers. The PMMUP estimates the MRMC LSI variables and provides each user with LSI estimates from other UCGs and the total power constraints at a particular node. Figure 4.1 illustrates the basic PMMUP based DTPC scheme for WBMNs. The MRMC LSI are estimated and coordinated to each power control system of a particular UCG set. Based on MRMC LSI estimates, the optimal power control signals are then obtained for each active user.

This work leads to two main new algorithms. The first is based on the LSI interaction prediction called multi-radio multi-channel LSI interaction prediction (MRSIP) and the other is based on the LSI unification prediction called multi-radio multi-channel LSI unification prediction (MRSUP). The interaction prediction concerns LSI estimates from lower layers, while the unification prediction concerns LSI estimates from both lower and higher layers [52]. Analytical results have demonstrated that asynchronous predictions (i.e., MRSIPA and MRSUPA) converge rapidly with a linear rate. The rate of convergence depends on the chosen iteration interval and the interaction among users of different UCGs. The power control system of multi-users is stabilized in the Lyapunov sense. The simulation results confirmed the efficacy of the proposed algorithms. The performance of the MRSIPA method yielded interesting results. At different traffic loads, this method on average provided between 8.11% and 87.87% transmission power saving after the system reached a steady state, compared to other related approaches. Also, at different traffic loads, the MRSIPA yielded on average between 16.67% and 80.00% throughput gain per node-pair while transmitting with steady state powers compared to recent works [41, 45, 183]. The reason for significant power saving and throughput gains has been attributed to the fact that MRSIP

(asynchronous) has a simple computational structure and low information interaction overhead costs across-multiple layers.

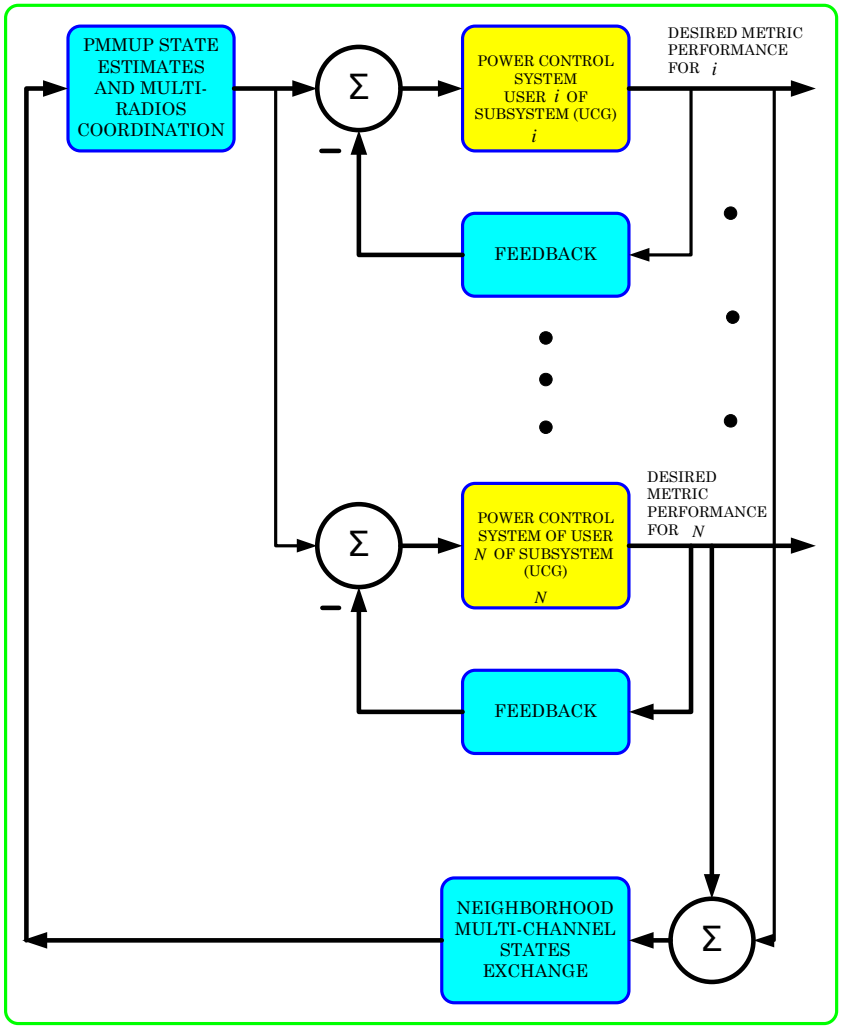

Figure 4.1: Basic block diagram of PMMUP based DTPC for BWMNs

Tables 4.1 and 4.2 summarize the definitions of abbreviations and notations used in the rest of this chapter.

Table 4.1: Abbreviation

Abbreviation	***Description***
ACI	Adjacent Channel Interference
DCA-DPC	Dynamic Channel Assignment with Power Control Protocol
EBIA	Effective Band Interference Aware Power Control Scheme
LSI	Link State Information
MRMC	Multi-radio Multi-channel Wireless System

MRSIP	MRMC LSI Interaction Prediction (Asynchronous and Synchronous)
MRSUP	MRMC LSI Unification Prediction (Asynchronous and Synchronous)
MUP	Multi-radio Unification Protocol
NICs	Network Interface Cards or radio interfaces or devices
PMMUP	Link Layer Power Selection MRMC Unification Protocol
UCG	Unified Channel Graph

Table 4.2: Notation

Notation	***Description***
Ω_i	A set of co-located radio devices in the neighbourhood of user i
$p_i(t+1)$	The next time-slot transmission power level of user i
$\tilde{I}_i(t)$	Effective band interference at both terminals of user i
$\tilde{\mathbf{x}}_i(t)$	LSI interaction vector of user i
$\mathbf{u}_i(t)$	Transmission power input control vector of user i
$\mathbf{y}_i(t)$	LSI available to user i and coordinated from other channels
$\boldsymbol{\pi}_t^i$	Cross-channel coordinated weight at user i and time slot t
$\boldsymbol{\varphi}_t^i$	Higher layers coordinated weight vector at user i and time slot t
H	Effective channel gain of user i
$\mathbf{P}_k$	Idempotent and stabilizing matrix solution to a control problem at time instant k
$\mathbf{F}$	Feedback regulator matrix of the control system

4.2 Network Model

4.2.1 Unified Channel Graph

Consider a wireless MRMC multi-hop WBMN (see Fig. 4.2), operating under dynamic channel conditions [142]. Let us assume that the entire WBMN is virtually divided into $\|L\|$ UCGs, each with a unique non-overlapping frequency channel. Further, let each UCG comprise $\|V\| = N_V$, network interface cards (NICs) or radio devices that connect to each other, possibly via multiple hops [54]. These transmit and receive NIC pairs are termed as users within a UCG. Successful communication is only possible within a common UCG; otherwise inter-channel communication is not feasible. Thus, each multi-radio mesh point (MP) node or wireless mesh router (WMR) is a member of at least one UCG. In practice, the

number of NICs denoted as $\|T_A\|$, at each MP node is less than the number of UCGs denoted as $\|L_A\|$, associated with that node, i.e., $\|T_A\| < \|L_A\|$. Each UCG set is represented as l, $\forall l \in L$ and the entire WBMN is viewed by the higher layers of the network protocol stack as unions of all UCG sets, that is, $l_1 \cup l_2 \cup l_3 \cup \ldots \cup l_{\|L\|}$. Utilizing the UCG model, transmission power optimization can then be locally performed within each UCG lower level, yet managed by the LL. The cross-channel LSI estimates are coordinated by the LL. Through higher level coordination, independent users are fairly allocated shared memory, central processor and energy resources [52].

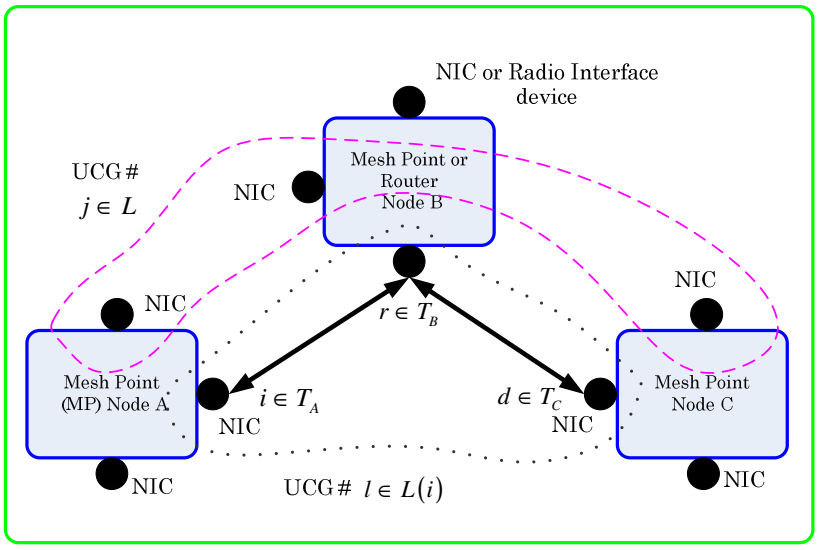

Figure 4.2: MRMC multi-hop WBMN:

In Figure 4.2, each Wireless Mesh Router (WMR) is assumed to have a single power supply. Node A has $\|T_A\|$ network interface cards (NICs) and $\|L_A\|$ non-overlapping frequency channels. Node B and C have, $\|T_B\|$ and $\|T_C\|$ NICs, respectively. Source NIC i can communicate with destination device d through multiple hop relays (routers), i.e., r. Devices can randomly switch among different channels so that each channel is maximally utilized during most of the operation time. However, the criterion of channel switching depends on the channel with the best channel quality as observed by the Link-Layer [41].

Based on the UCG model depicted in Figure 4.2, there exists an established logical topology, where some devices belonging to a certain UCG are *sources* of transmission, say $i \in T_A$ and some devices act as 'voluntary' *relays*, say $r \in T_B$ to *destinations*, say $d \in T_C$. A sequence of connected *logical links* forms a *route* originating from source i. It should be noted that each asymmetrical physical link may need to be regarded as multiple logical links due to multiple channels [84]. Adjacent channels actively transmitting packets

simultaneously cause adjacent channel interference (ACI) owing to their close proximity. The ACI can partly be reduced by dynamic channel assignment if implemented without run time overhead costs [19]. In this thesis, static channel assignment is assumed for every transmission time slot. Such an assumption is reasonable since the transmission power optimization is performed only by actively transmitting radios, to which channels have been assigned by the higher layers of the network protocol stack. It is pointless setting the time-scales for channel assignments greater than or matching that of power executions since the WMRs are stationary. Furthermore, modern WMRs are built on multiple cheap radio devices to simultaneously perform multi-point to multi-point (M2M) communication. Indeed, network accessing and backbone routing functionalities are effective while using separate radios [6]. Each actively transmitting user acquires the medium through carrier sensed multiple access with collision avoidance (CSMA/CA) [263]. Such users divide their access time into a transmission power optimization mini-slot time and a data packet transmission mini-slot time interval. For analytical convenience, time slots will be normalized to integer units $t \in \{0,1,2,\ldots\}$ in this chapter.

4.2.2 Adjacent Channel Interference

Let Figure 4.3 depict the interference modelling for a multi-hop UCG. If during time slot t NIC $i \in \Omega_i$ on channel $l \in L(i)\ \forall l$ randomly selects a transmission power $p_i^r(t) \in \Pi_i$ to multicast pending packets in its queue $q_i(t) > 0$ to a set of relaying devices, say $r \in \Omega_r$ on channel $l \in L(i)$, then its transmission interferes with simultaneous transmissions in its neighbourhood (a well known problem of exposed terminals [109]). Terminals, say $m \in \Omega_m$ transmitting to terminal $j \in \Omega_r$ (see Fig. 4.3) at time slot t cause interference at the receiving device r. The net instantaneous co-channel interference (CCI) at the beginning of time slot t at device r is given as in [142]. The net ACI, that is, from Figures 4.2 and 4.3 can be modelled as

$$I_{-i,l}^{ACI}(t) = \sum_{m \in \Omega_m, m \neq i} G_{m,l}^{r}(t) \sum_{l \in \{1,..L\}} \sum_{\substack{j \in \Omega_r \\ q_{m,l} > 0,\ x_{m,l}^{r} > 0}} c_{im} p_{m,l}^{j}(t) + c_{im} x_m^j \delta\left(p_{m,l-1}^{j}(t) + p_{m,l+1}^{j}(t)\right)$$

$$- G_{i,l}^{r}(t) \sum_{l \in \{1,\ldots,L\}} \sum_{\substack{j \in \Omega \\ j \neq r}} x_{i,l}^{j} \; p_{i,l}^{j}(t) \; + \delta \, x_{i}^{j} \left(p_{i,l-1}^{j}(t) + p_{i,l+1}^{j}(t) \right) + \eta_{r,l}(t),$$

$$= I_{r,l}^{ACI}(t) - G_{i,l}^{r}(t) \sum_{l \in \{1 \ldots L\}} P_{i,l}^{sum}(t) + \eta_{r,l}(t). \qquad (4\text{-}1)$$

Here, $G_{m,l}^{r}(t), G_{i,l}^{r}(t) \in \Re$ are asymmetrical wireless channel gains from senders m and i, respectively to receiver r on the lth UCG. The coding orthogonality coefficients at the senders are denoted as $c_{im}(t) \in \Re$ and defined as $c_{im}(t) = \begin{cases} 1 & \text{if i = m} \\ 0 & \text{otherwise} \end{cases}$. Such codes are spread along the common wireless spectrum to permit the interference-limited simultaneous transmissions of multiple neighbouring nodes [147]. The transmission activity constraints on the frequency channel l are $x_{m,l}^{j}(t), x_{i,l}^{j}(t) \in \{0,1\}$. These constraints describe whether a radio device is transmitting or dormant. The thermal noise at the receiver r is $\eta_{r,l}(t) \in \Re$. The transmission power leakage factor between neighbouring adjacent channels is $0 \leq \delta \leq 1$. This factor signifies the fraction of the transmission power causing interference between any two closely-separated wireless channels.

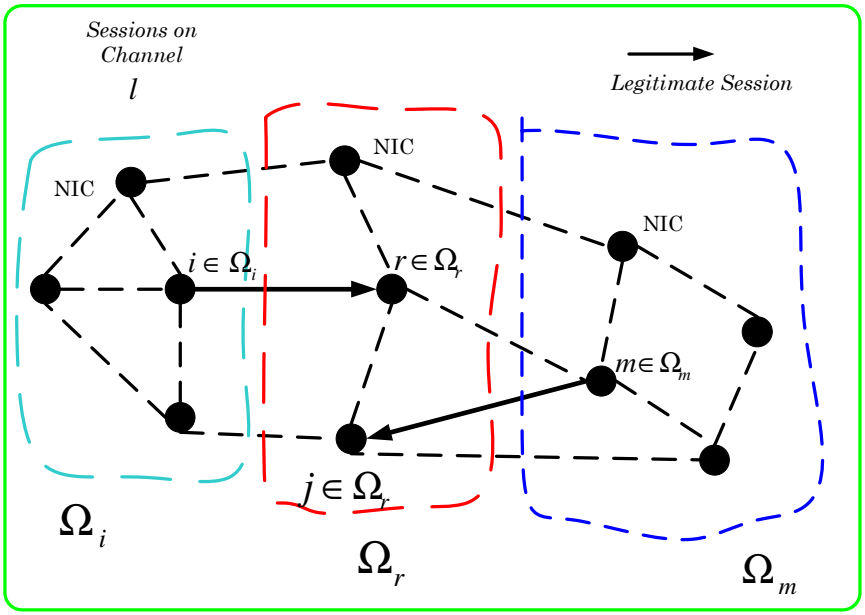

Figure 4.3: Interference model for *i*th transmission in a multi-hop UCG network

4.2.3 Basic Power Control

Each sender MP node initiates transmission by first gathering neighbour information using a fraction of a full or maximum power level known as the *probing power level* [142]. The probing power level is constrained by the amount of energy available at that node. For example, with respect to a communication link between a NIC a and a set of immediate neighbours Ω_a, the probing power level constraint at a multiple radio node is $\sum_{i\in\{1,\ldots N\}}\sum_{b\in\Omega_a} p_{ab}^{i}(t)\le p_{MP}^{\max}$, where i is an ith radio device and N the number of radios at the node. In addition to energy-awareness, NICs adapt transmission power levels based on the local channel environment $p_{ab}\left(G_{ab}(t),t\right)$. Conditions of the channel environment are probed through a request-to-send and clear-to-send (RTS/CTS) protocol [109]. This protocol allows NICs to sense whether the channel between the sender and the receiver pair is busy or not. The work in [45] utilized this protocol to extend the closed loop dynamic power control by [12]. The new algorithm is based on effective band interference (EBI) [45]. The algorithm is referred to as the EBIA and executes as

$$p_i(t+1)=\begin{cases} p_i(t)+\alpha_i(t)I_{(i,r)}(t) & \text{if } q_i(t)>0 \\ 0, & \text{otherwise} \end{cases}, \tag{4-2}$$

where EBI is denoted as $I_{(i,r)}(t)\triangleq\varsigma I_i(t)+(1-\varsigma)I_r(t)$, for $0\le\varsigma\le1$. Exploiting both forward and backward message signalling, each user autonomously estimates interferences at both the receiver and sender during each time slot [12, 45] in order that a node can choose power levels judiciously so as not to interrupt legitimate active sessions in its neighbourhood. Moreover, hidden terminal nodes at the receiver terminal can be exposed to allow the sender terminal to select an appropriate transmission power level. Finally, the feedback control gain $\alpha_i(t)\in\Re$ in equation (4-2) is defined as a time-variant sequence [12] because the channel quality is assumed to change from one time slot to the other. The well known Kalman filter is utilized to compensate for the channel condition uncertainties [156].

It is worth noting from (4-2) that if packets exist in a queue, that is, $q_i(t)>0$, then a device (NIC) decides to transmit with one step predicted power levels, that is, $p_i(t+1)\ge1$

*m*Watts. Otherwise it decides to become dormant, that is, $p_i(t+1) = 0$ *m*Watt, a condition that saves transmission power significantly [208].

In order to address the network capacity problem, we emphasize that the level of transmission power determines the quality of the received signal expressed in terms of signal-to-interference plus noise ratio (SINR) and the range of a transmission [76]. The range of the transmission determines the amount of interference a user creates for other users, hence the level of medium access contention. Interference, in turn, impacts on the link achievable rate [262]. These network capacity issues are what this thesis considers as Link State Information (LSI) based power control problems. Based on the LSI estimates, the decentralized power control strategy for each sender-receiver pair (i.e., user) on the *l*th UCG can be defined as [46, 52],

$$p_l(t+1) = \begin{cases} p_l(t) + f_l(\mathbf{x}) & \forall \mathbf{x} \in \{\mathbf{x}\} \quad \text{if Queue} > 0 \ \text{ and Residual\_Energy} > 0 \\ 0\,, & \text{otherwise} \end{cases} \quad , \quad (4\text{-}3)$$

where $f_l(\mathbf{x}) = f_l\left(\beta_l(t), I_l(t), \Gamma_l(t), R_l(t)\right)$. It is a non linear function of the LSI estimates. The LSI estimates are denoted by $\beta_l(t)$, $I_l(t)$, $\Gamma_l(t)$, $R_l(t)$ as the actual SINR, aggregate co-channel network interference, actual transmission rate and connectivity range of a particular user during time slot t. Using the Taylor series to obtain first order linear approximations to $f_l(\mathbf{x})$ gives

$$f_l(\mathbf{x}) \triangleq f\left(\gamma_l^{ss}, I_l^{ss}, \Lambda_l^{ss}, R_l^{ss}\right) + \alpha_\beta\left(\beta_l(t) - \gamma_l^{ss}\right) + \alpha_I\left(I_l(t) - I_l^{ss}(t)\right) + \alpha_\Gamma\left(\Gamma_l(t) - \Lambda_l^{ss}\right) + \alpha_R\left(R_l(t) - R_l^{ss}\right), \quad (4\text{-}4)$$

where γ_l^{ss}, I_l^{ss}, Λ_l^{ss} and R_l^{ss} are the steady state LSI values describing the target SINR, co-channel interference [12], link capacity and the transmission range values, respectively [264].

4.2.4 State Space Model

This subsection demonstrates the predictive LSI models that describe network capacity, transmission energy and connectivity. The LSI models permit the evaluation of the transmission power levels by each user in every UCG of the WBMN.

SINR deviation problem: The aim is to select a transmission power sequence $\{p_l(t)\}$ such that the actual SINR levels $\{\beta_l(t)\}$ will track the target SINR level $\{\gamma_l(t)\}$. Thus, using $p_l(t+1)$ in equation (4-3) and the EBIA scheme given by (4-2), the SINR state equation [12, 156] becomes,

$$\beta_l(t+1) = \frac{p_l(t+1)G_{ll}(t+1)}{I_l(t+1)} \ . \tag{4-5}$$

Let $\frac{G_{ll}(t+1)}{I_l(t+1)} = H(t)\frac{m(t)}{n(t)}$ be defined as the predicted effective channel gain with $m(t)$ and $n(t)$ which are Gaussian independent unit mean noise terms with the same variance σ_m^2. By Substituting $p_l(t+1)$ from (4-3) into (4-5) and maintaining the definition of $f_l(\mathbf{x})$ in (4-4), one obtains the SINR deviation:

$$e_\beta(t+1) = \beta_l(t+1) - \beta_l(t)\frac{m(t)}{n(t)} - H(t)\frac{m(t)}{n(t)} f\left(\gamma_l^{ss}, I_l^{ss}, \Lambda_l^{ss}, R_l^{ss}\right),$$

$$\begin{aligned} e_\beta(t+1) = {} & H(t)\frac{m(t)}{n(t)}\alpha_\beta\left(\beta_l(t) - \gamma_l^{ss}\right) + \\ & H(t)\frac{m(t)}{n(t)}\alpha_I\left(I_l(t) - I_l^{ss}\right) + H(t)\frac{m(t)}{n(t)}\alpha_\Gamma\left(\Gamma_l(t) - \Lambda_l^{ss}\right) + \\ & H(t)\frac{m(t)}{n(t)}\alpha_R\left(R_l(t) - R_l^{ss}\right). \end{aligned} \tag{4-6}$$

Here, $m(t)$ characterizes the slowly changing shadow-fading and the fast multipath-fading on top of the distance loss [265]. The noise term $n(t)$ models the fluctuation when radio interfaces increase or decrease their transmission power levels.

Aggregate interference problem: Each user desires to select the transmission power sequence $\{p_l(t)\}$ such that the actual network interference $\{I_l(t+1)\}$ including its own transmission interference to other network users is minimized. Making use of $p_l(t+1)$ in (4-3), the network interference state equation is modelled in a similar way to (4-6) and is given as

$$\begin{aligned} I_l(t+1) &= p_l(t+1)G_{ll}(t+1) + I_{(i,r),l}(t+1) \\ &= \left[p_l(t) + f_l(\mathbf{x})\right]G_{ll}(t)m(t) + I_{(i,r),l}(t)n(t) \\ e_I(t+1) &= G_{ll}(t)m(t)\alpha_\beta\left(\beta_l(t)-\gamma_l^{ss}\right) + G_{ll}(t)m(t)\alpha_I\left(I_l(t)-I_l^{ss}\right) + \\ &\quad G_{ll}(t)m(t)\alpha_\Gamma\left(\Gamma_l(t)-\Lambda_l^{ss}\right) + G_{ll}(t)m(t)\alpha_R\left(R_l(t)-R_l^{ss}\right). \end{aligned} \quad (4\text{-}7)$$

Link rate deviation problem: The aim is to select the power control sequence $\{p_l(t)\}$ in such a way that the actual transmission rate $\{\Gamma_l(t+1)\}$ will not exceed the achievable link capacity $\Lambda_l(t)$. Let the transmission power optimization be performed immediately after the neighbour discovery and frequency channel assignment so that $SINR_l(t) \gg 1$, that is, $G_{ll}(t)\,p_l(t) > I_l(t)$. The wireless link transmission rate then becomes

$$\begin{aligned} \Gamma_l(t+1) &= \log p_l(t+1) + \log G_{ll}(t+1) - \log I_{(i,r),l}(t+1), \\ &= \log\left[p_l(t) + f_l(\mathbf{x})\right] + \log G_{ll}(t) + \log m(t) - \log I_{(i,r),l}(t) - \log n(t). \end{aligned}$$

Let $p_l(t) \geq f_l(\mathbf{x})$, since $p_l(t) > 0$ when $q_l(t) > 0$ and $f_l(\mathbf{x}) \approx 0$ when $\mathbf{x} = 0$ [142]. Therefore,

$$\Gamma_l(t+1) \triangleq \log p_l(t) + \log\left[1 + \frac{f_l(\mathbf{x})}{p_l(t)}\right] + \log G_{ll}(t) + \log m(t) - \log I_{(i,r),l}(t) - \log n(t).$$

But, $\log[1+x] \approx x$, where $0 < x < 1$. Thus, the transmission rate deviation from the target value becomes [46]

$$e_{\Gamma}(t+1)=\frac{1}{p_l(t)}\begin{bmatrix}\alpha_{\beta}\left(\beta_l(t)-\gamma_l^{ss}\right)+\alpha_I\left(I_l(t)-I_l^{ss}\right)+\\ \alpha_{\Gamma}\left(\Gamma_l(t)-\Lambda_l^{ss}\right)+\alpha_R\left(R_l(t)-R_l^{ss}\right)\end{bmatrix}+\log m(t)-\log n(t). \quad (4\text{-}8)$$

Network connectivity problem: The connectivity range modelled as a function of the selected transmission power sequence $\{p_l(t)\}$ was given in [51]. Let

$\log R_l(t+1)=\frac{1}{\nu}\log\left(p_l(t)+f_l(\mathbf{x})-\kappa\right)$, with $\kappa\in\Re\geq 0$ and $2\leq\nu\leq 6$, where κ is a certain constant and ν is the path loss exponent (PLE). The PLE depends on the physical environmental conditions [146]. The connectivity range deviation from the target value is given as,

$$e_R(t+1)=\frac{1}{\nu p_l(t)}\alpha_{\beta}\left(\beta_l(t)-\gamma_l^{ss}\right)+\frac{1}{\nu p_l(t)}\alpha_I\left(I_l(t)-I_l^{ss}\right)+$$
$$\frac{1}{\nu p_l(t)}\alpha_{\Gamma}\left(\Gamma_l(t)-\Lambda_l^{ss}\right)+\frac{1}{\nu p_l(t)}\alpha_R\left(R_l(t)-R_l^{ss}\right). \quad (4\text{-}9)$$

Let $\mathbf{x}_l\triangleq\left(\beta_l-\gamma_l^{ss}\;\; I_l-I_l^{ss}\;\; \Gamma_l-\Lambda_l^{ss}\;\; R_l-R_l^{ss}\right)^T$ be LSI deviations of a control system [266]. Combining equations (4-6), (4-7), (4-8) and (4-9) and introducing a control input sequence term, we obtain

$$\mathbf{x}_l(t+1)=\mathbf{A}_l\,\mathbf{x}_l(t)\;+\mathbf{B}_l\,\mathbf{u}_l(t)\;+\;\varepsilon_l(t), \quad (4\text{-}10)$$

where $\mathbf{A}_l$ is a 4 x 4 coefficient matrix given by

$$\mathbf{A}_l=\begin{pmatrix}\frac{m}{n}H\alpha_{\beta} & \frac{m}{n}H\alpha_I & \frac{m}{n}H\alpha_{\Gamma} & \frac{m}{n}H\alpha_R\\ mG\alpha_{\beta} & mG\alpha_I & mG\alpha_{\Gamma} & mG\alpha_R\\ \frac{\alpha_{\beta}}{p_l} & \frac{\alpha_I}{p_l} & \frac{\alpha_{\Gamma}}{p_l} & \frac{\alpha_R}{p_l}\\ \frac{\alpha_{\beta}}{\nu p_l} & \frac{\alpha_I}{\nu p_l} & \frac{\alpha_{\Gamma}}{\nu p_l} & \frac{\alpha_R}{\nu p_l}\end{pmatrix},\quad\text{and}\quad \mathbf{B}_l\mathbf{u}_l(t)=\begin{bmatrix}u_{\beta}(t)\\ u_I(t)\\ u_{\Gamma}(t)\\ u_R(t)\end{bmatrix}$$ characterizes the

control sequence that needs to be *added* to the $p_l(t+1)$ equation (4-3) in order to maximize the network capacity. $\mathbf{B}_l$ is assumed to be a 4 x 1 coefficient matrix. The state stochastic

shock term $\varepsilon_l(t)$ is a 4 x 1 random Gaussian distributed vector with zero mean and covariance matrix

$$\Theta_\varepsilon = \mathrm{E}\varepsilon_l(t)\varepsilon_l^T(t) = diag\left(\sigma_\beta^2, \sigma_I^2, \sigma_\Gamma^2, \sigma_R^2\right). \tag{4-11}$$

From Equation (4-10), driving the SINR deviation and link rate deviation to as minimal a value as possible, benefits the individual user. On the other hand, ensuring low aggregate network interference is beneficiary to network users. It is important that each user selects the transmission power sequence so as to maintain joint user and network-centric LSI deviations as minimal a value as possible. This can be achieved by weighting the LSI deviation vector as

$$\boldsymbol{\omega}^T \mathbf{x}_l(t) \triangleq \tilde{\mathbf{x}}_l(t), \tag{4-12}$$

where $\boldsymbol{\omega}^T = \left(\omega_{l1} \quad \omega_{l2} \quad \omega_{l1} \quad \omega_{l1}\right)$ are weights such that the higher layer unification protocol assigns users according to the available energy constraints [12]. Intuitively, if $\omega_{l1} > \omega_{l2}$, then it implies the availability of more energy resources. Users adjust powers increasingly to maintain the target SINR, queue size level, throughput and proper connectivity range. Conversely, when $\omega_{l2} > \omega_{l1}$ it implies a energy supply shortage. Users judiciously adjust the transmission power to keep the network interference as low as possible. Consequently, denote the energy assignment ratio as $\omega_l = \omega_{l2} / \omega_{l1} \in \Re^+$ such that $\omega_l \in [0, \infty] \ \forall l \in L$.

4.3 MRMC Wireless System Controller

4.3.1 State Space Models for Multiple UCGs

If at each MP node there are N NICs tuneable to $\|L\|$ orthogonal channels (UCGs), then at each node the state space equation (4-10) becomes

$$\tilde{\mathbf{x}}(t+1) = \mathbf{A}(t)\tilde{\mathbf{x}}(t) + \mathbf{B}(t)\mathbf{u}(t), \ \tilde{\mathbf{x}}(0) = \tilde{\mathbf{x}}_0, \tag{4-13}$$

where $\tilde{\mathbf{x}} \in \Re^{nN}$, $\mathbf{u} \in \Re^{M}$, $\mathbf{A} \in \Re^{nN \times nN}$, $\mathbf{B} \in \Re^{nN \times M}$, M is the size of the control input vector for all active users associated with a single node and n is the dimension of LSI estimates at each user.

It should be noted from (4-13) that firstly, the structural complexity of the MRMC configuration increases with the size of NICs, the channels (UCGs), and the control input vector. Secondly, the number of NICs on one router may be different from that of another router, that is, owing to the heterogeneity of the WBMN [1]. Thirdly, owing to the diverse fading channel conditions, LSI dimensions may vary from one frequency channel or UCG set to the other. Therefore, channel power optimizations executed between multi-radio nodes may be complex and impractical with large network dimensions. For these reasons, (4-13) is decomposed into N interconnected subsystems (network users) each of LSI dimension n. Let $\|L\| \geq N$, without loss of generality. Because power control is only performed by actively transmitting radios on a pre-assigned number of channels at any given time, one can let $\|L\| = N$ as a worst case MRMC configuration at run time. The simplified multi-radio multi-channel state space (MMSS) model representation becomes [266, 267]

$$\tilde{\mathbf{x}}_i(t+1) = \mathbf{A}_i(t)\tilde{\mathbf{x}}_i(t) + \mathbf{B}_i(t)\mathbf{u}_i(t) + \mathbf{C}_i(t)\mathbf{y}_i(t) + \varepsilon_i(t), \quad \tilde{\mathbf{x}}_i(t_0) = \tilde{\mathbf{x}}_{i0}, \ \forall i \qquad (4\text{-}14)$$

where $\mathbf{y}_i(t)$, introduced in (4-14), is a linear combination of states (LCS) from other UCGs available to the ith network user belonging to UCG l. This LCS is defined as

$$\mathbf{y}_i(t) = \sum_{\substack{j=1 \\ j \neq i}}^{N} \mathbf{L}_{ij}(t)\tilde{\mathbf{x}}_j(t) + \varepsilon_i^{y}(t), \qquad (4\text{-}15)$$

where $\varepsilon_i^{y}(t)$ denotes Gaussian distributed coordination process shocks with zero mean and the covariance matrix is denoted as $\Theta_{\varepsilon} = \mathrm{E}\varepsilon_i^{y}(t)\varepsilon_i^{yT}(t)$, $\mathbf{C}_i(t)$ is considered to be a $n \times n$ identity matrix and $\mathbf{L}_{ij}(t)$ is the higher level interconnection matrix of states between ith network user and jth network user. This interconnection matrix needs to be evaluated by an energy-efficient multi-radio unification protocol (MUP) implemented at the LL.

4.3.2 Problem Formulation

In what follows, the control problem for each user is formulated as the minimization of the following stochastic quadratic cost function subject to the network interaction LSI equation (4-14) and coordination LSI in equation (4-15):

$$J_i = E\left[\lim_{t\to\infty}\frac{1}{t}\sum_{\tau=0}^{t-1}\tilde{\mathbf{x}}_i^T(\tau)\mathbf{Q}_i(\tau)\tilde{\mathbf{x}}_i(\tau)+\mathbf{u}_i^T(\tau)\mathbf{R}_i(\tau)\mathbf{u}_i\right],$$

$$=\lim_{t\to\infty}\frac{1}{t}\sum_{\tau=0}^{t-1}\sum_{\tilde{\mathbf{x}}_i\in\{\tilde{\mathbf{x}}\}}\sum_{\mathbf{u}_i\in\{\mathbf{u}\}}\left[\tilde{\mathbf{x}}_i^T(\tau)\mathbf{Q}_i(\tau)\tilde{\mathbf{x}}_i(\tau)+\mathbf{u}_i^T(\tau)\mathbf{R}_i(\tau)\mathbf{u}_i(\tau)\right]\rho_i(\tilde{\mathbf{x}}_i,\mathbf{u}_i)\cdot$$

Subject to: Equations (4-14) and (4-15). (4-16)

Here, $\mathbf{Q}_i(t)\in\Re^{n\times n}\geq\mathbf{0}$ is an assumed symmetric, positive semi-definite matrix and $\mathbf{R}_i(t)\in\Re^{M\times M}>\mathbf{0}$ is also an assumed symmetric, positive definite matrix. These matrices signify state and control input penalties, respectively [268]. In the sequel, for simplicity $\mathbf{Q}_i$ is chosen to be an identity matrix and $\mathbf{R}_i$ to be a matrix of unity entries. The quadratic cost function in (4-16) has a robust and fast tracking rate [107]. The joint probability density function (pdf) $\rho_i(\tilde{\mathbf{x}}_i,\mathbf{u}_i)$ denotes the cross-layer occupation measure (COM). The COM is defined as $\rho_i(\tilde{\mathbf{x}}_i,\mathbf{u}_i)=\Pr(\mathbf{u}_i\mid\tilde{\mathbf{x}}_i)\sum_{\mathbf{u}_i\in\{\mathbf{u}_i\}}\rho_i(\tilde{\mathbf{x}}_i,\mathbf{u}_i)$. It gives the steady state probability that the control system is in state $\tilde{\mathbf{x}}_i\in\{\tilde{\mathbf{x}}\}$ and the driving control parameter $\mathbf{u}_i\in\{\mathbf{u}_i\}$ is chosen [35]. Vector $\tilde{\mathbf{x}}_i$ is of dimension n, i.e., $n=4$ and is assumed to be Gaussian distributed [269]. The evaluation of the pdf follows the Gaussian multiple model adaptive estimator (MMAE) of parameters and states proposed by Ormsby, *et al.* [269]. Thus, we can seek an optimal $\mathbf{u}_i\in\{\mathbf{u}_i\}$ that solves the problem in (4-16). However, due to high level inter-channel LSI coordination matrices involved in the solution of (4-16), an energy-efficient power selection multi-radio multi-channel unification protocol (PMMUP) has been proposed recently [21, 46, 52].

4.4 PMMUP Description

4.4.1 Architecture

The PMMUP: V-MAC architecture is illustrated in Fig. 4.4. It is a *virtual* MAC built on top of the legacy IEEE 802.11 MAC and is required to operate with existing hardware [41]. The PMMUP periodically performs neighbour discovery using a probe power level equal to a fraction of the maximum power level. The PMMUP coordinates optimal power selection. State information from multiple channels, influencing power selection process is stored in the neighbour communication power and states (NCPS) table. The NCPS table is shown in Table 4.3. The PMMUP updates NICs with the unification variables such as the residual energy in a node, information from higher layers and coordinated variables from other UCGs.

Neighbour discovery: At start-up, the NICs of a node are tuned to orthogonal UCGs [58]. The PMMUP initiates communication using an address resolution protocol (ARP) message broadcast over all radio interfaces [41]. Each radio interface sends these messages to neighbours in their corresponding UCGs with a fraction of maximum power as instructed by the PMMUP. Upon receiving the ARP requests, the destination node sends the ARP responses with the MAC addresses of the NICs on which it received the ARP requests. Once the originating host receives the ARP responses it proceeds to communicate with the interface from which it received the ARP responses. The PMMUP begins the PMMUP discovery process with already discovered neighbours. Nodes that support PMMUP are classified as PMMUP enabled nodes, otherwise termed as legacy nodes.

Power selection process: The PMMUP chooses initial probing power and then broadcasts messages to all radio interfaces. This fraction of the maximum power level is vital for the neighbour discovery process with low network flooding effects. One can refer to the total probing power over the interfaces as *tot-ProbPow*. The energy residing in a node is referred to as *Energy Reserves.* The transmission power selection protocol is summarized by Algorithm 4.1.

Algorithm 4.1: Summary of the Energy-efficient power selection

1. If (*tot-ProbPow* > *the Energy Reserves* and *Load Queue* => *0 at the NICs)*
2. Each NIC selects a zero transmission power level => Dozing Mode.
3: else
4: PMMUP unicasts and/or multicasts "ps-Request" message
5: Neighbour NICs evaluate "Link State Information" and feedback "ps-Ack"
6: Sender NICs receive "ps-Ack" and evaluate "Link State Information"
7: Each sender NIC runs local power optimization algorithm (Cf. Section 4.5)
8: Each NIC unicasts pending DATA traffic to the Neighbour Destinations
9: Each sender NIC copies the optimal power values to the PMMUP table
10: end if

The PMMUP gathers "link state information" (LSI) by unicasting/multicasting power selection (i.e., ps-Request) message. Upon receiving ps-Request messages, neighbouring NICs evaluate the LSI such as SINR, interference, rate, queue status and energy reserves (i.e., line 5). After receiving the acknowledgement (i.e., ps-Ack) message, each sender NIC evaluates additional state information such as round trip time (RTT) (i.e., line 6). Transmission power is then optimally selected based on the LSI (i.e., line 7). Application or data traffic is transmitted using optimal power levels (i.e., line 8) and the PMMUP table is updated for the next time slot (i.e., line 9).

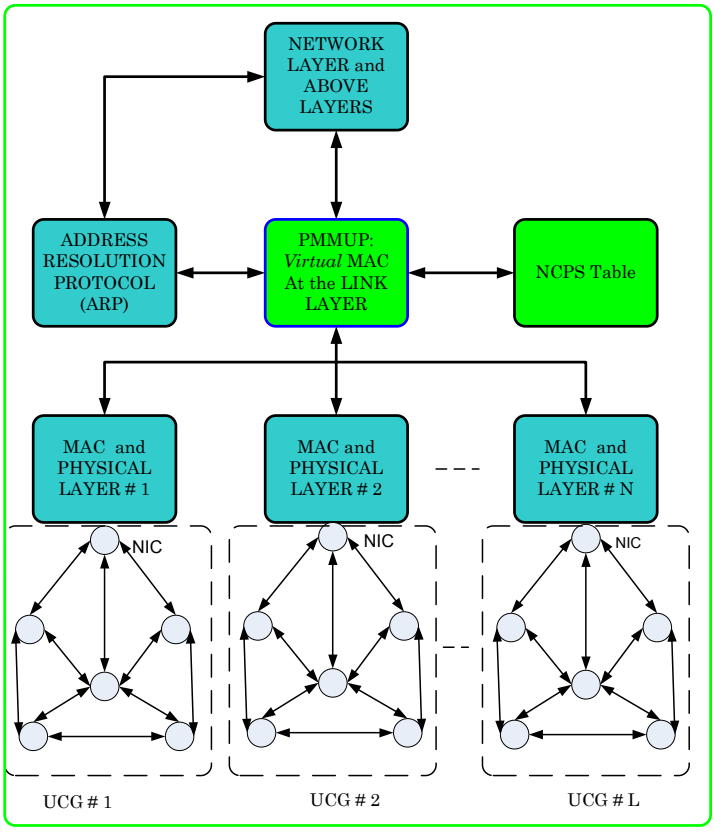

Figure 4.4: PMMUP: Virtual MAC architecture for Wireless Mesh Router (WMR)

Table 4.3: Entry in the PMMUP Table (NCPS)

FIELD	*DESCRIPTION (FOR EACH NEIGBOUR NODE, NEIGH)*
Neighbour	**IP address of the neighbour host**
Class	**Indicates whether *neigh* is PMMUP-enabled or not**
MAC list	**MAC address associated with *neigh* NICs**
States	**Recent measurements on: Channel Quality, Queue, RTT, and Energy Reserves**
TPL	**Recent transmit power level selected**

4.4.2 Advantages of PMMUP

The PMMUP does not require a global knowledge of the network topology; hence, it is a scalable protocol. Contents of a neighbourhood topology set are added or subtracted one node at a time. The PMMUP utilizes multiple parallel power controlled channels in order to enhance high data speed and capacity. It adapts to switched antenna beams for efficient spectral re-use. That is, neighbour discovery broadcasts require an omni-directional beam patterns while data transmissions can be effected using directional beam patterns. The

PMMUP is located at the Link layer (mid-way in the network protocol stack); thus, the top down or bottom up information flows with a reduced latency. The NCPS table at each node does not have too many LSI estimates, which determines the network capacity, in order to update. Neighbour discovery occurs once throughout the power optimization interval. This results in low overhead costs as regards exchanging control packets. Finally, the PMMUP coordinates the optimal executions by multiple MACs and radio interfaces in asynchronous and predictive manner.

4.4.3 Optimal Transmission Power Controller

In order to solve the minimization problem in (4-16), we introduce Lagrange multipliers $\boldsymbol{\pi}_t^i$ and a state unification (SU) vector $\boldsymbol{\varphi}_{t+1}^i$ to append the Linear Combination of Sates (LCS) equality in (4-15) and the multi-radio multi-channel states space (MMSS) constraint (4-14) respectively, to the cost function. The dynamic programming value function is then defined as

$$V\left(\tilde{\mathbf{x}}_t^i\right) = \min_{\{\mathbf{u}_t^i\}}\left\{\tilde{\mathbf{x}}_t^{iT}\mathbf{Q}_t^i\,\tilde{\mathbf{x}}_t^i + \mathbf{u}_t^{iT}\mathbf{R}_t^i\,\mathbf{u}_t^i\right\} + \min_{\{\mathbf{u}_t^i\}}\rho_i E\left[V\left(-\boldsymbol{\pi}_t^T\mathbf{y}_t^i + \boldsymbol{\pi}_t^T\sum_{\substack{j=1\\ j\neq i}}\mathbf{L}_t^{ij}\tilde{\mathbf{x}}_t^j + \boldsymbol{\pi}_t^T\boldsymbol{\varepsilon}_t^y\right)\right] +$$

$$\min_{\{\mathbf{u}_t^i\}}\rho_i\, E\left[V\left(\boldsymbol{\varphi}_{t+1}^T\mathbf{A}_t^i\tilde{\mathbf{x}}_t^i + \boldsymbol{\varphi}_{t+1}^T\mathbf{B}_t^i\mathbf{u}_t^i + \boldsymbol{\varphi}_{t+1}^T\mathbf{C}_t^i\mathbf{y}_t^i + \boldsymbol{\varphi}_{t+1}^T\boldsymbol{\varepsilon}_t^x\right)\right]. \tag{4-17}$$

Let us postulate a quadratic form for the DPF, in which $\mathbf{P}$ is an idempotent matrix so $\mathbf{P}^T = \mathbf{P}$,

$$V\left(\tilde{\mathbf{x}}_t^i\right) = \tilde{\mathbf{x}}_t^{iT}\mathbf{P}\,\tilde{\mathbf{x}}_t^i + \mathbf{D}\ . \tag{4-18}$$

We can proceed by substituting this form (with as yet undetermined matrices $\mathbf{P}$ and $\mathbf{D}$) into the value function (4-17). For convenience of notation, we drop the time slot subscripts and the user superscripts. In all cases, $\tilde{\mathbf{x}}$, $\mathbf{u}$, $\mathbf{y}$, $\boldsymbol{\pi}$, $\boldsymbol{\varphi}$ and $\boldsymbol{\varepsilon}$ refer to time slot t dated variables corresponding to the ith user on ith subsystem (UCG):

$$V\left(\tilde{\mathbf{x}}\right) = \min_{\mathbf{u}}\left\{\tilde{\mathbf{x}}^T\mathbf{Q}\,\tilde{\mathbf{x}} + \mathbf{u}^T\mathbf{R}\,\mathbf{u}\right\} + \rho\mathbf{D} + \min_{\mathbf{u}}\rho E\left[V\left(-\boldsymbol{\pi}^T\mathbf{y} + \boldsymbol{\pi}^T\sum_{\substack{j=1\\ j\neq i}}\mathbf{L}^{ij}\tilde{\mathbf{x}}^j + \boldsymbol{\pi}^T\boldsymbol{\varepsilon}^y\right)\right] +$$

$$\min_{\mathbf{u}} \rho E\left[\left(\boldsymbol{\varphi}^T\mathbf{A}\tilde{\mathbf{x}}+\boldsymbol{\varphi}^T\mathbf{B}\mathbf{u}+\boldsymbol{\varphi}^T\mathbf{C}\mathbf{y}+\boldsymbol{\varphi}^T\boldsymbol{\varepsilon}^x\right)^T\mathbf{P}\left(\boldsymbol{\varphi}^T\mathbf{A}\tilde{\mathbf{x}}+\boldsymbol{\varphi}^T\mathbf{B}\mathbf{u}+\boldsymbol{\varphi}^T\mathbf{C}\mathbf{y}+\boldsymbol{\varphi}^T\boldsymbol{\varepsilon}^x\right)\right]. \tag{4-19}$$

From (4-19), one expands the quadratic terms in the brackets and notes that $\left(\boldsymbol{\varphi}^T\mathbf{A}\,\mathbf{x}\right)^T=\mathbf{x}^T\mathbf{A}^T\boldsymbol{\varphi}$. Also, the expected value of the stochastic shocks is zero, so the terms of the form $\tilde{\mathbf{x}}^T\mathbf{A}^T\boldsymbol{\varphi}\mathbf{P}\boldsymbol{\varphi}^T\boldsymbol{\varepsilon}^x$, $\mathbf{u}^T\mathbf{B}^T\boldsymbol{\varphi}\mathbf{P}\boldsymbol{\varphi}^T\boldsymbol{\varepsilon}^x$, $\mathbf{y}^T\mathbf{C}^T\boldsymbol{\varphi}\mathbf{P}\boldsymbol{\varphi}^T\boldsymbol{\varepsilon}^x$, $\boldsymbol{\varepsilon}^{xT}\boldsymbol{\varphi}\mathbf{P}\boldsymbol{\varphi}^T\mathbf{A}\tilde{\mathbf{x}}$, $\boldsymbol{\varepsilon}^{xT}\boldsymbol{\varphi}\mathbf{P}\boldsymbol{\varphi}^T\mathbf{B}\mathbf{u}$, and $\boldsymbol{\varepsilon}^{xT}\boldsymbol{\varphi}\mathbf{P}\boldsymbol{\varphi}^T\mathbf{C}\mathbf{y}$, drop out. We are left with

$$V\left(\tilde{\mathbf{x}}\right)=\min_{\mathbf{u}}\left\{\tilde{\mathbf{x}}^T\mathbf{Q}\,\tilde{\mathbf{x}}+\mathbf{u}^T\mathbf{R}\,\mathbf{u}\right\}+\rho\mathbf{D}+\min_{\mathbf{u}}\rho E\left[V\left(-\boldsymbol{\pi}^T\mathbf{y}+\boldsymbol{\pi}^T\sum_{\substack{j=1\\ j\neq i}}\mathbf{L}^{ij}\tilde{\mathbf{x}}^j+\boldsymbol{\pi}^T\boldsymbol{\varepsilon}^y\right)\right]+$$

$$\min_{\mathbf{u}}\rho E\begin{bmatrix}\tilde{\mathbf{x}}^T\mathbf{A}^T\boldsymbol{\varphi}\mathbf{P}\boldsymbol{\varphi}^T\mathbf{A}\tilde{\mathbf{x}}+\tilde{\mathbf{x}}^T\mathbf{A}^T\boldsymbol{\varphi}\mathbf{P}\boldsymbol{\varphi}^T\mathbf{B}\mathbf{u}+\tilde{\mathbf{x}}^T\mathbf{A}^T\boldsymbol{\varphi}\mathbf{P}\boldsymbol{\varphi}^T\mathbf{C}\mathbf{y}\\ +\mathbf{u}^T\mathbf{B}^T\boldsymbol{\varphi}\mathbf{P}\boldsymbol{\varphi}^T\mathbf{A}\tilde{\mathbf{x}}+\mathbf{u}^T\mathbf{B}^T\boldsymbol{\varphi}\mathbf{P}\boldsymbol{\varphi}^T\mathbf{B}\mathbf{u}+\mathbf{u}^T\mathbf{B}^T\boldsymbol{\varphi}\mathbf{P}\boldsymbol{\varphi}^T\mathbf{C}\mathbf{y}\\ +\mathbf{y}^T\mathbf{C}^T\boldsymbol{\varphi}\mathbf{P}\boldsymbol{\varphi}^T\mathbf{A}\tilde{\mathbf{x}}+\mathbf{y}^T\mathbf{C}^T\boldsymbol{\varphi}\mathbf{P}\boldsymbol{\varphi}^T\mathbf{B}\mathbf{u}+\mathbf{y}^T\mathbf{C}^T\boldsymbol{\varphi}\mathbf{P}\boldsymbol{\varphi}^T\mathbf{C}\mathbf{y}\\ +\boldsymbol{\varepsilon}^{xT}\boldsymbol{\varphi}\mathbf{P}\boldsymbol{\varphi}^T\boldsymbol{\varepsilon}^x\end{bmatrix}. \tag{4-20}$$

The optimal control strategy from (4-20), after differentiating partially with respect to $\mathbf{u}$ and simplifying, is obtained as,

$$\mathbf{u}^*=-\left(\mathbf{R}+\rho\mathbf{B}^T\boldsymbol{\varphi}\mathbf{P}\boldsymbol{\varphi}^T\mathbf{B}\right)^{-1}\rho\begin{pmatrix}\mathbf{B}^T\boldsymbol{\varphi}\mathbf{P}\boldsymbol{\varphi}^T\mathbf{A}\tilde{\mathbf{x}}+\tilde{\mathbf{x}}^T\mathbf{A}^T\boldsymbol{\varphi}\mathbf{P}\boldsymbol{\varphi}^T\mathbf{B}\\ +\mathbf{B}^T\boldsymbol{\varphi}\mathbf{P}\boldsymbol{\varphi}^T\mathbf{C}\mathbf{y}+\mathbf{y}^T\mathbf{C}\boldsymbol{\varphi}\mathbf{P}\boldsymbol{\varphi}^T\mathbf{B}\end{pmatrix},$$

$$\mathbf{u}^*=-\left(\mathbf{R}+\rho\mathbf{B}^T\boldsymbol{\varphi}\mathbf{P}\boldsymbol{\varphi}^T\mathbf{B}\right)^{-1}\rho\left(\mathbf{B}^T\boldsymbol{\varphi}\mathbf{P}\boldsymbol{\varphi}^T\left(\mathbf{A}\tilde{\mathbf{x}}+\mathbf{C}\mathbf{y}\right)+\left(\tilde{\mathbf{x}}^T\mathbf{A}^T+\mathbf{y}^T\mathbf{C}\right)\boldsymbol{\varphi}\mathbf{P}\boldsymbol{\varphi}^T\mathbf{B}\right),$$

$$\mathbf{u}^*=-\left(\mathbf{R}+\rho\mathbf{B}^T\boldsymbol{\varphi}\mathbf{P}\boldsymbol{\varphi}^T\mathbf{B}\right)^{-1}\rho\left(\mathbf{B}^T\boldsymbol{\varphi}\mathbf{P}\boldsymbol{\varphi}^T\tilde{\mathbf{z}}+\tilde{\mathbf{z}}^T\boldsymbol{\varphi}\mathbf{P}\boldsymbol{\varphi}^T\mathbf{B}\right),\ \text{where}\ \tilde{\mathbf{z}}=\mathbf{A}\tilde{\mathbf{x}}+\mathbf{C}\mathbf{y},$$

$$\mathbf{u}^*=-\left(\mathbf{R}+\rho\mathbf{B}^T\boldsymbol{\varphi}\mathbf{P}\boldsymbol{\varphi}^T\mathbf{B}\right)^{-1}\rho\left(\mathbf{B}^T\boldsymbol{\varphi}\mathbf{P}\boldsymbol{\varphi}^T\tilde{\mathbf{z}}+\tilde{\mathbf{z}}^T\boldsymbol{\varphi}\mathbf{P}\boldsymbol{\varphi}^T\mathbf{B}\right),$$

$$\mathbf{u}^*=-\left(\mathbf{R}+\rho\mathbf{B}^T\boldsymbol{\varphi}\mathbf{P}\boldsymbol{\varphi}^T\mathbf{B}\right)^{-1}2\rho\left(\mathbf{B}^T\boldsymbol{\varphi}\mathbf{P}\boldsymbol{\varphi}^T\right)\tilde{\mathbf{z}},\ \text{with}\ \mathbf{B}^T\in\Re^{M\times n},\ \mathbf{P}\in\Re^{n\times n}\ \text{and}\ \boldsymbol{\varphi}\in\Re^{n\times 1}.$$

Or, more succinctly,

$$\mathbf{u}^*=-\mathbf{F}\left(\mathbf{A}\tilde{\mathbf{x}}+\mathbf{C}\mathbf{y}\right), \tag{4-21}$$

where $\mathbf{F}=-\left(\mathbf{R}+\rho\mathbf{B}^T\boldsymbol{\varphi}\mathbf{P}\boldsymbol{\varphi}^T\mathbf{B}\right)^{-1}2\rho\left(\mathbf{B}^T\boldsymbol{\varphi}\mathbf{P}\boldsymbol{\varphi}^T\right)$.

It can be noted from (4-21) that the optimal control strategy requires the control input vector $\mathbf{u}$ to depend linearly on the interaction LSI vector $\tilde{\mathbf{x}}$ and the coordination LSI vector $\mathbf{y}$. First order conditions for optimality of the other variables are given as follows [267]:

$$\frac{\partial V(\tilde{\mathbf{x}})}{\partial \boldsymbol{\pi}} = \rho V_{\boldsymbol{\pi}} \left(\mathbf{y} - \sum_{\substack{j=1 \\ j \neq i}} \mathbf{L}^{ij} \tilde{\mathbf{x}}_j - \boldsymbol{\varepsilon}^y \right) = 0 \text{ , with } V_{\boldsymbol{\pi}} = \frac{\partial V(\tilde{\mathbf{x}})}{\partial \boldsymbol{\pi}} \text{ .} \tag{4-22}$$

$$\frac{\partial V(\tilde{\mathbf{x}})}{\partial \mathbf{y}} = V_{\mathrm{y}}(\boldsymbol{\pi}) + \mathbf{C}^T \boldsymbol{\varphi} \mathbf{P} \boldsymbol{\varphi}^T \mathbf{A} \tilde{\mathbf{x}} + \mathbf{C}^T \boldsymbol{\varphi} \mathbf{P} \boldsymbol{\varphi}^T \mathbf{B} \mathbf{u} + 2\mathbf{C}^T \boldsymbol{\varphi} \mathbf{P} \boldsymbol{\varphi}^T \mathbf{C} \mathbf{y} = 0 \tag{4-23}$$

$$\frac{\partial V(\tilde{\mathbf{x}})}{\partial \boldsymbol{\varphi}} = \left(\tilde{\mathbf{x}}^T \mathbf{A}^T \mathbf{P} \mathbf{A} + \mathbf{u}^T \mathbf{B}^T \mathbf{P} \mathbf{A} + \mathbf{y}^T \mathbf{C}^T \mathbf{P} \mathbf{A} \right) \tilde{\mathbf{x}} + \left(\tilde{\mathbf{x}}^T \mathbf{A}^T \mathbf{P} \mathbf{B} + \mathbf{u}^T \mathbf{B}^T \mathbf{P} \mathbf{B} + \mathbf{y}^T \mathbf{C}^T \mathbf{P} \mathbf{B} \right) \mathbf{u} +$$

$$\left(\tilde{\mathbf{x}}^T \mathbf{A}^T \mathbf{P} \mathbf{C} + \mathbf{u}^T \mathbf{B}^T \mathbf{P} \mathbf{C} + \mathbf{y}^T \mathbf{C}^T \mathbf{P} \mathbf{C} \right) \mathbf{y} + \boldsymbol{\varepsilon}^{xT} \mathbf{P} \boldsymbol{\varepsilon}^x = 0 = \tilde{\mathbf{x}}_{t+1}, \quad \tilde{\mathbf{x}}(0) = \tilde{\mathbf{x}}_0 . \tag{4-24}$$

$$\frac{\partial V(\tilde{\mathbf{x}})}{\partial \tilde{\mathbf{x}}} = \left(\mathbf{Q} + \rho \mathbf{A}^T \boldsymbol{\varphi} \mathbf{P} \boldsymbol{\varphi}^T \mathbf{A} \right) \tilde{\mathbf{x}} + \left(\rho \mathbf{A}^T \boldsymbol{\varphi} \mathbf{P} \boldsymbol{\varphi}^T \mathbf{B} \right) \mathbf{u} + \left(\rho \mathbf{A}^T \boldsymbol{\varphi} \mathbf{P} \boldsymbol{\varphi}^T \mathbf{C} \right) \mathbf{y} = 0 = \boldsymbol{\varphi}_t \text{ , } \boldsymbol{\varphi}(\infty) = \boldsymbol{\varphi}_\infty \text{ .} \tag{4-25}$$

Equations (4-24) and (4-25) constitute a two-point boundary value problem (TPBVP). The TPBVP must be satisfied by an input control sequence $\{\mathbf{u}\}$ in (4-21) in order to achieve a stationary value of the value function (4-17). We demonstrate that the linear policy function in (4-21) (derived from a postulated quadratic value function) does actually imply a quadratic value function. In the process, we will be able to determine the two matrices $\mathbf{P}$ and $\mathbf{D}$. To do this, we substitute the policy function $\mathbf{u}^* = -\mathbf{F}\tilde{\mathbf{z}}$ back into the value function (4-17). Note that $-\tilde{\mathbf{x}}^T \mathbf{F}^T \mathbf{B}^T \mathbf{P} \mathbf{A} \tilde{\mathbf{x}}$ is a scalar and therefore equal to $-\tilde{\mathbf{x}}^T \mathbf{A}^{\mathbf{T}} \mathbf{P} \mathbf{B} \mathbf{F} \tilde{\mathbf{x}}$. Also, the postulated quadratic value function in (4-18) is assumed to be independent of the LSI estimates at steady state conditions or at the optimal control policy [265]. Thus, from (4-20) we have

$$V(\tilde{\mathbf{x}}) = \tilde{\mathbf{x}}^T \mathbf{P} \tilde{\mathbf{x}} + \mathbf{D} = \begin{bmatrix} \tilde{\mathbf{x}}^T \mathbf{Q} \tilde{\mathbf{x}} + \tilde{\mathbf{x}}^T \mathbf{F}^T \mathbf{Q} \mathbf{F} \tilde{\mathbf{x}} \\ + \rho E \begin{pmatrix} \tilde{\mathbf{x}}^T \mathbf{A}^T \mathbf{P} \mathbf{A} \tilde{\mathbf{x}} - 2\tilde{\mathbf{x}}^T \mathbf{A}^T \mathbf{P} \mathbf{B} \mathbf{F} \tilde{\mathbf{x}} \\ + \tilde{\mathbf{x}}^T \mathbf{F}^T \mathbf{B}^T \mathbf{P} \mathbf{B} \mathbf{F} \tilde{\mathbf{x}} \end{pmatrix} + \\ \rho E \boldsymbol{\varepsilon}^{xT} \mathbf{P} \boldsymbol{\varepsilon}^x + \rho \mathbf{D} \end{bmatrix} . \tag{4-26}$$

Comparing coefficients on constant terms in (4-26), that is, $\mathbf{D} = \rho E\boldsymbol{\varepsilon}^{xT}\mathbf{P}\boldsymbol{\varepsilon}^{x} + \rho\mathbf{D}$.

Simplifying this equation by applying the result $E\boldsymbol{\varepsilon}^{xT}\mathbf{P}\boldsymbol{\varepsilon}^{x} = tr\left(E\boldsymbol{\varepsilon}^{xT}\mathbf{P}\boldsymbol{\varepsilon}^{x}\right)$

$= tr\left(\mathbf{P}E\boldsymbol{\varepsilon}^{xT}\boldsymbol{\varepsilon}\right) = tr\left(\mathbf{P}\Theta_{\varepsilon}\right)$, we have

$$\mathbf{D} = \frac{\rho}{1-\rho} tr\left(\mathbf{P}\Theta_{\varepsilon}\right). \tag{4-27}$$

This equation shows how the additive uncertainty caused by the stochastic shocks $\boldsymbol{\varepsilon}_t$ does have an effect on the value function, but this effect is limited to the constant term, which is independent of the transmission power control policy.

Comparing coefficients of the terms quadratic in $\tilde{\mathbf{x}}$ from (4-26), we have

$$\mathbf{P} = \mathbf{Q} + \mathbf{F}^{T}\mathbf{R}\mathbf{F} + \rho\left(\mathbf{A}^{T}\mathbf{P}\mathbf{A} - 2\mathbf{A}^{T}\mathbf{P}\mathbf{B}\mathbf{F} + \mathbf{F}^{T}\mathbf{B}^{T}\mathbf{P}\mathbf{B}\mathbf{F}\right). \tag{4-28}$$

Rearranging,

$$\mathbf{P} = \mathbf{Q} + \rho\mathbf{A}^{T}\mathbf{P}\mathbf{A} - 2\rho\mathbf{A}^{T}\mathbf{P}\mathbf{B}\mathbf{F} + \mathbf{F}^{T}\left(\mathbf{R} + \rho\mathbf{B}^{T}\mathbf{P}\mathbf{B}\right)\mathbf{F} ,$$

$$= \mathbf{Q} + \rho\mathbf{A}^{T}\mathbf{P}\mathbf{A} - \rho^{2}\mathbf{A}^{T}\mathbf{P}\mathbf{B}\left(\mathbf{R} + \rho\mathbf{B}^{T}\mathbf{P}\mathbf{B}\right)^{-1}\mathbf{B}^{T}\mathbf{P}\mathbf{A} . \tag{4-29}$$

Here, $\mathbf{F} = \left(\mathbf{R} + \rho\mathbf{B}^{T}\mathbf{P}\mathbf{B}\right)^{-1}\rho\mathbf{B}^{T}\mathbf{P}\mathbf{A}$, is independent of the state unification weighting vector $\boldsymbol{\varphi}$.

Equation (4-29) confirms that a linear policy function does imply a quadratic value function. It is often known as the discrete in time algebraic matrix Riccati equation (DARE) [267]. This matrix is a non linear; therefore we simply use an iterative technique based on a matrix Riccati difference equation in order to solve the $\mathbf{P}$ matrix. Starting from an initial estimate of the $\mathbf{P}$ matrix in the value function, $\mathbf{P}_k$ is updated to $\mathbf{P}_{k+1}$ according to

$$\mathbf{P}_{k+1} = \mathbf{Q} + \rho\mathbf{A}^{T}\mathbf{P}_{k}\mathbf{A} - \rho^{2}\mathbf{A}^{T}\mathbf{P}_{k}\mathbf{B}\left(\mathbf{R} + \rho\mathbf{B}^{T}\mathbf{P}_{k}\mathbf{B}\right)^{-1}\mathbf{B}^{T}\mathbf{P}_{k}\mathbf{A} . \tag{4-30}$$

This equation is iterated until convergence, which is guaranteed to uniqueness under very mild weak conditions. That is, having eigenvalues in $\mathbf{A}$ of modulus less than unity is a sufficient condition [265].

At this stage it is worth noting that discrete equations (4-24) and (4-25) contain the lower level variables namely, $\mathbf{u}$ and $\tilde{\mathbf{x}}$ as well as higher level unification variables (UV) namely, $\mathbf{y}$, $\boldsymbol{\varphi}$, and $\boldsymbol{\pi}$. Hitherto, $\mathbf{y}$ signifies coordinated states (LSI estimates) from other UCGs, $\boldsymbol{\varphi}$ and $\boldsymbol{\pi}$ signify the *unification weight vectors* such as energy reserves and information from higher layers while $\tilde{\mathbf{x}}$ signifies the *interaction vector* of states (LSI estimates) within each UCG. Consequently, two PMMUP based power optimization algorithms called the MRSIP and MRSUP can be developed. MRSIP stands for synchronous (asynchronous) multi-radio multi-channel interaction LSI prediction. MRSUP stands for synchronous (asynchronous) multi-radio multi-channel unification LSI prediction. MRSIPA (i.e., asynchronous) and MRSIPS (i.e., synchronous) solve the power optimization with $\boldsymbol{\pi}$ and $\mathbf{y}$ as the PMMUP based coordinated variables. On the other hand MRSUPA (i.e., asynchronous) and MRSUPS (i.e., synchronous) solve the power optimization variables with $\boldsymbol{\varphi}$ and $\mathbf{y}$ as the PMMUP based coordinated variables.

4.5 PMMUP Based Power Control Algorithms

4.5.1 MRSIP Algorithm

Algorithm 4.2: MRSIP: Predicts Multi-Radio Multi-Channel Interaction Variables

Input: $\boldsymbol{\pi}$, $\mathbf{y}$; $\tilde{\mathbf{x}}_i$; ***A, B, C, Q*** *and* ***R***

Output: $\mathbf{u}_i^*$ /*i^{th} *user optimal power control signal*/

1: while $(k \geq 1)$ **do**

2: for each (user $i \in [1, N]$**) do**

3: Predict: $\tilde{\mathbf{x}}_i(k) \leftarrow \tilde{\mathbf{x}}_i(k+1)$;

4: if $(\tilde{\mathbf{x}}_i(k+1) \equiv \tilde{\mathbf{x}}_i^*$ ***for any*** $i \neq j$, $\forall j \in [1, N])$; /*if MRSIPA is executed*/

5: else if $(\tilde{\mathbf{x}}_i(k+1) \equiv \tilde{\mathbf{x}}_i^*$ ***for all*** $\forall i \in [1, N])$; /*if MRSIPS is executed*/

6: Update the PMMUP Table: $\mathbf{y}(k) \leftarrow \mathbf{y}(k+1)$; $\boldsymbol{\pi}(k) \leftarrow \boldsymbol{\pi}(k+1)$;

7: **if** $(e(k+1) \leq \varepsilon_{rr}$, *a small positive value);*

8: **Compute:** $\mathbf{u}_i^* = f(\boldsymbol{\pi}_i^*, \tilde{\mathbf{x}}_i^*, \mathbf{y}_i^*) = -\mathbf{F}_\pi \tilde{\mathbf{z}}_i^*$;

9: Add: $\mathbf{u}_i^*$ to Equation (4-3)

10: else

11: Repeat: Steps 2-6

12: end if

13: end for each

14: end while

Here,

$e(k+1) = \|\mathbf{g}(k+1) - \mathbf{g}(k)\|$, where

$\mathbf{g}(t) = \left[\mathbf{y}_i^T(k)\ \boldsymbol{\pi}_i^T(k)\right]^T$ and $\mathbf{g}(k+1) = \left[\mathbf{y}_i^T(k+1)\ \boldsymbol{\pi}_i^T(k+1)\right]^T$.

4.5.2 MRSUP Algorithm

Algorithm 4.3: MRSUP: Predicts Multi-Radio Multi-Channel Unification Variables

Input: $\boldsymbol{\varphi}$, $\mathbf{y}$; $\tilde{\mathbf{x}}_i$; ***A, B, C, Q*** *and* ***R***

Output: $\mathbf{u}_i^*$ /*i^{th} *user optimal power control signal*/

1: **while** $(k \geq 1)$ **do**

2: **for each** *(user* $i \in [1, N]$*)* **do**

3: **Predict:** $\tilde{\mathbf{x}}_i(k) \leftarrow \tilde{\mathbf{x}}_i(k+1)$; $\boldsymbol{\varphi}_i(k) \leftarrow \boldsymbol{\varphi}_i(k+1)$;

4: **if** $(\tilde{\mathbf{x}}_i(k+1) \equiv \tilde{\mathbf{x}}_i^* \;\&\&\; \boldsymbol{\varphi}_i(k) \leftarrow \boldsymbol{\varphi}_i(k+1)$ ***for any*** $i \neq j$, $\forall j \in [1, N])$; /*if MRSUPA is executed*/

5: **else if** $(\tilde{\mathbf{x}}_i(k+1) \equiv \tilde{\mathbf{x}}_i^* \;\&\&\; \boldsymbol{\varphi}_i(k) \leftarrow \boldsymbol{\varphi}_i(k+1)$ ***for all*** $\forall i \in [1, N])$; /*if MRSUPS is executed*/

6: **Update PMMUP table**: $\mathbf{y}(k) \leftarrow \mathbf{y}(k+1)$;

7: **if** $(e(k+1) \leq \varepsilon_{rr}$, *a small positive value);*

8: **Compute:** $\mathbf{u}_i^* = f(\boldsymbol{\varphi}_i^*, \tilde{\mathbf{x}}_i^*, \mathbf{y}_i^*) = -\mathbf{F}_{\boldsymbol{\varphi}} \tilde{\mathbf{z}}_i^*$;

9: **Add:** $\mathbf{u}_i^*$ to Equation (4-3).

10: **else**

11: **Repeat:** Steps 2-6.

12: **end if**

13: **end for each**

14: **end while**

Here,

$$e(k+1) = \left\| \mathbf{g}(k+1) - \mathbf{g}(k) \right\|, \text{with } \mathbf{g}(t) = \left[\mathbf{y}_i^T(k) \; \boldsymbol{\varphi}_i^T(k) \right]^T \text{ and}$$

$$\mathbf{g}(k+1) = \left[\mathbf{y}_i^T(k+1) \; \boldsymbol{\varphi}_i^T(k+1) \right]^T.$$

Each user automatically predicts the Interactive LSI affecting network throughput and transmission energy at the local UCG and the Unified LSI from the higher levels of the protocol stack (i.e., lines 1-3). If all users terminate their LSI predictions after a common iteration intervals then the convergence is termed as *synchronous,* otherwise *asynchronous* (i.e., lines 4-5). Using LSI trajectories, the coordination variables are updated at the PMMUP

table (i.e., line 6). Optimal power control signal is then computed using the converged LSI trajectories (i.e., line 8). After computing the optimal power control signal $\mathbf{u}_i^*(t) \in \Re^{1\times 1}$, the optimal dynamic power control law for each user is updated as

$$p_i(t+1) = p_i(t) + f_i(\mathbf{x}) + \mathbf{u}_i^*(t). \tag{4-31}$$

The optimal power law governing a multi-radio node and its neighbours is constrained by $0 \le \sum_{i\in\{1,\ldots,N\}} p_i(t+1) \le p_{MP}^{sum}$, where $p_{MP}^{sum} \le p_{MP}^{\max}$ are sum and maximum powers at each transmitting wireless MP (router).

It should be noted that local solutions for $\tilde{\mathbf{x}}$ depend on the converged *DARE* $\mathbf{P}$ matrix. Variables $\tilde{\mathbf{x}}$ and $\boldsymbol{\varphi}$ are functions of the coordinated variable $\mathbf{y}$ from the PMMUP. Asynchronous convergence of the PMMUP algorithms is non-trivial and is analysed in Section 4.5.3.

4.5.3 Analysis of Algorithms

Suppose $\mathbf{W}$ is a matrix of coupling variables between the *i*th user on *l*th UCG and other users on other UCGs [270, 271]. Let $\mathbf{W}$ be a discrete function representing a finite number of users performing a finite number of iterations. We write $\mathbf{W}$ in the form $\mathbf{W} = \left[\mathbf{W}_{\mathbf{x}} \;\; \mathbf{W}_{\boldsymbol{\varphi}}\right]$, where $\mathbf{W}_{\mathbf{x}}$ is the $\tilde{\mathbf{x}}$ component of $\mathbf{W}$ and $\mathbf{W}_{\boldsymbol{\varphi}}$ is the $\boldsymbol{\varphi}$ component of $\mathbf{W}$ given by $\mathbf{W}_{\mathbf{x}} = \left[\mathbf{w}_{\mathbf{x}1} \,|\, \mathbf{w}_{\mathbf{x}2} \,|\ldots|\, \mathbf{w}_{\mathbf{x}N}\right]$, $\mathbf{W}_{\boldsymbol{\varphi}} = \left[\mathbf{w}_{\boldsymbol{\varphi}1} \,|\, \mathbf{w}_{\boldsymbol{\varphi}2} \,|\ldots|\, \mathbf{w}_{\boldsymbol{\varphi}N}\right]$. Thus, the two-point boundary value problem derived from the value function (4-17) yields

$$\begin{pmatrix} \tilde{\mathbf{x}}_i^{(k+1)} \\ \boldsymbol{\varphi}_i^{(k)} \end{pmatrix} = \begin{pmatrix} \mathbf{z}_{i\mathbf{x}}^{T(k)}\mathbf{P}_{\mathbf{x}} & 0 \\ 0 & \mathbf{P}_{\boldsymbol{\varphi}}^{(k+1)} \end{pmatrix} \begin{pmatrix} \mathbf{z}_{i\mathbf{x}} \\ \mathbf{z}_{i\boldsymbol{\varphi}} \end{pmatrix}^{(k)} + \sum_{\substack{j=1 \\ j\neq i}}^{N} \begin{pmatrix} \mathbf{z}_{\mathbf{w}\mathbf{x}j}^{T(k)}\mathbf{P}_{\mathbf{w}\mathbf{x}j} & 0 \\ 0 & \mathbf{P}_{\mathbf{w}\boldsymbol{\varphi}j}^{(k+1)} \end{pmatrix} \begin{pmatrix} \mathbf{z}_{\mathbf{w}\mathbf{x}j}^{(k)} \\ \mathbf{z}_{\mathbf{w}\boldsymbol{\varphi}j}^{(k)} \end{pmatrix} + \begin{pmatrix} \mathbf{P}_{\varepsilon} & 0 \\ 0 & 0 \end{pmatrix} \begin{pmatrix} \boldsymbol{\varepsilon}_i^{\mathbf{x}} \\ \boldsymbol{\varepsilon}_i^{\boldsymbol{\varphi}} \end{pmatrix}^{(k)}. \tag{4-32}$$

If we define $\mathbf{z}_i^{(k)} = \left(\mathbf{z}_{i\mathbf{x}}^{(k)} \;\; \mathbf{z}_{i\boldsymbol{\varphi}}^{(k)}\right)^T, \mathbf{z}_{\mathbf{w}j}^{(k)} = \left(\mathbf{z}_{\mathbf{w}\mathbf{x}j}^{(k)} \;\; \mathbf{z}_{\mathbf{w}\boldsymbol{\varphi}j}^{(k)}\right)^T$, $\mathbf{v}_i^{(k+1)} = \left(\tilde{\mathbf{x}}_i^{(k+1)} \;\; \boldsymbol{\varphi}_i^{(k)}\right)^T$, then (4-32) can be written in the form

$$\mathbf{v}_i^{(k+1)} = \mathbf{H}_{\mathbf{x}\varphi}\mathbf{z}_i^{(k)} + \sum_{\substack{j=1 \\ j\neq i}}^{N}\mathbf{H}_{\mathbf{w}j}\mathbf{z}_{\mathbf{w}j}^{(k)} + \mathbf{H}_{\boldsymbol{\varepsilon}}\boldsymbol{\varepsilon}_i^{(k)} \;, \mathbf{H}_{\mathbf{w}i} = [\mathbf{0}] \;, \forall i,\; j \in [1, N] \;,$$

$$\mathbf{v}_i^{(k+1)} = \begin{pmatrix} \mathbf{H}_{\mathbf{x}\varphi} & \sum_{\substack{j=1 \\ j\neq i}}^{N}\mathbf{H}_{\mathbf{w}j} & \mathbf{H}_{\boldsymbol{\varepsilon}} \end{pmatrix} \begin{pmatrix} \mathbf{z}_i \\ \mathbf{z}_{\mathbf{w}j} \\ \boldsymbol{\varepsilon}_i \end{pmatrix}^{(k)} = \breve{\mathbf{A}}_i\, \mathbf{v}_i^{(k)} \;, \tag{4-33}$$

where $\mathbf{H}_{\mathbf{x}\varphi}$, $\mathbf{H}_{\mathbf{w}j}$ and $\mathbf{H}_{\boldsymbol{\varepsilon}}$ are functions of control system matrices, $\mathbf{A}, \mathbf{B}, \mathbf{C}, \mathbf{P}$, $\mathbf{Q}$ and $\mathbf{R}$. Let us now define the model uncertainty for (4-33) as

$$\delta\breve{\mathbf{A}} = \begin{pmatrix} \delta\mathbf{H}_{\mathbf{x}\varphi} & \sum_{\substack{j=1 \\ j\neq i}}^{N}\delta\mathbf{H}_{\mathbf{w}j} & \delta\mathbf{H}_{\boldsymbol{\varepsilon}} \end{pmatrix} , \tag{4-34}$$

where $\left\|\delta\breve{\mathbf{A}}_i\right\| < \varepsilon_0$ and ε_0 is a small positive value. Using this model uncertainty and invoking the Lyapunov test for stability, we show that the system is stable in every time slot [267].

Definition 4.1*:* Lyapunov Stability

The dynamic system in (4-33) is said to be stable in the sense of Lyapunov if there exists a Lyapunov scalar function, $Z(\breve{\mathbf{v}}):\Re^{\mathrm{O}} \to \Re$ *, defined in a region of state space near a solution of a dynamic system such that:*

$1:\; Z(\breve{\mathbf{v}}) = 0 \quad \forall \breve{v} = 0 \,,$

$2:\; Z(\breve{\mathbf{v}}) > 0 \quad \forall \breve{v} \in \mathrm{O},\; \breve{v} \neq 0,$

$3:\; Z(\breve{\mathbf{v}}(t+1)) - Z(\breve{\mathbf{v}}(t)) = \Delta Z(\breve{\mathbf{v}}) \leq 0 \quad \forall \breve{v} \in \mathrm{O},$

where $\breve{\mathbf{v}} = 0$ *represents a solution of the dynamic system,* $\Re^{\mathrm{O}}$ *represents the output space and* O *represents the region surrounding this solution of the system.*

Proposition 4.1: *The model in (4-34) with the system's asymptotic input* $\mathbf{u}_i^* = \breve{\mathbf{L}}_i\, \breve{\mathbf{v}}_i$*, where* $\breve{\mathbf{L}}_i = \left[0 \quad -\left(\mathbf{R} + \rho\mathbf{B}^T\mathbf{P}\mathbf{B}\right)^{-1}\mathbf{B}^T\mathbf{P}\mathbf{A}\right]$ *is stable if for some stationary* $\breve{\mathbf{A}}_{i0}$*, there exists a positive definite matrix* $\mathbf{N}$ *such that for any radio device belonging to user* $i \in \{1 \ldots N\}$*,*

$\breve{\mathbf{v}}_i^T \mathbf{D}_i \breve{\mathbf{v}}_i \le 0$, $\forall \breve{v}_i \in \mathrm{O}$, *where the equality holds only when* $\breve{\mathbf{v}}_i \equiv \mathbf{0}$. *Here,* $\mathbf{D}_i = \left(\breve{\mathbf{A}}_{i0} + \delta\breve{\mathbf{A}}_i\right)^T \mathbf{M}\left(\breve{\mathbf{A}}_{i0} + \delta\breve{\mathbf{A}}_i\right) - \mathbf{M}$. $\mathbf{M}$ *is assumed to be a positive definite matrix that solves the Lyapunov equation* $\breve{\mathbf{A}}_{i0}^T \mathbf{M}\breve{\mathbf{A}}_{i0} - \mathbf{M} = -\mathbf{N}$. *The uncertainty variable is* $\delta\breve{\mathbf{A}}_i$, *with the norm* $\left\|\delta\breve{\mathbf{A}}_i\right\|$ *as a small positive value.*

Proof: For a positive definite $\mathbf{N}$, the solution $\mathbf{M}$ of the Lyapunov equation is also a positive definite when $\breve{\mathbf{A}}_{i0}$ is stable. Thus from part 2 of the Lyapunov definition, $Z\left(\breve{\mathbf{v}}_i\right) = \breve{\mathbf{v}}_i^T \mathbf{M}\breve{\mathbf{v}}_i$ is always positive, $\forall \breve{\mathbf{v}}_i \in \mathrm{O}$, $\breve{\mathbf{v}}_i \neq 0$. From part 3 of the Lyapunov definition we proceed as:

$$
\begin{aligned}
\Delta Z\left(\breve{\mathbf{v}}_i\right) &= \breve{\mathbf{v}}_i^T \mathbf{D}_i \breve{\mathbf{v}}_i \qquad \forall \breve{v}_i \in \mathrm{O}, \\
&= \breve{\mathbf{v}}_i^T \left(\left(\breve{\mathbf{A}}_{i0} + \delta\breve{\mathbf{A}}_i\right)^T \mathbf{M}\left(\breve{\mathbf{A}}_{i0} + \delta\breve{\mathbf{A}}_i\right) - \mathbf{M}\right)\breve{\mathbf{v}}_i \\
&= \breve{\mathbf{v}}_i^T \left(\breve{\mathbf{A}}_{i0}^T \mathbf{M}\breve{\mathbf{A}}_{i0} + \delta\breve{\mathbf{A}}_i^T \mathbf{M}\breve{\mathbf{A}}_{i0} + \breve{\mathbf{A}}_{i0}^T \mathbf{M}\delta\breve{\mathbf{A}}_i + \delta\breve{\mathbf{A}}_i^T \mathbf{M}\delta\breve{\mathbf{A}}_i - \mathbf{M}\right)\breve{\mathbf{v}}_i \\
&= \breve{\mathbf{v}}_i^T \left(\underbrace{\breve{\mathbf{A}}_{i0}^T \mathbf{M}\breve{\mathbf{A}}_{i0} - \mathbf{M}}_{-\mathbf{N}} + \delta\breve{\mathbf{A}}_i^T \mathbf{M}\breve{\mathbf{A}}_{i0} + \breve{\mathbf{A}}_{i0}^T \mathbf{M}\delta\breve{\mathbf{A}}_i + \delta\breve{\mathbf{A}}_i^T \mathbf{M}\delta\breve{\mathbf{A}}_i\right)\breve{\mathbf{v}}_i \\
&= \breve{\mathbf{v}}_i^T \left(\delta\breve{\mathbf{A}}_i^T \mathbf{M}\breve{\mathbf{A}}_{i0} + \breve{\mathbf{A}}_{i0}^T \mathbf{M}\delta\breve{\mathbf{A}}_i + \delta\breve{\mathbf{A}}_i^T \mathbf{M}\delta\breve{\mathbf{A}}_i - \mathbf{N}\right)\breve{\mathbf{v}}_i \\
&= \breve{\mathbf{v}}_i^T \left(\delta\breve{\mathbf{A}}_i^T \mathbf{M}\breve{\mathbf{A}}_{i0} + \breve{\mathbf{A}}_{i0}^T \mathbf{M}\delta\breve{\mathbf{A}}_i + \delta\breve{\mathbf{A}}_i^T \mathbf{M}\delta\breve{\mathbf{A}}_i - \mathbf{N}\right)\breve{\mathbf{v}}_i .
\end{aligned}
\tag{4-35}
$$

Let $\mathbf{D}_i = \delta\breve{\mathbf{A}}_i^T \mathbf{M}\breve{\mathbf{A}}_{i0} + \breve{\mathbf{A}}_{i0}^T \mathbf{M}\delta\breve{\mathbf{A}}_i + \delta\breve{\mathbf{A}}_i^T \mathbf{M}\delta\breve{\mathbf{A}}_i - \mathbf{N}$ as extracted from (4-35). Consider long timeslot durations such that: $\lim_{t\to\infty}\left\|\delta\breve{\mathbf{A}}_i(t)\right\| \to 0$ if applied in (4-34). We can take the norm of $\mathbf{D}_i$ and obtain: $\left\|\mathbf{D}_i\right\| = -\left\|\mathbf{N}\right\|$. Since from the Lyapunov proposition, $\mathbf{N}$ is a positive definite matrix, $\mathbf{D}_i$ is a negative definite matrix denoted by $\mathbf{D}_i < [\mathbf{0}]$. Also, from the

proposition, $\breve{\mathbf{v}}_i^T \mathbf{D}_i \breve{\mathbf{v}}_i < 0$, $\forall \breve{\nu}_i \in \mathrm{O}$, $\breve{\nu}_i \neq 0$. Hence the system is said to be exponentially stable in the Lyapunov sense.

■

Theorem 4.1: *If the kth asynchronous iteration of the interaction state equation for the ith user is written as*

$$\tilde{\mathbf{x}}_i^{(k+1)} = \left(\tilde{\mathbf{x}}_i^T \ \mathbf{u}_i^T \ \mathbf{y}_i^T\right)^{(k)} \begin{pmatrix} \mathbf{A}^T\mathbf{P}\mathbf{A} & \mathbf{A}^T\mathbf{P}\mathbf{A} & \mathbf{A}^T\mathbf{P}\mathbf{C} \\ \mathbf{B}^T\mathbf{P}\mathbf{A} & \mathbf{B}^T\mathbf{P}\mathbf{B} & \mathbf{B}^T\mathbf{P}\mathbf{C} \\ \mathbf{C}^T\mathbf{P}\mathbf{A} & \mathbf{C}^T\mathbf{P}\mathbf{B} & \mathbf{C}^T\mathbf{P}\mathbf{C} \end{pmatrix} \begin{pmatrix} \tilde{\mathbf{x}}_i^{(k)} \\ \mathbf{u}_i^{(k)} \\ \mathbf{y}_i^{(k)} \end{pmatrix} + \boldsymbol{\varepsilon}_i^{xT(k)} \mathbf{P} \boldsymbol{\varepsilon}_i^{x(k)} \ \textit{with} \ \tilde{\mathbf{x}}_i^{(0)} = 0,$$

$$\tilde{\mathbf{x}}_i^{(k+1)} = \mathbf{z}_{\mathbf{x}i}^{T(k)} \ \mathbf{P}_{\mathbf{x}} \ \mathbf{z}_{\mathbf{x}i}^{(k)} + \ \boldsymbol{\varepsilon}_i^{xT} \mathbf{P} \boldsymbol{\varepsilon}_i^{x\,(k)} \ , \qquad (4\text{-}36)$$

$$\mathbf{y}_i^{(k)} = \sum_{\substack{j=1 \\ j \neq i}}^{N} \mathbf{L}_{ij}^{(k)} \mathbf{w}_{\mathbf{x}j}^{(k)} + \boldsymbol{\varepsilon}_j^{(k)}, \qquad (4\text{-}37)$$

and the unification state equation is given by

$$\boldsymbol{\varphi}_i^{(k)} = \begin{pmatrix} \mathbf{Q} + \rho \mathbf{A}^T \boldsymbol{\varphi}_i^{(k+1)} \mathbf{P} \boldsymbol{\varphi}_i^{T(k+1)} \mathbf{A} \\ \rho \mathbf{A}^T \boldsymbol{\varphi}_i^{(k+1)} \mathbf{P} \boldsymbol{\varphi}_i^{T(k+1)} \mathbf{B} \\ \rho \mathbf{A}^T \boldsymbol{\varphi}_i^{(k+1)} \mathbf{P} \boldsymbol{\varphi}_i^{T(k+1)} \mathbf{C} \end{pmatrix} \begin{pmatrix} \tilde{\mathbf{x}}_i^{(k)} \\ \mathbf{u}_i^{(k)} \\ \mathbf{y}_i^{(k)} \end{pmatrix}, \ \textit{with} \ \boldsymbol{\varphi}_i^{(K)} = 0,$$

$$\boldsymbol{\varphi}_i^{(k)} = \mathbf{P}_{\boldsymbol{\varphi}}^{(k+1)} \mathbf{z}_{\boldsymbol{\varphi}i}^{(k)}, \qquad (4\text{-}38)$$

$$\mathbf{y}_i^{(k)} = \sum_{\substack{j=1 \\ j \neq i}}^{N} \mathbf{L}_{ij}^{(k)} \mathbf{w}_{\boldsymbol{\varphi}j}^{(k)} + \boldsymbol{\varepsilon}_j^{(k)}, \qquad (4\text{-}39)$$

then

(a) The MRSIP and MRSUP algorithms satisfy a contraction property defined on a space S whereby

$$S = \sum_{i=1}^{N} S_i \ , \quad S_i = C_d\left(\left[k_0, k_\infty\right]; \Re^{2ni}\right), \qquad (4\text{-}40\ )$$

$C_d(.)$ denotes the set of discrete functions and n denotes the dimension of LSI at each user.

(b) MRSIP and MRSUP algorithms converge.

(c) The rate of convergence is linear and depends on the iteration interval and the interaction between users via exchange of states among separate UCGs.

Proof: **MRSIP**

Let each user $i \in \{1, \ldots, N\}$ iterate the discrete interaction and unification states *jointly* according to equation (4-32). Consequently from (4-33) one can re-write $\mathbf{v}_i^{(k+1)}$ as

$$\mathbf{v}_i^{(k+1)} = \mathbf{H}_{\mathbf{x}\varphi}\mathbf{z}_i^{(k)} + \mathbf{H}_{\mathbf{w}}\mathbf{z}_{\mathbf{w}}^{(k)} + \mathbf{H}_{\varepsilon}\boldsymbol{\varepsilon}_i^{(k)} \quad , \tag{4-41}$$

where $\mathbf{H}_{\mathbf{x}\varphi}$, $\mathbf{H}_{\mathbf{w}}$ and $\mathbf{H}_{\varepsilon}$ are the coefficient matrices in equation (4-32). The notations, $\mathbf{z}_i^{(k)}$, $\mathbf{z}_{\mathbf{w}}^{(k)}$ and $\boldsymbol{\varepsilon}_i^{(k)}$ are the interaction variable, coupling variable and stochastic shocks respectively, at time instant k.

Let the optimal solution to (4-41) be $\mathbf{v}_i^* = \left(\tilde{\mathbf{x}}_i^* \;\; \boldsymbol{\varphi}_i^*\right)^T$, where $\tilde{\mathbf{x}}_i^*$, $\boldsymbol{\varphi}_i^*$ are the *i*th user optimal values of interaction vector $\tilde{\mathbf{x}}$ and unification vector $\boldsymbol{\varphi}$. Define the interaction variable error of the *i*th user at iteration $k+1$ to be $\mathbf{e}_i^{(k+1)} = \mathbf{v}_i^{(k+1)} - \mathbf{v}_i^* = \left(\mathbf{e}_{i\mathbf{x}}^{(k+1)} \;\; \mathbf{e}_{i\boldsymbol{\varphi}}^{(k+1)}\right)^T$. The coupling variable iteration error at the *j*th user is given as $\mathbf{e}_{\mathbf{w}j}^{(k)} = \left(\mathbf{e}_{\mathbf{w}xj} \;\; \mathbf{e}_{\mathbf{w}\varphi j}\right)^T = \left(\mathbf{z}_{\mathbf{w}\mathbf{x}} - \tilde{\mathbf{x}}_j^* \;\; \mathbf{z}_{\mathbf{w}\boldsymbol{\varphi}} - \boldsymbol{\varphi}_j^*\right)^T$. Define the deviation of the stochastic shocks as $\mathbf{e}_{\varepsilon}^{(k)} = \boldsymbol{\varepsilon}_i^{(k)} - \boldsymbol{\varepsilon}_i^*$. Putting all this information together in (4-41), we have

$$\mathbf{e}_i^{(k+1)} = \mathbf{H}_{\mathbf{x}\varphi}\mathbf{e}_i^{(k)} + \mathbf{H}_{\mathbf{w}}\mathbf{e}_{\mathbf{w}}^{(k)} + \mathbf{H}_{\varepsilon}\mathbf{e}_{\varepsilon}^{(k)}. \tag{4-42}$$

In order to obtain sufficient conditions for the convergence, we introduce the norm for the global multi-radio system error vector $\mathbf{e}(k)$ over the time period $[k_0, k_\infty]$ and note the two point boundary conditions $\mathbf{e}_{i\boldsymbol{\varphi}}(k_\infty) = 0$ and $\mathbf{e}_{i\mathbf{x}}(k_0) = 0$ [267]. Also, we remember that after the large number of iteration $k \to k_\infty$, $\lim_{k\to k_\infty} \|\mathbf{e}_i(k)\|_2 = \mathbf{e}_i(k_\infty) = 0$, $\lim_{k\to k_\infty} \|\mathbf{e}_{\varepsilon i}(k)\|_2 = 0$ and the decentralized optimal control policy is $\mathbf{u}_i^* = -\mathbf{F}\tilde{\mathbf{x}}_i^*$. From (4-42) we have:

$$\max_{k\in[k0,k\infty]} \|\mathbf{e}(k)\|_2 \le (k_0 - k_\infty)\sum_{j=1}^{N}\left[\max_{\substack{k\in[k0,k\infty]\\ j\in[1,N]}}\left(\|\mathbf{H}_{\mathbf{x}\varphi}\|_2 \|\mathbf{e}_i(k)\|_2 + \|\mathbf{H}_{ij}\|_2 \|\mathbf{e}_{\mathbf{w}j}(k)\|_2 + \|\mathbf{H}_{\varepsilon}\|_2 \|\mathbf{e}_{\varepsilon i}(k)\|_2\right)\right],$$

$$\leq \left(k_0 - k_\infty\right) \sum_{\substack{j=1 \\ j\neq i}}^{N} \max_{\substack{k\in[k0,k\infty] \\ j\in[1,N]}} \left\|\mathbf{H}_{ij}\right\|_2 \max_{\substack{k\in[k0,k\infty] \\ j\in[1,N]}} \left\|\mathbf{e}_{\mathbf{w}j}(k)\right\|_2,$$

$$\max_{\substack{k\in[k0,k\infty] \\ i\in[1,N],\ \forall i}} \left\|\mathbf{e}(k)\right\|_2 \leq \alpha_i \max_{\substack{k\in[k0,k\infty] \\ j\in[1,N],\, j\neq i}} \left\|\mathbf{e}_{\mathbf{w}j}\right\|_2,\ \alpha_i = \left(k_0 - k_\infty\right) \sum_{\substack{j=1 \\ j\neq i}}^{N} \max_{\substack{k\in[k0,k\infty] \\ j\in[1,N]\, j\neq i}} \left\|\mathbf{H}_{ij}\right\|_2 \quad . \tag{4-43}$$

Here, the Norm of $\mathbf{e}(k) = \max_{k\in[k0,k\infty]} \left\|\mathbf{e}(k)\right\|_2$, is the Euclidean norm in $\Re^{2n}$.

Proof: **MRSUP**

On the other hand let each user, $i \in \{1, \ldots, N\}$ *separately* iterate the discrete interaction state equation (4-36) independent of the unification state equation (4-38). From (4-36), we have

$$\tilde{\mathbf{x}}_i^{(k+1)} = \mathbf{z}_{i\mathbf{x}}^{T(k)} \mathbf{P}_{\mathbf{x}} \mathbf{z}_{i\mathbf{x}}^{(k)} + \mathbf{z}_{\mathbf{wx}}^{T(k)} \mathbf{P}_{\mathbf{wx}} \mathbf{z}_{\mathbf{wx}}^{(k)} + \mathbf{P}_{\varepsilon} \boldsymbol{\varepsilon}_i^{x(k)}, \tag{4-44}$$

where $\mathbf{z}_{\mathbf{wx}}^{(k)} = \mathbf{y}_{i\mathbf{x}}^{(k)}$ and $\mathbf{z}_{i\mathbf{x}}^{(k)} = \left(\tilde{\mathbf{x}}_i^{(k)}\ \mathbf{u}_i^{(k)}\right)^T$.

At the optimal solution one obtains,

$$\tilde{\mathbf{x}}_i^{*} = \mathbf{z}_{i\mathbf{x}}^{T(*)} \mathbf{P}_{\mathbf{x}} \mathbf{z}_{i\mathbf{x}}^{(*)} + \mathbf{z}_{\mathbf{wx}}^{T(*)} \mathbf{P}_{\mathbf{wx}} \mathbf{z}_{\mathbf{wx}}^{(*)} + \mathbf{P}_{\varepsilon} \boldsymbol{\varepsilon}_i^{x(*)}, \tag{4-45}$$

where $\mathbf{z}_{\mathbf{wx}}^{(*)} = \mathbf{y}_{i\mathbf{x}}^{(*)}$ and $\mathbf{z}_{i\mathbf{x}}^{(*)} = \left(\tilde{\mathbf{x}}_i^{(*)}\ \mathbf{u}_i^{(*)}\right)^T$.

By subtracting (4-45) from (4-44), applying initial condition $\tilde{\mathbf{x}}_i^{(0)} = 0$, and simplifying we obtain

$$\mathbf{e}_{i\mathbf{x}}(k) = \mathbf{P}_{\mathbf{wx}} \mathbf{e}_{\mathbf{wx}}(k). \tag{4-46}$$

Taking the norm of both sides of (4-46) over the iteration period (k_0, k_∞), we have

$$\max_{k\in[k0,k\infty]} \left\|\mathbf{e}_{i\mathbf{x}}\right\|_2 \leq \left(k_0 - k_\infty\right) \max_{k\in[k0,k\infty]} \left\|\mathbf{P}_{\mathbf{wx}}\right\|_2 \max_{k\in[k0,k\infty]} \left\|\mathbf{e}_{\mathbf{wx}}\right\|_2. \tag{4-47}$$

In a similar procedure and noting the final value condition, one defines the norm error for the unification state equation as

$$\max_{k\in[k0,k\infty]}\left\|\mathbf{e}_{i\varphi}\right\|_2 \le \left(k_0-k_\infty\right)\max_{k\in[k0,k\infty]}\left\|\mathbf{P}_{w\varphi}\right\|_2\max_{k\in[k0,k\infty]}\left\|\mathbf{e}_{w\varphi}\right\|_2. \tag{4-48}$$

Combining the inequality (4-47) and (4-48) in a compact form for *i*th subsystem, we have

$$\max_{k\in[k0,k\infty]}\begin{pmatrix}\left\|\mathbf{e}_{i\mathbf{x}}\right\|_2\\ \left\|\mathbf{e}_{i\varphi}\right\|_2\end{pmatrix} \le \left(k_0-k_\infty\right)\max_{k\in[k0,k\infty]}\begin{pmatrix}\left\|\mathbf{P}_{w\mathbf{x}}\right\|_2 & 0\\ 0 & \left\|\mathbf{P}_{w\varphi}\right\|_2\end{pmatrix}\times\max_{k\in[k0,k\infty]}\begin{pmatrix}\left\|\mathbf{e}_{w\mathbf{x}}\right\|_2\\ \left\|\mathbf{e}_{w\varphi}\right\|_2\end{pmatrix},$$

$$\max_{\substack{k\in[k0,k\infty]\\ i\in[1,N],\,\forall i}}\left\|\mathbf{e}_i(k)\right\|_2 \le \left(k_0-k_\infty\right)\sum_{j=1}^{N}\Phi_{ij}\max_{\substack{k\in[k0,k\infty]\\ j\in[1,N],\,j\ne i}}\left\|\mathbf{e}_{wj}\right\|_2,$$

$$\max_{\substack{k\in[k0,k\infty]\\ i\in[1,N]}}\left\|\mathbf{e}_i(k)\right\|_2 \le \sigma_i\max_{\substack{k\in[k0,k\infty]\\ j\in[1,N],\,j\ne i}}\left\|\mathbf{e}_{wj}\right\|_2, \tag{4-49}$$

$$\sigma_i=\left(k_0-k_\infty\right)\sum_{j\ne i}\Phi_{ij}\,,\mathbf{e}_{wj}=\left(\mathbf{e}_{w\mathbf{x}j}\;\;\mathbf{e}_{w\varphi j}\right)^T. \tag{4-50}$$

Therefore,

(a) If one chooses $\left(k_\infty-k_0\right)$ such that $\sigma_i<1,\ \forall i\in[1,N]$, then inequalities (4-43) and (4-49) satisfy a contraction property on a space S which is defined as

$$S=\sum_{i=1}^{N}S_i\,,\quad S_i=C_d\left([k_0,k_\infty];\Re^{2ni}\right), \tag{4-51}$$

where $C_d(.)$ denotes the set of discrete functions.

(b) Consequently, satisfying a contraction property guarantees the convergence of asynchronous iterations [272].

(c) From (4-51) the asynchronous convergence depends on the iteration interval $\left(k_\infty-k_0\right)$ and the interaction matrix $\Phi_{ij}\left(k_\infty\right)$. Furthermore, each user is not expected to communicate its results after each iteration but only once at each power optimization period. Thus, some users execute more iterations than others. All users of a node-pair share the PMMUP layer and can access state trajectories simultaneously. This reduces the effects of communication delay across users of separate UCGs. Therefore, such asynchronous algorithms converge rapidly.

▪

4.6 Performance Evaluations

4.6.1 Simulation Environment

In all simulations, MATLAB™ version 7.1 was used. Fifty IEEE 802.11 wireless standard-based multiple radio nodes were randomly located in a 1200 m x 1200 m region. Each node was assumed to be equipped with 4 NICs or radios, each tuned to a unique frequency channel at any given time in operation. Radios operating in a common frequency channel form a UCG set, and fifty NIC-pairs were assumed to be fully interconnected over a wireless medium, forming network users. Each simulation run was performed long enough for the output statistics to stabilize (i.e., sixty seconds simulation time). Each datum point in the plots represented an average of five runs where each run used a different randomly generated topology. For evaluation purposes, we considered the frequency spectrum of 2412 MHz-2472 MHz, so that in each UCG, frequency carriers were: 2427 MHz, 2442 MHz, 2457 MHz and 2472 MHz. The direct sequence spread signalling in the IEEE 802.11 PHY layer was assumed. This is because of its potential for multi-user access through CDMA techniques. While the legacy MACs performed the CSMA/CA, the LL assigned orthogonal codes to NICs. Other simulation specifications per user were used as illustrated in Table 4.4 [21, 46].

Table 4.4: Simulation Specifications

Parameter	**Specification**	**Parameter**	**Specification**
Bandwidth	10 *MHz*	*Transmit & Interference ranges*	**240 m and 480 m**
Basic rate	2 *Mbps*	*Network probing power*	**Variable [Pmin,Pmax]**
Maximum link capacity	54 *Mbps*	*MAC scheme*	**CSMA/CA**
Minimum transmit power	10 *m*Watts	*Slot duration* *Power optimization duration*	**100 milliseconds** **40 milliseconds**
Target SINR threshold	Between 4 *dB*-20 *dB*	*Offered load* *Queue length*	**12.8,51.2,89.6,128 pkts/*s*** **50 *packets***
Thermal noise	90 *dBm*	*Packet sizes and FEC sizes*	**1000 *bytes and 50 bytes***
Maximum transmit power	**500 *m*Watts**	***Simulation time*** ***One measurement sample time***	**60 *seconds*** ***1 millisecond***

In order to evaluate LSI matrix **A,** the channel gain and the interference were estimated as follows: at each user associated with the *l*th channel, the channel gain conditions were given according to [125]

$$G_{Il} = L(d_0)\left(\frac{d_{Il}}{d_0}\right)^{-\nu} Y_l\left(X_{Il}^2 + X_{Ql}^2\right), \tag{4-52}$$

where $L(d_0) = \frac{\hbar_i \hbar_r \varpi^2}{16\pi^2 d_0^2}$ is the path loss of the close-in or reference distance d_0, with $\hbar_i$ and $\hbar_r$ as the antenna gains of the transmitter and the receiver radios assumed to be unity, respectively, and ϖ is the wavelength of the carrier signal. Let the close-in distance be $d_0 = 100$ meters and d_{Il} be the distance between the transmitter i and neighbourhood receiver r. The parameters $Y_l \ \forall l$ are independently identically distributed (i.i.d) lognormal shadowing random variables with the standard deviation σ_s, set to 8 dB. The random variables X_{Il} and $X_{Ql} \ \forall l$ are real and imaginary components, respectively, of a Rayleigh fading channel gain. Such variables possess zero mean and variance of 0.5. The path loss exponent (PLE) ν is assumed to be $2 \le \nu \le 6$, depending on the physical environment conditions. Using the channel autocorrelation function in [156] and assuming mobility-limited mesh devices, then $\sigma_m^2 = \sigma_s^2\left(1 - a^2\right)$, whereby picking $a = 0.95$ yields $\sigma_m = 1.56$ dB.

The work in [12, 156] revealed that a Kalman filter is utilized to predict the aggregate interference among users in a co-channel environment. However, the computational complexity of the filter would increase with the number of radio devices equipped at each node and the increased network state dimensions. Moreover, interference estimation in a distributed multicasting wireless network of multiple radios is an NP-hard problem [109]. Using Equation (4-1), interference becomes

$$\tilde{I}_l(t+1) \triangleq \tilde{I}_l(t) + n(t), \tag{4-53}$$

where $\tilde{I}_l(t)$ is the aggregate form of equation (4-1). The term $n(t)$ is a Gaussian distributed unit mean noise with variance σ_m^2 = 1.56 dB. The time-invariant effective channel gain is computed according to:

$$\lim_{t\to\infty} \frac{1}{t} \sum_{\tau=0}^{t-1} \mathrm{E}\left[\frac{G_{Il}}{\tilde{I}_l}\right](\tau) = H \ . \tag{4-54}$$

The LSI matrix coefficients, α_β, α_I, α_Γ were set to unity. The user and network and/or application weights ω_{I1} and ω_{I2} were both set to 0.5. The steady state pdf for the LSI deviation minimization ρ_i was set to 0.5 in order to offer a better trade-off between the system's states and control action regulation.

4.6.2 Simulation Results and Discussions

In a single unified channel graph (UCG), packets were transmitted by transmitter radio devices (or NICs) to target receivers of neighbouring nodes. The relationship between the transmission power consumed and the number of packets transmitted during a particular time slot was recorded in Fig. 4.5. The consumed transmission powers were recorded at different effective channel conditions. The results demonstrate that as the number of packets transmitted during each time slot increases, the amount of transmission energy needed to 'ferry' the packets increases linearly (i.e., see Fig. 4.5). Bad channel conditions, that is, H = 0.2 require additional transmission energy rate measured in $5\text{x}10^{-3}$ Watts-time slots per packet compared to ideal (favourable) channel conditions, that is, H = 1 with $7.33\text{x}10^{-4}$ Watts-time slots per packet. In order to transmit 500 packets in every time slot, transmissions when the gain was H = 1 demonstrated about 400%, 150%, 60%, 20% more power savings than when H = 0.2, 0.4, 0.6 and 0.8, respectively. Lossy channels occur as a result of wireless channel fading and interferences caused by multiple transmissions over a shared wireless medium.

Figure 4.6 depicts the number of packets successfully received by target receivers, divided by the transmission power used as a function of the inband packet transmission rate. The number of successfully received packets per unit transmission power decreases exponentially with the wireless link transmission rate. This is explained as follows. Increasing the transmission rate demands an increase in the transmission power for proper packet decoding against wireless fading conditions. Thus, throughput degrades with high wireless transmission power and rate, owing to the caused network interference and congestion. More signal losses would be noted when the channel gain, H = 0.2 than in situations when H = 1.0, and the associated explanations are similar to those of results in Fig. 4.5.

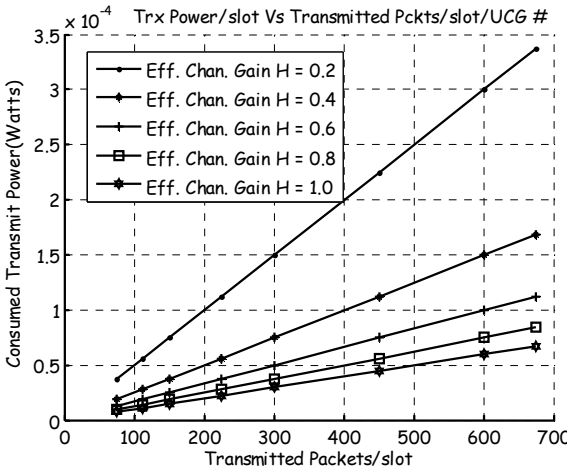

Figure 4.5: Transmit power versus packet transmission rate

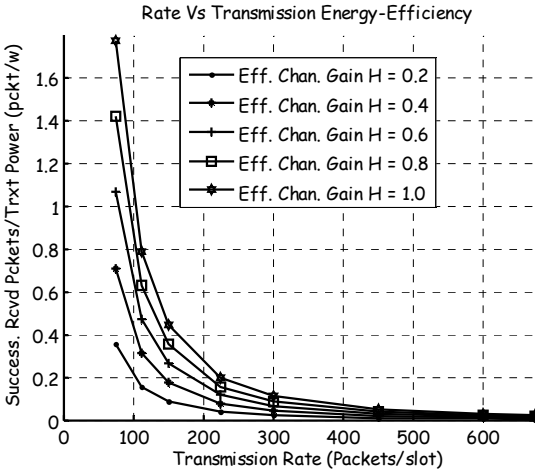

Figure 4.6: Energy-efficiency versus transmission rate

In Fig. 4.7, the PMMUP based power control algorithms were investigated for convergence. The simulations were run for a local UCG having carrier frequency of 2427 MHz. Operations of users belonging to other UCGs on separate frequency carriers were coordinated by the PMMUP layer. Intra-channel effective channel gain, $H = 0.4$ and adjacent channel interfering (ACI) power leakage factor was assumed to be 0.5 (i.e., strictly non-orthogonal channels). The LSI convergence time was allowed to be large enough (i.e., 4/5 of the time slot duration) in order to allow steady state values to be achieved. Each time slot consisted of a power optimization phase and data exchange phase. The Figure 4.7 demonstrates that all the algorithms converge at different rates. Specifically, at the 3rd time step, MRSIPA (asynchronous) recorded 25%, 37.5%, 50% and 75% superior convergence rates compared to MRSIPS (synchronous), MRSUPA (asynchronous), EBIA (co-channel interference estimation-based) and MRSUPS (synchronous) algorithms, respectively. The results are explained as follows. Asynchronous algorithms (e.g., MRSIPA and MRSUPA) require that any PMMUP user which has successfully completed the prediction of the link state information (LSI) terminates iterations regardless of the iterations of the other users on separate UCGs. However, synchronous algorithms (e.g., MRSIPS and MRSUPS) require that all users of a node must terminate executions at the same synchronized time. Thus, depending on various queue loads and network conditions, LSI executions by some users will converge faster than those of others. Prediction of unification variables tends to consume slightly more time than that of interaction variables, owing to the fact that the prediction of

the interaction variables by the PMMUP layer involves only intra-channel states and the coordinated variables. This simplifies the computational structure. On the other hand, the prediction of the Unification variables involves the intra-channel, the higher layers and the PMMUP coordinated variables. This complicates the computational structure. The latter approach faces the LSI exchange run time overhead costs. Furthermore, after receiving these variables the PMMUP layer updates the power table (i.e., NCPS) and subsequently broadcasts them to all users performing power optimization. This consumes a significant amount of the computational time. Finally, the EBIA approach estimates aggregate interference both at the sender and receiver nodes after a series of bidirectional information exchanges. Such bi-directional information exchanges minimize collisions and contentions at the expense of significant amount of convergence time. Nonetheless, EBIA works for user levels resulting in low information exchange overhead costs. Consequently, EBIA shows a slightly faster convergence rate than the MRSUPS method.

Fig. 4.8 illustrates the impacts of the transmission power sequence selection on the convergence of the LSI prediction. The simulation experiment was performed for each user on each UCG in a wireless multi-radio system. Specifically, the results indicate the difference between the actual and the target LSI values versus the measurement samples. The LSI estimates consist of the SINR, aggregate Interference within the neighbourhood of the transmitter, transmission bandwidth and the user connectivity range. It was noted that the control system stabilizes to steady states independent of the initial states. In fact, the system stability commences within the initial ten samples (i.e., 10% of one time slot duration) after short transients. This observation is justified as follows. A stabilizing solution of the idempotent matrix, $\mathbf{P}$ that finds an optimal control signal, $\mathbf{u}^*$ exists. This optimal control signal tracks the LSI deviation to convergence. Furthermore, a unique stabilizing value of $\mathbf{P}$ is always guaranteed under mild conditions (i.e., the LSI matrix $\mathbf{A}$ has eigenvalues with negative real components).

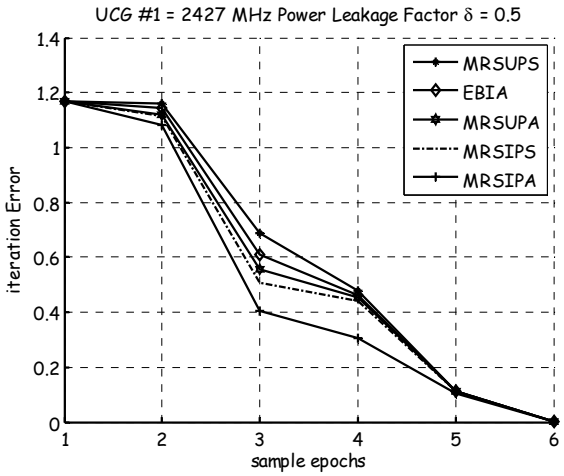

Figure 4.7: The LSI prediction convergence

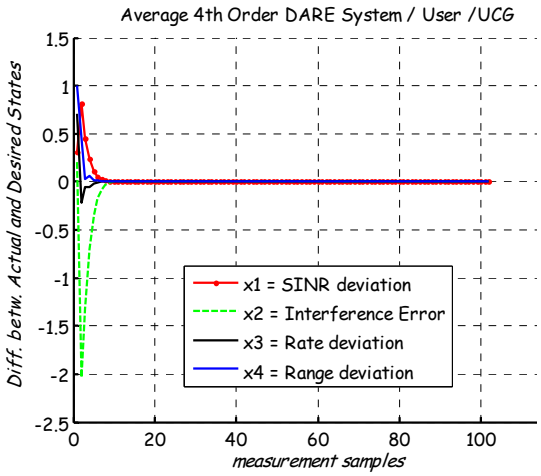

Figure 4.8: The LSI deviation in a single channel

Asynchronous LSI predictions demonstrated results in Figs. 4.9 and 4.10. For each UCG, inter-and intra-channel LSI is predicted and their differences from the target LSI values are noted. Rapid convergence was noted in both asynchronous Interaction and Unification predictions (i.e., MRSIPA and MRSUPA). Indeed, both MRSIPA and MRSUPA have occupied about 25% of power optimization period (i.e., 10 milliseconds out of 40 milliseconds), because the PMMUP layer coordinates the predictions of low level states across multiple channels. These states are stored at the NCPS table. The table-driven actual state tracking, to the predefined values, accelerates the convergence. However, Unification predictions have been shown to have a more complex structure and demonstrated a worse transient response than the Interaction prediction counterparts. Unification LSI predictions comprise states from multiple UCGs and a higher layer of the protocol stack, while Interaction LSI predictions require states only from the low level multiple UCGs.

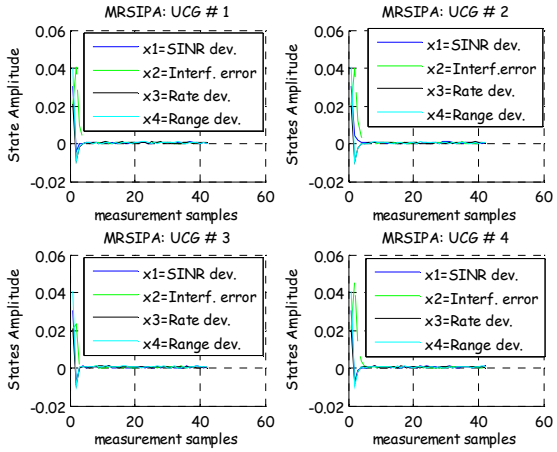

Figure 4.9: The LSI interaction prediction in multi-channels (i.e., MRSIPA)

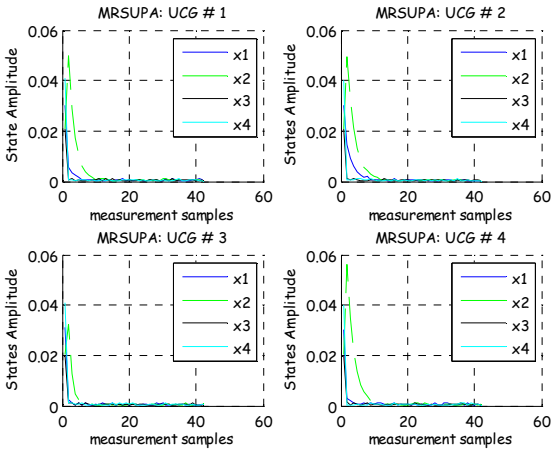

Figure 4.10: The LSI unification prediction in multi-channels (i.e., MRSUPA)

After the convergence of the Interaction and Unification LSI variables, the steady state response for transmission powers for each user is furnished in Figs. 4.11 to 4.14. The plots demonstrate transmission power executions for MRSIPA, MRSIPS, MRSUPA and MRSUPS. Simulation results indicate simultaneous transmission power executions by all active users on separate frequency channels: 2.427 GHz-2.472 GHz. Each frequency carrier is modelled as a single unified channel graph (UCG) set. States from multiple UCG sets are coordinated among independent radios by the PMMUP layer. The transmission power at each user evolves as a result of adding the optimal power control sequence $\{\mathbf{u}_i^*\}$, to the power update equation proposed at equation (4-3) in Section 4.2.3. It was noted that given the same initial prediction power value of 100 *m*Watts, the Interaction LSI prediction based power control approaches yielded more power saving at a steady state than the Unification LSI prediction based approaches. MRSIPA has presented slightly higher transmission power energy-efficiency compared to related counterparts. Specifically, MRSIPA consumes about 20.02% of the total amount of energy resource at a single node (i.e., 400.475 *m*Watts out of 2 Watts). On the other hand, MRSUPA consumes approximately 20.05% of the total amount of energy resources at a single node (i.e., 400.913 *m*Watts out of 2 Watts). Moreover, the Table 4.5 summarizes the statistical power savings by MRSIPA compared with other approaches.

Table 4.5: Percentage Transmission Power Saving Gain by MRSIPA Approach

	UCG 1 (2.427GHz)	*UCG 2 (2.442GHz)*	*UCG 3 (2.457GHz)*	*UCG 4 (2.472 GHz)*
MRSIPS	0.005%	0.010%	0.015%	0.010%
MRSUPA	0.128%	0.130%	0.064%	0.130%
MRSUPS	19.86%	23.84%	13.90%	21.850%

The explanation is as follows. Asynchronous algorithms require each autonomous user to terminate LSI predictions as soon as it attains the convergence level, while the convergence time of synchronous algorithms depends on the longest iteration interval set by the PMMUP. Thus, asynchronous algorithms have low computational run time overhead costs. Furthermore, each user autonomously updates the transmission power level immediately after attaining prediction convergence. Consequently, application or data packets are then exchanged without additional time delays. Interaction LSI prediction approaches provide better transmission energy saving than their Unification counterparts. Interaction LSI exchanges are simpler in structure and incur less overhead costs than the Unification LSI exchanges. The MRSIPA provided slightly improved energy conservation performance because it is asynchronous with a simple structure. The MRSIPA involves only Interaction LSI estimates from the lower level multiple UCGs.

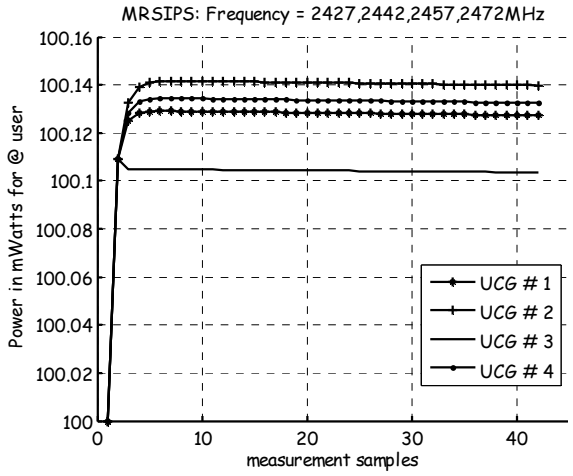

Figure 4.11: Steady state transmission power for each PMMUP user: MRSIPS algorithm

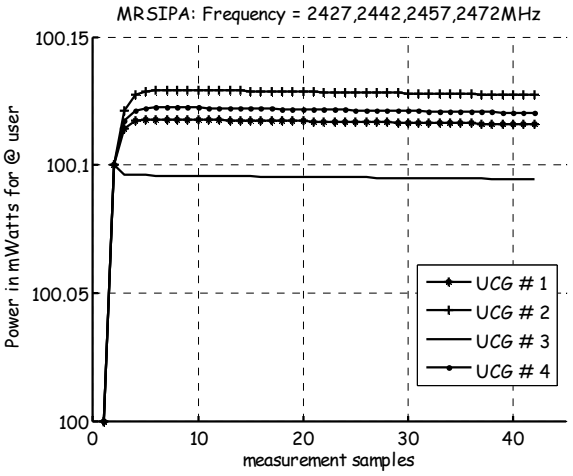

Figure 4.12: Steady state transmission power for each PMMUP user: MRSIPA algorithm

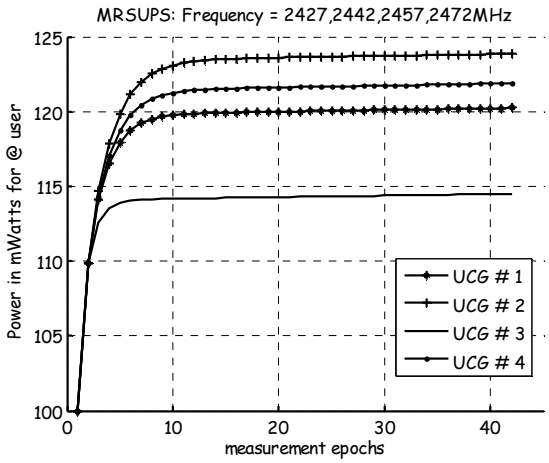

Figure 4.13: Steady state transmission power for each PMMUP user: MRSUPS algorithm

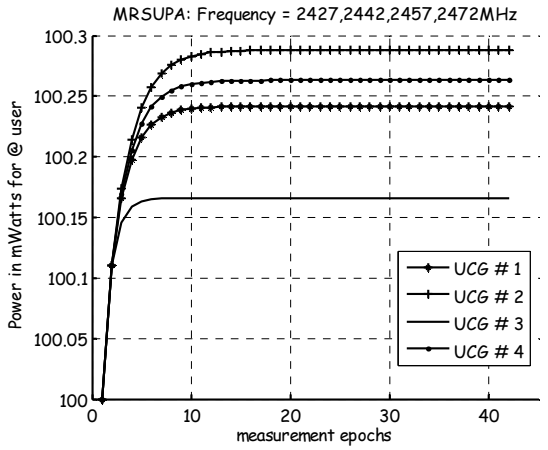

Figure 4.14: Steady state transmission power for each PMMUP user: MRSUPA algorithm

Fig. 4.15 depicts simulation results for transmission power after steady states per time slot duration per node-pair versus the amount of generated packets per time slot duration per node-pair. Fifty randomly generated nodes in a network of size 1200 m x 1200 m were considered. Five simulation runs were carried out; each run depicts a random topology. Packets were generated from each node and the amount of transmission power needed to reach the neighbouring nodes was measured. Three related approaches were compared with MRSIPA and MRSUPA under similar wireless channel conditions. Specifically, the dynamic channel assignment with power control (DCA-DPC) approach [183] uses two half-duplex transceivers per node. One transceiver operates in one control channel and the other in power controlled data channels which are switched dynamically. The effective band based interference prediction algorithm (EBIA) [12, 45] is a special case of the MRSIPA and/or the MRSUPA that uses one radio per node in a power controlled channel for both control and data packets. Finally, the multi-radio unification protocol (MUP) [41] uses multiple channels for control packets and then selects only one channel with the best link quality for data packets while keeping other radios dormant. For simulation purposes only, four non-overlapping UCGs with adjacent channel interference (ACI) leakage factor of 0.5 were used. The leakage factor depicts the fraction of transmission power causing interference across multiple adjacent channels. Simulation results reveal that increasing the amount of generated traffic increases the amount of transmission power needed. This suggests that a high data volume implies a high transmission energy consumption as demonstrated in Figs. 4.5 and 4.6. Over different amounts of generated traffics, the MRSIPA and the DCA-DPC method [183]

indicate impressive transmission power savings. Table 4.6 summarizes the MRSIPA power saving gain compared to the other methods:

Table 4.6: Percentage Transmission Power Saving Gain by MRSIPA

	5 pkts/slot	*10 pkts/slot*	*15 pkts/slot*	*20 pkts/slot*
DCA-DPC	9.09% (less)	8.33% (less)	14.29% (less)	8.11% (less)
MRSUPA	45.45%	50.00%	50.00%	56.76%
EBIA	63.64%	66.67%	57.14%	72.97%
MUP	81.82%	83.33%	82.86%	87.84%

The explanation follows. The DCA-DPC [183] approach offers the most superior power saving compared to others. This is because several data channels are assigned dynamically to hosts in "on-demand" manner. Owing to the on demand feature, the number of channels given to the network is a fixed number which is independent of the network size, topology and node degree. Furthermore, only subsets of nodes (i.e., each with only two transceivers) with the best channel qualities participate actively in data transmissions at controlled powers. The rest of the nodes go into the doze modes. This saves energy significantly, on average. Across the wide range of the packets generated, the MRSIPA yields significant transmission power savings compared to the rest of the related approaches, because the MRSIPA is a method which is both load and energy resource aware, that is, each user of a node autonomously performs dynamic power selection based on both node energy and queue status. Furthermore, Interaction LSI predictions depend on only local channel and coordinated states with low computational time. On the other hand, the MRSUPA approach is not only computationally complex but also demonstrates LSI prediction delays because it involves higher layers. The MUP approach [41] consumes a significant amount of transmission energy because it does not take power control into account, although it exploits only one channel with the best channel quality. The EBIA approach [12, 45] evaluates multiple access interference (MAI) by executing series of forward and backward information exchanges. Such procedures significantly increase the network "online" time and may translate to substantial energy consumption.

In Fig. 4.16 the simulation results on average throughput performance versus offered loads are illustrated. Each datum point in the plots was an average of five runs where each run used a different randomly generated topology of fifty nodes. The statistical averages were calculated with a 95% confidence interval. The adjacent channels transmission power leakage

factor was assumed to be 0.5. The plots demonstrate that MRSIPA provides the most superior throughput performance at various loads compared to the related methods. The performance gain of the MRSIPA approach compared with others is illustrated statistically by Table 4.7.

Table 4.7: Summary of Average Throughput Gain by MRSIPA

	12.8 pkts/s	*51.2 pkts/s*	*89.6 pkts/s*	*128 pkts/s*
MRSUPA	16.67%	21.74%	18.52%	20.69%
DCA-DPC	50.00%	45.65%	48.15%	48.28%
EBIA	66.67%	65.22%	64.81%	65.52%
MUP	80.00%	76.09%	77.78%	77.59%

The explanation now follows. MRSIPA records on average 16.67%, 21.74%, 18.52% and 20.69% average throughput gain over the MRSUPA versus various packet arrival rates. This observation is based on the view that the MRSIPA has a lower computational structure and faster convergence (i.e., less delay). Consequently, data packets are transmitted at faster rates than those of the MRSUPA approach. MRSIPA has on average 50%, 45.65%, 48.15% and 48.28% greater gain over the DCA-DPC across various arrival rates. This is because MRSIPA performs power control for all active wireless channels and strips data or application packets in parallel to improve the network traffic capacity. The PMMUP layer ensures node access and routes the traffic simultaneously. Each function is performed on a separate non-overlapping power controlled channel. On the other hand, the DCA-DPC performs dynamic channel assignments in which control packets are exchanged in one channel using the maximum transmission power level. This limits channel spatial re-use, causing poor network capacity. The data packets are transmitted using power controlled channels which are dynamically assigned to neighbouring hosts. The authors make no assumption to clock synchronization among these hosts. However, the DCA-DPC approach utilizes one transceiver per each node to transmit data packets. The DCA-DPC therefore provides a lower throughput performance than the MRSIPA approach.

MRSIPA records on average 66.67%, 65.22%, 64.81% and 65.52% greater gain over the EBIA at various packet arrivals. The MRSIPA approach performs power control for all channels based on intra-channel LSI states as well as LSI states from other neighbouring channels. The LSI states from other neighbouring channels are coordinated by the virtual MAC layer (i.e., PMMUP). In addition, the MRSIPA aims at minimizing the LSI deviation to enhance throughput. EBIA estimates interference at both the receiver and the transmitter end.

EBIA exploits this bi-directional interference information to adjust transmission power in such a manner that network aggregate interference is minimized [45]. This approach relies only on interference estimation and minimization to improve network capacity. Consequently, the resulting throughput per node pair is lower compared to the multi-radio approaches. The MRSIPA records on average 80.00%, 76.09%, 77.78% and 77.59% greater gain over the MUP approach at various packet arrivals. The MRSIPA is a multi-radio multi-channel (MRMC) power control approach and at the same time minimizes the LSI deviation. MUP on the other hand selects only one channel with the best channel quality for transmission of data or application traffic and no power control is guaranteed in each channel. The MRSIPA uses all power controlled channels for transmissions, yielding an average throughput gain over the MUP approach.

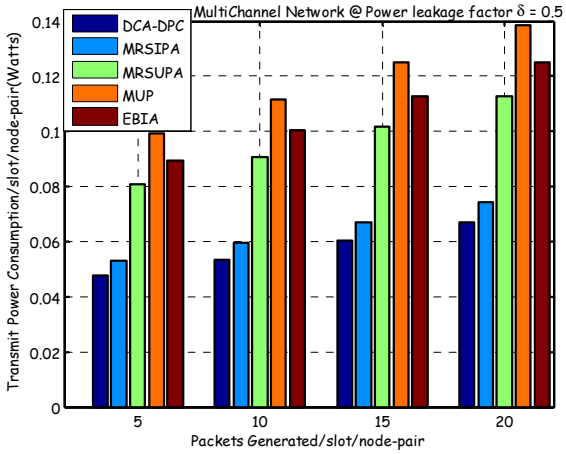

Figure 4.15: The transmission power after steady state versus packet generation rate

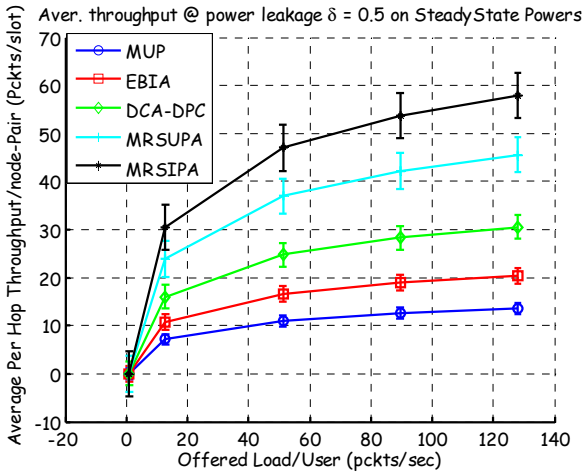

Figure 4.16: Average per hop throughput per node-pair versus the offered load per user

4.7 Chapter Conclusions and Remarks

In this chapter, a new power selection multi-radio multi-channel unification protocol (PMMUP) was developed. The PMMUP performed decentralized dynamic power control (DTPC) algorithms. Key PMMUP-based DTPC algorithms discussed were referred to as Asynchronous multi-radio multi-channel LSI Interaction and Unification predictions (i.e., MRSIPA and MRSUPA). The MRSIPA computes the optimal transmission power by allowing each network user to autonomously predict the Interaction LSI variables. The MRSUPA on the other hand predicts the Unification LSI variables. In order to achieve this goal, each user minimized a stochastic quadratic cost function. Analytical results showed that

the PMMUP-based DTPC algorithms converge linearly. The convergence rate depended on the iteration interval and the interaction between users through LSI exchanges. Simulation results revealed that PMMUP-based DTPC algorithms converge rapidly. The MRSIPA method, however, demonstrated the most superior convergence motivated by its simple computational structure. MRSIPA showed, on average, convergence power saving gains between 0.005% and 23.23% compared to other approaches. MRSIPA provided, on average, transmission power saving gains between 8.11% and 87.84% over different traffic loads compared to other approaches. MRSIPA also yielded, on average, throughput gains between 16.67% and 80.00% over different traffic loads compared to other approaches. Further simulation results regarding average throughput and energy performance can be found in our recent publications [21, 46, 48, 51].

It should be noted that the PMMUP based DTPC methods permit the transmission of application data only when the buffer and residual energy levels are greater than zero. However, speed differences involving both the buffer and energy variations introducing transmission power control problems have not been investigated. In other words, perturbation problems stemming from the energy and packet evolutions at various multi-radio queues have not been studied. Chapter 5 investigates a singularly-perturbed weakly-coupled based dynamic power control (SPWC-DTPC) method in MRMC wireless networks.

Chapter 5

Singularly-Perturbed Weakly-Coupled DTPC Scheme

5.1 Introduction

This chapter discusses a singularly-perturbed weakly-coupled dynamic transmission power control (SPWC-DTPC) problem at the Wireless Backbone Mesh Networks (WBMNs) configured with multi-radio multi-channel (MRMC) systems. Singular perturbations arise when different multiple packet queues on different channels evolve at various time-scales compared to the rate of energy depletions and/or charging by the multiple radios. Such a singular perturbation can effectively be modelled as a coefficient of the first order Taylor series expansion of steady state Markov Chain probability distributions. The MRMC wireless networks not only demonstrate singular perturbations at the multiple packet queues but also cross-channel interference problems owing to the fading of the diverse channels. Although orthogonal adjacent channels do not strongly interfere, the radio channel may affect this orthogonality. Indeed, time delays, lack of synchronization in the entire network and fading effects violate the orthogonality, resulting in significant packet losses. These MRMC configuration problems may substantially affect the capacity performance of the backbone WMNs. Owing to diverse multi-channel conditions, nodes may frequently be compelled to retransmit packets. Such retransmissions cause additional power control problems which have not received much research attention previously. Consequently, this study investigates a singular-perturbation and weak-coupling (SPWC) based transmission power control.

The theory of Singular perturbation and its applications is richly described [273-276]. Of interest here, the authors in [275] studied a singular perturbation approach for approximating steady state solutions of a two dimensional Markov chain. In particular, a queuing analysis of packet dropping over a wireless medium with retransmissions was undertaken. The Markov chain consisted of the channel state and the number of packets queued at the buffer. However, only good and bad levels of channel states were analysed. Based on a similar

paradigm, this chapter investigates a singular perturbation problem existing between the transmission energy availability and the buffer size evolutions at queue systems. In this case, energy levels are possibly larger than two and a multi-channel wireless framework is considered. The speed ratio between the buffer sizes and the transmission energy availability can be sufficiently represented by a singular perturbation parameter ε_s. On the other hand, weakly-coupled theory and its applications to large scale control systems can be found in numerous studies [271, 277-279]. In these contributions the emphasis has been mainly focused on the modelling of large scale interconnected control systems as differential Nash games [271]. In particular, assuming a large scale interconnected system, a strategy of one subsystem is decoupled from strategies of other subsystems [277] in the game so that a Nash equilibrium can then be attained [278]. Such a weak coupling parameter can be denoted as ε_w. Based on such modelling techniques, inter-channel wireless interference can be presented as a weakly-coupled power control problem. The transmission power control solutions are then obtained in terms of the sufficiently small positive parameter denoted as $\tilde{\varepsilon}$ and defined as $\tilde{\varepsilon} = \left|\sqrt{\varepsilon_s \varepsilon_w}\right|$. *To the best of our knowledge this is the first study to address a singularly-perturbed and weakly-coupled dynamic power control (SPWC-DTPC) problem in backbone wireless networks.*

In order to coordinate the functions of multiple MACs and radios, and to hide their complexities from the upper layers of the protocol stack, an energy-efficient power selection multi-radio multi-channel unification protocol (PMMUP) can be assumed at the Link Layer (LL). This PMMUP handles the SPWC problems of transmission power control. Based on differential Nash games, the SPWC higher order recursive algorithm (HORA) is then derived. This algorithm offers a stabilizing solution of the transmission power control problem for a decomposed system. Analytical results indicated that such an algorithm converges to the exact stationary solutions. The rate of convergence is linear. Numerical evaluations confirm that the algorithm converges to fixed points after about eight execution cycles. The dynamic power control based on the Link State Information (LSI) derived in Chapter 4 rapidly attains exact solutions. Several simulation results indicate that the SPWC-DTPC protocol is both energy and throughput superior compared to the conventional protocols. Specifically, the SPWC-PMMUP ensured that after 50 units of the simulation time and at $\tilde{\varepsilon} = 0.001$, the average number of "still alive links" gain over other protocols occurs between 12.50% and 33.30%. The resulting average throughput per node-pair gain statistically yields between 8%

and 36.36% at traffic loads $\lambda = 120$ packets/s and at the SPWC parameter $\tilde{\varepsilon} = 0.001$. This observation occurs because the SPWC-PMMUP scheme incorporates the queue perturbations and the cross-channel interference influence in the model. The SPWC conditions, in addition to the conventional LSI discussed in Chapter 4, have been shown to provide optimal power control solutions.

Tables 5.1 and 5.2 summarize the definitions of abbreviations and notations used in this Chapter.

Table 5.1: Abbreviation

Abbreviation	*Description*
ATIM	Ad Hoc Traffic Indication Message Window
LSI	Link State Information
MAC	Medium Access Control Protocol
MRMC	Multi-radio Multi-channel Wireless system
MUP	Multi-radio Unification Protocol
NIC	Network Interface Card or Radio Interface
PHY	Physical Layer
POWMAC	Power-Controlled Single-Channel MAC Protocol
PSM-MMAC	Power-Saving Multi-channel MAC Protocol
RTS/CTS	Request/Clear-To-Send Control Packets Exchanges
SPWC-PMMUP	Singularly-perturbed Weakly-coupled Power Selection MRMC Unification Protocol
SWARRE	SPWC-Continuous Algebraic Regulator Riccati Equation
UCGs	Unified Channel Graphs

Table 5.2:Notation

Notation	*Description*
ϕ	Probability of arrival in the queue system of a node
φ_i	Departure probability given the available energy level is i
$X(n)$	Markov chain sequence for singularly-perturbed queue system
$\pi(\varepsilon_s)$	Steady state perturbed Markov chain probability distribution
ε_s	The singular perturbation (SP) sufficiently small parameter
ε_w	The weakly coupling (WC) sufficiently small parameter
ε	Defines a MRMC wireless communication system which has both SP and WC properties, $0 \le \varepsilon = \frac{\varepsilon_w}{\varepsilon_s} < \infty$
$\tilde{\varepsilon}$	The SPWC sufficiently small parameter given by $\tilde{\varepsilon} = \sqrt{\lvert\varepsilon_s \varepsilon_w\rvert}$
$p_i(t+1)$	The next time slot transmission power level of the *i*th user.
$\mathbf{u}_i^*(t)$	The *i*th user optimal Nash strategy

$\mathbf{P}_{i\varepsilon}(t)$	The *i*th user decoupled SWARRE Solution
$\mathbf{F}_{i\varepsilon}(t)$	The *i*th user decoupled control feedback gain

5.2 System Model and Analysis

5.2.1 Perturbed Queue System

Suppose that N wireless links, each on a separate channel, emanate from a particular wireless MRMC node. Such links are assumed to contain N queues and use N times energy consumption associated with that node. The multiple queue system is depicted in Fig. 5.1. It is noted that at the sender (and, respectively, the receiver) packets from the PMMUP layer (respectively, multiple queues) are striped (respectively, resequenced) into multiple queues (respectively, PMMUP queues) [21, 46, 48, 52]. Queues can be assumed to control the rates of the input to the finite-sized buffers. Such admission control mechanisms are performed if the information about the energy residing in the node and the upper layers is known. Suppose that during a given time-slot, the application generates packets according to a Bernoulli process. Packets independently arrive at the multiple MAC and PHY queues with probability ϕ, where $\phi > 0$. Buffers' sizes of B packets are assumed. Suppose queues are initially nonempty and that new arriving packets are dropped when the queue is full; otherwise packets join the tail of the queue. The speed difference between the queue service rate and the energy level variations in the queue leads to the physical phenomenon called perturbation. Based on such perturbations, optimal transmission power is selected to send a serviced packet. It is noted that such a perturbation can conveniently be modelled by the Markov Chain as follows:

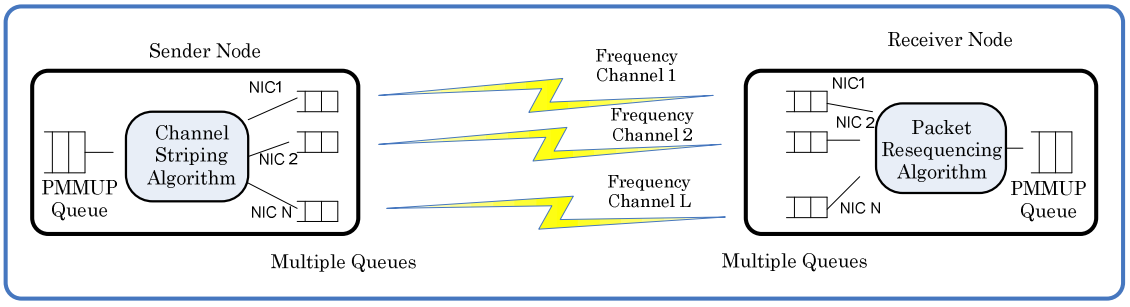

Figure 5.1: Multiple queue system for a MRMC router-pair

Denote $i \in \mathrm{E}$, where $\mathrm{E} = \{1, 2, \ldots, i, \ldots E\}$ as the energy level available for transmitting a packet over wireless medium by each NIC- pair (user). Denote φ_i, where $\varphi_i \in [0,1]$, as the probability of transmitting a packet with energy level i. The transition probability from energy state $X_n = i$ to state $X_{n+1} = j$ during the time transition $[n, n+1)$ is yielded by $\lambda_{ij} = \Pr(X_{n+1} = j \mid X_n = i)$. Let Λ, be the energy level transition matrix, where $\sum_{j=1}^{E} \lambda_{ij} = 1$ with the probability distribution denoted by $\vartheta = [\vartheta_1, \vartheta_2, \ldots, \vartheta_E]$ [275].

$$\Lambda = \begin{bmatrix} \lambda_{11} & \lambda_{12} & .. & \lambda_{1E} \\ \lambda_{21} & \lambda_{22} & .. & \lambda_{2E} \\ .. & .. & .. & .. \\ \lambda_{E1} & \lambda_{E2} & .. & \lambda_{EE} \end{bmatrix}, \tag{5-1}$$

It should be recalled that the power optimization phase requires information about the queue load and energy level dynamics. Such dynamics can be modelled as the Markov chain processes. Denote $X(n) = \{X_n(i(n), j(n))\}$ as a two dimensional Markov chain sequence, where $i(n)$ and $j(n)$ are respectively the energy level available for packet transmission and the number of packets in the buffer at the *n*th time step. Let the packet arrival and the energy-charging/discharging process at each interface in time step $n+1$ be independent of the chain $X(n)$. Arrivals are assumed to occur at the end of the time step so that new arrivals cannot depart in the same time step that they arrive [274]. Figure 5.2 depicts the two dimensional Markov chain evolution diagram with the transition probability matrix, $P_T(n)$, whose elements are $\lambda_{n,n+1}(i, j)$ for all $i = 1, 2, \ldots, E$ and $j = 0, 1, 2, \ldots, B$. The notation, $\lambda_{n,n+1}(i, j)$ represents the transition probability of the *i*th energy level and the *j*th buffer level from state at *n* to state at *n+1*. In general, similar Markov chain representations can be assumed for other queues in a multi-queue system.

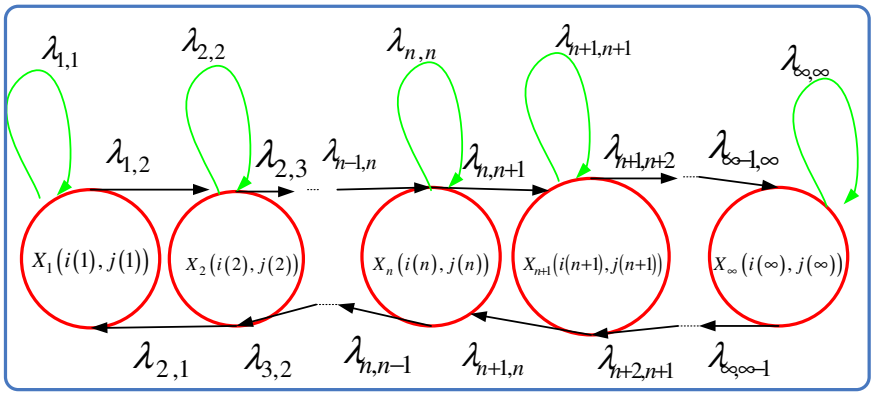

Figure 5.2: Markov chain diagram

The transition probability $E(B+1)\times E(B+1)$ matrix of the Markov chain $X(n)$ is yielded by

$$P_T(n)=\begin{pmatrix} \mathbf{B}_0 & \mathbf{B}_1 & 0 & \cdots & \cdots & \cdots & 0 \\ \mathbf{A}_2 & \mathbf{A}_1 & \mathbf{A}_0 & 0 & \cdots & \cdots & 1 \\ 0 & \mathbf{A}_2 & \mathbf{A}_1 & \mathbf{A}_0 & 0 & \cdots & . \\ \vdots & \ddots & \ddots & \ddots & \ddots & \vdots & . \\ \vdots & \ddots & \ddots & \ddots & \mathbf{A}_1 & \mathbf{A}_0 & . \\ 0 & \cdots & \cdots & 0 & \mathbf{A}_2 & \mathbf{F}_1 & B \end{pmatrix}, \tag{5-2}$$

where $P_T(n)$ consists of $B+1$ block rows and $B+1$ block columns each of size $E\times E$. The matrices $\mathbf{B}_0$, $\mathbf{B}_1$, $\mathbf{A}_0, \mathbf{A}_1$, $\mathbf{A}_2$ and $\mathbf{F}_1$ are all $E\times E$ non-negative matrices denoted as $\mathbf{B}_0=\bar{\phi}\Lambda$, $\mathbf{B}_1=\phi\Lambda$, $\mathbf{A}_0=\mathbf{diag}(\phi\bar{\varphi}_i,\ i=1,\ldots,E)\Lambda$, $\mathbf{A}_1=\mathbf{diag}(\phi\varphi_i+\bar{\phi}\bar{\varphi}_i,\ i=1,\ldots,E)\Lambda$, $\mathbf{A}_2=\mathbf{diag}(\bar{\phi}\varphi_i\ i=1,\ldots,E)\Lambda$ and $\mathbf{F}_1=\mathbf{diag}\,(\phi\varphi_i+\bar{\varphi}_i,\ i=1,\ldots,E)\Lambda$. Here $\bar{\phi}=1-\phi$ and $\bar{\varphi}_i=1-\varphi_i$ respectively denote the probability that no packet arrives in the queue and no packet is transmitted into the channel when the available energy level is i. If one assumes that the energy level transition matrix Λ is irreducible and aperiodic[2] and that $\phi>0$, then the Markov chain $X(n)$ is aperiodic and contains a single ergodic class[3] [38]. A unique row vector of steady state (or stationary) probability distribution can then be defined as $\pi(i,j)=\lim_{n\to\infty}P_T\left(l(n)=i\,,b(n)=j\right),\ i=1,2,\ldots,E,\ \ j=0,1,\ldots,B$ and

[2] A state evidences *aperiodic* behaviour if any return (returns) to the same state can occur at irregular multiple time steps.
[3] A Markov chain is called *ergodic* or *irreducible* if it is possible to go from every state to every other state

$\pi(i,j) \in \Re^{1 \times i(j+1)} \geq 0$.

Let $\pi(i,j,\varepsilon_s)$, $i = 1,\ldots,i,\ldots,E$, $j = 0,1,\ldots j\ldots,B$ be the probability distribution of the state of the available energy and the number of packets in the system in a steady state. Such a probability distribution $\pi(i,j,\varepsilon_s)$ can uniquely be determined by the following system

$$\pi(\varepsilon_s) P_T(\varepsilon_s) = \pi(\varepsilon_s),\ \pi(\varepsilon_s)\mathbf{1} = 1,\ \pi(\varepsilon_s) \geq 0\ , \tag{5-3}$$

where ε_s denotes the *singular perturbation* factor depicting the speed ratio between energy and queue state evolutions. The first order Taylor series approximation of the perturbed Markov chain $X(n)$ transition matrix can be represented as $P_T(\varepsilon_s) = Q_0 + \varepsilon_s Q_1$, where Q_0 is the probability transition matrix of the unperturbed Markov chain corresponding to strong interactions while Q_1 is the generator corresponding to the weak interaction [275], that is,

$$Q_0 = \begin{pmatrix} \bar{\phi} I & \phi I & 0 & \cdots & \cdots & \cdots \\ \bar{\mathbf{A}}_2 & \bar{\mathbf{A}}_1 & \bar{\mathbf{A}}_0 & 0 & \cdots & \cdots \\ 0 & \bar{\mathbf{A}}_2 & \bar{\mathbf{A}}_1 & \bar{\mathbf{A}}_0 & 0 & \cdots \\ \vdots & \ddots & \ddots & \ddots & \ddots & \vdots \\ \vdots & \ddots & \ddots & \ddots & \ddots & \bar{\mathbf{A}}_0 \\ 0 & \cdots & \cdots & 0 & \bar{\mathbf{A}}_2 & \bar{\mathbf{F}}_1 \end{pmatrix},\ Q_1 = \begin{pmatrix} \tilde{\mathbf{B}}_0 & \tilde{\mathbf{B}}_1 & 0 & \cdots & \cdots & \cdots \\ \tilde{\mathbf{A}}_2 & \tilde{\mathbf{A}}_1 & \tilde{\mathbf{A}}_0 & 0 & \cdots & \cdots \\ 0 & \tilde{\mathbf{A}}_2 & \tilde{\mathbf{A}}_1 & \tilde{\mathbf{A}}_0 & 0 & \vdots \\ \vdots & \ddots & \ddots & \ddots & \ddots & \vdots \\ \vdots & \ddots & \ddots & \ddots & \ddots & \tilde{\mathbf{A}}_0 \\ 0 & \cdots & \cdots & 0 & \tilde{\mathbf{A}}_2 & \tilde{\mathbf{F}}_1 \end{pmatrix}, \tag{5-4}$$

where

$\bar{\mathbf{A}}_2 = \mathbf{diag}(\bar{\phi}\varphi_i,\ i=1,\ldots,E)$, $\bar{\mathbf{A}}_1 = \mathbf{diag}(\phi\varphi_i + \bar{\phi}\bar{\varphi}_i,\ i=1,\ldots,E)$,

$\bar{\mathbf{A}}_0 = \mathbf{diag}(\phi\bar{\varphi}_i,\ i=1,\ldots,E)$, $\bar{\mathbf{F}}_1 = \mathbf{diag}(\phi\varphi_i + \bar{\varphi}_i,\ i=1,\ldots,E)$, $\tilde{\mathbf{B}}_0 = \bar{\phi}(\Lambda_1)$,

$\tilde{\mathbf{B}}_1 = \phi(\Lambda_1)$, $\tilde{\mathbf{A}}_2 = \mathbf{diag}\,(\bar{\phi}\varphi_i,\ i=1,\ldots E)\Lambda_1$,

$\tilde{\mathbf{A}}_1 = \mathbf{diag}\,(\phi\varphi_i\bar{\phi}\bar{\varphi}_i,\ i=1,\ldots,E)\Lambda_1$, $\tilde{\mathbf{A}}_0 = \phi\ \mathbf{diag}\,(\phi\bar{\varphi}_i,\ i=1,\ldots,E)\Lambda_1$ and

$\tilde{\mathbf{F}}_1 = \mathbf{diag}\,(\phi\varphi_i + \bar{\varphi}_i,\ i=1,\ldots,E)\Lambda_1$.

Here,

$$\Lambda(\varepsilon_s) = I + \varepsilon_s \Lambda_1 \tag{5-5}$$

where Λ_1 is the generator matrix [273], representing an aggregated Markov chain $X(n)$.

The model in (5-2) to (5-5) leaves us with the perturbation problem under the assumption that an ergodic class exists (i.e., has exactly one closed communicating set of states), and Q_0 contains E sub-chains (E ergodic class). The stationary probability $\pi(i, j, \varepsilon_s)$ from (5-3) of the perturbed Markov chain, therefore, takes a Taylor series expansion

$$\pi(i, j, \varepsilon_s) = \sum_{n=0}^{\infty} \pi^{(n)}(i, j)\, \varepsilon_s^n , \tag{5-6}$$

▪

where ε_s^n is the nth order singularly-perturbed parameter. Denote the aggregate Markov chain probability distribution as $\bar{\vartheta} = \left[\bar{\vartheta}_1, \bar{\vartheta}_2, \ldots, \bar{\vartheta}_E\right]$. The unperturbed stationary probability is then given by $\pi^{(0)}(i, j) = \bar{\vartheta}_i \nu_{\zeta_i}(j)$ where ν_{ζ_i} is the probability distribution of the recurrent class ζ_i, i.e., $\sum_{j=0}^{B} \zeta_i(j) = 1$ [275].

Lemma 5.1: *For each energy level, $i = 1, 2, \ldots, E$, the stationary distribution ν_{ζ_i} of the recurrent class ζ_i is given by:*

***1**-If $i \notin \mathrm{E}_H \cup \mathrm{E}_L$, then $\nu_{\zeta_i}(j+1) = \dfrac{\phi^{j+1}(1-\varphi_i)^j}{\varphi_i^{j+1}(1-\phi)^{j+1}} \nu_{\zeta_i}(0)$, $j = 1, 2, \ldots, B$. Here, $\nu_{\zeta_i}(0) = \dfrac{\varphi_i - \phi}{\varphi_i - \phi\alpha^B}$ with $\alpha = \dfrac{\phi(1-\varphi_i)}{\varphi_i(1-\phi)}$. E_H and E_L are sets respectively of the higher and lower energy levels than the minimum required for successful packet transmission.*

***2**-If $i \in \mathrm{E}_H$, then $\nu_{\zeta_i}(0) = 1 - \phi$ and $\nu_{\zeta_i}(1) = \phi$.*

***3**-If $i \in \mathrm{E}_L$, then $\nu_{\zeta_i}(B) = 1$.*

Proof: If the level of the available energy $i \notin \mathrm{E}_H \cup \mathrm{E}_L$ then we first consider $\nu_{\zeta_i}(1)$ in terms of $\nu_{\zeta_i}(0)$, i.e.,

$$\nu_{\zeta_i}(1) = \frac{1}{1-\varphi_i}\alpha\nu_{\zeta_i}(0).$$

Then by induction

$$\nu_{\zeta_i}(j) = \frac{1}{1-\varphi_i}\alpha^j\nu_{\zeta_i}(0),\ j = 1,2,\ \ldots,B,\ \alpha = \frac{\phi(1-\varphi_i)}{\varphi_i(1-\phi)}.$$ Thus,

$$\nu_{\zeta_i}(j+1) = \frac{1}{1-\varphi_i}\alpha^{j+1}\nu_{\zeta_i}(0);$$ alternatively,

$$\nu_{\zeta_i}(j+1) = \frac{\phi^{j+1}(1-\varphi_i)^j}{\varphi_i^{j+1}(1-\phi)^{j+1}}\nu_{\zeta_i}(0),\ \ j = 1,2,\ \ldots,B.$$ Using the normalization condition that $\sum_{j=0}^{B}\zeta_i(j) = 1$, one obtains $\nu_{\zeta_i}(0)$ by summing over all $j = 0,1,2,\ \ldots,B$,

$$\nu_{\zeta}(0) = \frac{1}{1+\frac{1}{1-\varphi_i}\alpha\frac{1-\alpha B}{1-\alpha}} = \frac{\varphi-\phi}{\varphi-\phi\alpha^B}. \tag{5-7}$$

▪

Suppose the level of the available energy is $i \in \mathrm{E}_H$, given that there is no packet in the queue then the condition $\nu_{\zeta_i}(0) = 1-\phi = \bar{\phi}$ holds. Consequently, one packet arrives with probability ϕ, implying that $\nu_{\zeta_i}(1) = \phi$. In a similar treatment, if the energy is $i \in \mathrm{E}_L$ given a full buffer then the stationary distribution of the recurrent class, ζ_i, is yielded by $\nu_{\zeta_i}(B) = 1$.

Lemma 5.2: *Assuming that there exists a perturbed Markov Chain* $X_n(i,j,\varepsilon_s)$, *the perturbed steady state transmission probability is given as follows:*

$$\psi(\varepsilon_s) = \sum_{(i,j)}\frac{\phi^{j+1}(1-\varphi_i)^{j-1}\varphi_i^{B+1}(1-\phi)^B(\varphi_i-\phi)}{\varphi_i^{B+j}(1-\phi)^{B+j}-\phi^{B+1}(1-\varphi_i)^{B-1}} + \phi\sum_{(i,j)}\sum_{n=1}^{\infty}\pi^{(n)}(i,j)\varepsilon_s^n\varphi_i\ , \tag{5-8}$$

where

$$\pi^{(n)} = \vartheta\left[\mathbf{R}(\mathbf{Q}_1\Delta_0)^n + \sum_{k=1}^{n-1}\left(\mathbf{R}\mathbf{Q}_1\Delta_0\tilde{\mathbf{R}}\Delta_1\right)^k(\mathbf{Q}_1\Delta_0)^{n-k}\right].$$

Here,

$\mathbf{R} \in \Re^{(E+1)\times(E+1)(B+1)}$ *denotes a matrix whose rows are a stationary distribution of the Markov chain* $\mathbf{Q}_0$, *i.e.,* $\mathbf{R} = \mathbf{diag}\left(\nu_{\zeta_i},\, i = 0,1,\, \ldots\, ,E\right)$. $\tilde{\mathbf{R}} \in \Re^{(E+1)(B+1)\times(E+1)}$ *denotes a matrix of eigenvectors corresponding to the zero eigenvalue of the unperturbed generator* $\mathbf{Q}_0 - I$, *i.e.,* $\tilde{\mathbf{R}} = \left(\theta_{\zeta_0}, \theta_{\zeta_1}, \ldots, \theta_{\zeta_E}\right)$. Δ_0 *denotes a deviation matrix of the unperturbed Markov chain* $\Delta_0 = \left[I - \mathbf{Q}_0 + \tilde{\mathbf{R}}\mathbf{R}\right]^{-1} - \tilde{\mathbf{R}}\mathbf{R}$. $\Delta_1 = \left[-\Lambda_1 + \Lambda^*\right]^{-1} - \Lambda^*$ *denotes a deviation of the aggregated Markov chain, where* $\Lambda^* = \mu_E \vartheta$, *with* $\mu_E = (1, \ldots, 1)^T \in \Re^{E+1}$ *[275].*

Proof: By definition and Lemma 5.1, the steady state transmission probability $\psi(\varepsilon_s)$ is given by the following

$$\begin{aligned}
\psi(\varepsilon_s) &= \phi \sum_{(i,j)} \sum_{n=0}^{\infty} \pi^{(n)}(i,j)\varepsilon_s^n \varphi_i, \quad i = 1,2, \ldots, E \text{ and } j = 0,1,2, \ldots, B \\
&= \phi \sum_{(i,j)} \pi^{(0)}(i,j)\varepsilon_s^0 \varphi_i + \phi \sum_{(i,j)} \sum_{n=1}^{\infty} \pi^{(n)}(i,j)\varepsilon_s^n \varphi_i, \\
&= \phi \sum_{(i,j)} \vartheta_i \nu_{\zeta_i}(j)\varphi_i + \phi \sum_{(i,j)} \sum_{n=1}^{\infty} \pi^{(n)}(i,j)\varepsilon_s^n \varphi_i, \\
&= \phi \sum_{(i,j)} \vartheta_i \frac{\alpha^j \nu_{\zeta_i}(0)}{(1-\varphi_i)}\varphi_i + \phi \sum_{(i,j)} \sum_{n=1}^{\infty} \pi^{(n)}(i,j)\varepsilon_s^n \varphi_i, \text{ with } \alpha = \frac{\phi(1-\varphi_i)}{\varphi_i(1-\phi)}, \\
&\qquad\qquad \nu_{\zeta_i}(0) = \frac{\varphi_i - \phi}{\varphi_i - \phi\alpha^B}, \\
&= \sum_{(i,j)} \vartheta_i \frac{\phi^{j+1}(1-\varphi_i)^{j-1}\varphi_i^{B+1}(1-\phi)^B(\varphi_i - \phi)}{\varphi_i^{B+j}(1-\phi)^{B+j} - \phi^{B+1}(1-\varphi_i)^{B-1}} + \phi \sum_{(i,j)} \sum_{n=1}^{\infty} \pi^{(n)}(i,j)\varepsilon_s^n \varphi_i,
\end{aligned} \tag{5-9}$$

with $\pi^{(n)}$ being recursively evaluated as given in Lemma 5.2.

■

Lemma 5.3: *Assuming that there exists a perturbed Markov Chain* $X_n(i,j,\varepsilon_s)$, *the expected delay in a singularly-perturbed queue,* $\mathrm{E}_D(\varepsilon_s)$ *is given as follows:*

$$\mathrm{E}_D(\varepsilon_s) = \frac{Nu}{De}, \tag{5-10}$$

where,

$$Nu = \sum_{(i,j)} \vartheta_i \frac{\phi^j (1-\varphi_i)^{j-1} \varphi_i^B (1-\phi)^B (\varphi_i - \phi) j}{\varphi_i^{B+j}(1-\phi)^{B+j} - \phi^{B+1}(1-\varphi_i)^{B-1}} + \sum_{(i.j)} \sum_{n=1}^{\infty} \pi^{(n)}(i,j) \varepsilon_s^n j, i = 1,2, \ldots, E,$$

$$j = 0,1,2, \ldots, B.$$

$$De = \phi - \sum_{i \notin E_H \cup E_L} \vartheta_i \frac{\phi^{B+1}(1-\varphi_i)^B}{(\varphi_i(1-\phi))^B} + \sum_{i \in E_L} \vartheta_i + \sum_{i=1} \sum_{n=1}^{\infty} \pi^{(n)}(i,B) \varepsilon_s^n, \text{ with}$$

$$\pi^{(n)} = \vartheta \left[\mathbf{R}(\mathbf{Q}_1 \Delta_0)^n + \sum_{k=1}^{n-1} \left(\mathbf{R}\mathbf{Q}_1 \Delta_0 \tilde{\mathbf{R}} \Delta_1 \right)^k (\mathbf{Q}_1 \Delta_0)^{n-k} \right].$$

Proof: By definition, the average number of packets in the queue is yielded by

$$Nu = \mathrm{E}[X_n] = \sum_{(i,j)} \pi(i,j,\varepsilon_s) j, \; i = 1,2, \ldots, E, \; j = 0,1,2, \ldots, B.$$

$$= \sum_{(i,j)} \sum_{n=0}^{\infty} \pi^{(n)}(i,j) \varepsilon_s^n j, \; i = 1,2, \ldots, E, \; j = 0,1,2, \ldots, B.$$

$$= \sum_{(i,j)} \pi^{(0)}(i,j) j + \sum_{(i,j)} \sum_{n=1}^{\infty} \pi^{(n)}(i,j) \varepsilon_s^n j, i = 1,2, \ldots, E,$$

$$j = 0,1,2, \ldots, B.$$

After expanding the above and using the results in Lemma 5.1, we obtain

$$Nu = \sum_{(i,j)} \vartheta_i \frac{\phi^j (1-\varphi_i)^{j-1} \varphi_i^B (1-\phi)^B (\varphi_i - \phi) j}{\varphi_i^{B+1}(1-\phi)^{B+j} - \phi^{B+1}(1-\varphi_i)^{B-1}} + \sum_{(i,j)} \sum_{n=1}^{\infty} \pi^{(n)}(i,j) \varepsilon_s^n j, \text{ for all}$$

i and j.

Suppose ϕ^* denotes the packet acceptance rate into the queue at steady state. Define ϕ^* as,

$$\phi^* = De = \phi \left(1 - \sum_{i=1}^{E} \pi(i,B,\varepsilon_s) \varphi_i \right),$$

$$= \phi \left(1 - \sum_{i=1}^{E} \sum_{n=0}^{\infty} \pi^{(n)}(i,B) \varepsilon_s^n \varphi_i \right),$$

$$= \phi \left(1 - \sum_{i=1}^{E} \pi^{(0)}(i,B) \varphi_i + \sum_{i=1}^{E} \sum_{n=1}^{\infty} (i,B) \varepsilon_s^n \varphi_i \right).$$

Applying results of Lemma 5.1, we obtain

$$De = \phi\left(1 - \sum_{i \in \mathrm{E}_H \cup \mathrm{E}_L} \vartheta_i \frac{\phi^B \left(1-\varphi_i\right)^B}{\left(\varphi_i\left(1-\phi\right)\right)^B} + \phi^{-1} \sum_{i=\mathrm{E}_L} \vartheta_i + \phi^{-1} \sum_{i=1}^{E} \sum_{n=1}^{\infty} \pi^{(n)}\left(i, B\right) \varepsilon_s^n\right).$$

Using Little's Theorem [273, 280], the average delay in a perturbed queue is calculated by

$$\mathrm{E}_D\left(\varepsilon_s\right) = \frac{Nu}{De}. \tag{5-11}$$

■

It should be noted from the results of Lemma 5.1 and 5.2 that the steady state transmission probability of a packet from the queue and the expected packet queue delay are decomposable into an unperturbed component (i.e., independent of ε_s) and a perturbed component expressed in terms of a higher order Taylor series expansion (i.e., dependent on ε_s). A higher order Taylor series expansion with sufficiently large step size n results in significantly small values of perturbation, hence such terms can be neglected. The first order Taylor series expansion in terms of the perturbation factor presents a reliable approximation of the exact steady state probability distribution of the Markov chain $X_n\left(i, j, \varepsilon_s\right)$.

5.2.2 Weakly-Coupled Wireless System

Theoretically, simultaneous transmitting links on different non-overlapping and orthogonal channels are expected not to conflict with each other. However, wireless links emanating from the same node of a multi-radio system do conflict with each other owing to their close vicinity. The radiated power coupling across multiple channels results in the following: loss in signal strength owing to inter-channel interference; hence packet losses over multi-channel wireless links. Such losses lead to packet retransmissions and hence queue instabilities along a link(s). Retransmissions also cause high energy consumption in the network. Highly energy-depleted networks result in poor network connectivity. Therefore, one can model the wireless cross-channel interference (interaction) as a weakly-coupled system [271]. Each NIC-pair (i.e., transmit-receive or user) operating on a particular channel (i.e., UCG) adjusts its transmission power dynamically, based on a sufficiently small positive parameter denoted as ε_w.

Consider a two-dimensional node placement consisting of two co-located orthogonal wireless channels labelled i and j with simultaneous radial transmissions. Such a

configuration is illustrated in Fig. 5.3. The coupled region is denoted by surface area A_ε. Since power coupling is considered, the weak coupling factor can be derived as a function of the region or surface A_ε, i.e., $O\left(d_{ij}^2\right)$, where d_{ij} is the distance between point i and j. From the geometry of Fig. 5.3, it is easy to demonstrate that the weak coupling parameter is obtained as

$$\varepsilon_{ij} = \frac{\mathrm{A}_{\varepsilon i}}{\mathrm{A}_\varepsilon} = \frac{d_i^2\left[\theta_i - \frac{\sin\theta_i}{\sqrt{2}}\right]}{d_i^2\left[\theta_i - \frac{\sin\theta_i}{\sqrt{2}}\right] + d_j^2\left[\theta_j - \frac{\sin\theta_j}{\sqrt{2}}\right]},$$

$$\varepsilon_{ji} = \frac{\mathrm{A}_{\varepsilon j}}{\mathrm{A}_\varepsilon} = \frac{d_j^2\left[\theta_j - \frac{\sin\theta_j}{\sqrt{2}}\right]}{d_i^2\left[\theta_i - \frac{\sin\theta_i}{\sqrt{2}}\right] + d_j^2\left[\theta_j - \frac{\sin\theta_j}{\sqrt{2}}\right]}. \tag{5-12}$$

Thus, the weakly-coupled scalar is generally a function of the square of the transmission radius and the coupling-sector angle. The weak coupling parameter is bounded by $0 < \varepsilon_{ij} = \varepsilon_w < 1$. The sectored angle has a bound, $0 \le \theta \le 2\pi$ radians.

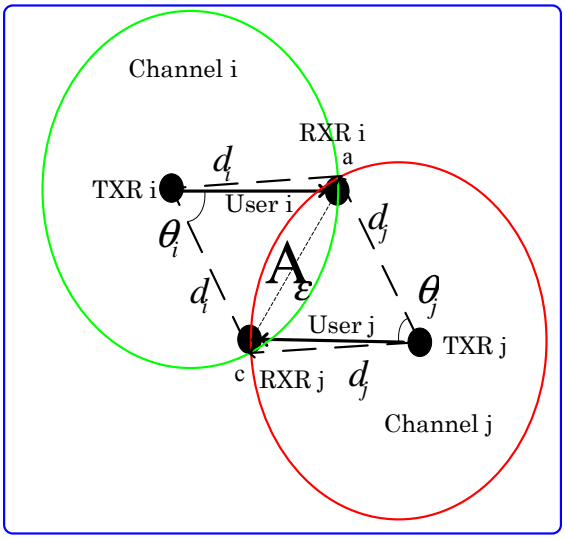

Figure 5.3: Weak coupling between two channels

In Figure 5.3, two simultaneously co-located transmitting users i and j described by infinitesimally small radiating points TXR i and RXR i pair, and TXR j and RXR j pair, respectively. Transmitters i and j are assumed to radiate signals omni-directionally with radii d_i and d_j and cause weak inter channel connections. Here, d_i refers to the conflict edge from a sender on channel i to a receiver on channel j while d_j is the conflict edge from a sender on channel j to a receiver on channel i. The region denoted by A_ε is the weakly coupling region described by d_i and d_j as well as by the coupling beamwidth angles θ_i and θ_j in radians.

It should be noted that both the singular perturbation and weak coupling models at the multiple MACs and radio interfaces are coordinated by the virtual MAC protocol at the Link Layer. The motivation is to conceal the complexity of lower layers from the higher layers of the protocol stack.

5.3 SPWC-PMMUP Architecture

In order to manage SPWC models based DTPC scheme at the complex MAC and PHY layers, a *singularly-perturbed weakly-coupled power selection multi-radio multi-channel unification protocol* (SPWC-PMMUP) is suggested. The SPWC-PMMUP firmware architecture is depicted in Figure 5.4. The design rationale of the firmware is to perform an energy-efficient power control in a multi-radio system with minimal change to the existing standard compliant wireless technologies. Such power control can adapt even to a heterogeneous multi-radio system (i.e., each node has a different number of radios) experiencing singular perturbations. Like the PMMUP discussed in Chapter 4, SPWC-PMMUP coordinates the power control executions in UCGs. Power optimization is based on the *Link State Information* (LSI) from the same channel or coordinated channels. In addition, this chapter deals with queue perturbation and cross-channel interference. It also furnishes the medium access timing phases.

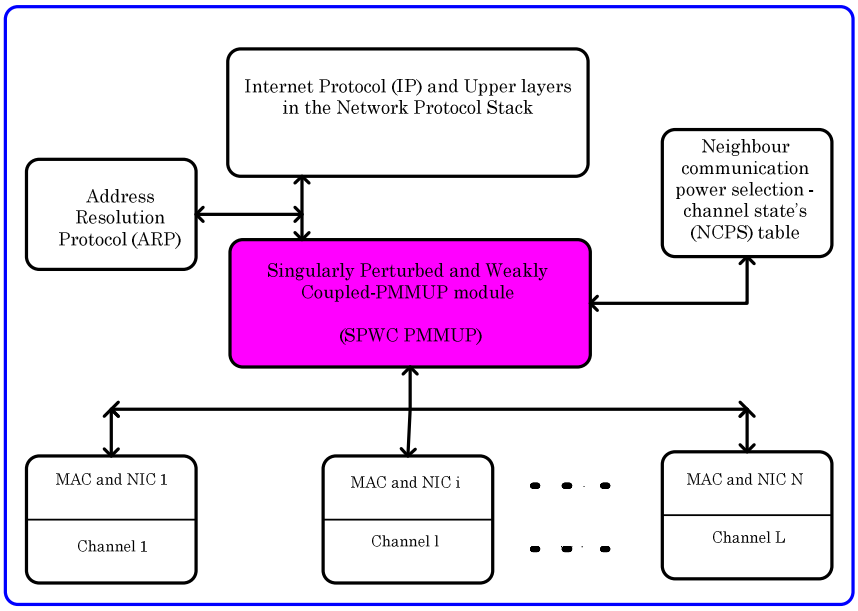

Figure 5.4: Singularly-perturbed weakly-coupled PMMUP architecture

5.3.1 Timing Phase Structure

The SPWC-PMMUP contains L parallel channel sets with the virtual timing structure shown in Fig. 5.5. Channel access times are divided into identical time-slots. There are three phases in each time slot after slot synchronization. Phase I serves as the channel probing or LSI estimation phase. Phase II serves as the *Announcement Traffic Indication Message* (ATIM) window which is on when power optimization occurs. Nodes stay awake and exchange an ATIM (indicating such nodes' intention to send the queue data traffic) message with their neighbours. Each node is faced with a power control problem formulated in section 5.4. Based on the exchanged ATIM and probe messages, each user performs an optimal power selection for eventual data exchange. Phase III serves as the data exchange phase over power controlled multiple channels.

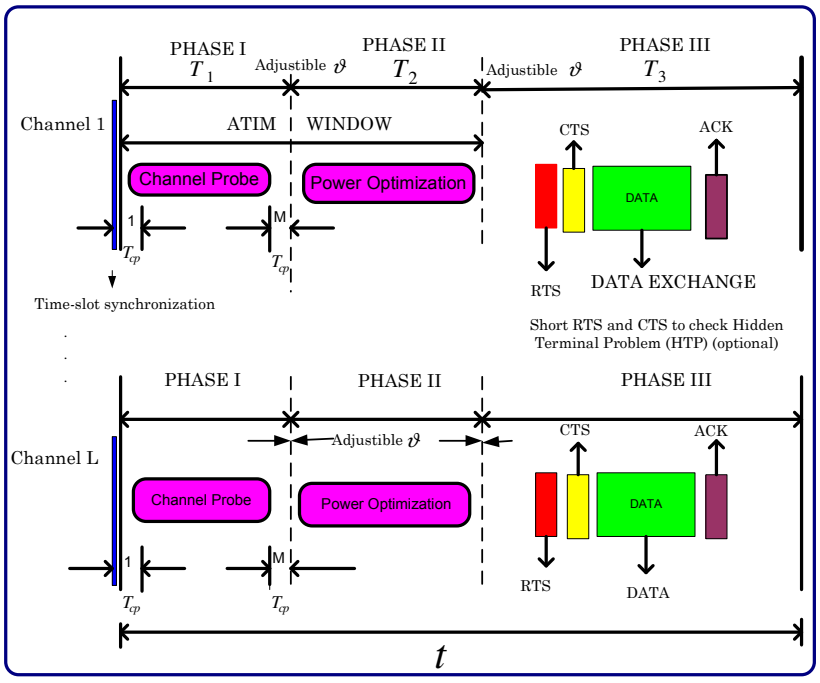

Figure 5.5: The virtual SPWC-PMMUP timing structure

Phase I: In order for each user to estimate the number of active links in the same UCG, Phase I is divided into M mini-slots. Each mini-slot lasts a duration of channel probing time T_{cp}, which is set to be large enough for judging whether the channel is busy or not. If a link has traffic in the current time-slot, it may randomly select one probe mini-slot and transmit a

busy signal. By counting the busy mini-slots, all nodes can estimate how many links intend to advertise traffic at the end of Phase I. Additionally, the SPWC-PMMUP estimates: the inter channel interference (i.e., weak coupling powers), the intra-UCG interference (i.e., the strong coupling powers), the queue perturbation and the LSI addressed in Chapter 4 [46]. It should be noted that the number of links intending to advertise traffic, if not zero, could be greater than the observed number of busy mini-slots. This occurs because there might be at least one link intending to advertise traffic during the same busy mini-slot.

Denote the number of neighbouring links in the same UCG intending to advertise traffic at the end of Phase I as n. Given M and n, the probability that the number of observed busy mini-slots equals to m, is calculated by

$$P_r(M,n,m) = \frac{\binom{M}{m}\binom{n-1}{m-1}}{\binom{n+M-1}{M-1}} \tag{5-13}$$

Let n remain the same for the duration of each time-slot t. Denote the estimate of the number of active links as $\hat{n}(t)$ and the probability mass function (PMF) that the number of busy mini-slots observed in the previous time-slot equals k as $f_k(t)$. Denote $m(t)$ as the number of the current busy mini-slots. The estimate $\hat{n}(t)$ is then derived from the estimation error process as,

$$\hat{n}(t) = \arg\min_{n \geq m(t)} \left\{ \sum_{k=m(t)}^{n} P_r(M,n,k) - \sum_{k=m(t)}^{n} f_k(t) \right\}, \tag{5-14}$$

where $f_k(t)$ from one time-slot to other is updated as

$$f_k(t) = \begin{cases} (1-\alpha(t)) f_k(t-1), & k \neq m(t) \\ (1-\alpha(t)) f_m(t-1) + \alpha(t), & k = m(t) \end{cases}, \tag{5-15}$$

and $\alpha(t)$, $(0 < \alpha(t) < 1)$ is the PMF update step size, which needs to be chosen appropriately to balance the convergence speed and the stability. Of course, selecting a large value of M

when Phase I is adjusted to be narrower will imply short T_{cp} periods and negligible delay during the probing phase. Short channel probing phase time allows time for large actual data payload exchange, consequently improving network capacity.

Phase II: Suppose the number of busy mini-slot is non-zero then the SPWC-PMMUP module performs a power optimization following the $p-$persistent algorithm or back-off algorithm [249]. Otherwise, the transmission power optimization depends on the queue status only (i.e., the evaluation of the singular perturbation of the queue system). The time duration of the power optimization is denoted as T_2 and the minimal duration to complete power optimization as a function of the number of participating users in a p-persistent CSMA, is denoted as $T_{succ}\left(n, p^*\right)$ [281]. The transmission power optimization time allocation T_2 is then adjusted according to

$$T_2 = \min\left\{T_2^{\max}, \vartheta \sum_{n=1}^{\hat{n}} T_{succ}\left(n, p^*\right)\right\}, \tag{5-16}$$

where $T_2^{\max}$ is the power allocation upper bound time, ϑ is the power allocation time adjusting parameter and $\hat{n}$ is the estimated number of actively interfering neighbour links in the same UCG. The steady state medium access probability p in terms of the minimal average service time can be computed as [208],

$$p^* = \arg\min_{0<p<1}\left\{T_{succ}\left(n, p\right)\right\}. \tag{5-17}$$

It should be noted that due to energy conservation, T_1 and T_2 should be short enough and the optimal p^* can be obtained from a look up table rather than from online computation. The transmission power problem and solution can be formulated according to the optimization criteria in Sections 5.4 and 5.5.

Phase III: Data is exchanged by NICs over parallel multiple non-overlapping channels within a time period of T_3. The RTS/CTS are exchanged at the probe power level sufficient enough in order to resolve collisions due to hidden terminal nodes. Furthermore, the optimal

medium access probability p^* resolves RTS/CTS collisions. After sending data traffic to the target receiver, each node may determine the achievable throughput according to [208, 249],

$$Th_r(t) = \frac{\tilde{L}}{t}\left\{\sum_i \left\{ P_i^{swp}\left(\vec{n}_{swp}, \vec{p}_{swp,} T_2\right) \times \sum_{l=1}^{L} \sum_j j\, P_j^{l,data}\left(\vec{n}_{l,data}, \vec{p}_{l,data}, T_3\right)\right\}\right\}. \quad (5\text{-}18)$$

Here, $\tilde{L}$ is the application/data packet length and t is the length of one virtual time-slot which equals $T_1 + T_2 + T_3$. Denote $P_i^{swp}\left(\vec{n}_{swp}, \vec{p}_{swp}, T_2\right)$ as the SPWC based probability that i actively interfering links successfully exchange ATIM in Phase II, given the number of links intending to advertise traffic as, $\vec{n}_{swp}$ and the medium access probability sequence as, $\vec{p}_{swp}$ during time T_2 period. Denote $P_i^{l,data}\left(\vec{n}_{l,data}, \vec{p}_{l,data}, T_3\right)$ as the probability that i data packets are successfully exchanged on channel l in Phase III, given the number sequence $\vec{n}_{l,data}$ and the medium access probability sequence as $\vec{p}_{l,data}$ during time T_3 period. The computations of such probabilities have been provided in [282]. If several transmissions are executed, then an average throughput performance can be evaluated. The energy efficiency in joules per successfully transmitted packets then becomes

$$E_{eff} = \frac{optimal\, transmission\, power\, per\, node\left(watts\right)}{average Throughput\, per\, node\ \left(packets/\mathrm{s}\right)}. \quad (5\text{-}19)$$

It should be noted that a high throughput implies a low energy-efficiency for a given optimal power level, because of the high data payload needed to successfully reach the intended receiver within a given time slot. The use of an optimal power level creates better spectrum efficiency and improved throughput measurement. Such optimal power levels can be formulated according to Section 5.4 while managed by the SPWC-PMMUP developed at the LL.

5.4 Problem Formulation

5.4.1 Preliminaries

Based on the virtual SPWC-PMMUP timing structure discussed in Section 5.3, the transmission power optimization is performed during Phase II. Indeed, the study can be simplified by *decomposing* the WMN into separate but interconnected single channels (i.e., each being a set of users forming the *Unified Channel Graphs* (UCGs)). This concept naturally leads to a decentralized optimization for large scale systems [283]. The higher order state variables are then reflected by the wireless interconnected system [271]. As a result, the transmission power control problem can be formulated as Nash Equilibrium differential games [284].

For N users at each WMR, the SPWC large-scale linear dynamic system is written as [271, 277-279],

$$\mathbf{x}_i(t+1) = \mathbf{A}_{ii}(\varepsilon)\mathbf{x}_i(t) + \mathbf{B}_{ii}(\varepsilon)\mathbf{u}_i(t) + \mathbf{W}_{ii}(\varepsilon)\mathbf{w}_i(t)$$

$$+ \sum_{\substack{j=1 \\ j\neq i}}^{N} \varepsilon_{ij}\mathbf{A}_{ij}\mathbf{x}_j(t) + \sum_{\substack{j=1 \\ j\neq i}}^{N} \varepsilon_{ij}\mathbf{B}_{ij}\mathbf{u}_j(t) + \sum_{\substack{j=1 \\ j\neq i}}^{N} \varepsilon_{ij}\mathbf{W}_{ij}\mathbf{w}_j(t),$$

$$\mathbf{y}_i(t) = \mathbf{C}_{ii}(\varepsilon)\mathbf{x}_i(t) + \sum_{\substack{j=1 \\ j\neq i}}^{N} \varepsilon_{ij}\mathbf{C}_{ij}\mathbf{x}_j(t) + \mathbf{v}_i(t), \quad \mathbf{x}_i(0) = \mathbf{x}_i^0, \; i = 1, \ldots, N, \qquad (5\text{-}20)$$

where $\mathbf{x}_i \in \Re^{n_i}$ represents the state (LSI) vector of the ith user, $\mathbf{u}_i \in \Re^{m_i}$ is the control input of the ith user, $\mathbf{w}_i \in \Re^{q_i}$ represents the Gaussian distributed zero mean disturbance noise vector to the ith user, $\mathbf{y}_i \in \Re^{l_i}$ represents the observed output and $\mathbf{v}_i \in \Re^{l_i}$ are the Gaussian distributed zero mean measurement noise vectors. The white noise processes $\mathbf{w}_i \in \Re^{q_i}$ and $\mathbf{v}_i \in \Re^{l_i}$ are independent and mutually uncorrelated with intensities $\Theta_{\mathbf{w}} > 0$ and $\Theta_{\mathbf{v}} > 0$, respectively. The problem system matrices **A**, **B**, **C** and **W** are defined in the same way as discussed in Chapter 4.

Let the partitioned matrices for the wireless MRMC node pair with the weak-coupling to the singular-perturbation ratio $0<\varepsilon=\frac{\varepsilon_w}{\varepsilon_s}<\infty$, be defined as follows:

$$\mathbf{A}_\varepsilon=\begin{bmatrix}\mathbf{A}_{11}(\varepsilon) & \varepsilon_{12}\mathbf{A}_{12} & \dots & \varepsilon_{1N}\mathbf{A}_{1N}\\ \varepsilon_{21}\mathbf{A}_{21} & \mathbf{A}_{22}(\varepsilon) & \dots & \varepsilon_{2N}\mathbf{A}_{2N}\\ . & . & . & .\\ \varepsilon_{N1}\mathbf{A}_{N1} & \varepsilon_{N2}\mathbf{A}_{N2} & \dots & \mathbf{A}_{NN}(\varepsilon)\end{bmatrix},\ \mathbf{B}_{i\varepsilon}=\begin{bmatrix}\varepsilon^{1-\delta_{1i}}\mathbf{B}_{1i}\\ \varepsilon^{1-\delta_{2i}}\mathbf{B}_{2i}\\ .\\ \varepsilon^{1-\delta_{Ni}}\mathbf{B}_{Ni}\end{bmatrix},\ \delta_{ij}=\begin{cases}0\ (i\neq j)\\ 1\ (i=j)\end{cases},$$

$$\mathbf{W}_\varepsilon=\begin{bmatrix}\mathbf{W}_{11}(\varepsilon) & \varepsilon_{12}\mathbf{W}_{12} & \dots & \varepsilon_{1N}\mathbf{W}_{1N}\\ \varepsilon_{21}\mathbf{W}_{21} & \mathbf{W}_{22}(\varepsilon) & \dots & \varepsilon_{2N}\mathbf{W}_{2N}\\ . & . & . & .\\ \varepsilon_{N1}\mathbf{W}_{N1} & \varepsilon_{N2}\mathbf{W}_{N2} & \dots & \mathbf{W}_{NN}(\varepsilon)\end{bmatrix},\ \mathbf{C}_\varepsilon=\begin{bmatrix}\mathbf{C}_{11}(\varepsilon) & \varepsilon_{12}\mathbf{C}_{12} & \dots & \varepsilon_{1N}\mathbf{C}_{1N}\\ \varepsilon_{21}\mathbf{C}_{21} & \mathbf{C}_{22}(\varepsilon) & \dots & \varepsilon_{2N}\mathbf{C}_{2N}\\ . & . & . & .\\ \varepsilon_{N1}\mathbf{C}_{N1} & \varepsilon_{N2}\mathbf{C}_{N2} & \dots & \mathbf{C}_{NN}(\varepsilon)\end{bmatrix}.\quad(5\text{-}21)$$

Each strategy user is faced with the *minimization problem* along trajectories of a linear dynamic system in (5-20),

$$J_i\left(u_1,\dots,u_N,\mathbf{w},\mathbf{x}(0)\right)=$$

$$=\frac{1}{2}\mathrm{E}\left\{\lim_{t\to\infty}\frac{1}{t}\sum_{\tau=0}^{t-1}\begin{bmatrix}\mathbf{z}^T(\tau)\mathbf{z}(\tau)+\mathbf{u}_i^T(\tau)\mathbf{R}_{ii}\mathbf{u}_i(\tau)\\ +\sum_{\substack{j=1\\ j\neq i}}^{N}\varepsilon_{ij}\mathbf{u}_j^T(\tau)\mathbf{R}_{ij}\mathbf{u}_j(\tau)-\ \mathbf{w}^T(t)\Theta_{\mathbf{w}i\varepsilon}\mathbf{w}(t)\end{bmatrix}\right\},\quad(5\text{-}22)$$

where $\mathbf{z}\in\Re^s$ is the controlled output with dimension equal to s, given by [271],

$$\mathbf{z}_i(t)=\mathbf{D}_{ii}(\varepsilon)\mathbf{x}_i(t)+\sum_{\substack{j=1\\ j\neq i}}^{N}\varepsilon_{ij}\mathbf{D}_{ij}\mathbf{x}_j(t),\quad(5\text{-}23)$$

with

$$\mathbf{D}_\varepsilon=\begin{bmatrix}\mathbf{D}_{11}(\varepsilon) & \varepsilon_{12}\mathbf{D}_{12} & \dots & \varepsilon_{1N}\mathbf{D}_{1N}\\ \varepsilon_{21}\mathbf{D}_{21} & \mathbf{D}_{22}(\varepsilon) & \dots & \varepsilon_{2N}\mathbf{D}_{2N}\\ . & . & . & .\\ \varepsilon_{N1}\mathbf{D}_{N1} & \varepsilon_{N2}\mathbf{D}_{N2} & \dots & \mathbf{D}_{NN}(\varepsilon)\end{bmatrix},$$
$$\in\ \Re^{\bar{n}\times\bar{n}}$$

$$\mathbf{R}_{ii} = \mathbf{R}_{ii}^T > 0 \in \Re^{m_i \times m_i}, \mathbf{R}_{ij} = \mathbf{R}_{ij}^T \geq 0 \in \Re^{m_j \times m_j},$$

$$\Theta_{\mathbf{w}i\varepsilon} = \mathbf{block\ diag}\left(\varepsilon_{i1}^{-(1-\delta_{i1})}\Theta_{\mathbf{w}i1} \ldots \varepsilon_{iN}^{-(1-\delta_{iN})}\Theta_{\mathbf{w}iN}\right) \geq 0 \in \Re^{\bar{q}\times\bar{q}},\ i,\ j=1,\ldots,N\ .$$

5.4.2 Nash Strategies

The optimal solution to the given problem (5-22) with the conflict of interest and simultaneous decision making leads to the so called Nash strategies [271] $\mathbf{u}_1^*,...,\mathbf{u}_i^*,...,\mathbf{u}_N^*$ satisfying

$$J_i\left(\mathbf{u}_1^*,\ldots,\mathbf{u}_i^*,\ldots,\mathbf{u}_N^*,\mathbf{x}(0)\right) \leq J_i\left(\mathbf{u}_1^*,\ldots,\mathbf{u}_i,\ldots,\mathbf{u}_N^*,\mathbf{x}(0)\right), \mathbf{u}_i^* \neq \mathbf{u}_i,\ i=1,\ldots,N\ . \quad (5\text{-}24)$$

Assumption 5.1*: Each* ith *user has optimal closed-loop Nash strategies yielded by*

$$\mathbf{u}_i^*(t) = -\mathbf{F}_{i\varepsilon}^*\mathbf{x}(t), \quad i=1,\ldots,N\ . \quad (5\text{-}25)$$

Here, the decoupled $\mathbf{F}_{i\varepsilon}^*$ is the regulator feedback gain with singular-perturbation and weak-coupling components defined as

$$\mathbf{F}_{i\varepsilon} = \left[\varepsilon^{1-\delta_{1i}}\mathbf{F}_{1i}\ \varepsilon^{1-\delta_{2i}}\mathbf{F}_{2i}\ \ldots\ \varepsilon^{1-\delta_{Ni}}\mathbf{F}_{Ni}\right] \in \Re^{\bar{n}}\ , \quad (5\text{-}26)$$

with $\bar{n} = \sum_{i=1}^N n_i$, n_i is the size of the vector $\mathbf{x}_i$ and $\delta_{ij} = \begin{cases} 0\ (i \neq j) \\ 1\ (i = j) \end{cases}$.

Define the N-tuple discrete in time Nash strategies by

$$\mathbf{u}_i^*(t) = -\mathbf{F}_{i\varepsilon}^*\mathbf{x}(t) = -\left(\mathbf{R}_{ii} + \mathbf{B}_{i\varepsilon}^T\mathbf{P}_{i\varepsilon}\mathbf{B}_{i\varepsilon}\right)^{-1}\mathbf{B}_{i\varepsilon}^T\mathbf{P}_{i\varepsilon}\mathbf{A}_\varepsilon\mathbf{x}(t), \quad i=1,\ldots,N, \quad (5\text{-}27)$$

where $\left(\mathbf{F}_{1\varepsilon}^*,\ldots,\mathbf{F}_{N\varepsilon}^*\right) \in F_N$ and N-tuple $\mathbf{u}_i^*(t)$, form a soft constrained Nash Equilibrium represented as

$$J_i\left(\mathbf{F}_{1\varepsilon}^{*}\mathbf{x},\ldots,\mathbf{F}_{N\varepsilon}^{*}\mathbf{x},\,\mathbf{x}(0)\right)=\mathbf{x}(0)^T\,\mathbf{P}_{i\varepsilon}\mathbf{x}(0). \tag{5-28}$$

Here, the decoupled $\mathbf{P}_{i\varepsilon}$ is a positive semi-definite stabilizing solution of the discrete-time algebraic regulator Riccati equation (DARRE) with the following structure:

$$\mathbf{P}_{i\varepsilon}=\mathbf{P}_{i\varepsilon}^T=\begin{bmatrix}\varepsilon_{i1}^{1-\delta_{i1}}\mathbf{P}_{i1} & \varepsilon_{i2}\mathbf{P}_{i12} & . & \varepsilon_{iN}\mathbf{P}_{i1N}\\ \varepsilon_{i2}\mathbf{P}_{i12}^T & \varepsilon_{i2}^{1-\delta_{i2}}\mathbf{P}_{i2} & . & \varepsilon_{iN}\mathbf{P}_{i2N}\\ . & . & . & .\\ \varepsilon_{iN}\mathbf{P}_{i1N}^T & \varepsilon_{iN}\mathbf{P}_{i2N}^T & . & \varepsilon^{1-\delta_{iN}}\mathbf{P}_{iN}\end{bmatrix}, \tag{5-29}$$
$$\in\ \Re^{\bar{n}\times\bar{n}}$$

where the DARRE is given by

$$\mathbf{P}_{\varepsilon}=\mathbf{D}_{\varepsilon}^T\mathbf{D}_{\varepsilon}+\mathbf{A}_{\varepsilon}^T\mathbf{P}_{\varepsilon}\mathbf{A}_{\varepsilon}-\mathbf{A}_{\varepsilon}^T\mathbf{P}_{\varepsilon}\mathbf{B}_{\varepsilon}\left(\mathbf{R}_{\varepsilon}+\mathbf{B}_{\varepsilon}^T\mathbf{P}_{\varepsilon}\mathbf{B}_{\varepsilon}\right)^{-1}\mathbf{B}_{\varepsilon}^T\mathbf{P}_{\varepsilon}\mathbf{A}_{\varepsilon}\ , \tag{5-30}$$

with

$$\mathbf{R}=\mathbf{diag}\left(\mathbf{R}_1\ldots\mathbf{R}_N\right),$$

$$\mathbf{D}_{\varepsilon}=\begin{bmatrix}\mathbf{D}_{11}(\varepsilon) & \varepsilon_{12}\mathbf{D}_{12} & \ldots & \varepsilon_{1N}\mathbf{D}_{1N}\\ \varepsilon_{21}\mathbf{D}_{21} & \mathbf{D}_{22}(\varepsilon) & \ldots & \varepsilon_{2N}\mathbf{D}_{2N}\\ . & . & . & .\\ \varepsilon_{N1}\mathbf{D}_{N1} & \varepsilon_{N2}\mathbf{D}_{N2} & \ldots & \mathbf{D}_{NN}(\varepsilon)\end{bmatrix}.$$
$$\in\ \Re^{\bar{n}\times\bar{n}}$$

It should be noted that the inversion of the partitioned matrices $\mathbf{R}_{\varepsilon}+\mathbf{B}_{\varepsilon}^T\mathbf{P}_{\varepsilon}\mathbf{B}_{\varepsilon}$ will produce numerous terms and cause the DARRE approach to be computationally very involved, even though one is faced with the reduced-order numerical problem [271]. This problem is resolved by using bilinear transformation to transform the discrete-time Riccati equations (DARRE) into the continuous-time algebraic Riccati equation (CARRE) with equivalent co-relation [271].

The differential game Riccati matrices $\mathbf{P}_{i\varepsilon}$ satisfy the singularly-perturbed and weakly-coupled, continuous in time, algebraic Regulator Riccati equation (SWARREs) [271, 277, 278] which is given below,

$$\Omega_i\left(\mathbf{P}_{1\varepsilon},\ldots,\mathbf{P}_{i\varepsilon},\ldots,\mathbf{P}_{N\varepsilon}\right) = \mathbf{P}_{i\varepsilon}\left(\mathbf{A}_{\varepsilon} - \sum_{\substack{j=1\\ j\neq i}}^{N}\mathbf{S}_{j\varepsilon}\mathbf{P}_{j\varepsilon}\right) + \left(\mathbf{A}_{\varepsilon} - \sum_{\substack{j=1\\ j\neq i}}^{N}\mathbf{S}_{j\varepsilon}\mathbf{P}_{j\varepsilon}\right)^{T}\mathbf{P}_{i\varepsilon}$$

$$- \mathbf{P}_{i\varepsilon}\mathbf{S}_{i\varepsilon}\mathbf{P}_{i\varepsilon} + \sum_{\substack{j=1\\ j\neq i}}^{N}\varepsilon_{ij}\mathbf{P}_{j\varepsilon}\mathbf{S}_{ij\varepsilon}\mathbf{P}_{j\varepsilon} + \mathbf{P}_{i\varepsilon}\mathrm{M}_{i\varepsilon}\mathbf{P}_{i\varepsilon} + \mathbf{D}^{T}{}_{i\varepsilon}\mathbf{D}_{i\varepsilon} = \mathbf{0}, \quad (5\text{-}31)$$

where

$$\mathbf{S}_{i\varepsilon} = \mathbf{B}_{i\varepsilon}\mathbf{R}_{ii}^{-1}\mathbf{B}_{i\varepsilon}^{T}, \quad i = 1,\ldots,N.$$

$$\mathbf{S}_{ij} = \mathbf{B}_{j\varepsilon}\mathbf{R}_{jj}^{-1}\mathbf{R}_{ij}\mathbf{R}_{jj}^{-1}\mathbf{B}_{j\varepsilon}^{T}, \; i = 1,\ldots,N.$$

$$\mathrm{M}_{i\varepsilon} = \mathbf{W}_{\varepsilon}\Theta_{\mathbf{w}i\varepsilon}^{-1}\mathbf{W}_{\varepsilon}, \; i = 1,\ldots,N.$$

■

5.4.3 Auxiliary SWARRE

By substituting the partitioned matrices of $\mathbf{A}_{\varepsilon}$, $\mathbf{S}_{i\varepsilon}$, $\mathbf{S}_{ij\varepsilon}$, $\mathrm{M}_{i\varepsilon}$, $\mathbf{D}_{i\varepsilon}$, and $\mathbf{P}_{i\varepsilon}$ into SWARRE (5-31), and by letting $\varepsilon_w = 0$ and any $\varepsilon_s \neq 0$, then simplifying the SWARRE (5-31), the following reduced order (auxiliary) algebraic Riccati equation is obtained,

$$\mathbf{P}_{ii}\mathbf{A}_{ii} + \mathbf{A}_{ii}^{T}\mathbf{P}_{ii} - \mathbf{P}_{ii}\left(\mathbf{S}_{ii} - \mathrm{M}_{ii}\right)\mathbf{P}_{ii} + \mathbf{D}_{ii}^{T}\mathbf{D}_{ii} = 0, \quad (5\text{-}32)$$

where $\mathbf{S}_{ii} = \mathbf{B}_{ii}\mathbf{R}_{ii}^{-1}\mathbf{B}_{ii}^{T}$ and $\mathrm{M}_{ii} = \mathbf{W}_{ii}\Theta_{ii}^{-1}\mathbf{W}_{ii}^{T}$, and $\mathbf{P}_{ii}$, $i = 1,\ldots,N$ is the 0-order approximation of $\mathbf{P}_{i\varepsilon}$ when the weakly-coupled component is set to zero, i.e., $\varepsilon_w = 0$. It should be noted that a unique positive semi-definite optimal solution $\mathbf{P}_{i\varepsilon}^{*}$ exists if the following assumptions are taken into account [277].

Assumption 5.2: *The triples* $\mathbf{A}_{ii}$, $\mathbf{B}_{ii}$ *and* $\mathbf{D}_{ii}$, $i = 1,\ldots,N$, *are stabilizable and detectable.*

Assumption 5.3: *The auxiliary (5-32) has a positive semidefinite stabilizing solution such that* $\tilde{\mathbf{A}} = \mathbf{A}_{ii} - \mathbf{S}_{ii}\mathbf{P}_{ii}$ *is stable.*

Lemma 5.4*: Under assumption 5.3 there exists a small constant* ∂^* *such that for all* $\tilde{\varepsilon}(t) \in (0, \partial^*)$*, SWARRE admits a positive definite solution* $\mathbf{P}_{i\varepsilon}^*$ *represented as*

$$\begin{aligned} \mathbf{P}_{i\varepsilon} &= \mathbf{P}_{i\varepsilon}^* = \mathbf{P}_i + O(\varepsilon(t)),\ i=1,\ldots,N \text{ and } \tilde{\varepsilon}(t) = \left|\sqrt{\varepsilon_w \varepsilon_s}\right|, \\ &= \textbf{block diag}(0 \ldots \mathbf{P}_{ii} \ldots 0) + O(\tilde{\varepsilon}(t)). \end{aligned} \tag{5-33}$$

Proof: This can be achieved by demonstrating that the Jacobian of SWARRE is non-singular at $\tilde{\varepsilon}(t) = 0$ and its neighbourhood, i.e., $\varepsilon(t) \to +0$. Differentiating the function $\Omega_i(\tilde{\varepsilon}(t), \mathbf{P}_{1\varepsilon}, \ldots, \mathbf{P}_{N\varepsilon})$ with respect to the decoupled matrix $\mathbf{P}_{i\varepsilon}$ produces,

$$\begin{aligned} \mathbf{J}_{ii} &= \frac{\partial}{\partial\, vec\ \mathbf{P}_{i\varepsilon}}\, vec\ \Omega_i(\tilde{\varepsilon}(t), \mathbf{P}_{1\varepsilon}, \ldots, \mathbf{P}_{N\varepsilon})^T \\ &= \Delta_{ii}^T \otimes I_{n_i} + I_{n_i} \otimes \Delta_{ii}^T. \\ \mathbf{J}_{ij} &= \frac{\partial}{\partial\, vec\ P_{ij}}\, vec\ \Omega_i(\tilde{\varepsilon}(t), \mathbf{P}_{1\varepsilon}, \ldots, \mathbf{P}_{N\varepsilon})^T, \\ &= -\left(\mathbf{S}_{j\varepsilon}\mathbf{P}_{i\varepsilon} - \tilde{\varepsilon}_{ij}\mathbf{S}_{ij\varepsilon}\mathbf{P}_{j\varepsilon}\right)^T \otimes I_{n_i} - I_{n_i} \otimes \left(\mathbf{S}_{j\varepsilon}\mathbf{P}_{i\varepsilon} - \tilde{\varepsilon}_{ij}\mathbf{S}_{ij\varepsilon}\mathbf{P}_{j\varepsilon}\right)^T, \end{aligned} \tag{5-34}$$

where $i \neq j$, $j = 1, \ldots, N$ and $\Delta = \mathbf{A}_\varepsilon - \sum_{\substack{j=1 \\ i \neq j}}^{N} \mathbf{S}_{j\varepsilon}\mathbf{P}_{j\varepsilon} + \mathrm{M}_{i\varepsilon}\mathbf{P}_{i\varepsilon}$.

Exploiting the fact that $\mathbf{S}_{j\varepsilon}\mathbf{P}_{i\varepsilon} = O(\tilde{\varepsilon}(t))$ for $i \neq j$, the Jacobian of SWARRE with $\tilde{\varepsilon}(t) \to +0$ can be verified as

$$\begin{aligned} \hat{\mathbf{J}} &= \textbf{block diag}\,(\Delta_{11} \ldots \Delta_{NN}), \\ \mathbf{J} &= \textbf{block diag}\,(\hat{\mathbf{J}} \ldots \hat{\mathbf{J}}). \end{aligned}$$

Since the determinant of $\Delta_{ii} = \mathbf{A}_{ii} - \mathbf{S}_{ii}\mathbf{P}_{ii} + \mathbf{M}_{ii}\mathbf{P}_{ii}$ with $\tilde{\varepsilon}(t) = 0$ is non-zero by following assumption 5.3 for all $i = 1, \ldots, N$, thus $\det \mathbf{J} \neq 0$ i.e., $\mathbf{J}$ is non-singular for $\tilde{\varepsilon}(t) = 0$. As a consequence of the implicit function theorem coined in [285], $\mathbf{P}_{ii}$ is a positive definite matrix at $\tilde{\varepsilon}(t) = 0$ and for sufficiently small parameters $\tilde{\varepsilon}(t) \in (0, \partial^*)$, one can conclude that $\mathbf{P}_{i\varepsilon} = P_{ii} + O(\tilde{\varepsilon}(t))$ is also a positive definite solution.

▪

5.5 Recursive Algorithm and Analysis

5.5.1 Conventional Approach

For analytical brevity, let N = 2 users. Substitute matrices, namely $\mathbf{A}_\varepsilon$, $\mathbf{P}_\varepsilon, \mathbf{S}_\varepsilon$, $\mathbf{M}_\varepsilon$ and $\mathbf{D}_\varepsilon$ into the following steady state Riccati equation

$$\mathbf{P}_\varepsilon\mathbf{A}_\varepsilon + \mathbf{A}_\varepsilon^T\mathbf{P}_\varepsilon - \mathbf{P}_\varepsilon(\mathbf{S}_\varepsilon - \mathrm{M}_\varepsilon)\mathbf{P}_\varepsilon + \mathbf{D}_\varepsilon^T\mathbf{D}_\varepsilon = 0\ , \tag{5-35}$$

so that after tedious algebraic calculations, three decomposed matrix algebraic equations are produced according to [271]:

$$\begin{aligned}
&\mathbf{P}_{11}\mathbf{A}_{11} + \mathbf{A}_{11}^T\mathbf{P}_{11}\,\mathbf{D}_{11}^T\mathbf{D}_{11} - \varepsilon_w^4\mathbf{P}_{12}(\mathbf{S}_{21} - \mathbf{M}_{21})\mathbf{P}_{12}^T - \\
&\mathbf{P}_{11}(\mathbf{S}_{11} - \mathbf{M}_{11})\mathbf{P}_{11} + \varepsilon_w^2(\mathbf{A}_{21}^T\mathbf{P}_{12}^T + \mathbf{P}_{12}\mathbf{A}_{21}) - \\
&\varepsilon_w^2(\mathbf{P}_{11}(\mathbf{S}_{12} - \mathbf{M}_{12})\mathbf{P}_{11} + \mathbf{P}_{12}\mathbf{Z}^T\mathbf{P}_{11} + \mathbf{P}_{11}\mathbf{Z}\mathbf{P}_{12}^T + \mathbf{P}_{12}(\mathbf{S}_{22} - \mathbf{M}_{22})\mathbf{P}_{12}^T) = \mathbf{0}\ .
\end{aligned} \tag{5-36}$$

$$\begin{aligned}
&\mathbf{P}_{12}\mathbf{A}_{22} + \mathbf{D}_{12}^T\mathbf{D}_{12} + \mathbf{P}_{11}\mathbf{A}_{12} + \\
&\alpha(\mathbf{A}_{21}^T\mathbf{P}_{22} - \mathbf{P}_{12}(\mathbf{S}_{22} - \mathbf{M}_{22})\mathbf{P}_{22} - \mathbf{P}_{11}\mathbf{Z}\mathbf{P}_{22}) - \\
&\varepsilon_w^2\alpha\mathbf{P}_{12}(\mathbf{S}_{21} - \mathbf{M}_{21})\mathbf{P}_{22} + \\
&\varepsilon_s(\mathbf{A}_{11}^T\mathbf{P}_{12} - \mathbf{P}_{11}(\mathbf{S}_{11} - \mathbf{M}_{11})\mathbf{P}_{12}) - \\
&\varepsilon_w^s\varepsilon_s(\mathbf{P}_{11}(\mathbf{S}_{12} - \mathbf{M}_{12})\mathbf{P}_{12} + \mathbf{P}_{12}\mathbf{Z}^T\mathbf{P}_{12}) = \mathbf{0}\ .
\end{aligned} \tag{5-37}$$

$$\alpha \mathbf{P}_{22}\mathbf{A}_{22} + \alpha \mathbf{A}_{22}^T\mathbf{P}_{22} + \mathbf{D}_{22}^T\mathbf{D}_{22} -$$
$$\alpha^2\mathbf{P}_{22}\left(\mathbf{S}_{22}-\mathbf{M}_{22}\right)\mathbf{P}_{22} + \varepsilon_w^2\varepsilon_s\left(\mathbf{P}_{12}^T\mathbf{A}_{12}+\mathbf{A}_{12}^T\mathbf{P}_{12}\right)-$$
$$\varepsilon_w^2\varepsilon_s\alpha\left(\mathbf{P}_{22}\mathbf{Z}^T\mathbf{P}_{12}+\mathbf{P}_{12}^T\mathbf{Z}\mathbf{P}_{22}\right)-\varepsilon_w^2\alpha^2\mathbf{P}_{22}\left(\mathbf{S}_{21}-\mathbf{M}_{21}\right)\mathbf{P}_{22} -$$
$$\varepsilon_w^2\varepsilon_s^2\left(\mathbf{P}_{12}^T\left(\mathbf{S}_{11}-\mathbf{M}_{11}\right)\mathbf{P}_{12}+\varepsilon_w^2\mathbf{P}_{12}^T\left(\mathbf{S}_{12}-\mathbf{M}_{12}\right)\mathbf{P}_{12}\right)=\mathbf{0}\ . \tag{5-38}$$

where $\mathbf{S}_{ij}=\mathbf{B}_{ij}\mathbf{R}_i^{-1}\mathbf{B}_{ij}^T$, $i=1,2$, $j=1,2$, $\mathbf{M}_{ij}=\mathbf{W}_{ij}\Theta_{ij}^{-1}\mathbf{W}_{ij}^T$, $i=1,2$, $j=1,2$, and $\mathbf{Z}=\mathbf{B}_{11}\mathbf{R}_1^{-1}\mathbf{B}_{21}^T+\mathbf{B}_{12}\mathbf{R}_2^{-1}\mathbf{B}_{22}^T$, with $\alpha=\left|\sqrt{\frac{\varepsilon_w}{\varepsilon_s}}\right|$. The recursive algorithm solving the stabilizing solution $\mathbf{P}_{i\varepsilon}^*$ from Equations (5-36)-(5-38) has conventionally been established in Gajic and Shen [271]. Since ε_w and ε_s are sufficiently small parameters, $O(\varepsilon)$ approximation of (5-36)-(5-38) can be defined as follows:

$$\mathbf{P}_{11}^{(0)}\mathbf{A}_{11}+\mathbf{A}_{11}^T\mathbf{P}_{11}^{(0)}+\mathbf{D}_{11}^T\mathbf{D}_{11}-\mathbf{P}_{11}^{(0)}U_{11}\mathbf{P}_{11}^{(0)}=\mathbf{0}\,,\ U_{ii}=\mathbf{S}_{ii}-\mathbf{M}_{ii}\,,\ i=1,2\,. \tag{5-39}$$

$$\mathbf{P}_{12}^{(0)}\left(\mathbf{A}_{22}-\alpha U_{22}\mathbf{P}_{22}^{(0)}\right)+\mathbf{D}_{12}^T\mathbf{D}_{12}+\mathbf{P}_{11}^{(0)}\mathbf{A}_{12}+\alpha\left(\mathbf{A}_{21}^T\mathbf{P}_{22}^{(0)}-\mathbf{P}_{11}^{(0)}Z\mathbf{P}_{22}^{(0)}\right)=0\ . \tag{5-40}$$

$$\alpha\mathbf{P}_{22}^{(0)}\mathbf{A}_{22}+\alpha\mathbf{A}_{22}^T\mathbf{P}_{22}^{(0)}+\mathbf{D}_{22}^T\mathbf{D}_{22}-\alpha^2\mathbf{P}_{22}^{(0)}\mathbf{S}_{22}\mathbf{P}_{22}^{(0)}=\mathbf{0}\ . \tag{5-41}$$

The decomposed solution of (5-35) is now yielded by

$$\mathbf{P}^{(0)}=\begin{bmatrix}\mathbf{P}_{11}^{(0)} & \varepsilon_w\varepsilon_s\mathbf{P}_{12}^{(0)}\\ \varepsilon_w\varepsilon_s\mathbf{P}_{12}^{(0)T} & \sqrt{\varepsilon_w\varepsilon_s}\mathbf{P}_{22}^{(0)}\end{bmatrix}=\mathbf{P}+O(\varepsilon)\,. \tag{5-42}$$

The unique positive semi-definite stabilizing solution $P^{(0)}$ from (5-39)-(5-41), exists under the assumption 5.2. It should be noted that [271] considered specific cases when only U_{ii}, $\mathbf{P}_{ii}$ and $\mathbf{P}_{ij}$ with $i\neq j$, $i=1,2$, and $j=1,2$ are present in the problem. A more general case would be to take into account U_{i12}, U_{ij}, $\mathbf{P}_{ij}$ and $\mathbf{P}_{i12}$ as non zeros for all $i\neq j$, $i=1,2$, and $j=1,2,\ldots$

▪

5.5.2 Generalized Recursive Algorithm

Suppose an alternative generalized algorithm for solving SWARREs (5-31) can be obtained. Let $N=2$ and $\mathbf{S}_{i\varepsilon}-\mathbf{M}_{i\mu}=\begin{bmatrix}\varepsilon_w^{1-\delta_{i1}}U_{i1} & \varepsilon U_{i12}\\ \varepsilon U_{i12}^T & \varepsilon_w^{1-\delta_{i2}}\varepsilon_s U_{i2}\end{bmatrix}$ so that the tedious algebra manipulations involved with high order MRMC dimensions can be analytically simplified. The SPWC Higher Order Recursive Algorithm (HORA) is assumed to be decentralized with reduced information exchange overhead costs. Thus, HORA demonstrates a low computational complexity. Consequently, SWARRE can easily be solved at a user's perspective.

In order to solve the SWARREs (5-31), it is crucial to first define the approximation error equations decomposed as follows:

$$\mathbf{P}_{ii}=\mathbf{P}_{ii}^{(0)}+\tilde{\varepsilon}\,\mathbf{E}_{ii},\ \mathbf{P}_{ij}=\mathbf{P}_{ij}^{(0)}+\tilde{\varepsilon}\,\mathbf{E}_{ij},\ i\neq j,\ \mathbf{P}_{i12}=\mathbf{P}_{i12}^{(0)}+\tilde{\varepsilon}\,\mathbf{E}_{i12}, \tag{5-43}$$

where i, $j=1,2$, $\tilde{\varepsilon}=\left|\sqrt{\varepsilon_w\varepsilon_s}\right|$, $U_{ii}=\mathbf{S}_{ii}-\mathbf{M}_{ii}$ and $\mathbf{P}_{ii}^{(0)}$, $\mathbf{P}_{ij}^{(0)}$, $\mathbf{P}_{i12}^{(0)}$ are the 0-order approximations of $\mathbf{P}_{i\varepsilon}$ corresponding to ε. Define the asymptotic equations of the SWARREs (5-31) as follows:

$$\begin{aligned}
&\mathbf{P}_{ii}^{(0)}\mathbf{A}_{ii}+\mathbf{A}_{ii}^T\mathbf{P}_{ii}^{(0)}-\mathbf{P}_{ii}^{(0)}U_{ii}\mathbf{P}_{ii}^{(0)}+\mathbf{D}_{ii}^T\mathbf{D}_{ii}=\mathbf{0}.\\
&\mathbf{P}_{ij}^{(0)}\mathbf{A}_{jj}+\mathbf{A}_{jj}^T\mathbf{P}_{ij}^{(0)}-\mathbf{P}_{ij}^{(0)}U_{ij}\mathbf{P}_{ij}^{(0)}+\mathbf{D}_{ij}^T\mathbf{D}_{ij}=\mathbf{0}.\\
&\mathbf{P}_{112}^{(0)}\mathbf{A}_{22}+\mathbf{A}_{11}^T\mathbf{P}_{112}^{(0)}-\mathbf{P}_{112}^{(0)}U_{112}^T\mathbf{P}_{112}^{(0)}+\mathbf{D}_{112}^T\mathbf{D}_{112}=\mathbf{0}.\\
&\mathbf{P}_{212}^{(0)}\mathbf{A}_{21}+\mathbf{A}_{11}^T\mathbf{P}_{212}^{(0)}-\mathbf{P}_{212}^{(0)}U_{212}^T\mathbf{P}_{212}^{(0)}+\mathbf{D}_{212}^T\mathbf{D}_{212}=\mathbf{0}.
\end{aligned} \tag{5-44}$$

Theorem 5.1: *Under assumptions 1-3, the aid of approximation error equation (5-43) and the asymptotic equations (5-44), the following Lyapunov form recursive algorithm that solves the SWARREs (5-31) for N=2 can be obtained:*

$$\begin{aligned}
&\mathbf{E}_{11}^{(k+1)}\Delta_{11}+\Delta_{11}^T\mathbf{E}_{11}^{(k+1)}=\\
&-\varepsilon\alpha\left(\mathbf{P}_{112}^{(k)}\mathbf{A}_{21}+\tilde{\varepsilon}\,\mathbf{E}_{112}^{(k)}\mathbf{A}_{21}+\mathbf{A}_{21}^T\mathbf{P}_{112}^{(k)T}+\tilde{\varepsilon}\,\mathbf{A}_{21}^T\mathbf{E}_{112}^{(k)}\right)\\
&+\varepsilon_1^3\tilde{\varepsilon}^2\mathbf{E}_{11}^{(k)}U_{11}\mathbf{E}_{11}^{(k)}+\varepsilon_1\varepsilon^2\left(\mathbf{P}_{112}^{(k)}U_{112}^T\mathbf{P}_{11}^{(k)}+\mathbf{P}_{11}^{(k)}U_{112}\mathbf{P}_{112}^{(k)T}\right)
\end{aligned}$$

$$+\varepsilon_1\varepsilon^2\tilde{\varepsilon}\left(\mathbf{P}_{112}^{(k)}U_{112}^{T}\mathbf{E}_{11}^{(k)}+\mathbf{E}_{112}^{(k)}U_{112}^{T}\mathbf{P}_{11}^{(k)}+\tilde{\varepsilon}\,\mathbf{E}_{112}^{(k)}U_{112}^{T}\mathbf{E}_{11}^{(k)}\right)$$

$$+\varepsilon_1\varepsilon^2\tilde{\varepsilon}\left(\mathbf{P}_{11}^{(k)}U_{112}\mathbf{E}_{112}^{(k)}+\mathbf{E}_{11}^{(k)}U_{112}\mathbf{P}_{112}^{(k)T}+\tilde{\varepsilon}\,\mathbf{E}_{11}^{(k)}U_{112}\mathbf{E}_{112}^{(k)}\right)$$

$$+\varepsilon^2\varepsilon_2\left(\mathbf{P}_{112}^{(k)}U_{12}\mathbf{P}_{112}^{(k)T}+\tilde{\varepsilon}\,\mathbf{P}_{112}^{(k)}U_{12}\mathbf{E}_{112}^{(k)}+\tilde{\varepsilon}\,\mathbf{E}_{112}^{(k)}U_{12}\mathbf{P}_{112}^{(k)T}+\tilde{\varepsilon}^2\mathbf{E}_{112}^{(k)}U_{12}\mathbf{E}_{112}^{(k)}\right). \tag{5-45}$$

$$\mathbf{E}_{112}^{(k+1)}\Delta_{112}+\Delta_{112}^{T}\mathbf{E}_{112}^{(k+1)}=$$

$$-\varepsilon_1\varepsilon_w\left(\mathbf{P}_{11}^{(k)}\mathbf{A}_{12}+\tilde{\varepsilon}\,\mathbf{E}_{11}^{(k)}\mathbf{A}_{12}\right)-\alpha\varepsilon_2\left(\mathbf{A}_{21}^{T}\mathbf{P}_{12}^{(k)}+\tilde{\varepsilon}\,\mathbf{A}_{21}^{T}\mathbf{E}_{12}^{(k)}\right)$$

$$\varepsilon_1^3\tilde{\varepsilon}\left(\mathbf{P}_{11}^{(k)}U_{11}\mathbf{P}_{112}^{(k)}+\tilde{\varepsilon}\,\mathbf{E}_{11}^{(k)}U_{11}\mathbf{P}_{112}^{(k)}+\tilde{\varepsilon}^2\mathbf{E}_{11}^{(k)}U_{11}\mathbf{E}_{112}^{(k)}+\tilde{\varepsilon}\,\mathbf{P}_{11}^{(k)}U_{11}\mathbf{E}_{112}^{(k)}\right)$$

$$+\varepsilon^3\tilde{\varepsilon}\left(\tilde{\varepsilon}\,\mathbf{E}_{112}^{(k)}U_{112}^{T}\mathbf{E}_{112}^{(k)}\right)$$

$$+\varepsilon_1\varepsilon_2\varepsilon\left(\mathbf{P}_{11}^{(k)}U_{112}\mathbf{P}_{12}^{(k)}+\tilde{\varepsilon}\,\mathbf{P}_{11}^{(k)}U_{112}\mathbf{E}_{12}^{(k)}+\tilde{\varepsilon}\,\mathbf{E}_{11}^{(k)}U_{112}\mathbf{P}_{12}^{(k)}+\tilde{\varepsilon}^2\mathbf{E}_{11}^{(k)}U_{112}\mathbf{E}_{12}^{(k)}\right)$$

$$+\varepsilon\varepsilon_2^2\left(\mathbf{P}_{112}^{(k)}U_{12}\mathbf{P}_{12}^{(k)}+\tilde{\varepsilon}\,\mathbf{P}_{112}^{(k)}U_{12}\mathbf{E}_{12}^{(k)}+\tilde{\varepsilon}\,\mathbf{E}_{11}^{(k)}U_{12}\mathbf{P}_{12}^{(k)}+\tilde{\varepsilon}^2\mathbf{E}_{11}^{(k)}U_{12}\mathbf{E}_{12}^{(k)}\right). \tag{5-46}$$

$$\mathbf{E}_{12}^{(k+1)}\Delta_{12}+\Delta_{12}^{T}\mathbf{E}_{12}^{(k+1)}=$$

$$-\varepsilon\varepsilon_w\left(\mathbf{P}_{112}^{(k)T}\mathbf{A}_{12}+\tilde{\varepsilon}\,\mathbf{E}_{112}\mathbf{A}_{12}+\mathbf{A}_{12}^{T}\mathbf{P}_{112}^{(k)}+\tilde{\varepsilon}\,\mathbf{A}_{12}^{T}\mathbf{E}_{112}\right)$$

$$+\varepsilon_1\varepsilon^2\left(\mathbf{P}_{112}^{(k)T}U_{11}\mathbf{P}_{112}^{(k)}+\tilde{\varepsilon}\,\mathbf{P}_{112}^{(k)T}U_{11}\mathbf{E}_{112}^{(k)}+\tilde{\varepsilon}\,\mathbf{E}_{112}^{(k)}U_{11}\mathbf{P}_{112}^{(k)}+\tilde{\varepsilon}^2\mathbf{E}_{112}^{(k)}U_{11}\mathbf{E}_{112}^{(k)}\right)$$

$$+\varepsilon_2\varepsilon^2\left(\mathbf{P}_{12}^{(k)}U_{112}^{T}\mathbf{P}_{112}^{(k)}+\mathbf{P}_{112}^{(k)T}U_{112}\mathbf{P}_{12}^{(k)}\right)$$

$$+\varepsilon_2\varepsilon^2\tilde{\varepsilon}\left(\mathbf{P}_{12}^{(k)}U_{112}^{T}\mathbf{E}_{112}^{(k)}+\mathbf{E}_{12}^{(k)}U_{112}^{T}\mathbf{P}_{112}^{(k)}+\tilde{\varepsilon}\,\mathbf{E}_{12}^{(k)}U_{112}^{T}\mathbf{E}_{112}^{(k)}+\mathbf{P}_{112}^{(k)T}U_{112}\mathbf{E}_{12}^{(k)}+\mathbf{E}_{112}^{(k)}U_{112}\mathbf{P}_{12}^{(k)}+\tilde{\varepsilon}\,\mathbf{E}_{112}^{(k)}U_{112}\mathbf{E}_{12}^{(k)}\right)$$

$$+\varepsilon_2^3\tilde{\varepsilon}^2\mathbf{E}_{12}^{(k)}U_{12}\mathbf{E}_{12}^{(k)}. \tag{5-47}$$

$$\mathbf{E}_{21}^{(k+1)}\Delta_{21}+\Delta_{21}^{T}\mathbf{E}_{21}^{(k+1)}=$$

$$-\varepsilon\alpha\left(\mathbf{P}_{212}^{(k)}\mathbf{A}_{21}+\tilde{\varepsilon}\,\mathbf{E}_{212}^{(k)}\mathbf{A}_{21}+\mathbf{A}_{21}^{T}\mathbf{P}_{212}^{(k)T}+\tilde{\varepsilon}\mathbf{A}_{21}^{T}\mathbf{E}_{212}^{(k)}\right)$$

$$+\varepsilon_1\left(\varepsilon_1^2\tilde{\varepsilon}^2\mathbf{E}_{21}^{(k)}U_{21}\mathbf{E}_{21}^{(k)}+\varepsilon^2\mathbf{P}_{212}^{(k)}U_{212}^{T}\mathbf{P}_{21}^{(k)}+\varepsilon^2\mathbf{P}_{21}^{(k)}U_{212}\mathbf{P}_{212}^{(k)T}\right)$$

$$\varepsilon_1\varepsilon^2\tilde{\varepsilon}\left(\mathbf{P}_{212}^{(k)}U_{212}^{T}\mathbf{E}_{21}^{(k)}+\mathbf{E}_{212}^{(k)}U_{212}^{T}\mathbf{P}_{21}^{(k)}+\tilde{\varepsilon}\,\mathbf{E}_{212}^{(k)}U_{212}^{T}\mathbf{E}_{21}^{(k)}+\mathbf{P}_{21}^{(k)}U_{212}\mathbf{E}_{212}^{(k)}+\mathbf{E}_{21}^{(k)}U_{212}\mathbf{P}_{212}^{(k)T}+\tilde{\varepsilon}\,\mathbf{E}_{21}^{(k)}U_{212}\mathbf{E}_{212}^{(k)}\right)$$

$$+\varepsilon_2\varepsilon^2\left(\mathbf{P}_{212}^{(k)}U_{22}\mathbf{P}_{212}^{(k)T}+\tilde{\varepsilon}\,\mathbf{P}_{212}^{(k)}U_{22}\mathbf{E}_{212}^{(k)}+\tilde{\varepsilon}\,\mathbf{E}_{212}^{(k)}U_{22}\mathbf{P}_{212}^{(k)T}+\tilde{\varepsilon}^2\mathbf{E}_{212}^{(k)}U_{22}\mathbf{E}_{212}^{(k)}\right). \tag{5-48}$$

$$\mathbf{E}_{212}^{(k+1)}\Delta_{212}+\Delta_{212}^{T}\mathbf{E}_{212}^{(k+1)}=$$

$$-\varepsilon_1\varepsilon_w\left(\mathbf{P}_{21}^{(k)}\mathbf{A}_{12}+\tilde{\varepsilon}\,\mathbf{E}_{21}^{(k)}\mathbf{A}_{12}\right)-\alpha\varepsilon_2\left(\mathbf{A}_{21}^{T}\mathbf{P}_{22}^{(k)}+\tilde{\varepsilon}\,\mathbf{A}_{21}^{T}\mathbf{E}_{22}^{(k)}\right)$$

$$+\varepsilon_1^2\varepsilon\left(\tilde{\varepsilon}\,\mathbf{P}_{21}^{(k)}U_{21}\mathbf{E}_{212}^{(k)}+\mathbf{P}_{21}^{(k)}U_{21}\mathbf{P}_{212}^{(k)}+\tilde{\varepsilon}\,\mathbf{E}_{21}^{(k)}U_{21}\mathbf{P}_{212}^{(k)}+\tilde{\varepsilon}^2\mathbf{E}_{21}^{(k)}U_{21}\mathbf{E}_{212}^{(k)}\right)$$

$$+\varepsilon^3\tilde{\varepsilon}\left(\tilde{\varepsilon}\,\mathbf{E}_{212}^{(k)}U_{212}^{T}\mathbf{E}_{212}^{(k)}\right)$$

$$+\varepsilon_1\varepsilon_2\varepsilon\left(\mathbf{P}_{21}^{(k)}U_{212}\mathbf{P}_{22}^{(k)}+\tilde{\varepsilon}\,\mathbf{P}_{21}^{(k)}U_{212}\mathbf{E}_{22}^{(k)}+\tilde{\varepsilon}\,\mathbf{E}_{21}^{(k)}U_{212}\mathbf{P}_{22}^{(k)}+\tilde{\varepsilon}^2\mathbf{E}_{21}^{(k)}U_{212}\mathbf{E}_{22}^{(k)}+\tilde{\varepsilon}\,\mathbf{E}_{212}^{(k)}U_{22}\mathbf{P}_{22}^{(k)}\right)$$

$$+\varepsilon\varepsilon_2^2\left(\mathbf{P}_{212}^{(k)}U_{22}\mathbf{P}_{22}^{(k)}+\tilde{\varepsilon}\,\mathbf{P}_{212}^{(k)}U_{22}\mathbf{E}_{22}^{(k)}+\tilde{\varepsilon}^2\mathbf{E}_{212}^{(k)}U_{22}\mathbf{E}_{22}^{(k)}\right). \qquad (5\text{-}49)$$

$$\mathbf{E}_{22}^{(k+1)}\Delta_{22}+\Delta_{22}^{T}\mathbf{E}_{22}^{(k+1)}=$$

$$-\varepsilon\varepsilon_w\left(\mathbf{P}_{212}^{(k)T}\mathbf{A}_{12}+\tilde{\varepsilon}\,\mathbf{E}_{212}^{(k)}\mathbf{A}_{12}+\mathbf{A}_{12}^{T}\mathbf{P}_{212}^{(k)}+\tilde{\varepsilon}\mathbf{A}_{12}^{T}\mathbf{E}_{212}^{(k)}\right)$$

$$+\varepsilon_1\varepsilon^2\left(\mathbf{P}_{212}^{(k)T}U_{21}\mathbf{P}_{212}^{(k)}+\tilde{\varepsilon}\,\mathbf{P}_{212}^{(k)T}U_{21}\mathbf{E}_{212}^{(k)}+\tilde{\varepsilon}\mathbf{E}_{212}^{(k)}U_{21}\mathbf{P}_{212}^{(k)}+\tilde{\varepsilon}^2\mathbf{E}_{212}^{(k)}U_{21}\mathbf{E}_{212}^{(k)}\right)$$

$$+\varepsilon_2\varepsilon^2\left(\mathbf{P}_{22}^{(k)}U_{212}^{T}\mathbf{P}_{212}^{(k)}+\mathbf{P}_{212}^{(k)T}U_{212}\mathbf{P}_{22}^{(k)}\right)$$

$$+\varepsilon_2\varepsilon^2\tilde{\varepsilon}\left(\mathbf{P}_{22}^{(k)}U_{212}^{T}\mathbf{E}_{212}^{(k)}+\mathbf{E}_{22}^{(k)}U_{212}^{T}\mathbf{P}_{212}^{(k)}+\tilde{\varepsilon}\,\mathbf{E}_{22}^{(k)}U_{212}^{T}\mathbf{E}_{212}^{(k)}+\mathbf{P}_{212}^{(k)T}U_{212}\mathbf{E}_{22}^{(k)}+\mathbf{E}_{212}^{(k)}U_{212}\mathbf{P}_{22}^{(k)}+\tilde{\varepsilon}\,\mathbf{E}_{212}^{(k)}U_{212}\mathbf{E}_{22}^{(k)}\right)$$

$$+\varepsilon_2^3\tilde{\varepsilon}^2\mathbf{E}_{22}^{(k)}U_{22}\mathbf{E}_{22}^{(k)}\ . \qquad (5\text{-}50)$$

where

$\mathbf{E}_{ii}^{(0)}=\mathbf{E}_{ij}^{(0)}=\mathbf{E}_{i12}^{(0)}=\mathbf{0}$, $i,j=1,2$, $\varepsilon_1=\varepsilon_w^{1-\delta_{i1}}s$, $\varepsilon_2=\varepsilon_w^{1-\delta_{i2}}\varepsilon_s$, $\varepsilon=\varepsilon_w\varepsilon_s$, $\alpha=\varepsilon_w/\varepsilon_s$ and $\tilde{\varepsilon}=\left|\sqrt{\varepsilon_w\varepsilon_s}\right|$.

Proof: Due to space constraints and the tedious algebra manipulations involved, the proof is outlined as follows: Substitute the approximations error equations (5-43) into the SWARREs (5-31). Set N = 2 and expand the result. After subtracting the asymptotic equations (5-44) one obtains the Lypunov form recursive equations (5-45)-(5-50) whereby Δ_{ii}, Δ_{ij} and Δ_{i12} and their corresponding transpositions are defined as follows:

$\Delta_{11}=\varepsilon_1\tilde{\varepsilon}\mathbf{A}_{11}-\varepsilon_1^3\tilde{\varepsilon}U_{11}\mathbf{P}_{11}^{(0)}$, $\Delta_{11}^{T}=\varepsilon_1\tilde{\varepsilon}\mathbf{A}_{11}^{T}-\varepsilon_1^3\tilde{\varepsilon}\,\mathbf{P}_{11}^{(0)}U_{11}$, $\Delta_{112}=\varepsilon\tilde{\varepsilon}\mathbf{A}_{22}/\varepsilon_s-\varepsilon^3\tilde{\varepsilon}U_{112}^{T}\mathbf{P}_{112}^{(0)}$,

$\Delta_{112}^{T}=\varepsilon\tilde{\varepsilon}\mathbf{A}_{11}^{T}-\varepsilon^3\tilde{\varepsilon}\,\mathbf{P}_{112}^{(0)}U_{112}^{T}$, $\Delta_{12}=\varepsilon_2\tilde{\varepsilon}\mathbf{A}_{22}/\varepsilon_s-\varepsilon_2^3\tilde{\varepsilon}U_{12}\mathbf{P}_{12}^{(0)}$, $\Delta_{12}^{T}=\varepsilon_2\tilde{\varepsilon}\mathbf{A}_{22}^{T}/\varepsilon_s-\varepsilon_2^3\tilde{\varepsilon}\,\mathbf{P}_{12}^{(0)}U_{12}$,

$\Delta_{21} = \varepsilon_1\tilde{\varepsilon}\mathbf{A}_{11} - \varepsilon_1^3\tilde{\varepsilon}U_{21}\mathbf{P}_{21}^{(0)}$, $\Delta_{21}^T = \varepsilon_1\tilde{\varepsilon}\mathbf{A}_{11}^T - \varepsilon_1^3\tilde{\varepsilon}\mathbf{P}_{21}^{(0)}U_{21}$, $\Delta_{212} = \varepsilon\tilde{\varepsilon}\mathbf{A}_{21}/\varepsilon_s - \varepsilon^3\tilde{\varepsilon}U_{212}^T\mathbf{P}_{212}^{(0)}$,

$\Delta_{212}^T = \varepsilon\tilde{\varepsilon}\mathbf{A}_{11}^T - \varepsilon^3\tilde{\varepsilon}\mathbf{P}_{212}^{(0)}U_{212}^T$, $\Delta_{22} = \varepsilon_2\tilde{\varepsilon}\mathbf{A}_{22}/\varepsilon_s - \varepsilon_2^3\tilde{\varepsilon}U_{22}\mathbf{P}_{22}^{(0)}$, $\Delta_{22}^T = \varepsilon_2\tilde{\varepsilon}\mathbf{A}_{22}^T - \varepsilon_2^3\tilde{\varepsilon}\mathbf{P}_{22}^{(0)}U_{22}$.

▪

Theorem 5.2: *Under assumptions 5.1-5.3, the recursive algorithm (5-45)-(5-50) converges to the exact solutions of the error terms* $\mathbf{E}_{ii}$, $\mathbf{E}_{ij}$, *and* $\mathbf{E}_{i12}$, $i, j = 1,2$ *in the Lyapunov form equations (5-51)-(5-54):*

$$\mathbf{E}_{ii}\Delta_{ii} + \Delta_{ii}^T\mathbf{E}_{ii} + L_{ii} = \mathbf{0}. \tag{5-51}$$

$$\mathbf{E}_{ij}\Delta_{ij} + \Delta_{ij}^T\mathbf{E}_{ij} + L_{ij} = \mathbf{0}. \tag{5-52}$$

$$\mathbf{E}_{112}\Delta_{112} + \Delta_{112}^T\mathbf{E}_{112} + L_{112} = \mathbf{0}. \tag{5-53}$$

$$\mathbf{E}_{212}\Delta_{212} + \Delta_{212}^T\mathbf{E}_{212} + L_{212} = \mathbf{0}. \tag{5-54}$$

with $L_{ii} = L_i\left(\tilde{\varepsilon}, \tilde{\varepsilon}\mathbf{E}_{11}, \ldots, \tilde{\varepsilon}\mathbf{E}_{22}\right)$, $i, j = 1,2$, *The rate of convergence is linear,* $\kappa = O\left(\tilde{\varepsilon}\right)$, *and satisfies the following conditions*:

$$\left\|\mathbf{E}_{ii} - \mathbf{E}_{ii}^{(k)}\right\| = O\left(\tilde{\varepsilon}^k\right), \left\|\mathbf{E}_{ij} - \mathbf{E}_{ij}^{(k)}\right\| = O\left(\tilde{\varepsilon}^k\right) \text{ and } \left\|\mathbf{E}_{i12} - \mathbf{E}_{i12}^{(k)}\right\| = O\left(\tilde{\varepsilon}^k\right), \; k = 1,2,\ldots, i = 1,2. \tag{5-55}$$

Proof: The proof follows a mathematical induction. If we set $k = 0$ in the recursive algorithm (5-45)-(5-50) then the first order error term approximations, $\mathbf{E}_{ii}^{(1)}$, $\mathbf{E}_{ij}^{(1)}$ and $\mathbf{E}_{i12}^{(1)}$ corresponding to the small parameter $\tilde{\varepsilon}$, satisfy the Lyapunov equations (5-51)-(5-54). Subtracting (5-45)-(5-50) from (5-51)-(5-54) and taking the norm when $k = 0$, the following equations are obtained,

$$\left\|\mathbf{E}_{ii} - \mathbf{E}_{ii}^{(1)}\right\| = O\left(\tilde{\varepsilon}^1\right), \left\|\mathbf{E}_{ij} - \mathbf{E}_{ij}^{(1)}\right\| = O\left(\tilde{\varepsilon}^1\right), \left\|\mathbf{E}_{i12} - \mathbf{E}_{i12}^{(1)}\right\| = O\left(\tilde{\varepsilon}^1\right), \quad i, j = 1,2. \tag{5-56}$$

Correspondingly, if we set $k = n$, for all $n \geq 1$ then the following hold.

$$\left\|\mathbf{E}_{ii} - \mathbf{E}_{ii}^{(n)}\right\| = O\left(\tilde{\varepsilon}^n\right), \left\|\mathbf{E}_{ij} - \mathbf{E}_{ij}^{(n)}\right\| = O\left(\tilde{\varepsilon}^n\right), \left\|\mathbf{E}_{i12} - \mathbf{E}_{i12}^{(n)}\right\| = O\left(\tilde{\varepsilon}^n\right) i, j = 1,2. \tag{5-57}$$

Subtracting the (5-45)-(5-50) when $k=n$, from (5-51)-(5-54) and after invoking assumptions (5-57) and the closed loop Nash strategy assumption in (5-25), we obtain the following results, provided that Δ_{ii}, $\forall i=1,2$ are stable.

$$\left\|\mathbf{E}_{ii}-\mathbf{E}_{ii}^{(n+1)}\right\|=O\left(\tilde{\varepsilon}^{n+1}\right),\quad \left\|\mathbf{E}_{ij}-\mathbf{E}_{ij}^{(n+1)}\right\|=O\left(\tilde{\varepsilon}^{n+1}\right),\quad \left\|\mathbf{E}_{i12}-\mathbf{E}_{i12}^{(n+1)}\right\|=O\left(\tilde{\varepsilon}^{n+1}\right)\ i,j=1,2,$$

and for all $k=1,2,\ldots$

Note that with $O\left(\tilde{\varepsilon}\right)\ll 1$ and $O\left(\tilde{\varepsilon}\right)>O\left(\tilde{\varepsilon}^{n+1}\right)$ for $n\gg 1$, the generalized recursive algorithm (HORA) also converges to the exact solution of the error terms, $\mathbf{E}_{ii}$, $\mathbf{E}_{ij}$, and $\mathbf{E}_{i12}$, $i,j=1,2$.

To indicate the rate of convergence one can proceed as follows:

$$\kappa=\frac{\left\|E_{ii}-E_{ii}^{(1)}\right\|}{\left\|E_{ii}-E_{ii}^{(0)}\right\|}=\frac{\left\|E_{ij}-E_{ij}^{(1)}\right\|}{\left\|E_{ij}-E_{ij}^{(0)}\right\|}=\frac{\left\|E_{i12}-E_{i12}^{(1)}\right\|}{\left\|E_{i12}-E_{i12}^{(0)}\right\|},$$

$$\kappa=\frac{\left\|E_{ii}-E_{ii}^{(n+1)}\right\|}{\left\|E_{ii}-E_{ii}^{(n)}\right\|}=\frac{\left\|E_{ij}-E_{ij}^{(n+1)}\right\|}{\left\|E_{ij}-E_{ij}^{(n)}\right\|}=\frac{\left\|E_{i12}-E_{i12}^{(n+1)}\right\|}{\left\|E_{i12}-E_{i12}^{(n)}\right\|},$$

$$\approx\frac{O\left(\tilde{\varepsilon}^{n+1}\right)}{O\left(\tilde{\varepsilon}^{n}\right)}=O\left(\tilde{\varepsilon}\right).\qquad(5\text{-}58)$$

■

The above rate is linear and satisfies the condition of the convergence theorem.

Upon obtaining the stabilizing solution $\mathbf{P}_{i\varepsilon}^{*}$, the high-order Nash equilibrium strategy for the sign-indefinite linear quadratic games can then be determined. Such a strategy is obtained by using the iterative solution (5-45)-(5-50).

$$\mathbf{u}_i^{(k)*}\left(t\right)=-\mathbf{R}_{ii}^{-1}\mathbf{B}_{i\varepsilon}^{T}\mathbf{P}_{i\varepsilon}^{(k)}\mathbf{x}\left(t\right),\ i=1,\ldots,N,\qquad(5\text{-}59)$$

where $\mathbf{u}_i^{*}\left(t\right)=\mathbf{u}_i^{(k)*}+O\left(\tilde{\varepsilon}\right)$ and k is an iteration step. The optimal $\mathbf{u}_i^{*}\left(t\right)$ is added to the power law $p_i\left(t+1\right)$ equation such that $\sum_{i=1}^{N}p_i\left(t+1\right)\le P_{probe}^{tot}$. Notation N denotes the

number of all users whose operations are managed by a single MRMC node-pair while P_{probe}^{tot}, denotes the total channel probe power level which a node uses to upper bound greedy strategies.

The degradation of the cost performance via the high-order soft constrained Nash equilibrium strategy (5-59) is outlined in the following theorem.

Theorem 5.3: *Under assumptions 5.1-5.3, the use of a soft constrained Nash equilibrium (5-59) results in the following condition.*

$$J_i\left(\mathbf{u}_1^{(k)*}, \ldots, \mathbf{u}_N^{(k)*}, \mathbf{x}(0)\right) \approx J_i\left(\mathbf{u}_1^{*}, \ldots, \mathbf{u}_N^{*}, \mathbf{x}(0)\right) + O\left(\tilde{\varepsilon}^{2^k+1}\right). \tag{5-60}$$

Proof: Due to space constraints, we outline the proof. A detailed related analysis can be found in [277, 278].

If the iterative strategy is $\mathbf{u}_i^{(k)*}(t) = -\mathbf{F}_{i\varepsilon}^{(k)*}\mathbf{x}(t)$ then the value of the cost function is given by

$$J_i\left(\mathbf{u}_1^{(k)*}, \ldots, \mathbf{u}_N^{(k)*}, \mathbf{x}(0)\right) = \mathbf{x}^T(0)\mathbf{Y}_{i\varepsilon}\mathbf{x}(0), \tag{5-61}$$

where $\mathbf{Y}_{i\varepsilon}$ is a *positive semi-definite solution* of the following algebraic Riccati equation

$$\mathbf{Y}_{i\varepsilon}\left(\mathbf{A}_\varepsilon - \sum_{\substack{j=1\\ j\neq i}}^{N}\mathbf{S}_{j\varepsilon}\mathbf{P}_{j\varepsilon}^{(k)}\right) + \left(\mathbf{A}_\varepsilon - \sum_{\substack{j=1\\ j\neq i}}^{N}\mathbf{S}_{j\varepsilon}\mathbf{P}_{j\varepsilon}^{(k)}\right)^T\mathbf{Y}_{i\varepsilon}$$

$$+ \mathbf{Y}_{i\varepsilon}\mathbf{M}_{i\varepsilon}\mathbf{Y}_{i\varepsilon} + \varepsilon\sum_{\substack{j=1\\ j\neq i}}^{N}\mathbf{P}_{j\varepsilon}^{(k)}\mathbf{S}_{ij\varepsilon}\mathbf{P}_{j\varepsilon}^{(k)} - \mathbf{P}_{i\varepsilon}^{(k)}\mathbf{S}_{i\varepsilon}\mathbf{P}_{i\varepsilon}^{(k)} + \mathbf{D}_{i\varepsilon}^T\mathbf{D}_{i\varepsilon} = \mathbf{0}. \tag{5-62}$$

Let $\mathbf{Z}_{i\varepsilon} = \mathbf{Y}_{i\varepsilon} - \mathbf{P}_{i\varepsilon}$, then subtracting SWARRE (5-31) from (5-62) satisfies the following equation

$$\mathbf{Z}_{i\varepsilon}\bar{\mathbf{A}}_\varepsilon^{(k)} + \bar{\mathbf{A}}_\varepsilon^{(k)T}\mathbf{Z}_{i\varepsilon} + \sum_{\substack{j=1\\ j\neq i}}^{N}\mathbf{P}_{i\varepsilon}\mathbf{S}_{j\varepsilon}\left(\mathbf{P}_{j\varepsilon} - \mathbf{P}_{j\varepsilon}^{(k)}\right)$$

$$+ \sum_{\substack{j=1\\ j\neq i}}^{N}\left(\mathbf{P}_{j\varepsilon} - \mathbf{P}_{j\varepsilon}^{(k)}\right)\mathbf{S}_{j\varepsilon}\mathbf{P}_{i\varepsilon} + \varepsilon\left[\sum_{\substack{j=1\\ j\neq i}}^{N}\left(\mathbf{P}_{j\varepsilon}^{(k)}\mathbf{S}_{ij\varepsilon}\mathbf{P}_{j\varepsilon}^{(k)} - \mathbf{P}_{j\varepsilon}\mathbf{S}_{ij\varepsilon}\mathbf{P}_{j\varepsilon}\right)\right] + \left(\mathbf{P}_{i\varepsilon} - \mathbf{P}_{i\varepsilon}^{(k)}\right)\mathbf{S}_{i\varepsilon}\left(\mathbf{P}_{i\varepsilon} - \mathbf{P}_{i\varepsilon}^{(k)}\right) = 0, \tag{5-63}$$

where $\bar{\mathbf{A}}_{\varepsilon}^{(k)} = \mathbf{A}_{\varepsilon} - \sum_{j=1}^{N} \mathbf{S}_{j\varepsilon}\mathbf{P}_{j\varepsilon}^{(k)} + \mathbf{M}_{i\varepsilon}\mathbf{P}_{i\varepsilon}^{(k)} + \mathbf{M}_{i\varepsilon}\left(\mathbf{P}_{i\varepsilon} - \mathbf{P}_{i\varepsilon}^{(k)}\right)$. Suppose $\left\|\mathbf{P}_{i\varepsilon} - \mathbf{P}_{i\varepsilon}^{(k)}\right\| \approx O\left(\tilde{\varepsilon}^{2^k}\right)$, (i.e., has a quadratic rate of convergence) then from the proof of *lemma 5.4,* one can have,

$$\theta(\mathbf{Z}_{i\varepsilon}) = \mathbf{Z}_{i\varepsilon}\left(\hat{\mathbf{J}} + O(\tilde{\varepsilon})\right) + \left(\hat{\mathbf{J}} + O(\tilde{\varepsilon})\right)^{T}\mathbf{Z}_{i\varepsilon} + \mathbf{Z}_{i\varepsilon}\mathbf{M}_{i\varepsilon}\mathbf{Z}_{i\varepsilon} + O\left(\tilde{\varepsilon}^{2^k+1}\right) = 0, \quad (5\text{-}64)$$

where $\theta(\mathbf{0}) = O\left(\tilde{\varepsilon}^{2^k+1}\right)$ and $\hat{\mathbf{J}} = \mathbf{block\ diag}\left(\Delta_{11} \ldots \Delta_{NN}\right)$ with $\Delta_{ii} = \mathbf{A}_{ii} - (\mathbf{S}_{ii} - \mathbf{M}_{ii})\mathbf{P}_{ii}$ [278]. Thus, let $\|\mathbf{Z}_{i\varepsilon} - \mathbf{0}\| \le O\left(\tilde{\varepsilon}^{2^k+1}\right)$ and from the cost function definition it is evident that:

$$\begin{aligned}\mathbf{x}^{T}(0)\mathbf{Z}_{i\varepsilon}\mathbf{x}(0) &= \mathbf{x}^{T}(0)\mathbf{Y}_{i\varepsilon}\mathbf{x}(0) - \mathbf{x}^{T}(0)\mathbf{P}_{i\varepsilon}\mathbf{x}(0)\\ &= J_i\left(\mathbf{u}_1^{(k)*}, \ldots, \mathbf{u}_N^{(k)*}, \mathbf{x}(0)\right) - J_i\left(\mathbf{u}_1^{*}, \ldots, \mathbf{u}_N^{*}, \mathbf{x}(0)\right)\\ &\le O\left(\tilde{\varepsilon}^{2^k+1}\right) . \end{aligned} \quad (5\text{-}65)$$

5.6 Numerical Examples

5.6.1 Apparatus

The efficiency of the proposed model and algorithm is studied by means of numerical examples. The MATLAB™ tool was used to evaluate the design optimization parameters, because of its efficiency in numerical computations. The wireless MRMC network being considered was modelled as a large scale interconnected control system. Upto 50 wireless nodes were randomly placed in a 1200 m by 1200 m region. The random topology depicts a non-uniform distribution of the nodes. Each node was assumed to have at most four network interface cards (NICs) or radios, each tuned to a separate non-overlapping unified channel graph (UCG) as shown in Fig. 5.6. Although 4 radios are situated at each node, it should be noted that such dimension only simplifies the simulation. The higher dimension of radios per node may be used without loss of generality. The MRMC configurations depict the weak coupling to each other among different non-overlapping channels. In other words, those radios of the same node operating on separate frequency channels (or UCGs) do not

communicate with each other. However, due to their close vicinity such radios significantly interfere with each other and affect the process of optimal power control. The ISM carrier frequency band of 2.427 GHz-2.472 GHz was assumed for simulation purposes only. Figure 5.6 illustrates the typical wireless network scenario with 4 nodes, each with 4 radio-pairs or users able to operate simultaneously. The rationale is to stripe application traffic over power controlled multiple channels and/or to access the WMCs as well as backhaul network cooperation.

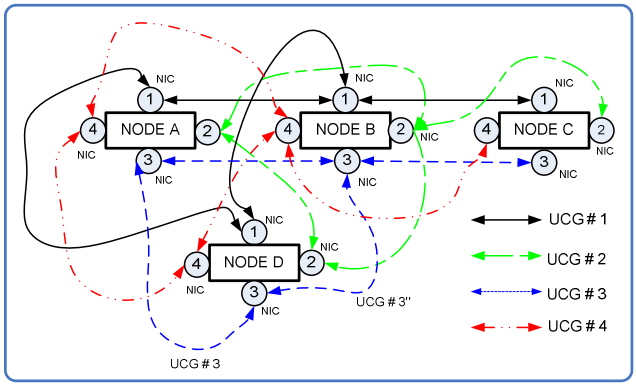

Figure 5.6: MRMC wireless network:

In Figure 5.6, each node has 4 NICs that can operate simultaneously on 4 disjoint channels (or UCGs). Node A reaches Node B and D via one hop and reaches C via 2 hops (i.e., through Node B) or 3 hops (i.e., through Nodes D and B). For example, NIC (radio) B1 has transparent neighbours: (A1,C1,D1), radio B2 has transparent neighbours: (A2,C2,D2) and radio B3 has transparent neighbours: (A3,C3,D3). Radio A1 can communicate with radio B1 if tuned to UCG # 1 during current timeslot and radio B1 can relay traffic of radio A1 to radio C1 if both are switched to UCG # 1" during the next timeslot. Aware of the queue system perturbation and cross-channel interference coupling influence, each radio-pair (user) optimizes transmission power levels while the Link Layer manages fairness in energy resource allocation [46].

5.6.2 Cost Function and LSI System Behaviour

Given static WMRs and allowing each multi-radio node to send queue traffic to its target receivers (neighbours) after successful neighbour discovery, the channel state coefficient matrices in (5-21) can be generated. In order to ensure, a low computational complexity problem, the number of immediate neighbours has been assumed to be, at most, five. Furthermore, to reduce the involved complex manipulations with regards to matrices, only two active radios at each node may suffice. In such situation, one radio may access the

WMCs while the other may voluntarily forward the backhaul traffic. Consequently, the numerical parameters are specified as follows.

$B_{11}=[0.1\ 0.59\ 0\ 1]^T$, $B_{12}=[0\ 0.001\ 0\ 0.002]^T$, $B_{21}=[0\ 0.059\ 0\ 0.095]^T$,

$B_{22}=[0.01\ 4\ 0\ 0.002]^T$, $\Theta_{ii}=\mathbf{diag}(0.9\ \ 0.9\ \ 0.9\ \ 0.9)$, $\Theta_1=\mathbf{block\ diag}\left(\Theta_{ii}\quad \varepsilon_w^{-1}I_{4\times4}\right)$,

$\Theta_2=\mathbf{block\ \ diag}\left(\varepsilon_w^{-1}I_{4\times4}\quad \Theta_{ii}\right)$, $\mathbf{D}_1=\mathbf{block\ \ diag}\left(0.5I_{4\times4}\ O_{4\times4}\right)$,

$\mathbf{D}_2=\mathbf{block\ diag}\left(O_{4\times4}\ 0.5I_{4\times4}\right)$, $\mathbf{R}_{11}=\mathbf{R}_{22}=1$; $\mathbf{R}_{12}=\mathbf{R}_{21}=0.1$,

$\varepsilon_w=0.001$; $\varepsilon_s=0.001$.

By means of a numerical example, an average transmission probability and a queue delay plotted against packet arrival probability, given the known level of buffer size and energy availability, are obtained in Fig. 5.7. The intuitive explanation is as follows. As packets arrive at the queues, the probability of transmitting a packet slightly increases but is inversely proportional to the system perturbation. A highly perturbed queue system results in packet drops, hence losses occur. The slowly rising exponential delay behaviour versus packet arrivals under the influence of system perturbation suggests buffer overflows, and consequently undesirable queue delays. Figure 5.8 illustrates the energy levels and buffer size in order to attain a lower bounded transmission probability. The plotted levels are considered at different perturbations. For each value of the lower bounded and singular perturbation factor, the energy level and buffer size are determined in such a manner that the transmission probability should be no smaller than the lower bound transmission probability.

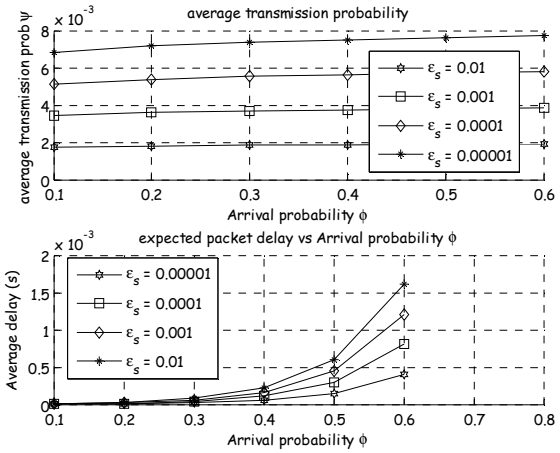

Figure 5.7: Average transmission probability and delay versus arrival probability:

The buffer size, $B = 20$. Available energy levels for packet transmission, $E = 2$. The service probability, $\varphi_1 = 1$ and $\varphi_2 = 0.2$ and the arrival probability, $\phi = 0.6$. The energy transition process, $\lambda_{11} = 0.3$ and $\lambda_{22} = 0.5$. The probability distribution of the aggregated Markov chain Λ_1, $\bar{\vartheta}_1 = 2/7$ and $\bar{\vartheta}_2 = 5/7$.

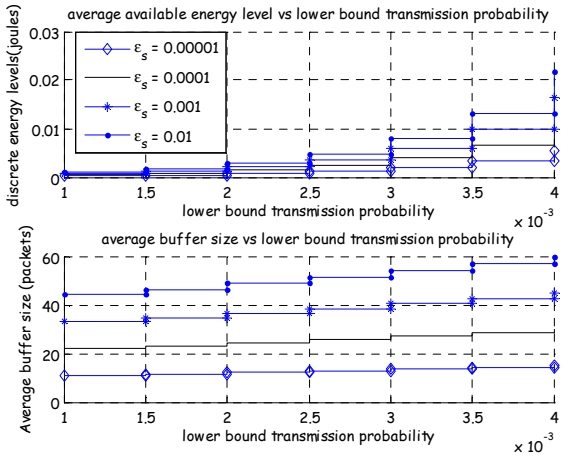

Figure 5.8: Average energy and buffer levels versus lower transmission probability:

The average energy and the buffer size per network interface card needed to ensure a transmission probability of not less than the lower bound $pr_l, \phi = 0.6, \varphi_1 = 1, \varphi_2 = 0.2, \lambda_{11} = 0.3, \lambda_{22} = 0.4,$ $\lambda_{33} = \ldots \lambda_E = 0.1$ and $E = 7$. The probability distribution of the aggregated Markov chain Λ_1, $\bar{\vartheta}_1 = 1/7 = \ldots \bar{\vartheta}_7 = 1/7$.

Stabilizing solution

The SWARREs solution $\mathbf{P}_{i\varepsilon}^{(8)*}$ and the corresponding feedback matrix $\mathbf{F}_{i\varepsilon}^{(8)*}$ are tabulated as in Tables 5.3 and 5.4, respectively. A close examination of the $\mathbf{P}_{i\varepsilon}^{(8)*}$ matrices reveals an 8 x 8

positive semi-definite stabilizing solution to the system matrices $\mathbf{A}_{ii}, \mathbf{B}_{ii}$ and $\mathbf{D}_{ii}$. This is in accordance with *assumption 5.2* in such a way that the stability condition of *assumption 5.3* is satisfied, that is, the matrix $\mathbf{A}_{ii} - \mathbf{S}_{ii}\mathbf{P}_{ii}$ has strictly negative real-part eigenvalues. This is valid because the high-order approximate soft-constrained Nash strategies (5-59) are yielded by $\mathbf{u}_i^{(8)*}(t) = -\mathbf{F}_{i\varepsilon}^{(8)*}\mathbf{x}(t)$, $i = 1,2$, with $\mathbf{F}_{1\varepsilon}^{(8)*}$ and $\mathbf{F}_{2\varepsilon}^{(8)*}$ also calculated numerically from the SWARREs as shown in Table 5.4.

Cost function performance

The high-order soft constrained Nash strategy (approximation) and the zero-order (optimal) cost functions are, respectively, computed as follows.

$$J_{i,approx}^{*} = J_i\left(\mathbf{u}_1^{(8)*}, \ldots, \mathbf{u}_N^{(8)*}, \mathbf{x}(0)\right) = \mathbf{x}(0)^T \mathbf{P}_{i\varepsilon}^{(8)*}\mathbf{x}(0),$$
$$J_{i,opt}^{*} = J_i\left(\mathbf{u}_1^{*}, \ldots, \mathbf{u}_N^{*}, \mathbf{x}(0)\right) = \mathbf{x}(0)^T \mathbf{P}_{i\varepsilon}^{*}\mathbf{x}(0), \qquad (5\text{-}66)$$

where $i = 1,2$ for $N = 2$. The initial state vector $\mathbf{x}(0)$ is numerically chosen as $x(0) = [1\ 1\ 1\ 1\ 1\ 1\ 1\ 1]^T$. The cost function (5-66) and the degradation for decomposed subsystem 1 are tabulated in Table 5.5. The table illustrates that the cost function deviation at the 8th iteration yields an accuracy of $\left\| J_{1,opt}^{*} - J_{1,approx}^{(8)*} \right\| < 7.294787e-11$. This observation confirms that the proposed Higher Order Recursive Algorithm (HORA) converges practically to the exact solution. Furthermore, at the system's convergence point it can be shown that the ratio between the cost function deviation and the SPWC factor is very large, that is, $\varsigma_i \geq 7.294787e+246$, for all $i = 1,2,\ldots,N$,

where $\varsigma_i = \dfrac{\left| J_{i,opt.}^{*} - J_{i,approx}^{(k)*} \right|}{\tilde{\varepsilon}^{2^k+1}}$ is the ratio between the cost function deviation and the SPWC factor.

The curve in Fig. 5.9 illustrates how the system's cost functions converge exponentially faster. This rapid response implies that the SWARRE solutions can be obtained relatively quickly if both system perturbation and inter-channel interference information can be known before hand. The power control input can fast track the wireless MRMC system states to steady state solutions. The driving input control signal for power control is given by Fig.

5.10. For a two wireless multi-radio multi-channel system, the input control signal converges rapidly, thus the total CPU time can be significantly shortened.

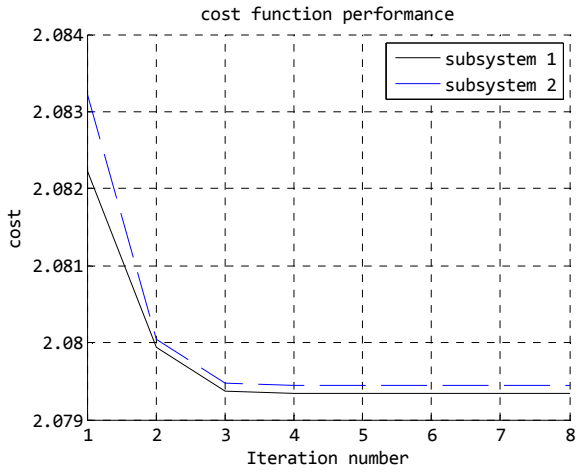

Figure 5.9: Cost function performance

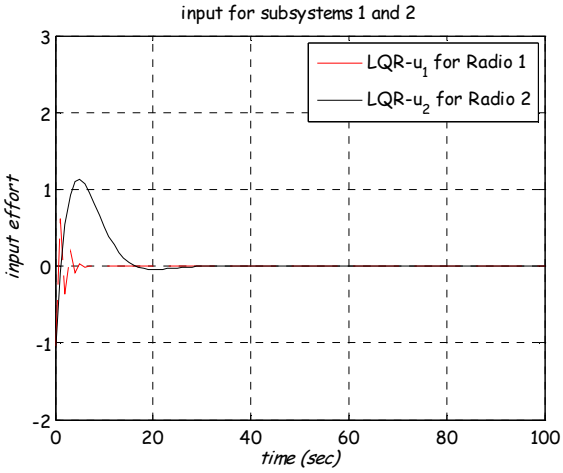

Figure 5.10: A 2 subsystems control input signal

Table 5.3: Numerical Values for the Decomposed SWARRE

$\mathbf{P}_{1\varepsilon}^{(8)*}$	5.6703 0.0408 −0.1739 −0.0155 0.0062 0.0004 0.0038 0.0003 0.0408 0.5431 0.0299 −0.0147 −0.0004 0.0007 −0.0003 0.0004 −0.1739 0.0299 2.4611 0.0301 −0.0141 −0.0008 −0.0007 0.0002 −0.0155 −0.0147 0.0301 0.1302 −0.0002 −0.0003 −0.0001 −0.0001 0.0062 −0.0004 −0.0141 −0.0002 0.2368 0.0054 −0.0027 0.0001 0.0004 0.0007 −0.0008 −0.0003 0.0054 0.0212 −0.0001 −0.0002 0.0038 −0.0003 −0.0007 −0.0001 −0.0027 −0.0001 0.2488 0.0031 0.0003 0.0004 0.0002 −0.0001 0.0001 −0.0002 0.0031 0.0132
$\mathbf{P}_{2\varepsilon}^{(8)*}$	2.3676 0.0537 −0.0267 0.0013 0.0062 0.0004 0.0038 0.0003 0.0537 0.2116 −0.0012 −0.0022 −0.0004 0.0007 −0.0003 0.0004 −0.0267 −0.0012 2.4880 0.0314 −0.0141 −0.0008 −0.0007 0.0002 0.0013 −0.0022 0.0314 0.1321 −0.0002 −0.0003 −0.0001 −0.0001 0.0062 −0.0004 −0.0141 −0.0002 0.2368 0.0054 −0.0027 0.0001 0.0004 0.0007 −0.0008 −0.0003 0.0054 0.0212 −0.0001 −0.0002 0.0038 −0.0003 −0.0007 −0.0001 −0.0027 −0.0001 0.2488 0.0031 0.0003 0.0004 0.0002 −0.0001 0.0001 −0.0002 0.0031 0.0132

Table 5.4: Near Optimal (Approximated) Regulator Feedback Values

$\mathbf{F}_{1\varepsilon}^{(8)*}$	−0.5755 −0.3086 −0.0303 −0.1200 −0.0002 −0.0003 −0.0001 −0.0003
$\mathbf{F}_{2\varepsilon}^{(8)*}$	−0.2386 −0.8470 0.0049 0.0088 0.0014 −0.0029 0.0013 −0.0016

Table 5.5: The Cost Function and Degradation Performance

k	$J^{*}_{1,optimum}$	$J^{(k)*}_{1,approximation}$	$\left\|J^{*}_{1,opt.} - J^{(k)*}_{1,approx.}\right\|$	ς_1
1	2.079347e+001	2.082221e+001	2.874104e-002	2.874104e+001
2	2.079347e+001	2.079944e+001	5.971379e-003	5.971379e+002
3	2.079347e+001	2.079371e+001	2.336666e-004	2.336666e+005
4	2.079347e+001	2.079348e+001	2.324894e-006	2.324894e+011
5	2.079347e+001	2.079347e+001	6.377017e-008	6.377017e+025
6	2.079347e+001	2.079347e+001	1.048373e-008	1.048373e+121
7	2.079347e+001	2.079347e+001	1.048373e-008	1.048373e+121
8	2.079347e+001	2.079347e+001	7.294787e-011	7.294787e+246

5.7 Performance Evaluations

In order to evaluate the performance of the singularly-perturbed weakly-coupled dynamic transmission power control (SPWC-DTPC) scheme in terms of power and throughput, our additional simulation parameters to those in section 5.6.1 were outlined as follows: The Distributed Inter Frame Space (DIFS) time = 50 μs, Short Inter Frame Space (SIFS) time = 10 μs and Back-off slot time = 20 μs. The number of mini-slots in the probe phase, M = 20, duration of probe mini-slot, T_{pc} = 40 μs and ATIM and Power Selection window adjustment parameter, ϑ = 1.2-1.5 as well as a virtual time slot duration consisting of probe, power optimization and data packet transmission times, t = 100 ms.

An arrival rate of λ packets/sec of packets at each queue was assumed. For each arriving packet at the sending queue, a receiver was randomly selected from its immediate neighbours. Each simulation run was performed long enough for the output statistics to stabilize (i.e., sixty seconds simulation time). Each datum point in the plots represents an average of four runs where each run exploits a different randomly generated network topology. Saturated transmission power consumption and throughout gain performance were evaluated. Saturation conditions, means that packets are always assumed to be in the queue for transmission; otherwise, the concerned transmitting radio goes to doze/sleep mode to conserve energy (i.e., back-off amount of time).

The following parameters were varied in the simulation: the number of active links (transmit-receive radio-pairs) interfering (i.e., co-channel and cross-channel), from 2 to 50 links, the channels availability, from 1 to 4 and the traffic load, from 12.8 packets/s to 128

packets/s. The maximum possible power consumed by a radio in the transmit state, the receive state, the idle state and the doze state was assumed as 0.5 Watt, 0.25 Watt, 0.15 Watt and 0.005 Watt, respectively. A user being in the transmitting state means that the radio at the head of the link is the transmit state and the radio at the tail of the link is in the receive state. A user in the receive state, in the idle state, and in the doze state means that both the radio at the head of the link and the radio at the tail of the link are in the receive state, in the idle state, and in the doze state, respectively [208]. In order to evaluate the transmission power consumption, packets must be assumed to be always available in all the sending queues of nodes. This is a condition of network saturation.

Figure 5.11 illustrates an average transmission power per node pair at steady state, versus the number of active radios relative to the total number of adjacent channels. During each time slot, each node evaluates steady state transmission powers in the ATIM phase. Average transmission power was measured as the number of active radio interfaces was increased at different values of the queue perturbations and the weak couplings of the MRMC systems. An increase in the number of active interfaces results in a linear increase in the transmission powers per node-pairs. At 80%, the number of radios relative to the number of adjacent channels with $\varepsilon = \sqrt{|\varepsilon_s \varepsilon_w|} = 0.0001$ yields about 0.61%, 7.98%, 9.51% respectively, a greater power saving than with $\varepsilon = 0.001$, 0.01 and 0.1. This is explained as follows. Stabilizing a highly perturbed queue system and strongly interfered disjoint wireless channels consumes more source energy. Packets are also re-transmitted frequently because of high packet drop rates. Retransmitting copies of previously dropped packets results in perturbations at the queue system owing to induced delays and energy-outages.

A number of previously studied MAC protocols for throughput enhancement were compared with the SPWC-PMMUP based power control scheme. The multi-radio unification protocol (MUP) [41] was compared with SPWC-PMMUP scheme because the latter is a direct extension of the former in terms of the energy- efficiency. Both protocols are implemented at the LL and with the same purpose (i.e., to hide the complexity of the multiple PHY and MAC layers from the unified higher layers, and to improve throughput performance) [4]. However, MUP scheme chooses only one channel with the best channel quality to exchange data and does not take power control into consideration. The power-saving multi-radio multi-channel medium access control (MAC) (PSM-MMAC) [208] was compared with SPWC-PMMUP scheme, because both protocols share the following characteristics: they are energy-efficient, and they select channels, radios and power states

dynamically based on estimated queue lengths, channel conditions and the number of active links. The single-channel power-control medium access control (POWMAC) protocol [18] was compared with the SPWC-PMMUP because both are power controlled MAC protocols suitable for wireless Ad Hoc networks (e.g., IEEE 802.11 schemes). Such protocols perform the carrier sensed multiple access with collision avoidance (CSMA/CA) schemes. Both protocols possess the capability to exchange several concurrent data packets after the completion of the operation of the power control mechanism. Both are distributed, asynchronous and adaptive to changes of channel conditions.

Figure 5.12 depicts the plots for energy-efficiency versus the number of active links per square kilometre of an area. Energy-efficiency is measured in terms of the steady state transmission power per time slot divided by the amount of packets that successfully reach the target receiver. It is observed that low active network densities generally provide higher energy-efficiency gain than highly active network densities. This occurs because low active network densities have better spatial re-use and proper multiple medium accesses. Except for low network densities, the SPWC-PMMUP scheme outperforms the POWMAC [18], the power saving multi-channel MAC (i.e., PSM-MMAC) [208] and the MUP schemes. In low active network density, a single channel power controlled MAC (i.e., POWMAC) records a higher degree of freedom with spatial re-use. As a result, it indicates a low expenditure of transmission power. As the number of active users increases, packet collisions and retransmissions become significantly large. The POWMAC uses an adjustable access window to allow for a series of RTS/CTS exchanges to take place before several concurrent data packet transmissions can commence. Unlike its counterparts, the POWMAC does not make use of control packets (i.e., RTS/CTS) to silence neighbouring terminals. Instead, collision avoidance information is inserted in the control packets and is used in conjunction with the received signal strength of these packets to dynamically bound the transmission power of potentially interfering terminals in the vicinity of a receiving terminal. This allows an appropriate transmission power selection that ensures multiple-concurrent transmissions in the vicinity of the receiving terminal. On the other hand, both SPWC-PMMUP and PSM-MMAC contain an adjustable ATIM window for traffic loads and the LL information. The ATIM window is maintained moderately narrow in order that less energy is wasted for being idle. Statistically, the simulation results indicated that for between 4 and 16 users per deployment area, the POWMAC scheme was on average 50%, 87.50%, and 137.50% more energy-efficient than the SPWC-PMMUP, PSM-MMAC and MUP, respectively. However, between 32 and 50 users per deployment area, SPWC-PMMUP scheme yielded on average

14.58%, 66.67%, and 145.83% more energy efficiency than the POWMAC, PSM-MMAC and MUP schemes, respectively.

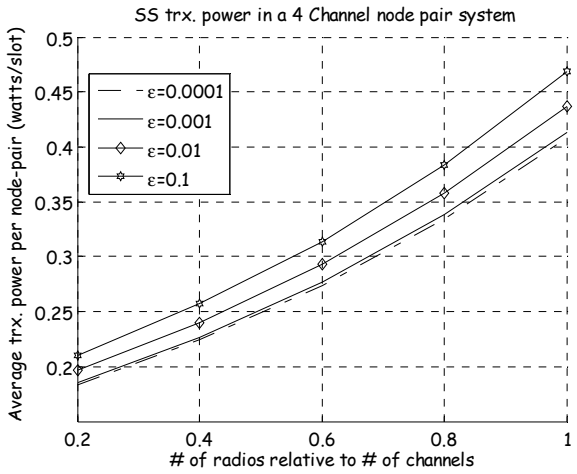

Figure 5.11: Steady state transmission power versus relative number of radios per channel

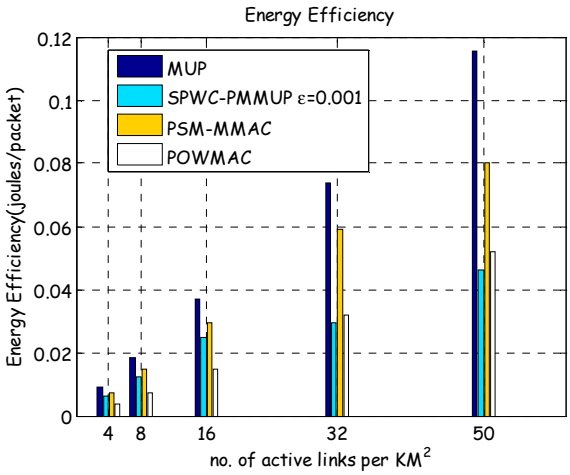

Figure 5.12: Energy-efficiency versus density of active links

Figure 5.13 depicts the performance of the network lifetime observed for the duration of the simulation. The number of active links using steady state transmission power levels was initially assumed to be 36 links per square kilometre area. Under the saturated traffic generated by the queue systems, different protocols were simulated and compared to the SPWC-PMMUP scheme. The links which were still alive were defined as those which were operating on certain stabilized transmission power levels and which remained connected at the end of the simulation time. The SPWC-PMMUP scheme evaluates the network lifetime based on the stable connectivity measure. That is, if a transmission power level, $p_{ij} = p_{ij}^*$ then the link (i, j) exists; otherwise if $p_{ij} < p_{ij}^*$, then there is no link between the transmitting interface i and the receiving interface j (i.e., the tail of the link). The notation, p_{ij}^* represents the minimum transmission power level needed to successfully send a packet to the target receiver at the immediate neighbours. After 50 units of simulation time, SPWC-PMMUP scheme records, on average, 12.50%, 22.22% and 33.33%, of links still alive, more than the POWMAC, PSM-MMAC and MUP schemes, respectively. This is because SPWC-PMMUP scheme uses a fractional power to perform the medium access control (i.e., RTS/CTS control packets are executed at a lower power than the maximum possible) while the conventional protocols employ maximum transmission powers to exchange control packets. The SPWC-PMMUP also transmits application or data packets using a transmission power level which is

adaptive to queue perturbations, the intra and inter-channel interference, the receiver SINR, the wireless link rate and the connectivity range. The performance gains of the POWMAC scheme are explained as follows. The POWMAC uses a collision avoidance inserted in the control packets, and in conjunction with the received signal strength of these packets to dynamically bound the transmission powers of potentially interfering terminals in the vicinity of a receiving terminal. This promotes mutual multiple transmissions of the application packets at a controlled power over a relatively long time. The PSM-MMAC scheme offers the desirable feature of being adaptive to energy, channel, queue and opportunistic access. However, its RTS/CTS packets are executed on maximum power. The MUP scheme does not perform any power control mechanism and hence records the worst lifetime performance.

Figure 5.14 illustrates an average throughput performance versus the offered traffic load at different singular-perturbation and weak-coupling conditions. Four simulation runs were performed at different randomly generated network topologies. The average throughput per send and receive node-pairs was measured when packets were transmitted using steady state transmission powers. Plots were obtained at confidence intervals of 95%, that is, with small error margins. In general, the average throughput monotonically increases with the amount of the traffic load subjected to the channels. The highly-perturbed and strongly-coupled multi-channel systems, that is, $\varepsilon = \sqrt{|\varepsilon_s \varepsilon_w|} = 0.1$, degrades average per hop throughput performance compared to the lowly-perturbed and weakly-coupled system, that is, $\varepsilon = 0.0001$. On average, and at 100 packets/s of the traffic load, the system described by $\varepsilon = 0.0001$ can provide 4%, 16% and 28% more throughput performance gain over the system at $\varepsilon = 0.001$, $\varepsilon = 0.01$ and $\varepsilon = 0.1$, respectively. This may be explained as follows. In large queue system perturbations (i.e., $\varepsilon = 0.1$) the SPWC-PMMUP scheme wastes a large portion of the time slot in stabilizing the queue and in finding optimal transmission power levels. This means that only lesser time intervals are allowed for actual application packet transmission. Furthermore, the inherently high inter channel interference degrades the spatial re-use. Consequently, smaller volumes of application/data packets actually reach the receiving destination successfully (i.e., low throughput). Conversely, with a low perturbation and inter-channel interference (i.e., $\varepsilon = 0.001$), data packets have a larger time interval for transmission; the wireless medium is spectrally efficient and hence achieves an enhanced average throughput.

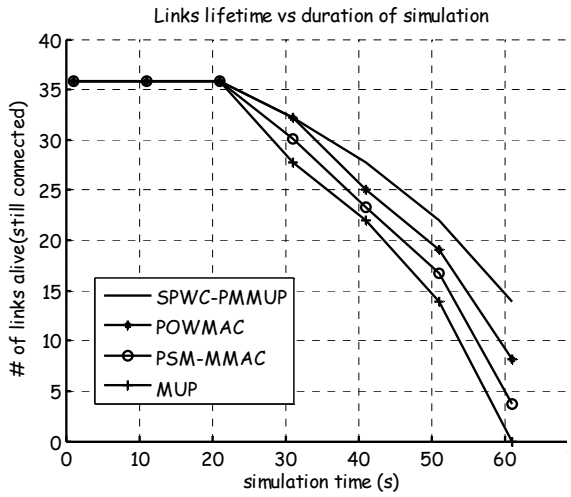

Figure 5.13: Active links lifetime performance

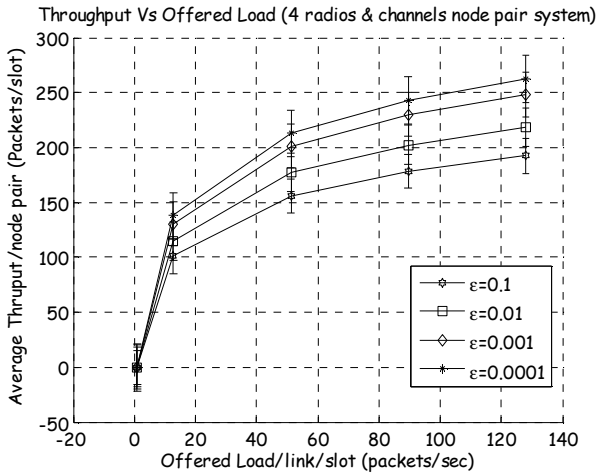

Figure 5.14: Average Throughput versus offered Load

Figure 5.15 depicts the average throughput per node pair versus the probability at steady state that a multi-radio multi-channel (MRMC) node will transmit application or data packets given a traffic load of $\lambda = 120$ packets/s, different queue system perturbations and inter channel interference. In order to obtain the average saturated throughput, each queue was assumed always to have data packets destined for the target receivers at the immediate neighbours. The steady state transmission probability (rate) was evaluated as a function of the Markov chains (i.e., chains consisting of the queue and energy size dynamics) and packet arrival probabilities. The simulation results indicated that the average throughput per node-pair increases linearly with the transmission probability. The average linear rate was 200 packets/slot (i.e., change in average throughput divided by the transmission rate). The average throughput increased with the increase in the number of channels and the information regarding queue perturbation and inter-channel interference. Specifically, at 80% of the transmission probability and with the traffic load of $\lambda = 120$ packets/s in each channel, the multi-radio node with 4 number of channels at $\varepsilon = 0.001$ network system provided an 8%, 20% and 36% average throughput performance gain over a node-pair with 2 channels, $\varepsilon = 0.001$, 4 channels MUP and 1 channel, $\varepsilon = 0$, respectively. This is now explained. The high performance rate suggests that each link always possess enough energy for transmitting the application packets from its buffer. Packets arriving at the buffer of the link are always served and transmitted using the appropriate transmission power. Striping application packets over several parallel network interfaces on to a number of power-controlled orthogonal

channels provides more throughput gain over a single interface-channel system. The power-controlled multiple channel data stream reduces data delay over the wireless medium. The fact of data occupying less transmission time suggests an improved successful transmission rate. The wireless MRMC system perturbation and inter channel parameter evaluation allows the power optimization system to scale the transmission power appropriately. Consequently, one establishes a more realistic energy level for transmission of data packets. In contrast, naïve approaches to the perturbation and inter channel coupling produce improper energy levels for data payloads. The MUP scheme, however, uses one channel with the best channel quality to send data traffic. The MUP does not take into account power control. Compared to the MUP, the SPWC PMMUP scheme exploits the advantages of the MUP and in addition evaluates the impact of system perturbation and interference on throughput performance. The SPWC- PMMUP scheme also stripes data/application traffic over at least one wireless channel in order to enhance channel diversity.

Figure 5.16 depicts the average saturated throughput per node-pair versus the number of active links per square kilometre when the queue traffic load of $\lambda = 120$ packets/s. Densities of the active links were varied from 4 to 50 and the average throughput per node pair was measured by running conventional protocols. Saturated throughput degrades with the densities of the active links. On average, the SPWC-PMMUP scheme at $\varepsilon = 0.001$ provides 8%, 20% and 36.36% more throughput performance gain than PSM-MMAC, MUP and POWMAC schemes, respectively. Large densities of active links in a unit of an area limit the spectral efficiency. Inefficient use of the space spectrum promotes traffic collisions and packet drops, consequently resulting in a degraded throughput performance. The PSM-MMAC scheme offers two desirable features: the ATIM window is adjustable and the medium access probability is optimized. Both features are aimed at minimising control packet exchange time (i.e., channel probing time) while maximizing the actual application or data exchange time so that throughput is improved. However, the data packets are not transmitted at the optimal power, contrary to the case of the SPWC-PMMUP scheme. The MUP scheme's most desirable feature is that only one out of many channels with the best channel quality (i.e., based on round trip time), is exploited for data transmission. However, multiple channels are used for striping control packet exchanges among neighbouring nodes. The MUP does not take into account power control. The POWMAC scheme is, on the other hand, a single-channel power controlled MAC scheme. The POWMAC uses an adjustable access window to allow for a series of RTS/CTS exchanges to occur before several

concurrent data packets can be exchanged. Collision avoidance information is inserted into the CTS packet to bound the transmission power of potentially interfering terminals in the vicinity of the receiver, rather than silencing them. This procedure improves the spatial re-use factor of the network and consequently produces good throughput. However, control packets are exchanged at maximum power and only one channel is available for the exchange of data packets, compared to the SPWC-PMMUP scheme.

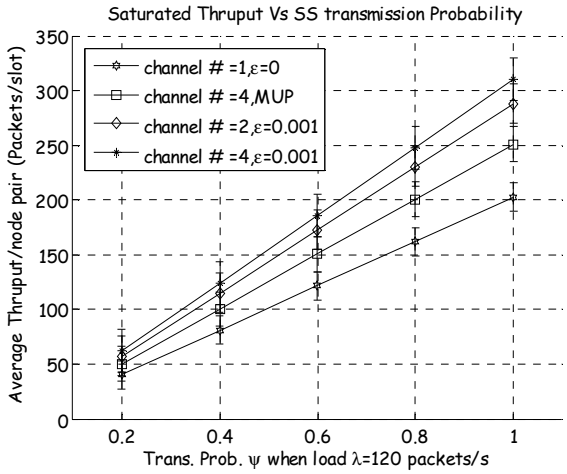

Figure 5.15: Average saturated throughput versus transmission probability

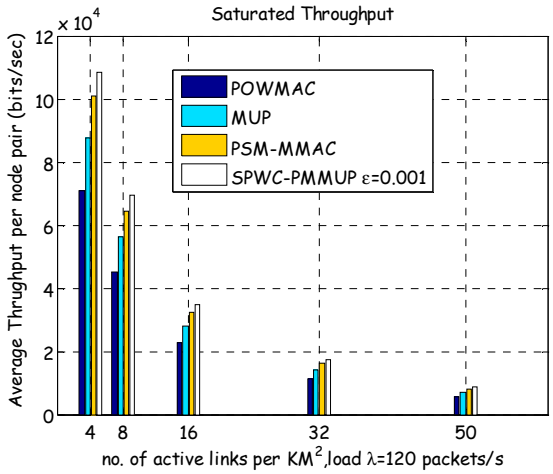

Figure 5.16: Average saturated throughput versus density of active links

5.8 Chapter Conclusions and Remarks

In this chapter, a new transmission power control scheme based on singular-perturbations at the co-located multiple queues and the weak-coupling of multiple wireless channels has been developed. In order to coordinate the functions of wireless multi-radio and multi-channel (MRMC) network configurations, a corresponding Link Layer power selection multi-radio multi-channel unification protocol (SPWC-PMMUP) has also been incorporated. Using the differential Nash game techniques for large scale interconnected weakly-coupled and singularly-perturbed control systems, a generalized higher order recursive algorithm (HORA) has been derived. The algorithm was proved to converge at a linear rate both analytically and numerically. Performance evaluations by means of several simulations demonstrated that the SPWC-PMMUP scheme was superior to other conventional related protocols. Simulation results were recorded as follows. A larger number, relatively speaking, of radios to the number of channels at $\tilde{\varepsilon} = 0.01$ recorded higher transmission power consumption than at

$\tilde{\varepsilon} = 0.001$ (i.e., Fig. 5.11). The SPWC-PMMUP scheme was, between 14.58% and 145.83%, more energy-efficient on average than the POWMAC, PSM-MMAC and MUP schemes, respectively (i.e., Fig. 5.12). The SPWC-PMMUP scheme provided a longer network lifetime on average, ranging from 12.50% to 33.30%, than the POWMAC, PSM-MMAC and MUP schemes, respectively (i.e., Fig. 5.13). The average throughput per node pair was better, with $\tilde{\varepsilon} = 0.1$, than with $\tilde{\varepsilon} = 0.001$ (i.e., Fig. 5.14). Average throughput per node-pair plotted against the transmission probability was better at $\tilde{\varepsilon} = 0.001$ in a multi-radio network than in a single radio network (i.e., Fig. 5.15). Finally, the SPWC-PMMUP schemes, at $\tilde{\varepsilon} = 0.001$ and arrival rate of $\lambda = 120$ packets/s, yielded between 8% and 36.36% more average saturated throughput per node pair plotted against the active density of nodes (i.e., Fig. 5.16).

The main reasons for these observations are as follows. Multi-radio multi-channel wireless networks do face both queue perturbations and cross-channel interference phenomena. Such phenomena result in dropping of the transmitted packets. In order to guarantee network throughput, nodes can choose to retransmit the packets opportunistically (i.e., when link conditions are favourable). This may result in the wastage of the transmission energy. The reduced system perturbations and the cross-channel interference would allow the network to operate for a longer time. In contrast, a strongly perturbed queue system and the cross-channel interference would shorten the operation time of a network. The SPWC-PMMUP scheme determines the optimal transmission power signals dynamically in response to the queue status, the residual-energy and the conventional LSI discussed in Chapter 4 (e.g., received signal to noise ratio, aggregate co-located network interference, the packet transmission rate and the link connectivity range). Such factors directly affect the optimality of the transmission power and hence are worth investigating. On the other hand, the PSM-MMAC scheme performs both power saving and opportunistic medium access scheduling. However, there are no guarantees regarding the optimality of the transmission power signal. The POWMAC protocol performs transmission power control on a single wireless transceiver and channel. However, control packets are exchanged at maximum transmission power. The MUP method does not guarantee power control on the optimally selected wireless channels. Lastly, the MUP scheme records a fairly efficient throughput performance but its energy-efficiency is comparatively poorer than that of the SPWC-PMMUP counterpart.

Chapter 6

Conclusions and Future Work

The work presented in this dissertation has addressed one of the most crucial issues in a distributed Wireless Backbone Mesh Network (WBMN): the dynamic transmission power control (DTPC) problem. The distinctive feature of the WBMN is the ability to access and route traffic both simultaneously and in a distributed fashion. In order to ensure this high traffic carrying capacity, the WBMN nodes are often equipped with at least one independent radio, each operating on a separate frequency channel. Or else, each node may be configured with a fast switching radio capable of performing dynamic channel assignment. While attempting to increase network traffic carrying capacity, battery energy outage and connectivity issues may arise. This is the problem which this dissertation addressed. In this work, dynamic mathematical programming models are developed for formulating this problem in terms of both user-centric and network-centric objectives. If each node has at least two radios operating simultaneously on separate channels, the entire WBMN is first divided into sets of unified channel graphs (UCGs). Each UCG is assigned a unique frequency channel so that different nodes can interconnect with each other. A Stochastic Quadratic Cost Function is then formulated subject to the linear combination of Link-Layer State Information (LSI) from other UCGs. Indeed, predictive algorithms are proposed at the Link-Layer (LL) to solve this problem by means of a reduced delay. Based on the convex cost function formulation, the proposed algorithms provide fast convergence with global system stability. They are also robust in the sense that they can tackle the DTPC problem under a diverse range of input parameters, e.g., diverse channel conditions, multiple access interference (MAI), diverse Signal-to-Interference plus Noise ratio (SINR), different wireless link rates, heterogeneous connectivity ranges, singular queue perturbations, cross-channel weak-couplings, diverse dimensions of radios and various sizes of network et cetera. The distinctive attributes of our proposed DTPC solutions meet the following specifications of generalized WBMNs:

1. Scalability. That is, the network performance indexed by energy-efficiency, high throughput, fairness and fault-tolerant connectivity do not degrade significantly on an

increase in the number of nodes or hops from the sender to destination. This has been achieved by ensuring that the Link-Layer protocol provides good trade-off modularity with minimal overhead costs as regards the cross-layering information exchanges.

2. Self-organization and Self-configuration. That is, each node or link in the network individually exploits local LSI to build-up a network or, if at least one link/route fails it auto-heals (auto-configures) channels, links and routes in real-time. The objective is to allow all protocols to be distributive and collaborative or decentralized.
3. Heterogeneity. That is, the DTPC algorithms are adaptive to different connectivity ranges, dimensions and/or different technologies of radios at each node, variable channel switching speeds, memory sizes, energy battery constraints, queue traffic loads, etc.
4. Multi-point to Multi-point (M2M) communication. That is, our models and algorithms are adaptive to high speed operation of nodes or those with software defined radios. This is to ensure timely channel assignments and/or the use of multiple radios for accessing several mesh clients and forwarding network traffic simultaneously, to a few fixed gateways.
5. Multi-hop communication. That is, due to limitations on the transmission ranges, the nodes relay multi-hop forms of traffic from the access networks to the back-haul gateway networks. This feature is ensured by allowing each node to use power controlled channels for every packet.
6. Energy and memory diversity. That is, the possibility of possessing multiple radios with diverse energy consumption and memory capability at the backbone network. The proposed predictive and/or recursive asynchronous algorithms based on residual energy support both energy and memory-efficiency.

The following sections summarize in brief our findings, contributions, provide concluding remarks and describe some directions for future extension of our work.

6.1 Summary of Contributions

In addition to the survey presented in this thesis, we have developed mathematical programming models managed by Link-Layer protocol based on predictive algorithms with respect to the DTPC problem. The main contributions may be outlined as follows:

- ***Survey:*** In this thesis, an overview of the proposed algorithms to the DTPC problem is presented. The algorithms are classified according to the solution techniques: mathematical programming, game-theoretical, dynamic control-theoretical, and

network protocol heuristics [286]. The survey provided in this study presents a starting point for choosing a DTPC method to be used in different scenarios of wireless backbone networks. It may also be used by researchers for selecting an algorithm against which to compare and/or develop new schemes.

- ***Modelling:*** In this thesis, three mathematical programming models are formulated, as regards the DTPC problem, for the WBMNs. One for single radio wireless backbone networks and the other two for a generalized multi-radio multi-channel (MRMC) wireless network. Each model formulates the decentralized DTPC problem as an optimization problem at link/user level composed of a cost function subject to a set of LL based constraints imposed by both the user and the network.

  The first model is developed in chapter three for single radio wireless networks. The objective is to minimize the convex cost function composed of SIR-deviation (i.e., maximizing the *user quality of service (QoS)*) and the aggregate interference (i.e., maximizing the *network spatial reuse/capacity*). Two sets of LL constraint models are provided in this formulation. One constraint model is based on the medium access control transmission scheduling probability (MAC-TSP) while the other is based on a generalized cross-layer occupation measure (GCOM). These models describe how message interactions among the layers of the protocol stack affect the optimality of DTPC supported at the LL.

  The second model is formulated in chapter four for MRMC wireless networks. The MRMC wireless network is first modelled as sets of UCGs. Link State Information (LSI) is then derived for each UCG set and represented as state space control models. The objective is to minimize stochastic quadratic cost function (i.e., *composed of LSI from one user*) subject to the network interaction LSI (i.e., *from the same UCG where the user is located*) and the coordination LSI (i.e., *derived from other UCGs*).

  The third model is presented in chapter five for a Singularly-Perturbed Weakly-Coupled (SPWC) MRMC wireless system. The idea is to model energy and packet dynamics of a multiple queue system as a singular perturbation problem [287]. This problem is mathematically represented in terms of a two dimensional Markov chain model. From the Markov chain perspective, steady state probabilities of the system can be obtained. In addition, practical transmission power interference among multiple channels within close vicinity is modelled as a weak coupling problem. The objective is to minimize the stochastic quadratic cost function of the SPWC-LSI in addition to the *queue perturbation* and *cross-channel interference* problems.

The proposed mathematical models may be used by analytical research to discover solutions to the problem of DTPC in generalized WBMN applications.

- ***Algorithms:*** In this thesis, several algorithms based on three Link-Layer protocols are developed to solve the DTPC problem for WBMNs.

  In chapter three, a multiple access transmission aware (MATA) protocol is proposed for single radio wireless networks. The said protocol is based on scalable MAC-TSP and GCOM models. The MAC-TSP model defines the probability that a packet will successfully be transmitted by each user with the selected transmission power level knowing the physical, MAC and topological characteristics of the Bi-directional Logical Visible Neighbour (BLVN) set. The GCOM model is a generalized type of the MAC-TSP model that spans all the layers of the protocol stack. It defines the probability that an individual user chooses a certain transmission power level knowing the states across the layers of the protocol stack. Based on these models, the MATA-DTPC algorithm is developed. Correspondingly, the optimal power controller gain is designed and analysed for system convergence.

  In chapter four, an energy-efficient power selection multi-radio multi-channel unification protocol (PMMUP) supported at the LL is developed. The PMMUP is a virtual MAC, composed of two predictive algorithms. One of these is called a multi-radio multi-channel LSI interaction prediction (MRSIP); the other is termed a multi-radio multi-channel LSI unification prediction (MRSUP). MRSIP predicts LSI from multiple MACs and UCGs at a lower level, while MRSUP predicts LSI from the upper layers of the protocol stack. The rationale is that interaction variables provide wireless system constraints while the unification variables provide application constraints to the DTPC at the LL. Based on the predicted LSI states, both algorithms determine an optimal transmission power level for each user, subject to the node energy constraints. These algorithms are further analysed for convergence and system stability.

  In chapter five, an extension of PMMUP called Singularly-Perturbed Weakly-Coupled PMMUP (or simply, SPWC-PMMUP) is developed in order to generalize the DTPC problem to large-scale wireless networks [287]. The protocol optimally selects the transmission power level based on the knowledge of the queue perturbation, and interference across different neighbouring channels or UCGs. A differential Nash games algorithm is presented to perform the transmission power control for a SPWC system. The rationale is to decompose independent actions and to

have a Nash equilibrium solution for the whole system such that each user's transmission power choice is completely decoupled from those of others in a large scale wireless network. In order to devise an optimal power control strategy, the SPWC algebraic regulator Riccati equation (SWARRE) is developed. A generalized Higher-Order Recursive Algorithm (HORA) is then derived that provides a stabilizing solution for the decoupled SWARRE. The derived HORA is analysed for system convergence.

6.2 Concluding Remarks

The proposed DTPC algorithms from the survey are difficult to evaluate and compare with each other as they strictly depend on the various wireless network architectures, technologies and structural configurations both for user and network applications. Most researchers have attempted to compare their work against those of others and claim that their findings are better than those reported by the latter. Based on this trend, it may be difficult to select a single approach/algorithm that can provide the best DTPC solutions for a wide range of WBMN attributes.

From the perspective of single radio WBMNs, the following analytical conclusions have been deduced: Because the distributed cost function of both the user and network objectives is convex, it records at most one local minimum; however, if such a local minimum exists, it records a global minimum for all users operating within an interference range (i.e., BLVN). The dynamic controller and thus transmission power level were shown to be optimal globally with respect to the minimization of the convex cost function. The uniqueness of the optimal controller gain/vector has implied that the transmission power update has a unique fixed point at optimal transmission power level. Furthermore, the following results from simulation experiments have been found: the controller gain and transmission power executions, on average, have proved to exponentially converge to a steady state for the MATA based algorithm. This is because the chosen convex cost function is minimized iteratively as the MATA information is exchanged locally among nodes. This implies that the controller gain and the adjusted transmission power must also steadily drive this message exchange until all MATA state prediction converges. For the MATA based algorithm, the autonomous executions of the transmission power level allow some nodes to be energy-efficient by lowering their transmission powers while others are permitted to be overly greedy by raising

their powers. On average, such power executions have shown a better trade-off between energy conservation and the network capacity of active users than either employing greedy strategy alone or the energy-efficient method. The average steady state power consumption and average per link throughput have indicated desirable performance with regards to multiple concurrent active users when the MATA based algorithm is compared with conventional methods. The average feasibility rate per network scenario versus number of admitted users has proved to be more robust with the MATA based algorithm than conventional algorithms. Here, the feasibility rate defines the probability that active users will co-exist and send packets successfully to their target receivers. Based on this simulation experiment, the MATA based algorithm has yielded good scalability measures for the WBMNs irrespective of the network size. The main reasons for these observations are two-fold: first, the MATA based algorithm executes both the user-centric objectives (i.e., optimizing user QoS e.g., throughput, delay, etc.) and the network centric-objectives (i.e., maximizing the network lifetime, network co-existence/spatial reuse, fault-tolerant connectivity, etc). Second, the MATA based algorithm is executed at the LL and deals with both forward and backward power controlled LSI exchanges that take into account the MAI at both the receiver and transmitter sides.

As far as the multi-radio WBMNs are concerned, the following analytical conclusions can be drawn from the PMMUP algorithms developed: The two PMMUP algorithms (e.g., MRSIP and MRSUP), during an optimization time slot, have proved to be exponentially stable in the Lyapunov sense. This is because the derived stabilizing solution to the Riccati Equation has been employed to compensate for model uncertainties in the dynamic programming function of our work. It has also been shown that MRSIP and MRSUP converge asynchronously with a linear rate. The convergence rate depends on the iteration interval and interaction between users as they exchange LSI estimates among different UCGs because, these algorithms have been proved to satisfy a contraction property defined in terms of a set of discrete functions. Therefore, satisfying a contraction property implies convergence of asynchronous iterations. The following results were observed from the simulation results: based on its simple computational structure, asynchronous MRSIP (MRSIPA) demonstrated convergence superior to that of the asynchronous MRSUP (MRSUPA). Of interest, MRSIPA have shown, on average, between 0.005% and 23.23% more transmission power adaptation saving gains than other approaches. MRSIPA has provided, on average, steady transmission power savings versus different traffic loads, of between 8.11% and 87.84% greater than other approaches. MRSIPA has also yielded, on

average, throughput gains, versus different traffic loads, of between 16.67% and 80.00% more than other approaches. The motivations behind these observations are: MRSIPA is asynchronous and each user, having attained convergence does not have to wait for other iterating users before transmitting its packets in the queue. MRSIPA possesses a simple computational structure with localized information exchange among multiple MACs and radios at a lower level. This attribute not only improves delay/real-time applications but also reduces message overhead costs. The closest in performance is the MRSUPA which is asynchronous but exhibits a complex computational structure. It relies heavily on information from higher layers at the expense of extra transmission power and message overhead costs.

According to the Singularly-Perturbed Weakly-Coupled protocol (SPWC-PMMUP), the following analytical results have been noted:

The steady state transmission probability of a packet from the queue and the expected packet queue delay are decomposable into an unperturbed component and a perturbed component expressed in terms of higher order Taylor series expansion. The first order Taylor series expansion in terms of the perturbation factor presents a reliable approximation of the exact steady state probability distribution of the two-dimensional Markov chains for both energy and packet queue dynamics in multiple queues. Under the assumptions that (i) each user has an optimal closed-loop Nash Strategy, (ii) the wireless system matrices are stabilizable and detectable, and (iii) the auxiliary SWARRE has a positive semi-definite stabilizing solution, the generalized Higher-Order Recursive Algorithm (HORA) converges to the exact solutions of the error terms in the Lyapunov sense and the rate of convergence is linear (i.e., *Theorem 5.2*). Furthermore, under similar assumptions, the use of a high-order soft constrained Nash Equilibrium results in the condition that: the cost function of the high-order (i.e., iterative) input control sequences is approximately equal to the cost function of the zero-order (i.e., optimal) input control sequences plus a higher-order function of SPWC factor (i.e., *Theorem 5.3*). This observation confirms that the proposed generalized algorithm converges to the exact solution. As a consequence, the system's cost function converges exponentially, implying that the optimal transmission power level for each user is obtainable. In addition to the analytical results, the following summary of performance evaluations is offered: The proposed SPWC-PMMUP, on average, has shown between 14.58% and 145.83% more energy-efficiency than conventional protocols. On average, the new protocol has demonstrated a longer network lifetime ranging from 12.50% to 33.30% longer than conventional methods. The average throughput per node-pair at a high SPWC factor is worse than throughput measured at a low SPWC factor. The average throughput per node-pair

versus the transmission probability in a multi-radio network at a low SPWC factor is better than the case for a single-radio network. On average, the SPWC-PMMUP has yielded between 8% and 36% more saturated throughput per node-pair versus the density of nodes at an arrival rate of 120 packets/s, than the conventional methods. The reasons for these remarks are outlined as follows. Multi-radio multi-channel (MRMC) wireless systems/networks do face both queue perturbations due to energy and packet dynamics, and cross-channel interference due to the power of transmissions radiated by different radios in the close vicinity. Such phenomena result in the dropping of the transmitted packets and hence re-transmissions at the expense of extra transmission power consumption. Indeed, a single radio wireless network experiencing packet re-transmissions and pessimistic with respect to queue status, would incur higher transmission power consumption than its SPWC power controlled counterpart. Therefore, the SPWC-PMMUP allows the evaluation of optimal transmission power signals to be selected dynamically in response to the knowledge of queue status, the residual energy at the node and Link State Information (LSI) (i.e., *in chapter 4*). The optimal transmission power signals ameliorate the condition of a tendency to re-transmit, thus more energy-efficiency and throughput enhancement are evident in a MRMC network. Conversely, the PSM-MAC protocol performs power management but guarantees no optimal transmission power levels. The POWMAC protocol executes transmission power control but takes no account of the queue status of the network. The MUP method performs unification of MRMC systems to enhance throughput under transmission power which is unconstrained and is thus energy-inefficient.

6.3 Future Work

The work described in this thesis may be extended in several directions. Some possible areas could be discussed as follows:

- **Analysing the DTPC Algorithms for energy-efficiency in backbone nodes deployed in energy-constrained areas:**

  One of the most challenging directions is to extend the applicability of the proposed algorithms to WBMNs operating in energy-constrained environments. In rural and remote areas, nodes are battery-powered and have limited capacity. However, the

proposed algorithms involve computationally intensive mathematical models that may in turn compromise the energy costs. Analysis of computational time, memory and energy costs with respect to their applicability to energy-constrained nodes would constitute interesting future work.

- **Adapting the DTPC Algorithms to include Dynamic Channel Assignment:**

  The algorithms proposed in this thesis assume that there is no Channel Assignment within every time slot except that channels are hard-coded for the entire duration of the time-slot. The channel assignment remains static until the completion of at least one DTPC cycle. This implies that the power optimization time-scales are assumed to be typically faster than that of the Channel Assignment. However, under fast fading channel conditions, the channel assignment time-scale should be, on average, a one-to-one matching with that of the transmission power optimization. Furthermore, automatic accessing and forwarding traffic by the WMRs require a dynamic and scalable channel assignment. This would offer a challenging and interesting research topic.

- **Adapting the DTPC Algorithms to include network Routing:**

  As the next step to future research, the proposed Algorithms should include scalable routing at the backbone networks. Most previous studies have shown that most routing algorithms performed at the network layer of the protocol stack are not energy-efficient and are un-scalable. Adapting routing and the DTPC at the Link-Layer may improve network throughput irrespective of the size of the network. This is because the Link-Layer utilizes local information to perform hop by hop routing. Research into joint DTPC and routing at the Link-Layer would be interesting future study.

- **Applying the DTPC Algorithms to backbone emerging wireless technologies such as IEEE 802.16 Broadband Wireless Metropolitan Area Network (BWMAN) and IEEE 802.22 Wireless Regional Area Network (WRAN):**

Although the thesis has made it clear that the DTPC Algorithms are generic with respect to any distributed wireless backbone technologies, the major focus has been placed on the IEEE 802.11 based wireless backbone mesh networks (WBMNs). Performance evaluations of the Algorithms with respect to other backbone technologies would represent worthwhile research areas.

- **Hardware-implementation of the energy-efficient protocols at the network protocol stack:**

  This thesis has furnished the analytical and simulation investigations of the proposed Link-Layer protocols. An extension of this work to actual prototype implementations and field-testing on backbone wireless nodes would similarly be a challenging yet an interesting topic for future studies.

List of Publications

• Peer Reviewed International Journals:

1. **Olwal, T. O**., Djouani, K., Van Wyk, B. J., Hamam, Y., Siarry, P and Ntlatlapa, N., **"**A Multiple-State Based Power Control for Multi-Radio Multi-Channel Wireless Mesh Networks,**"** *International Journal of Computer Science***,** Vol. 4, no. 1, pp. 53-61,August 2009, ISSN 2070-3856.
2. Aron, F., **Olwal, T. O.,** Kurien, A. & Odhiambo, M., "A distributed Topology Control to Conserve Energy in Heterogeneous Wireless Mesh Networks," *Proceedings of the World Academy of Science, Engineering and Technology* (PWASET), Vol. 30, September 2008, ISSN 1307-6884, pp. 530-536.
3. **Olwal, T. O**., Djouani, K., Van Wyk, B. J., Hamam, Y., Siarry, P, **"**A Multi-Radio Multi-Channel Unification Power Control for Wireless Mesh Networks,**"** *International Journal of Computer Science***,** Vol. 5, no. 1, pp. 38-50, March 2010, ISSN 2070-3856.
4. **Olwal, T. O**., Van Wyk, B. J., Djouani, K., Hamam, Y and Siarry, P., "Singularly-Perturbed Weakly-Coupled Based Power Control for Multi-Radio Multi-Channel Wireless Networks," *International Journal of Applied Mathematics and Computer Sciences,* Vol. 6, no. 1, pp. 4-14, April 2010, ISSN 2070-3902.
5. **Olwal, T**.O., Van Wyk, B. J., Ntlatlapa, N., Djouani, K., Siarry, P and Hamam, Y., "Dynamic Power Control for Wireless Backbone Mesh Networks: a Survey," *International Journal of Network Protocols and Algorithms,* Vol. 2, no. 1, pp. 1-44, May 2010, ISSN 1943-3581.

• Chapters in Edited Books:

1. **Olwal, T. O.,** Aron, F., van Wyk, B. J., Hamam, Y., Ntlatlapa, N. & Odhiambo, M., "Improved Distributed Dynamic Power Control for Wireless Mesh Networks", in *Ad Hoc, Mobile and Wireless Networks***,** LNCS 5198, vol. 5198/2008, ISBN 978-3-540-85208-7, pp. 357-368, DOI: 10. 1007/978-3-540-85209-4- 28, Springer-Verlag, Berlin Heidelberg, September 20, 2008.
2. **Olwal, T. O**., van Wyk, B. J., Djouani, K., Hamam, Y., Siarry, P. & Ntlatlapa, N., "Autonomous Transmission Power Adaptation for Multi-Radio Multi-Channel Wireless Mesh Networks", in *Ad Hoc, Mobile and Wireless Networks*, LNCS 5793, Springer-Verlag, Berlin Heidelberg, pp. 284-297, DOI: 10.1007/978-3-642-04383-3, ISBN: 978-3-642-04382-6,August 29, 2009.
3. **Olwal, T. O.,** Djouani, K., van Wyk, B. J., Hamam, Y. & Siarry, P., "Optimal Control of Transmission Power Management in Wireless Backbone Mesh Networks," Accepted in *Wireless Mesh Networks*, INTECH Open Access Publisher, pp. 1-26, ISBN: 978-953-7619-X-X, December 2010.

• Peer Reviewed International Conference Proceedings:

1. **Olwal, T. O.,** Aron, F., Van Wyk, B. J., Hamam, Y., Ntlatlapa, N. & Odhiambo, M., "Improved Distributed Dynamic Power Control for Wireless Mesh Networks," in Proc. *7th International Conference*

on the Ad Hoc Networks and Wireless, AD HOC NOW' 2008, Sophia Antipolis, France, September 10-12, 2008, ISSN 0302-9743, pp. 357-368.

2. **Olwal, T. O.,** Aron, F., Van Wyk, B. J., Hamam, Y., Ntlatlapa, N. & Johnson, D., "Transmission Probability based Dynamic Power Control for multiple radio mesh networks," In *Proc. SATNAC'2008,* Wild Coast, Eastern Cape, 7-10 September, 2008.
3. **Olwal, T. O.,** van Wyk, B. J., Hamam, Y. & Ntlatlapa, N., "Decentralized Cross-layer Dynamic Power Control for Wireless Mesh Networks," in *IEEE Computer Society, 3rd International Conference on Broadband communications, Information Technology and Biomedical Applications, Broadcom'2008,* pp. 245-253, 23-26 November 2008, Pretoria, South Africa.
4. **Olwal, T. O.,** Van Wyk, B. J., Hamam, Y. & Ntlatlapa, N., "Scalable Power Selection Method for Wireless Mesh Networks," in *Proc. IEEE/ACM 3rd Annual workshop Wireless Systems: Advanced Research and Development (WISARD 2009),* 05-06 Jan 2009, Bangalore, India.
5. **Olwal, T. O.,** Van Wyk, B. J., Djouani, K., Hamam, Y., Siarry, P and Ntlatlapa, N., "Autonomous Transmission Power Control Adaptation for Multi-Radio Multi-Channel Wireless Mesh Networks," I*n 8th Proc. Of International Conference on Ad Hoc Networks and Wireless*, LNCS 5793, pp. 284-297, 22-25 September, 2009, Murcia, Spain.
6. **Olwal, T. O.,** Van Wyk, B. J., Djouani, K., Hamam, Y., Siarry, P and Ntlatlapa, N., "Interference-Aware Power Control for Multi-Radio Multi-Channel Wireless Mesh Networks," *in Proc. Of IEEE Africon 2009*, pp. 1-6, ISBN: 978-1-4244-3919-5, 23-25 September 2009, Nairobi, Kenya.
7. **Olwal, T. O.,** Van Wyk, B. J., Djouani, K., Hamam, Y., Siarry, P and Ntlatlapa, N., "Range Based Power Control for Multi-Radio Multi-Channel Wireless Mesh Networks," I*n SATNAC 2009,* pp. 49-54, ISBN: 978-0-620-44106-3, 30 Aug-2 September 2009, Royal Swazi Spa, Swaziland.
8. Aron, F., **Olwal, T. O.,** Kurien, A. & Hamam, Y., "Network Preservation through a Topology Control Algorithm for Wireless Mesh Networks," in *Proc. International Conference, IASTED on Modeling and Simulation (AfricaMs 2008),* ISSN 603-080, http://www.iasted.org/, September 8-10, 2008, Gaborone, Botswana.
9. Aron, F., **Olwal, T. O.,** Kurien, A. & Odhiambo, M., "Energy Efficient Topology Control Algorithm for Wireless Mesh Networks," in *Proc. International Conference, IEEE Region 8, Wireless Communication and Mobile Computing (IWCMC'2008),* pp. 135-140, ISBN: 978-1-4244-22012-2, Aug 6-8, 2008, Crete, Greece.
10. Mhlanga, M., Nyandeni, T., **Olwal, T. O.,** Ntlatlapa, N. and Adigun, M. "Energy-Aware Path Selection Metric for IEEE 802.11s Wireless Mesh Networks,"*WIP in SATNAC 2009*, ISNB: 978-0-620-44106-3, 30 August-2 September 2009, Royal Swazi Spa, Swaziland.
11. Masonta, M. T., **Olwal, T** and Ntlatlapa, N., "An Energy Saving Scheme for Internet Provision in Rural Africa: LESS," *International Conference paper accepted* at IST-Africa', May 2010, Durban, South Africa.
12. **Olwal, T. O.,** Van Wyk, B. J., Djouani, K., Hamam, Y., Siarry, P and Ntlatlapa, N., "Decentralized Power Control in Multi-Radio Multi-Channel Wireless Mesh Networks," Accepted at *SATNAC 2010, September 5-8, Spier Wine Estate, Cape Town, South Africa.*

- **Papers Submitted to Peer Review Journal**

1. **Olwal**, **T. O**., Djouani, K., Siarry, P., Van Wyk, B. J and Hamam, Y., "Singularly-perturbed Weakly-coupled Power Control for Wireless Backbone Networks: A Decentralized Approach," ***Journal*** *under Review in IEEE Transactions on Mobile Computing, November 2009.*

Bibliography

[1] I. F. Akyildiz, X. Wang, and W. Wang, "Wireless Mesh Networks: a Survey," *Computer Networks,* vol. 47, pp. 445-487, March 2005.

[2] Z. J. Haas, *Wireless Ad Hoc Networks*: Institute of Electrical and Electronics Engineers (IEEE), 1999.

[3] I. F. Akyildiz, W. Su, Y. Sankarasubramaniam, and E. Cayirci, "Wireless Sensor Networks: a survey," *Computer Networks,* vol. 38, pp. 393-422, 2002.

[4] I. S. 802.11, " Wireless LAN Media Access Control (MAC) and Physical Layer (PHY) Specifications," 1999.

[5] M. Chiang, P. Hande, T. Lan, and C. W. Tan, *Power Control in Wireless Cellular Networks, Foundation and Trends in Networking* vol. x. Hanover MA 02339 USA: now Publishers Inc, 2008.

[6] I. F. Akyildiz and X. Wang, *Wireless Mesh Networks*: John Wiley & Sons Ltd, 2009.

[7] J. D. Camp and E. W. Knightly, "The IEEE 802.11s Extended Service Set Mesh Networking Standard," *IEEE Communications Magazine,* vol. 46, pp. 120-126, August 2008.

[8] I. Working Group, "IEEE 802.15.5 Mesh Networking Standards," in *http://www.ieee802.org/15/*. vol. 2010: IEEE 802.15. Working Group.

[9] J. Dicman, K. Rath, and L. Kotecha, "Proposal for IEEE 802.16 Connection Oriented Mesh," *IEEE 802.16 Standard Proposal,* March 2003.

[10] V. C. Gungor, E. Natalizio, P. Pace, and S. Avallone, "Challenges and Issues in Designing Architectures and Protocols for Wireless Mesh Networks," in *Wireless Mesh Networks: architecture and protocols*, E. Hossain and K. K. Leung, Eds.: Spinger, 2008.

[11] J. Ishmael, S. Bury, D. Pezaros, and N. Race, "Rural Community Wireless Mesh Networks," *IEEE Internet Computer Journal,* vol. 2008, pp. 22-29, 2008.

[12] S. Sorooshyari and Z. Gajic, "Autonomous Dynamic Power Control for Wireless Networks: User-centric and Network centric consideration," *IEEE Trans. On Wireless Communications,* vol. 7, pp. 1004-1015, March 2008.

[13] A. A. Hanbali, E. Altman, and P. Nain, "A Survey of TCP over Ad Hoc networks," *IEEE Communications Surveys and Tutorials,* vol. 7, pp. 22-36, June 2005.

[14] X. Li, F. Cao, and D. Wu, "QoS-driven power allocation for Multi-channel communication under delayed channel side information," in *Proc. IEEE Consumer Communications & Networking (CCNC'09) Conference*, Las Vegas, Nevada, USA, 2009.

[15] P. Mohapatra and S. Krishnamurthy, *Ad Hoc Networks: Technologies and Protocols*: Springer, 2005.

[16] B. Alawieh, C. Assi, and H. Mouftah, "Investigating the performance of power-aware IEEE 802.11 in Multi-hop wireless networks," *IEEE Transactions on Vehicular Technology,* vol. 58, pp. 287-300, January 2009.

[17] E. S. Jung and N. H. Vaidya, "A power control MAC protocol for ad hoc networks," *Wireless Networks,* vol. 11, pp. 55-66, 2005.

[18] A. Muqattash and M. Krunz, "POWMAC: A Single-Channel Power-Control Protocol for Throughput Enhancement in Wireless Ad Hoc Networks," *IEEE Journal, Selected Areas in Communications, (JSAC)-Special Issue on Advances in Military Communications,* vol. 23, pp. 1067-1084, 2005.

[19] Y. Feng, M. Li, and M.-Y. Wu, "Improving Capacity and Flexibility of Wireless Mesh Networks by Interface Switching," in *Proc. IEEE International conference on communications (ICC'2008)*, Beijing, 2008, pp. 4729-4733.

[20] J. Olafsson, X. Gu, and Y. Yang, "Joint design of distributed power control and dynamic channel allocation in scalable WLANs," in *Proc. IEEE 4th International Conf. Wireless Communication, Networking and Mobile Computing (WiCOM'08)*, Dalian, 2008, pp. 1-4.

[21] T. O. Olwal, B. J. V. Wyk, K. Djouani, Y. Hamam, P. Siarry, and N. Ntlatlapa, "Autonomous Transmission Power Adaptation for Multi-radio Multi-channel Wireless Mesh Networks," in *Proc. Ad Hoc Now 2009 Conference*, Spain, 2009, pp. 284-297.

[22] M. Hajiaghayi, N. Immorlica, and V. S. Mirrokni, "Power Optimization in Fault-tolarant Topology Control Algorithms for Wireless Multi-hop Networks," in *Proc. MobiCom'03 Conference*, San Diego, California, USA, 2003, pp. 300-312.

[23] T. Olwal, B. J. V. Wyk, Y. Hamam, and N. Ntlatlapa, "Scalable Power Selection Method for Wireless Mesh Networks," in *Proc. IEEE/ACM 3rd Annual Workshop Wireless Systems: Advanced Research and Development (WISARD 2009)*, Bangalore, India., 2009, pp. 1-8.

[24] V. Kawadia and P. R. Kumar, "A cautionary perspective on cross-layer design," in *IEEE Wireless Communications Magazine*. vol. 12, 2005.

[25] A. Iqbal and S. A. Khayam, "An energy-efficient link-layer protocol for reliable transmission over wireless networks," *EURASIP journal on Wireless Communications and Networking,* vol. 2009, p. 10, July 2009.

[26] M. Krunz and A. Muqattash, "Transmission Power Control in Wireless Ad Hoc Networks: Challenges, Solutions, and Open Issues," *IEEE Network,* vol. 18, pp. 8-14, September/October 2004.

[27] F. Aron, T. O. Olwal, A. Kurien, and M. O. Odhiambo, "Network Preservation through a Topology Control Algorithm for Wireless Mesh Networks," in *Proc. International*

Conference on Modelling and Simulation (IASTED AfricaMs 2008), Gaborone, Botswana, 2008.

[28] F. O. Aron, A. Kurien, and Y. Hamam, "A Topology Control Algorithm for Effective Power Efficiency and Throughput for Wireless Mesh Networks," in *Proc. IEEE 3rd International Conference on Broadband communications, Information Technology and Biomedical Applications (Broadcom'08)*, CSIR, Pretoria, South Africa, 2008, pp. 89-96.

[29] F. O. Aron, T. O. Olwal, A. Kurien, and M. O. Odhiambo, "A Distributed Topology Control Algorithm to Conserve Energy in Heterogeneous Wireless Mesh Networks," *Proceedings of World Academy of Science, Engineering and Technology,* vol. 30, pp. 530-536, July 2008.

[30] F. O. Aron, T. O. Olwal, A. Kurien, and M. O. Odhiambo, "Energy Efficient Topology Control for Wireless Mesh Networks," in *Proc. IEEE Region 8, International Conference on Wireless Communication and Mobile Computing (IWCMC'2008)*, Crete, Greece, 2008.

[31] N. Ramachandran, E. M. Belding, K. C. Almeroth, and M. M. Buddikot, "Interference-Aware Channel Assignment in Multi-Radio Wireless Mesh Networks," in *Proc. IEEE INFOCOM 2006*, Barcelona, Spain, 2006.

[32] K. K. Leung, "A Kalman-filter method for power control in broadband wireless networks," in *Proc. IEEE INFOCOM 1999 Conference*, New York, 1999, pp. 948-956.

[33] F. Gunnarsson, "Power Control in Cellular Radio Systems: Analysis, Design and Estimation," in *Electrical Engineering*. vol. PhD Thesis Linkoping Sweden: Linkoping Studies in Science and Technology, 2000, p. 262.

[34] J. E. Suris, "Cooperative Game Theory and Non-Convex Optimization for Distributed Spectrum Sharing." vol. PhD Thesis USA: Virginia Polytechnic Institute and State University, 2007.

[35] E. Altman, K. Avrachenkov, G. Millen, and B. Prabhu, "Discrete Power Control: Cooperative and Non-Cooperative Optimization," in *Proc. IEEE INFOCOM 2007 Conference*, Alaska, USA, 2007.

[36] R. Branzei, D. Dimitrov, and S. Tijs, *Models in Cooperative Game Theory*, Second ed. vol. 556. Berlin: Springer, 2008.

[37] J. E. Suris, L. A. DaSilva, Z. Han, A. B. MacKenzie, and R. S. Komali, "Asympototic Optimality for Distributed Spectrum Sharing Using Bargaining Solutions," *IEEE Trans. Wirel. Communications,* vol. 8, pp. 5225-5237, October 2009.

[38] E. Altman, K. Avrachenkov, N. Bonneau, M. Debbah, R. El-Azouzi, and D. Menasche, " Constrained Stochastic Games in Wireless Networks," www.cs.umass.edu/~sadoc/mdp 2007.

[39] M. J. Osborne and A. Rubinstein, *Bargaining and Markets* vol. 2005-3-2. New York: Academic Press, Inc., 1990.

[40] M. A. Aldajani and A. H. Sayed, " Adaptive Predictive Power Control for the Uplink Channel in DS-CDMA cellular systems," *IEEE Trans. Vehicular Technology,* vol. 52, pp. 1447-1463, November 2003.

[41] A. Adya, P. Bahl, J. Padhye, A. Wolman, and L. Zhou, "A multi-radio unification protocol for IEEE 802.11 wireless networks," in *Proc. International Conference on Broadband Networks (Broadnets'04)*, San Jose, CA, 2004.

[42] H. T. Cheng, H. Jiang, and W. Zhuang, "Distributed medium access control for wireless mesh networks," *Journal of Wireless Communications and mobile computing,* vol. 6, pp. 845-864, 2006.

[43] J. P. Monks, "Transmission power control for enhancing the performance of wireless packet data networks," in *Faculty of Engineering*. vol. PhD Thesis Urbana-Champaign: University of Illinois at Urbana-Champaign, 2001.

[44] L. Jia, X. Liu, G. Noubir, and R. Rajaraman, "Transmission power control for Ad Hoc wireless networks: throughput, energy and fairness," in *Proc. IEEE Wireless Communications and Networks Conference (WCNC'05)*, New Orleans, LA, USA, 2005, pp. 619-625.

[45] T. Olwal, F. Aron, B. J. V. Wyk, Y. Hamam, N. Ntlatlapa, and M. Odhiambo, "Improved Distributed Dynamic Power Control for Wireless Mesh Networks," in *Proc. 7th International conference on Ad Hoc Networks and Wireless (DHOC-NOW 2008)*, Sophia Antipolis, France, 2008, pp. 357-368.

[46] T. Olwal, B. J. V. Wyk, K. Djouani, Y. Hamam, P. Siarry, and N. Ntlatlapa, "A Multi-State Based Power Control for Multi-Radio Multi-Channel Wireless Mesh Networks," *International Journal of Computer Science (WASET),* vol. 4, pp. 53-61, 2009.

[47] T. Olwal, B. J. V. Wyk, Y. Hamam, and N. Ntlatlapa, "Decentralized Cross-layer Dynamic Power Control for Wireless Mesh Networks," in *Proc. 3rd IEEE International conference on Broadband communications, Information Technology and Biomedical Applications (Broadcom'08)*, Pretoria, South Africa, 2008, pp. 245-253.

[48] T. O. Olwal, B. J. V. Wyk, K. Djouani, Y. Hamam, P. Siarry, and N. Ntlatlapa, "Interference-Aware Power Control for Multi-Radio Multi-Channel Wireless Mesh Networks," in *Proc. IEEE Africon 2009 conference*, Nairobi, Kenya, 2009, pp. 1-6.

[49] T. Olwal, F. Aron, B. J. V. Wyk, Y. Hamam, N. Ntlatlapa, and D. Johnson, "Transmission Probability-based Dynamic Power Control for Multi-Radio Mesh Networks," in *Proc. Southern Africa Telecommunication Network Application Conference (SATNAC 2008)*, Wild Coast, Eastern Cape, 2008, pp. 1-6.

[50] K. Wang, C. F. Chiasserini, J. G. Proakis, and R. R. Rao, "Joint scheduling and power control supporting multicasting in wireless Ad Hoc networks," *Ad Hoc Networks,* vol. 4, pp. 532-546, 2006.

[51] T. O. Olwal, B. J. V. Wyk, K. Djouani, Y. Hamam, P. Siarry, and N. Ntlatlapa, "Range Based Power Control for Multi-radio Multi-channel Wireless Mesh Networks," in *Proc. Southern Africa Telecommunication Networks Application Conference (SATNAC'09)*, Royal Swazi Spar, Swaziland, 2009, pp. 49-54.

[52] T. O. Olwal, K. Djouani, B. J. V. Wyk, Y. Hamam, and P. Siarry, "A multi-radio Multi-Channel Unification Power Control for Wireless Mesh Networks," *International Journal of Computer Science (WASET),* vol. 5, pp. 38-50, March 2010.

[53] T. O. Olwal, K. Djouani, P. Siarry, B. J. V. Wyk, and Y. Hamam, "Singularly-perturbed Weakly-coupled Power Control for Wireless Backbone Networks: A Decentralized Approach," *Submitted to IEEE Transactions on Mobile Computing,* November 2009.

[54] I. 802.11s, "IEEE 802.11s Standard Working Group, Draft amendment," 2007.

[55] K. C. Lan, Z. Wang, R. Berriman, T. Moors, and M. Hassan, "Implimentation of a Wireless Mesh Network Testbed for Traffic Control," in *Proc. IEEE 1st International Workshop on Wireless Mesh and Ad Hoc Networks (WiMAN'07)*, Honolulu, Hawaii, USA, 2007.

[56] D. Li, D. Dai, X. Zhang, and Hang, "Joint adaptive modulation and power control in cognitive radio networks," in *Proc. IET Conf. Wireless, Mobile and Sensor Networks (CCWMSN'07)*, Shanghai, China, 2007, pp. 739-741.

[57] Y. Shi and Y. T. Hou, "Optimal Power Control for Multi-hop software Defined Radio Networks," Bradley Department of ECE, Virginia Tech., Virginia 2006.

[58] E. Inc, "Multiple Channel 802.11 Chipset.," 2004.

[59] R. S. Komal and A. B. Mackenzie, "Analyzing Selfish Topology Control in Multi-Radi Multi-Channel Multi-hop Wireless Networks," in *Proc. IEEE International Conference on Communications (ICC'09)*, 2009.

[60] S. Merlin, N. Vaidya, and M. Zorzi, "Resource Allocation in Multi-Radio Multi-Channel Wireless Networks," in *Proc. IEEE INFOCOM 2008*, Phoenix, USA, 2008, pp. 610-618.

[61] I. Khemapech, A. Miller, and I. Duncan, "A Survey of Transmission Power Control in Wireless Sensor Networks," in *Proc. of the 8th Annual Postgraduate symposium on the Convergence of Telecommunications, Networking and Broadcasting (PGNet 2007)*, 2007, pp. 15-20.

[62] S. Koskie and Z. Gajic, "Signal-To-Interference-Based Power Control for Wireless Networks: a Survey, 1992—2005," *Dynamics of continuous, Discrete and Impulsive Systems B: Applications and Algorithms,* vol. 13, pp. 187-220, 2006.

[63] L. T. H. A. Correia, D. F. Macedo, D. A. C. Silva, A. L. d. Santos, A. A. F. Loureiro, and J. M. S. Noguerira, "Transmission Power Control in MAC Protocols for Wireless Sensor Networks," in *Proc. of the 8th ACM/IEEE International Symposium on Modelling, Analysis and Simulation of Wireless and Mobile Systems (MSWiM'05)*, Montreal, Quebec, Canada, 2005, pp. 282-289.

[64] N. A. Pantazis, D. D. Vergados, N. I. Miridakis, and D. J. Vergados, "Power control schemes in wireless sensor networks for homecare e-health applications," in *ACM International Conference Proceeding Series*, Athens, Greece, 2008.

[65] M. J. Neely and R. Urgoankar, "Cross-layer Adaptive Control for Wireless Mesh Networks," *Ad Hoc Networks,* vol. 5, pp. 719-743, August 2007.

[66] E. Altman, A. Kumar, and Y. Hayel, "A Potential Game Approach for Uplink Resource Allocation in a Multichannel Wireless Access Networks," in *Proc. ACM/ICST International Workshop on Game Theory for Comm. Networks*, Pisa, Italy, 2009.

[67] G. He, S. Gault, M. Debbah, and E. Altman, "Distributed Power Allocation Game for Uplink OFDM Systems," in *Proceedings of 2nd International Workshop on Wireless Networks: Communication, Cooperation and Competition*, Berlin, Germany, 2008.

[68] T. Chahed, E. Altman, and S. E. Elayoubi, "On Design of TDD for Joint Uplink and Downlink Resource Allocation in OFDMA-based WiMAX," in *Proceedings of 68th IEEE Vehicular Technology Conference*, Calgary, Canada, 2008.

[69] E. Altman, R. El-Azouzi, Y. Hayel, and H. Tembine, "Evolutionary Power Control Games in Wireless Networks," in *Proc. IFIP Networking*, Singapore, 2008.

[70] F. Gunnarsson and F. Gustafsson, "Control Theory Aspects of Power Control in UMTS," *Control Engineering Practice,* vol. 11, pp. 1113-1125, October 2003.

[71] R. Yellapantula, Y. Yao, and R. Ansari, "Antenna Selection and Power Control in MIMO Systems with Continuously Varying Channels," *IEEE Communications Letters,* vol. 13, pp. 480-482, July 2009.

[72] M. P. J. Baker and T. J. Moulsley, "Power Control in UMTS release'99," in *Proc. 1st International Conference on 3G Mobile Technologies*, 2000.

[73] J. Zhu, T. Li, P. Barber, J. Carlo, D. Xiang, D. Dang, L. Chen, and J. Lee, "Correction to Power Control for OFDMA PHY in IEEE 802.16 Broadband Wireless Access Working Group," in *IEEE 802.16 Broadband Wireless Acess*: IEEE, 2005.

[74] I. Marin, E. Arceredillo, A. Zuloaga, and J. Arias, "Wireless Sensor Networks: A Survey on Ultra-Low Power-Aware Design," *Journal of Proceedings of World Academy of Science, Engineering and Technology (PWASET),* vol. 8, pp. 44-49, October 2005.

[75] C. R. Anderson, J. H. Reed, R. M. Buehrer, D. Sweeney, and S. Griggs, *An Introduction to Ultra Wideband Communication Systems*. Indiana: Prentice Hall, 2005.

[76] V. Kawadia and P. R. Kumar, "Principles and Protocols for Power Control in Ad hoc Networks," *IEEE Journal on Selected Areas in Communications,* vol. 23, pp. 78-88, January 2005.

[77] S. Narayanaswamy, V. Kawadia, R. S. Screenivas, and P. R. Kumar, "Power Control in Ad Hoc Networks: Theory, Architecture, Algorithm and Implementation of the COMPOW

Protocol," in *Proceedings of the European Wireless Conference*, Florence, Italy, 2002, pp. 156-162.

[78] A. Capone and F. Martignon, "Power-controlled Directional Medium Access Control for Wireless Mesh Networks," in *Wireless System and Network Architecture*. vol. 2883/2006 Berlin: Springer Berlin, 2006, pp. 34-46.

[79] A. C. a. G. Carello, "Scheduling Optimization in Wireless Mesh Networks with Power Control and Rate Adaptation," in *Proc. IEEE SECON 2006 conference*, Reston, USA, 2006.

[80] L. Georgiadis, M. J. Neely, and L. Tassiulas, *Resource Allocation and Cross-Layer Control in Wireless Networks, Foundations and Trends in Networking* vol. 1. USA: now Publishers Inc., 2006.

[81] J. Yuan, Z. Li, W. Yu, and B. Li, "A cross-layer Optimization Framework for Multi-hop multi-cast in Wireless Mesh Networks," *IEEE Journal Selected Areas in Communications,* vol. 24, November 2006.

[82] S. Max and T. Wang, "Transmit Power Control in Wireless Mesh Networks Considered Harmful," in *Proc. 2nd International Conference on Advances in Mesh Networks*, Athens, Greece, 2009, pp. 73-78.

[83] J. C. Chiang, K. K. Leung, and X. Qiu, "Power control for packet voice service with application to EDGE wireless system," *International Journal of Wireless Information Networks,* vol. 11, pp. 29-39, 2004.

[84] M. Chiang, "Balancing Transport and Physical Layers in Wireless Multi-hop Networks: Jointly Optimal Congestion Control and Power Control," *IEEE Journal on Selected Areas in Communications,* vol. 23, January 2005.

[85] M. Chiang, C. W. Tan, D. P. Palmar, D. O'Neill, and D. Julian, "Power Control by Geometric Programming," *IEEE Trans. Wirel. Communications,* vol. 6, pp. 2640-2651, July 2007.

[86] R. Montemanni and L. M. Gambardella, " Minimum Power Symmetric Connectivity problem in wireless networks: a new approach," in *Mobile and Wireless Communication Networks*. vol. 162: Springer, 2004, pp. 496-508.

[87] R. Montemanni, L. M. Gambardella, and A. K. Das, "The Minimum Power Broadcast problem in Wireless Networks: a Simulated Annealing approach," in *Proc. Of the IEEE Wireless Communications and Networking Conference (WCNC'2005)*, New Orleans, USA, 2005.

[88] C. Fischione and M. Butussi, "Power and Rate Control Outage Based in CDMA Wireless Networks under MAI and Heterogeneous Traffic Sources," in *Proc. of IEEE International Conference on Communications 2007 (IEEE ICC 07)*, Glasgow, UK, 2007.

[89] B. Z. Ares, P. G. Park, C. Fischione, A. Speranzon, and K. H. Johansson, "On Power Control for Wireless Sensor Networks: System Model, Middleware Component and Experimental Evaluation," in *Proc. of IFAC European Control Conference*, Kos, Greece, 2007.

[90] A. Arora and M. Krunz, "Power-Controlled medium access for Ad Hoc networks with directional antennas," *Ad Hoc Networks,* vol. 5, pp. 145-161, 2007.

[91] L. Dongsheng, X. Yong, and S. Meilin, "A Multi-Channel Based Power Control Protocol for Mobile Ad Hoc Networks," in *Proc. International Conference on Wireless Networks (ICWN'2006)*, Las Vegas, USA, 2006, pp. 237-243.

[92] J. Gomez, A. T. Campbell, M. Naghshineh, and C. Bisdikian, "PARO: Supporting Dynamic Power Controlled Routing in Wireless Ad Hoc Networks," *ACM/Kluwer, Journal Wireless Networks,* vol. 9, pp. 443-460, September 2003.

[93] V. Kawadia and P. R. Kumar, "Power control and clustering in Ad Hoc networks," in *Proc. IEEE INFOCOM 2003 Conference*, San Fransisco, California, USA, 2003, pp. 459-469.

[94] S. Singh, M. Woo, and C. S. Raghavendra, "Power Aware Routing in Mobile Ad Hoc Networks," in *Proc. ACM MobiCom 1998 Conference*, Dallas, Texas, USA, 1998, pp. 181-190.

[95] C. Tadonki and J. Rolim, " Integer Programming Heuristic for the Dual Power Setting Problem in Wireless Sensors Networks," *Sensors Networks,* vol. 1, 2008.

[96] J. Huang, R. Berry, and M. L. Honig, " Performance of Distributed Utility-Based Power Control for Wireless Ad Hoc Networks," in *Proc. Military Communication Conference (MILCOM'2005)*, Atlantic City, New Jersey, 2005.

[97] J. Huang, R. A. Berry, and M. L. Honig, "A Game Theoretic Analysis of Distributed Power Control for Spread Spectrum Ad Hoc Networks," in *Proc. IEEE International Symposium Information Theory (ISIT 2005) Conference*, Adelaide, Australia.

[98] F. Meshkati, M. Chiang, H. V. Poor, and S. C. Schwartz, "A Game-Theoretic Approach to Energy-Efficient Power Control in Multi-carrier CDMA systems," *IEEE Journal Selected Areas in Communications,* vol. 24, pp. 1115-1129, June 2006.

[99] Y. Xing and R. Chandramouli, "Stochastic Learning Solution for Distributed Discrete Power Control Game in Wireless Data Networks," in *Proceedings of IEEE International Conf. on Communications (ICC)*, Paris, 2004.

[100] S. Koskie and Z. Gajic, "Optimal SIR-Based Power Control Strategies for Wireless CDMA Networks," *International Journal of Information and Systems Sciences,* vol. 1, pp. 1-18, 2007.

[101] K. Shoarinejad, J. L. Speyer, and G. J. Pottie, "A distributed scheme for integrated predictive dynamic channel and power allocation in cellular radio networks," in *Proc. Global Telecommunication (GLOBECOM 2001) Conference*, San Antonio, TX, 2001, pp. 3623-3627.

[102] K. K. Leung, "Power Control by interference predictions for wireless packet networks," *IEEE Trans. Wireless Communications,* vol. 1, pp. 256-265, April 2002.

[103] E. Altman, J. Galtier, and C. Touati, "Fair Power and Transmission Rate Control in Wireless Networks," in *Proc. 3rd Annual Conference on Wireless on Demand Network System and Services (WONS)*, Les Menuires, France, 2006.

[104] E. Altman, A. Kumar, D. Kumar, and R. Venkatesh, "Cooperative and Non-Cooperative Control in IEEE 802.11 WLANs," in *Proc. 19th International Teletraffic Congress*, Beijing, China, 2005.

[105] D. Kumar, V. Ramaiyan, A. Kumar, and E. Altman, "Capacity Optimization Hop Distance in a Mobile Ad Hoc Network with Power Control," in *Proc. 4th International Symposium on Modelling and Optimization in Mobile, Ad Hoc and Wireless Networks (WiOpt'06)*, Boston, Massachussets, 2006.

[106] V. Ramaiyan, A. Kumar, and E. Altman, "Jointly Optimal Power Control and Routing for a Single Cell, Dense, Ad Hoc Wireless Network," in *Proc. Work on Modelling and Optimization in Mobile, Ad Hoc and Wireless Networks*, Limasol, Cyprus, 2007.

[107] A. Subramanian and A. H. Sayed, "Joint Rate and Power Control Algorithms for Wireless Networks," *IEEE Trans. On Signal Processing,* vol. 53, November 2005.

[108] S. Boyd and L. Vandenberge, *Convex Optimization*. Cambridge, U. K.: Cambridge University Press, 2004.

[109] K. Jain, J. Padhaye, V. N. Padmanabhan, and L. Qiu, "Impact of Interference On Multi-hop Wireless Network Performance," in *Proc. Mobile Computing and Networks (MobiCom'03)*, San Diego, California, USA, 2003.

[110] G. M. A. Attiya, "Assignment of Tasks on Parallel and Distributed Computer Systems," in *Computer Science*. vol. PhD Thesis Paris: University of Marne-La-Valley, 2004, p. 225.

[111] S. A. Grandhi and J. Zander, "Constrained power control in cellular radio systems," in *Proc. IEEE 44th Vehicular Technology Conference (VTC'94)*, Stockhom, Sweden, 1994, pp. 824-828.

[112] M. M. Olama, S. M. Djouadi, and C. D. Charalambous, "Stochastic power control for time-varying long-term fading wireless," *EURASIP Journal on Applied Signal Processing,* vol. 2006, pp. 1-13, 2006.

[113] M. M. Olama, S. M. Shajaat, S. M. Djouadi, and D. Charalambous, "Stochastic power control for time-varying short term flat fading wireless channels," in *Proc. 16th IFAC World Congress*, Prague, Czech Republic, 2005.

[114] C. Fischione, M. Butussi, K. H. Johansson, and M. D'Angelo, "Power and Rate Control with Outage Constraints in CDMA Wireless Networks," *IEEE Transactions on Communications,* 2009.

[115] J. Tang, G. Xue, C. Chaudler, and W. Zhang, "Link Scheduling with power control for throughput enhancement in multi-hop wireless networks," *IEEE Transaction Vehicular Technology,* vol. 55, pp. 733-742, May 2006.

[116] V. Ramamurthi, A. Reaz, S. Dixit, and B. Mukherjee, "Link Scheduling and Power Control in Wireless Mesh Networks with Directional Antennas," in *Proc. IEEE ICC 2008 conference*, Beijing, China, 2008, pp. 4835-4839.

[117] R. Montemanni and L. M. Gambardella, " An exact algorithm for the min-power symmetric connectivity problem in wireless networks," IDSIA-23-03 December 2003.

[118] R. Montemanni and L. M. Gambardella, "Exact algorithms for the minimum power symmetric connectivity problem in wireless networks," *Computers and Operations Research,* vol. 32, pp. 2891-2904, November 2005.

[119] R. Montemanni, L. M. Gambardella, and A. K. Das, "Models and exact algorithms for the min-power symmetric connectivity problem: an overview," in *Handbook on Theoretical and Algorithmic Aspects of Sensor, Ad Hoc Wireless, and Peer-to-Peer Networks*: Auerbach Publications, 2006, pp. 133-146.

[120] J. Wieselthier, G. Nguyen, and A. Ephremides, "On the construction of energy-efficient broadcast and multi-cast trees in wireless networks," in *Proc. IEEE INFOCOM 2000 Conference*, Israel, 2000, pp. 585-594.

[121] P. Belotti and F. Malucelli, "Row-column generation for multi-layer network design," in *Proc. International Network Optimization Conference (INOC'05)*, Lisbon, Portugal, 2005.

[122] C. Tadonki and J. Rolim, "Integer programming heuristic for the dual power management problem in sensor networks," in *Proc. 2nd International Workshop on Managing Ubiquitous Communication and Services (MUCS'2004)*, Dublin, 2004.

[123] Y. Xi and E. M. Yeh, "Distributed algorithms for spectrum allocation, power control, routing and congestion control in wireless networks," in *Proc. ACM 8th International Symposium on Mobile Ad Hoc Networking and Computing*, Montreal, Quebec, Canada, 2007, pp. 180-189.

[124] S. Vasudevan, C. Zhang, D. Goeckel, and D. Towsley, "Optimal power allocation in wireless networks with transmitter-receiver power tradeoffs," in *Proc. IEEE 25th International Conference on Computer Communications (INFOCOM'06)*, Barcelona, 2006, pp. 1-11.

[125] T. Shu, M. Krunz, and S. Vrudhula, "Joint optimization of transmit power-time and bit energy efficiency in CDMA wireless sensor networks," *IEEE Transactions on Communications,* vol. 5, pp. 3109-3118, November 2006.

[126] I. Broustis, J. Eriksson, S. V. Krishnamurthy, and M. Faloutsos, "Implications of Power Control in Wireless Networks: A Quantitative study," in *Proc. Passive and Active Measurements Conference (PAM'07)*, Louvain-la-neuve, Belgium, 2007.

[127] S. Koskie, "Contributions to Dynamic Nash Games and Applications to Power Control for Wireless Networks." vol. PhD thesis: Rutgers University, 2003.

[128] S. Koskie and J. Zapf, "Acceleration of Static Nash Power Control Algorithm using Newton Iterations," *Dynamics of Continuous, Discrete and Impulse Systems B: Applications and Algorithms,* vol. 12, pp. 685-690, 2005.

[129] V. Srivastava, J. Neel, A. B. MacKenzie, R. Menon, L. A. DaSilva, J. E. Hicks, J. H. Reed, and R. P. Gilles, "Using Game Theory to Analyze Wireless Ad Hoc Networks," *IEEE Communications Surveys and Tutorials 4th Quarter 2005,* 2005.

[130] J. Levin, *Super Modular Games*. Palo Alto, California: Stanford University Working Paper, 2003.

[131] D. J. Goodman and N. B. Mandayam, "Network Assisted power control for wireless data," *Mobile Networks and Applications,* vol. 6, pp. 409-418, September 2001.

[132] C. A. S. Jean and B. Jabbari, " Game-Theoretic Delay-Sensitive Multi-rate Power Control for CDMA Wireless Networks with Variable Path Loss " in *Proc. IEEE Wireless Communications and Networking Conference (WCNC)*, Las Vegas, Nevada, 2006.

[133] C. Liang and K. R. Dandekar, "Power Management in MIMO ad hoc networks: a game theoretic approach," *IEEE Transaction on Wireless Communication,* vol. 6, pp. 1164-1170, April 2007.

[134] D. Famolari, N. B. Mandayam, D. J. Goodman, and V. Shah, "A new framework for power control in wireless data networks: games, utility and pricing," *Wireless multimedia network technologies, Kluwer Academic Publishers,* pp. 289-310, 1999.

[135] K. Viswanath and K. Obraczka, "Modelling the Performance of Flooding in Wireless Multi-Hop Ad Hoc Networks," *Proc. Computer Communications Journal (CCJ'05),* 2005.

[136] E. Altman, K. Avrachenkov, and A. Garnaev, "Transmission power control game with SINR as

objective function," in *Network Control and Optimization*. vol. LNCS 5425/2009: Springer Berlin, 2009, pp. 112-120.

[137] V. M. DaSilva and E. S. Sousa, "Performance of orthogonal CDMA codes for quasi-synchronous communication systems," in *Proc. IEEE 2nd International Conference on Universal Personal Communications*, Ottawa, Canada, 1993, pp. 995-999.

[138] R. W. Thomas, R. S. Komali, A. B. MacKenzie, and L. A. DaSilva, "Joint Power and Channel Minimization in Topology Control: A cognitive Network Approach," in *Proc. IEEE International Conference on Communication (ICC'2007)*, Glasgow, Scotland, 2007, pp. 6538-6542.

[139] P. Closas, A. Pages-Zamora, and J. A. Fernadez-Rubio, "A game theoretical algorithm for joint power and topology control in distributed WSN," in *Proc. IEEE International Conference on Acoustics, Speech and Signal Processing (ICASSP'09)*, Taipei, Taiwan, 2009, pp. 2765-2768.

[140] J. Huang, Z. Han, M. Chiang, and H. V. Poor, "Distributed Power Control and Relay Selection for Cooperative Transmission Using Auction Theory," *IEEE Journal Selected Areas in Communications,* vol. 26, pp. 1226-1237, September 2008.

[141] N. Jindal, S. Weber, and J. G. Andrews, "Fractional Power Control for Decentralized Wireless Networks," *IEEE Transactions on Wireless Communications,* vol. 7, pp. 5482-5492, December 2008.

[142] M. J. Neely, E. Modiano, and C. E. Rohrs, "Dynamic Power Allocation and Routing for Time-Varying Wireless Networks," *IEEE Journal on Selected Areas of Communication,* vol. 23, pp. 89-103, January 2005.

[143] N. Bambos, "Toward Power-Sensitive Network Architectures in Wireless Communications: Concepts, Issues, and Design Aspects," in *IEEE Personal Communication Magazine*: IEEE, 1998, pp. 50-59.

[144] T. Holliday, A. Goldsmith, P. Glynn, and N. Bambos, "Distributed Power and Admission control for time varying wireless networks," in *Proc. IEEE International Symposium on Information Theory (ISIT'04)*, Chicago, Illinois, 2004.

[145] S. Lin, J. Zhang, G. Zhou, L. Gu, T. He, and J. A. Stankovic, "ATPC: Adaptive Transmission Power Control for Wireless Sensor Networks," in *Proc. 4th ACM Conf. Embedded Networked Sensor (SenSys'06)*, Boulder, Colorado, USA, 2006.

[146] T. S. Rappaport, *Wireless Communications, Principles and Practice*: Prentice-Hall, 1996.

[147] M. M. Carvalho and J. J. Garcia-Luna-Aceves, "A scalable model for channel access protocols in multi-hop Ad Hoc Networks," in *Proc. ACM MobiCom'04 Conference*, Philadelphia, USA, 2004, pp. 1-9.

[148] G. J. Foschini and Z. Miljanic, "A simple distributed autonomous power control algorithm and its convergence," *IEEE Trans. On Vehicular Technology,* vol. 42, pp. 641-647, November 1993.

[149] R. D. Yates, "A framework for uplink power control in cellular radio systems," *IEEE Journal on Selected Areas in Communications,* vol. 13, pp. 1341-1348, 1995.

[150] D. Kim, "Rate regulated power control for supporting flexible transmission in future CDMA mobile networks," *IEEE Journal on Selected Areas Communication,* vol. 17, pp. 968-977, May 1999.

[151] A. H. Sayed, " A framework for state space estimation with uncertain models," *IEEE Transactions Automatic Control,* vol. 46, pp. 998-1013, July 2001.

[152] H.-J. Su and E. Geraniotis, "Adaptive closed-loop control with quantized feedback and loop filtering," *IEEE Trans. Wireless Communications,* vol. 1, pp. 76-86, 2002.

[153] S. Agarwal, R. H. Katz, S. V. Krishnamurthy, and S. K. Dao, "Distributed power control in Ad-Hoc wireless networks," in *Proc. IEEE 12th International Symposium on Personal, Indoor and Mobile Radio Communications*, 2002.

[154] P. Hande, S. Rangan, M. Chiang, and X. Wu, " Distributed uplink power control for optimal SIR assignment in cellular data networks," *IEEE/ACM Transactions on Networking,* vol. 16, pp. 1430-1443, November 2008.

[155] M. L. Sim, E. Gunawan, C. B. Soh, and B. H. Soong, "Study on the Characteristics of Predictive Closed-loop Power Control Algorithms for a cellular DS/CDMA System," *IEEE Transactions on Vehicular Technology,* vol. 48, pp. 911-921, May 1999.

[156] K. Shoarinejad, J. L. Speyer, and G. J. Pottie, "An Integrated Predictive Power Control and dynamic channel assignment in mobile radio systems," *IEEE Transactions on Wireless Communications,* vol. 2, pp. 976-988, September 2003.

[157] K. Shoarinejad, "On Stochastic Decentralised Systems in Communications and Controls," in *Electrical Engineering Department*. vol. PhD Dissertation: University of California Los Angeles, 2001.

[158] K. K. Leung, "Power Control by Kalman Filter with Error Margin for Wireless IP Networks." vol. US6519705 US patent, 2003.

[159] K. K. Leung, P. F. Driesson, and K. Chaula, "Link Adaptation and Power Control for Streaming Services in EGPRS wireless networks," *IEEE Journal Selected Areas in Communication,* vol. 19, pp. 2029-2039, 2001.

[160] H.-H. Chen, Z. Fan, and J. Li, "Autonomous power control MAC protocol for mobile ad hoc networks," *EURASIP Journal on Wireless Communications and networking,* vol. 2006, pp. 1-10, 2006.

[161] C. E. Koksal, H. I. Kassab, and H. Balakrishnan, "An analysis of short term fairness in wireless media access protocols," in *Proc. ACM SIGMETRICS*, Santa Clara, California, USA, 2000.

[162] A. Sheth and R. Han, "SHUSH: Reactive transmission power for wireless MAC protocols," in *Proc. IEEE 1st International Conference on the Wireless Internet (WICON'05)*, Budapest, Hungary, 2005, pp. 18-25.

[163] A. Sheth and R. Han, "SHUSH: A MAC protocol for Transmit Power Controlled Wireless Networks," Department of Computer Science, University of Colorado December 2004.

[164] A. Muqattash and M. Krunz, "Power controlled dual channel (PCDC) medium access protocol for wireless ad hoc networks," in *Proc. IEEE INFOCOM 2003 Conference*, San Francisco, 2003.

[165] A. Muqattash and M. Krunz, "A distributed transmission power control protocol for mobile ad hoc networks," *IEEE Transactions on Mobile Computing,* vol. 3, pp. 113-128, April/June 2004.

[166] M. Siam and M. Krunz, "Throughput-Oriented power control in MIMO-based ad hoc networks," in *Proc. IEEE ICC 2007 Conference: Wireless Ad Hoc and Sensor Symposium*, Glasgow, Scotland, 2007.

[167] P. Ding, J. Holliday, and A. Celik, "Demac: an adaptive power control MAC protocol for Ad Hoc networks," in *Proc. IEEE 16th International Symposium Personal, Indoor Mobile Radio Communication (PIMRC'05)*, Berlin, Germany, 2005.

[168] P. Li, X. Gang, and Y. Fang, "An Adaptive power controlled MAC protocol for wireless Ad Hoc networks," *IEEE Transactions on Wireless Communication,* vol. 8, pp. 226-233, January 2009.

[169] D. Qiao, S. Choi, and K. G. Shin, "Interference analysis and transmit power control in IEEE 802.11a/h wireless LANs," *IEEE/ACM Transaction Network,* vol. 15, pp. 1007-1020, October 2007.

[170] W. H. Ho and S. C. Liew, "Distributed Adaptive Power Control in IEEE 802.11 Wireless Networks," in *Proc. IEEE International Conference on Mobile Ad-Hoc and Sensor System (MASS'06)*, Vancouver, Canada, 2006.

[171] W. H. Ho and S. C. Liew, "Impact of power control on performance of IEEE 802.11 Networks," *IEEE Transaction on Mobile computing,* vol. 6, pp. 1245-1258, November 2007.

[172] W. H. Ho and S. C. Liew, "Achieving Scalable Capacity in Wireless Networks with Adaptive Power Control," in *Proc. IEEE 5th International Workshop on Wireless Local Networks (WLN)*, 2005, pp. 720-728.

[173] L. Jiang and S. C. Liew, "Removing Hidden Nodes in IEEE 802.11 Wireless Networks," in *Proc. IEEE Vehicular Technology Conference (VTC'05)*, Dallas,TX, 2005.

[174] L. Fu, S. C. Liew, and J. Huang, " Fast Algorithms for joint power control and scheduling in wireless networks," *To appear in IEEE Transactions on Wireless Communication,* 2010.

[175] J. Polastre, J. Hill, and D. Culler, "Versatile low power medium access for wireless sensor networks," in *Proc. 2nd International Conf. on Embedded networked sensor systems*, 2004, pp. 95-107.

[176] L. T. H. A. Correia, D. F. Macedo, D. A. C. Silva, A. L. d. Santos, A. A. F. Loureiro, and J. M. S. Noguerira, "Challenges and Experiences in the Design of Transmission Power Control Protocols for Wireless Sensor Networks," Department of Computer Science, Federal University of Minas Gerais, Brazil 2006.

[177] J. Jeong, D. Culler, and J.-H. Oh, "Empirical Analysis of Transmission Power Control Algorithms for Wireless Sensor Networks," in *Proc. 4th International Conference on Networked Sensing Systems (INSS'07)*, Braunschweig, Germany, 2007, pp. 27-34.

[178] J. Jeong, D. Culler, and J.-H. Oh, " Design and Analysis of micro-solar systems for Wireless Sensor Networks," in *Proc. 4th International Conference on Networked Sensing Systems (INSS'08)*, Kanazawa, Japan, 2008, pp. 181-188.

[179] R. O'Dell, "Understanding Ad Hoc Networks From Geometry to Mobility," in *Computer Science*. vol. PhD Thesis Zurich: Swiss Federal Institute of Technology Zurich, 2006.

[180] A. Hasan, K. Yang, and J. G. Andrews, "Clustered CDMA AD HOC networks without closed-loop power control," in *Proc. IEEE MILCOM 2003 Conference*, Boston, MA, 2003.

[181] W. K. Lai, H.-S. Tsai, C. Li, and C.-S. Shieh, "A power efficient solution to the large interference range problem in ad hoc networks," *Journal of Wireless Communications and Mobile Computing,* vol. 9, pp. 1264-1273, 2009.

[182] W. K. Lai and C. Li, "PCIA: A Power control interference avoidance scheme for ad hoc networks," in *Proc. International Conference on Wireless Networks (ICWN'06)*, Las Vegas, USA, 2006, pp. 186-192.

[183] S.-L. Wu, Y.-C. Tseng, C.-Y. Lin, and J.-P. Shen, "A multi-channel MAC protocol with power control for multi-hop mobile ad hoc networks," *the Computer Journal* vol. 45, pp. 101-110, 2002.

[184] Y. Kim, H. Shin, and H. Cha, "Y-MAC: An Energy-Efficient Multi-Channel MAC protocol for dense wireless sensor networks," in *Proc. of 7th International Conference on Information Processing in Sensor Networks*, St. Louis, Missouri, USA, 2008, pp. 53-63.

[185] Q. Qu, L. B. Milstein, and D. R. Vaman, "Distributed power and scheduling management for mobile ad hoc networks with delay constraints," in *Proc. IEEE Military Commun., Conf., (Milcom 2006)*, Washington, DC, 2006.

[186] Z. Tang, Q. Hu, and G. Yu, "Power control strategies for multi-channel cognitive wireless networks with opportunistic interference cancellation," *Journal of Electronics (China),* vol. 25, pp. 268-273, April 2008.

[187] C.-M. Wu and Y.-Y. Wang, "Adaptive distributed channel assignment in wireless mesh networks," *International Journal of the Wireless Personal Communications,* vol. 47, pp. 363-382, November 2008.

[188] A. Arora, M. Krunz, and A. Muqattash, "Directional Medium Access Protocol with Power Control for Wireless Ad Hoc Networks," in *Proc. IEEE Global Telecommunication Conference (Globecom'04)*, Dallas, USA, 2004, pp. 2797-2801.

[189] R. R. Choudhary, X. Yang, R. Ramanathan, and N. H. Vaidya, "Using directional antennas for media access control in ad hoc networks," in *Proc. ACM MobiCom (MobiCom'02) Conference*, Atlanta, Georgia, USA, 2002, pp. 59-70.

[190] A. Capone, F. Martignon, and L. Fratta, "Directional MAC and Routing Schemes for Power Controlled Wireless Mesh Networks with adaptive Antennas," *Ad Hoc Networks Journal,* 2008.

[191] B. Alawieh, C. Assi, and H. Mouftah, "Power-aware ad hoc networks with directional antennas: Models and Analysis," *Ad Hoc Networks,* vol. 7, pp. 486-499, May 2009.

[192] N. S. Fahmy, T. D. Todd, and V. Kezys, "Distributed power control for ad hoc networks with smart antennas," in *Proc. IEEE Vehicular Technology Conference (VTC)*, Vancouver, BC, Canada, 2002, pp. 2141-2144.

[193] R. H. Ha, P.-H. Ho, and X. S. Shen, "Optimal sleep scheduling with transmission range assignment in application-specific wireless sensor networks," *to appear in International Journal Sensor Networks,* pp. 1-17, 2010.

[194] R. Zheng, J. C. Hou, and N. Li, "Power management and power control in wireless networks," in *Ad Hoc and Sensor Networks*: Nova Science Publishers, 2006, pp. 1-25.

[195] K. Jamieson, B. Chen, H. Balakrishnan, and R. Morris, "Span: Topology Maintenance for Energy Efficiency in Ad Hoc Wireless Networks," in *Proc. ACM MobiCom 2001 conference*, Rome, Italy, 2001.

[196] Y. Xu, S. Bien, Y. Mori, J. Heidemann, and D. Estrin, "Topology Control Protocols to Conserve Energy in Wireless Ad Hoc Networks," University of Los Angeles, Los Angeles January 2008.

[197] H.-Y. Hsu and A. R. Hurson, "PEAN: A Probabilistic Energy Aware Neighbour Monitoring Protocol for Mobile Ad Hoc Networks," in *Proc. IEEE 21st International Conference Advanced Information Networking and Applications (AINAW'07),*, Niagara Falls, Ontario, 2007, pp. 201-206.

[198] L. M. Feeney, "An Asynchronous Power Save Protocol for Wireless Ad Hoc Networks," T2002:9, SICS 2002.

[199] L. M. Feeney, C. Rohner, and B. Ahlgren, "The impact of wakeup schedule distribution in asynchronous power save protocols on the performance of multi-hop wireless networks," in *Proc. IEEE Wireless Communication Networks Conference (WCNC'07)*, Hong Kong, 2007.

[200] G. Dhiman and T. S. Rosing, "Dynamic power management using machine learning," in *Proc. International Conference on Computer-Aided Design (ICCAD'06)*, San Jose, CA, 2006.

[201] K. Klues, G. Xing, and C. Lu, "A Unified architecture for Flexible Radio Power Management in Wireless Sensor Networks," Washington University, School of Engineering 2006.

[202] K. Klues, G. Xing, and C. Lu, "Link layer support for unified radio power management in wireless sensor networks," in *Proc. ACM 6th International Conference on Information Processing in Sensor Networks (IPSN'07)*, Massachusetts, USA, 2007, pp. 460-469.

[203] G. Xing, M. Sha, G. Hackmann, K. Klues, O. Chipara, and C. Lu, "Towards unified radio power management for wireless sensor networks," *Wireless Communications and Mobile Computing,* 2008.

[204] G. Xing, C. Lu, Y. Zhang, and Q. Huang, "Minimum Power Configuration for Wireless Communication in Sensor Networks," *to appear ACM Journal* pp. 1-29, 2010.

[205] R. Zheng and R. Kravets, "On-demand power management for ad hoc network," in *Proc. IEEE INFOCOM 2003 Conference*, San Franscisco, California, 2003.

[206] N. Li and J. C. Hou, "Localised topology control algorithms for heterogeneous wireless networks," *IEEE/ACM Transactions on Networking (TON),* vol. 13, pp. 1313-1324, December 2005.

[207] J. Zhang, G. Zhou, C. Huang, S. H. Son, and J. A. Stankovic, "TMMAC: An Energy Efficient Multi-Channel MAC Protocol for Ad Hoc Networks," *ACM SIGMOBILE Mobile Computing and Communications Review (ACM MC2R), Special Issue on Localization Techniques and Algorithms,* January 2007.

[208] J. Wang, Y. Fang, and D. Wu, "A Power-Saving Multi-Radio Multi-Channel MAC protocol for wireless local area networks," in *Proc. IEEE INFOCOM 2006 conference*, Barcelona, Spain, 2006, pp. 1-13.

[209] H. Park, J. Jee, and C. Park, "Power management of multi-radio mobile nodes using HSDPA interface sensitive APs," in *Proc. IEEE 11th International Conference Advanced Communication Technology (ICACT'09)*, Phoenix Park, South Korea, 2009, pp. 507-511.

[210] M. Miller and N. Vaidya, " Improving Power Save Protocols Using Carrier Sensing and Busy-Tones for Dynamic Advertisement Window," Technical Report December 2004.

[211] D. Qiao and K. G. Shin, "Smart Power-Saving Mode for IEEE 802.11 Wireless LANs," in *Proc. IEEE INFOCOM 2005 Conference*, Miami, 2005.

[212] R. Bhatia, A. Kashyap, and L. Li, "The Power balancing problem in energy constrained multi-hop wireless networks," in *Proc. IEEE INFOCOM 2007 Conference*, Anchorage, Alaska, USA, pp. 553-562.

[213] R. Ramanathan and R. R. Hain, "Topology Control of Multi-hop Wireless Using Transmit Power Adjustment," in *Proc. IEEE INFOCOM 2000 Conference*, Tel-Aviv, Israel, 2000, pp. 404-413.

[214] M. Gerharz, C. d. Waal, M. Frank, and P. Martini, "Influence of Transmission Power Control on the Transport capacity of Wireless Multi-hop Networks," in *Proc. 75th IEEE International Symposium on Personal, Indoor and Mobile Radio Communication (PIMRC'04)*, Barcelona, Spain, 2004.

[215] R. Wattenhofer, L. Li, P. Bahl, and Y.-M. Wang, "Distributed Topology Control for Power Efficient Operation in Multi-hop Wireless Ad Hoc Networks," in *Proc. IEEE INFOCOM 2001 Conference*, Achorage, Alaska, 2001.

[216] R. Gallager, P. Humblet, and P. Spira, "A distributed algorithm for minimum-weight spanning trees," *ACM Transactions on Programming Languages and Systems,* vol. 5, pp. 66-77, January 1983.

[217] M. Khan, G. Pandurangan, and V. S. A. Kumar, "Energy-Efficient distributed constructions of minimum spanning tree for wireless ad hoc networks," Department of Computer Science, Purdue University 2006.

[218] Y. Wang and X.-Y. Li, "Minimum Power Assignment in Wireless Ad Hoc Networks with Spanner Property," *Kluwer Academic Publishers, Netherlands,* pp. 1-15, June 2005.

[219] D. Li, H. Du, L. Liu, and S. C.-H. Huang, "Joint Topology Control and Power Conservation for Wireless Sensor Networks Using Transmit Power Adjustment," in *Computing and Combinatorics*. vol. 5092/2008 Berlin/Heidelberg: SpringerLink, 2008, pp. 541-550.

[220] P. v. Richenback, "Interference and Topology Control in Ad Hoc Networks," in *Computer Science*. vol. Masters Thesis Zurich: Swiss Federal Institute of Technology Zurich, 2004.

[221] H. X. Tan and W. K. G. Seah, "Dynamic Topology Control to Reduce Interference in MANETs," Institute for Infocomm Research Technical Report:NET-2004-AHN-General-0027 November 2004.

[222] G. Calinescu, S. Kapoor, A. Olshevsky, and A. Zelikovsky, "Summary of Network Lifetime and Power Assignment in ad hoc Wireless networks," March 2005.

[223] G. Calinescu, S. Kapoor, A. Olshevsky, and A. Zelikovsky, "Network Lifetime and Power Assignment in ad hoc Wireless networks," in *Proc. 11th Annual European Symp. Algorithms (ESA 2003)* Berlin: Springer-Verlag, 2003, pp. 114-126.

[224] X.-Y. Li, P.-J. Wan, and Y. Wang, "Power Efficient and Sparse Spanner for Wireless Ad Hoc Networks," in *Proc. 35th Annual Hawaii International Conference on System Sciences (HICSS'02)*, Hilton Waikoloa Village, Island of Hawaii, 2002, pp. 296-299.

[225] Y. Choi, M. Khan, V. S. A. Kumar, and G. Pandurangan, "Energy-Optimal Distributed Algorithms for Minimum Spanning Trees," *IEEE Journal on Selected Areas in Communication, Issue on Stochastic Geometry and Random Graphs in Wireless Networks,* vol. 27, September 2009.

[226] M. Gerharz, C. d. Waal, P. Martini, and P. James, "A Cooperative Nearest Neighbours Topology Control Algorithm for Wireless Ad Hoc Networks," in *Proc. 12th International Conference on Computer Communications and Networks (ICCCN'03)* Dallas, TX, USA, 2003, pp. 412-417.

[227] X.-Y. Li, W.-Z. Song, and Y. Wang, "Efficient Topology Control for Ad Hoc Wireless Networks with Non-Uniform Transmission Ranges," August 23 2003.

[228] A. C.-C. Yao, "On constructing minimum spanning trees in k-dimensional spaces and related problems," *SIAM Journal of Computing,* vol. 11, pp. 721-736, 1982.

[229] A. Ghosh, Y. Wang, and B. Krishnamachari, "Efficient Distributed Topology Control in 3-Dimensional Wireless Networks," in *Proc. IEEE 4th Communication Society Conference on Sensor, Mesh and Ad Hoc communication and Networks (SECON'07)*, San Diego, California, USA, 2007.

[230] A. Muqattash, M. Krunz, and T. Shu, "On the Performance of Joint rate/power control with adaptive modulation in Wireless CDMA networks," in *Proc. IEEE INFOCOM 2006 Conference*, Barcelona, Spain, 2006.

[231] X. Li and D. Wu, "Power control and Dynamic Channel Allocation for Delay Sensitive Applications in Wireless Networks," in *Proc. IEEE Global Telecommunication Conference (Globecom 2006)*, San Francisco, CA, USA, 2006.

[232] C.-C. Chen and D.-S. Lee, "A Joint Design of Distributed QoS Scheduling and Power Control for Wireless Networks," in *Proc. IEEE INFOCOM 2006 Conference*, Barcelona, Spain, 2006.

[233] P. Bergamo, A. Giovanardi, A. Travasoni, D. Maniezzo, G. Mazzini, and M. Zorzi, "Distributed power control for energy efficient routing in ad hoc networks," *Wireless Networks,* vol. 10, January 2004.

[234] S.-J. Park and R. Sivakumar, "Load-Sensitive Transmission Power Control in Wireless Ad Hoc Network," in *Proc. IEEE Global Telecommunication Conference (Globecom'02)*, Taiwan, 2002.

[235] S.-J. Park and R. Sivakumar, "Quantitative analysis of transmission power control in wireless ad hoc networks," in *Proc. IEEE International Conference on Parallel Processing*, Vancouver, Canada, 2003.

[236] O. Chipara, Z. He, G. Xing, Q. Chen, X. Wang, C. Lu, J. Stankovic, and T. Abdelzaher, "Real-time Power-Aware Routing in Sensor Networks," in *Proc. IEEE 14th International Workshop on Quality of Service (IWQoS'06)*, Yale University, New Haven, CT, USA, 2006, pp. 83-92.

[237] J. Gomez, A. T. Campbell, M. Naghshineh, and C. Bisdikian, "Conserving transmission power in wireless ad hoc networks," in *Proc. 9th International Conf. on Network protocols (ICNP'01)*, Riverside, California, USA, 2001, pp. 24-34.

[238] J. Gomez and A. T. Campbell, "A case for Variable-Range transmission power control in wireless multi-hop networks," in *Proc. IEEE International Conference on Computer Communications (INFOCOM'04)*, Hong Kong, 2004.

[239] P. Gupta and P. R. Kumar, " The Capacity of Wireless Networks," *IEEE Trans. Information Theory,* vol. 46, 2000.

[240] O. Savas, M. Alanyali, and B. Yener, "Joint route and power assignment in asynchronous multi-hop wireless networks," in *Proc. MedHocNet 2004 Conference*, Bodrum, Turkey, 2004.

[241] P. Li, Q. Shen, Y. Fang, and H. Zhang, "Power Controlled Network Protocols for Multi-rate Ad Hoc Networks," *IEEE Transaction on Wireless Communication,* vol. 8, pp. 2142-2149, April 2009.

[242] R. L. Cruz and A. V. Santhanam, "Optimal Routing, Link scheduling and Power Control in Multi-hop wireless networks," in *Proc. IEEE INFOCOM 2003 Conference*, San Fransisco, California, 2003.

[243] D. K. Gupta, "Joint scheduling, routing and power control for single-channel wireless mesh networks," in *Computer Engineering*. vol. MSc. Thesis: North Carolina State University, 2006.

[244] S. Hengstler, "Performance of Joint routing, scheduling and power control in energy-constrained wireless sensor networks," Electrical Engineering: Technical Report EE360 2007.

[245] A. Kashyap, S. Senguta, R. Bhatia, and M. Kodialam, "Two-phase routing, scheduling and power control for wireless mesh networks with variable traffic," in *Proc. ACM SIGMETRICS Conference*, San Diego, California, USA, 2007, pp. 85-96.

[246] Y. Xi and E. M. Yeh, "Optimal Distributed Power Control, routing and congestion control in wireless networks," Department of Electrical Engineering, Yale University May 2006.

[247] G. L. Stuber, *Principles of Mobile Communication*. USA: Kluwer Academic Publishers, 2000.

[248] Y. Shen, Y. Cai, and X. Xu, "A shortest path-based topology control algorithm in wireless multi-hop networks," *Computer Communication Review,* vol. 37, pp. 29-38, 2007.

[249] H. Wu, Y. Lin, S. Cheng, Y. Peng, and K. Long, "IEEE 802.11 Distributed Coordination Function: Enhancement and Analysis," *Journal Computer Science and Technology,* vol. 18, pp. 607-614, September 2003.

[250] M. Gudmundson, "Correlation model for shadow fading in mobile radio systems," *Electronic Letters,* vol. 27, pp. 2145-2146, November 1991.

[251] G. Welch and G. Bishop, " An Introduction to the Kalman Filter," University of North Carolina, Chapel Hill July 2006.

[252] M.-S. Alouini and A. Goldsmith, "Adaptive M-QAM modulation over Nakagami Fading Channels," in *Proceedings IEEE Global Communication Conference*, 1997, pp. 218-223.

[253] N. D. Bambos, S. C. Chen, and D. Mitra, "Channel probing for distributed access control in wireless communication networks," in *Proc. IEEE Globecom'95 Conference*, 1995, pp. 322-326.

[254] S. I. Gauss, *Linear programming methods and applications*. New York, 2003.

[255] E. Altman, K. Avrachenkov, I. Menache, G. Miller, B. Prabhu, and A. Shwartz, "Dynamic Discrete Power Control in Cellular Networks," *IEEE Transaction on Automatic Control,* vol. 54, pp. 2328-2340, 2009.

[256] Math Works Inc., "http://www.mathworks.com," in *Math Works Inc* USA.

[257] S. Banerjee and A. Misra, "Adapting transmission power for optimal energy reliable multi-hop wireless communications," Dept. Compt. Science, University of Maryland, College Park, USA November 2002.

[258] A. Brzezinski, G. Zussman, and E. Modiano, "Enabling distributed throughput maximization in wireless mesh networks: a portioning approach," in *Proc. ACM MobiCom'06 Conference*, Los Angeles, California, USA, 2006.

[259] J. So and N. H. Vaidya, "Multi-channel MAC for ad hoc networks: handling multi-channel hidden terminals using a single transceiver," in *Proc. ACM Intl. Symposium on Mobil. Ad Hoc Netw. Comp. (MOBIHOC'04)*, Tokyo, Japan, 2004, pp. 222-233.

[260] A. P. Subramanian, H. Gupta, and S. Das, "Minimum-Interference Channel Assignment in Multi-radio Wireless Mesh Networks," *IEEE Trans. Mobile Computing (TMC'08),* vol. 7, November 2008.

[261] H. Zhu, K. Lu, and M. Li, "Distributed Topology Control in Multi-Channel Multi-Radio Mesh Networks," in *Proc. IEEE International Conference on Communications (ICC'08)*, Beijing, China, 2008, pp. 2958-2962.

[262] J. Tang, G. Xue, and W. Zhang, "End-to-end rate allocation in multi-radio wireless networks: cross-layer schemes," in *Proc. 3rd International conference (QShine'06)*, Waterloo, 2006.

[263] G. Bianch, "Performance analysis of the IEEE 802.11 distributed coordination function," *IEEE Jnl. Select. Areas in Communication,* vol. 18, pp. 535-547, March 2000.

[264] B. O'Hara and A. Petrick, *The IEEE 802.11 Handbook: A designer's Companion*: IEEE, 1999.

[265] T. Kailath, A. H. Sayed, and B. Hassibi, *Linear Estimation*: NJ: Prentice Hall, 2000.

[266] M. S. Mahmoud, M. F. Hassan, and M. G. Darwish, *Large Scale Control Systems Theories and Techniques*. Dekkar, New York, 1985.

[267] R. L. W. II and D. A. Lawrence, *Linear state space controls systems*. New Jersey: John Wiley & Sons, Inc.,, 2007.

[268] V. Dragan and T. Morozan, "The linear Quadratic Optimization Problem for a class of Discrete-Time Stochastic Linear Systems," *International Journal of Innovative Computing, Information and Control,* vol. 4, pp. 2127-2137, 2008.

[269] C. D. Ormsby, J. F. Raquet, and P. S. Maybeck, "A new generalized residual multiple model adaptive estimator of parameters and states," *Mathematical and Computer Modeling,* vol. 43, pp. 1092-113, 2006.

[270] S. S. Abdelwahed, M. F. Hassan, and M. A. Sultan, "Parallel Asynchronous Algorithms for optimal control of large scale dynamic systems," *Journal of Optimal Control Applications and Methods,* vol. 18, pp. 1-15, 1997.

[271] Z. Gajic and X. Shen, *Parallel Algorithms for Optimal Control of Large Scale Linear Systems*. New York: Spinger-Verlag, 1993.

[272] M. M. El-Tarazi, "Some Convergence results for asynchronous algorithms," *Numreish Mathematik,* vol. 39, pp. 325-344, 1982.

[273] K. E. Avrachenkov, "Analytic Perturbation Theory and its Applications," in *Electrical Engineering*: University of South Australia, 1999.

[274] F. Delebecque and J. Quadrat, "Optimal control of Markov chains admitting strong and weak interactions," *Automatic,* vol. 17, pp. 281-296, 1981.

[275] R. El-Azouzi and E. Altman, "Queueing Analysis of Link-Layer Losses in Wireless Networks," in *Proc. of Personal Wireless Communications* Venice, Italy, 2004, pp. 1-24.

[276] P. J. Schweitzer, "Perturbation series expansions for nearly completely-decomposable Markov Chains," *Teletraffic Analysis and computer performance evaluation,* pp. 319-328, 1986.

[277] H. Mukaidani, "Soft-constrained stochastic Nash games for weakly coupled large-scale systems " *Elsevier Automatica,* vol. 45, pp. 1272-1279, 2009.

[278] M. Sagara, H. Mukaidani, and T. Yamamoto, "Efficient Numerical Computations of Soft Constrained Nash Strategy for Weakly Coupled Large-Scale Systems," *Journal of Computers,* vol. 3, pp. 2-10, November 2008.

[279] X. Shen and Z. Gajic, "Optimal Reduced Solution of the weakly coupled discrete Riccati Equation," *IEEE Transactions on Automatic Control,* vol. 35, October 1990.

[280] H. Wang and N. B. Mandayam, "Dynamic power control under energy and delay constraints," in *Proc. IEEE Globecom'01 Conference*, San Fransisco, 2001.

[281] A. Nasipuri, J. Zhuang, and S. R. Das, "A Multichannel CSMA MAC Protocol for Multihop Wireless Networks," in *Proc. Of IEEE WCNC'99*, Hong Kong, 1999.

[282] H. Zhai, Y. Kwon, and Y. Fang, "Performance analysis of IEEE 802.11 MAC Protocol in Wireless LAN," *Wiley Journal of Wireless Communication and Mobile Computing (WCMC),* vol. 4, pp. 917-931, 2004.

[283] L. S. Lasdon, *Optimization Theory for Large Systems*. New York: Mac Millan, 1970.

[284] M. Krawczak, "Suboptimal strategies for Nash Nonlinear differential games," in *Control and Information Sciences*. vol. vol. 82/1986 Berlin: Springer Berlin/Heidelberg, 2006, pp. 185-202.

[285] K. Jittorntrum, "An implicit function theorem," *Journal of Optimization Theory and Applications,* vol. 25, pp. 285-288, 1978.

[286] T. O. Olwal, B. J. V. Wyk, N. Ntlatlapa, K. Djouani, P. Siarry, and Y. Hamam, "Dynamic Power Control for Wireless Backbone Mesh Networks: a Survey," *International Journal of Network Protocols and Algorithms,* vol. 2, pp. 1-44, April 2010.

[287] T. Olwal, B. J. V. Wyk, K. Djouani, Y. Hamam, and P. Siarry, "Singularly-Perturbed Weakly-Coupled Based Power Control for Multi-Radio Multi-Channel Wireless Networks," *International Journal of Applied Mathematics and Computer Sciences,* vol. 6, pp. 4-14, April 2010.